
Structure and Function of Flavin-containing Monoxygenases 3 and 5



Dissertation

zur Erlangung des Doktorgrades

der Mathematisch Naturwissenschaftlichen Fakultät

der Christian Albrechts-Universität

zu Kiel

vorgelegt von

Meike Motika

Kiel 2010

Referent: Prof. Dr. B. Clement

Korreferent: Prof. Dr. A. Scheidig

Tag der mündlichen Prüfung: 12.03.2010

Zum Druck genehmigt: 12.03.2010

Prof. Dr. Lutz Kipp
(Dekan)

List of Abbreviations

5-DPT	10-(<i>N,N</i> -Dimethylamino pentyl)-2-trifluoromethyl) phenothiazine
8-DPT	10-(<i>N,N</i> -Dimethylamino octyl)-2-trifluoromethyl) phenothiazine
Abs	Absorption
ACES	<i>N</i> -(2-Acetamido)-2-aminoethanesulfonic acid
APS	Ammonium persulfate
AUC	Area under the curve
BCHP	4'-(4''-Bromophenyl)- ω -[4-chlorophenyl]-4-hydroxypiperidinyl]-butyrophenone
BDAB	4'-(4-Bromophenyl)- ω -dimethylaminobutyrophenone
Bis-tris	Bis-(2-hydroxyethyl)-imino-tris-(hydroxymethyl)-methan
bp	Base pair
BPPB	4'-(4''-Bromophenyl)- ω -(4-phenylpiperazinyl)butyrophenone
BSA	Bovine serum albumine
C ₁₂ E ₈	Octa(ethylene glycol) dodecylmonoether
C ₈ E ₄	Tetra(ethylene glycol) monooctylether
cDNA	Complementary DNA
cGMP	Cyclic guanosine monophosphate
CHAPS	3-[(3-Cholamidopropyl)dimethylammonio]-1-propane sulfonate
C-HEGA [®] -10	Cyclohexylbutanoyl- <i>N</i> -hydroxyethylglucamide
CIP	Calf intestinal phosphatase
CMC	Critical micelle concentration
CTAB	Cetyltrimethylammonium bromide
Cymal [®] -1-7	Cyclohexyl-alkyl- β -D-maltoside
DDAO	<i>N,N</i> -Dimethyl-1-dodecanamine- <i>N</i> -oxide
DDM	n-Dodecyl- β -D-maltoside
DETAPAC	Diethylenetriaminepentaacetic acid
DLS	Dynamic light scattering
DM	n-Decyl- β -D-maltoside
DNA	Desoxyribonucleic acid
dNTP	Desoxyribonucleotide triphosphate
DTT	1,4-Dithiothreitol

<i>E. coli</i>	<i>Escherichia coli</i>
EDTA	Ethylenediaminetetraacetic acid
ESI	Electrospray ionization
FA	Facial amphiphile
FMO	Flavin-containing monooxygenase
FOS-CHOLINE [®] 10	n-Decylphosphocholine
FOS-CHOLINE [®] 12	n-Dodecylphosphocholine
FPLC	Fast performance liquid chromatography
fXa	Factor Xa
GSH	Glutathione
HECAMEG	Methyl-6-O-(<i>N</i> -heptylcarbamoyl)- α -D-glucopyranoside
Hox	Homeodomain protein
HPLC	High performance liquid chromatography
HT	High-throughput
IEF	Isoelectric focusing
IPTG	Isopropyl- β -D-thiogalactopyranoside
kb	Kilo bases
kDa	Kilo dalton
LB	Lysogenic broth (Luria-Bertani broth)
MBP	Maltose-binding protein
MeDDC	<i>S</i> -Methyl- <i>N,N</i> -diethyldithiocarbamate
MEGA-8	Octanoyl- <i>N</i> -methylglucamide
MMI	Mercaptoimidazole
MPTP	1-Methyl-4-phenyl-1,2,3,6-tetrahydropyridine
MPDP ⁺	1-Methyl-4-phenyl-2,3-dihydropyridinium cation
MPP ⁺	1-Methyl-4-phenylpyridinium cation
mRNA	Messenger ribonucleic acid
MW	Molecular weight
NADP	Nicotinamide adenine dinucleotide phosphate, oxidized form
NADPH	Nicotinamide adenine dinucleotide phosphate, reduced form
NFY	Nuclear transcription factor Y
NO	Nitric oxide
ODG	n-Octyl- β -D-glucoside
P450	Cytochrome P450

Pbx2	Pre-B-cell leukemia transcription factor 2
PDI	Polydispersity index
PEG	Polyethylene glycol
PEG MME	Polyethylene glycol monomethylether
pI	Isoelectric point
PMSF	Phenylmethylsulfonyl fluoride
RT	Room temperature
RT-PCR	Reverse transcription polymerase chain reaction
SDS	Sodium dodecyl sulfate
SDS-PAGE	Sodium dodecyl sulfate polyacrylamide gelelectrophoreses
SEC	Size exclusion chromatography
SNP	Single-nucleotide polymorphism
SOC	Super-optimal broth (SOB) with catabolite repression
<i>S. pombe</i>	<i>Schizosaccharomyces pombe</i>
TEMED	<i>N,N,N',N'</i> -Tetramethylethylenediamine
TMA	Trimethylamine
TMAu	Trimethylaminuria
TPN	Total parenteral nutrition
Tris	Tris-(hydroxymethyl) aminomethan
Triton [®] X-100	α -[4-(1,1,3,3-Tetramethylbutyl)phenyl]-hydroxy-poly(oxy-1,2-ethanediyl)
USF1	Upstream transcription factor 1
YY1	YY1 transcription factor
ZWITTERGENT [®] 3-10	n-Decyl- <i>N,N</i> -dimethyl-3-ammonio-1-propanesulfonate

Amino Acid Code

Amino acid	3-Letter-code	1-Letter-code
Alanine	Ala	A
Arginine	Arg	R
Asparagine	Asn	N
Aspartic acid	Asp	D
Cysteine	Cys	C
Glutamine	Gln	Q
Glutamic acid	Glu	E
Glycine	Gly	G
Histidine	His	H
Isoleucine	Ile	I
Leucine	Leu	L
Lysine	Lys	K
Methionine	Met	M
Phenylalanine	Phe	F
Proline	Pro	P
Serine	Ser	S
Threonine	Thr	T
Tryptophan	Trp	W
Tyrosine	Tyr	Y
Valine	Val	V

Flavin-containing monooxygenases (FMOs) are a family of NADPH dependent enzymes mainly catalyzing the oxygenation of heteroatom-containing nucleophilic xenobiotics. It consists of five isoforms with FMO3 and 5 having highest mRNA levels in adult human liver. Thus particular interest was paid to these two isoforms and their structural and functional properties were characterized.

Several mutations of FMO3 have been reported to be associated with the disorder trimethylaminuria (TMAu). In phenotyping and genotyping studies of self-reporting TMAu patients at the Human BioMolecular Research Institute, a novel FMO3 variant (V187A) was discovered that occurred in combination with E158K, E308G, and E305X. FMO3 V187A as well as V187A/E158K were recombinantly expressed as maltose-binding fusion proteins (MBP-FMO3) and characterized. In combination with the common mutations E158K and E308G the novel variant impairs FMO3 oxygenation activity and leads to TMAu.

In order to investigate structure and function of human FMO5 (hFMO5) sufficient quantities of highly purified, well characterized enzyme was needed. Thus, hFMO5 was successfully expressed as MBP-fusion protein (MBP-hFMO5), purified and characterized in terms of activity, purity, comparability to commercially available FMO5, stability at 4 °C, and monodispersity. These studies showed that MBP-hFMO5 was suitable for further studies including crystallization attempts. During these, MBP-hFMO5 proved to be stable without detergent although detergent was inevitable for extraction from *E. coli* suggesting that FMO5 is not an integral membrane protein but rather only associated with the membrane. Further, MBP-hFMO5 was crystallized. However, no satisfactory diffraction pattern could be obtained. Crystallization of FMO5 separated from the MBP-tag might improve crystals.

Also, species-dependent pK_a differences of the FMO5 enzyme were investigated. pH dependence studies of human and mouse MBP-FMO5 (MBP-mFMO5) were performed showing that residues at positions 227 and 228 of MBP-hFMO5 were responsible for the higher *N*-oxygenation activity of the human enzyme at low pH (i.e. pH 6).

Finally, in order to identify new substrates to further the knowledge of FMO5 active site structure and to identify a possible physiological function of FMO5, a high-throughput compatible enzyme activity assay was developed and several compounds were screened. Of all compounds tested, one (i.e., 4'-(4-bromophenyl)- ω -dimethylaminobutyrophenone HCl) was found to be *N*-oxygenated by MBP-hFMO5. This compound fits into the proposed selectivity range of FMO5, having a tertiary amine group on a long carbon side-chain. Overall, further compound screens will be needed to identify additional FMO5 substrates and gain more knowledge of substrate specificity and of its structure-function relationship.

Flavin-haltige Monooxygenasen (FMOs) gehören zu einer Familie von NADPH-abhängigen Enzymen, die die Oxygenierung von hauptsächlich Heteroatom-haltigen nucleophilen Xenobiotika katalysieren. Die Enzymfamilie besteht aus fünf Isoenzymen, von denen die mRNA Level von FMO3 und 5 in der Leber von Erwachsenen am höchsten sind. Daher bestand ein besonderes Interesse an diesen zwei Isoformen und an der Charakterisierung ihrer strukturellen und funktionellen Eigenschaften.

Viele in der Literatur beschriebene Mutationen der humanen FMO3 werden mit der Stoffwechselerkrankung Trimethylaminurie (TMAu) in Zusammenhang gebracht. In Phäno- und Genotypisierungsstudien von TMAu-Patienten, durchgeführt am Human BioMolecular Research Institute in San Diego, wurde eine neue FMO3 Variante (V187A) entdeckt, die in Kombination mit E158K, E308G und E305X auftrat. Sowohl FMO3 V187A als auch V187A/E158K wurden rekombinant als Maltose-bindende Fusionsproteine hergestellt (MBP-FMO3), gereinigt und näher charakterisiert. Die durchgeführten Studien zeigten, dass diese neu entdeckte FMO3 Variante in Kombination mit den häufig vorkommenden Mutationen E158K und E308G die Oxygenierungsaktivität der FMO3 beeinträchtigt und so zu TMAu führt.

Um Struktur- und Funktionsstudien der humanen FMO5 (hFMO5) durchzuführen, wurden ausreichende Mengen an hochgereinigtem, gut charakterisiertem Enzym benötigt. Dazu wurde hFMO5 als MBP-Fusionsprotein exprimiert, gereinigt und hinsichtlich Reinheit, Ausbeute, Aktivität, Vergleichbarkeit mit kommerziell-erhältlicher FMO5, Stabilität und Monodispersität charakterisiert. Diese Studien zeigten, dass MBP-hFMO5 für weitere Studien (u.a. Kristallisationsstudien) geeignet ist. In diesen stellte sich heraus, dass MBP-hFMO5 auch in Abwesenheit von Detergens stabil und aktiv ist, obwohl zu ihrer Extraktion aus *E. coli* Detergens benötigt wird. Daher liegt die Vermutung nahe, dass FMO5 kein integrales Membranprotein ist sondern vielmehr nur mit der Membran assoziiert ist. Weiterhin konnte MBP-hFMO5 kristallisiert werden. Allerdings wurde kein angemessenes Diffraktionsmuster erhalten. Kristallisation mit dem vom MBP-Tag getrennten FMO5 Protein könnte hierbei die Qualität der Kristalle verbessern.

In einer weiteren Studie wurden Spezies-abhängige pK_a -Unterschiede der FMO5 untersucht, indem pH-Abhängigkeitsstudien von humaner und muriner MBP-FMO5 (MBP-mFMO5) durchgeführt wurden. Diese zeigten, dass die Aminosäuren an Position 227 und 228 der hFMO5 für die erhöhte *N*-Oxygenierungsaktivität bei niedrigem pH (d.h. bei pH 6) verantwortlich sind.

Zuletzt wurde zur Identifizierung von neuen Substraten ein 'high-throughput'-fähiger Enzymaktivitätstest entwickelt, mit dem zahlreiche Verbindungen getestet wurden. Ein neues Substrat der FMO5 (4'-(4-Bromphenyl)- ω -dimethylaminobutyrophenon HCl) konnte auf diese Weise identifiziert werden, welches gut in das bisher bekannte Selektivitätsmuster des Enzyms paßt. Um weitere Erkenntnisse über die Struktur des aktiven Zentrums der FMO5 zu erhalten, sind allerdings weitere Untersuchungen nötig.

Table of Contents

1	Introduction	1
1.1	Introduction to Flavin-containing Monooxygenases	1
1.2	Nomenclature of FMO Enzymes	2
1.3	FMO Gene Organization	3
1.4	Regulation	4
1.4.1	Regulation of FMO Gene Expression	4
1.4.2	Species-, Tissue-, Age-, and Gender-Dependence of FMO Expression	4
1.4.3	Hormonal Regulation	7
1.4.4	Transcriptional Regulation	9
1.4.5	Posttranscriptional Regulation	10
1.5	Prominent FMO Polymorphisms	11
1.6	FMO Catalytic Mechanism	12
1.7	Differences between P450 and FMO Enzymes	14
1.8	Toxicity	15
1.9	Clinical Significance	19
1.10	Aim	21
2	Novel Variant of the Human FMO3 Gene Associated with Trimethylaminuria	24
2.1	Introduction	24
2.1.1	FMO3 Polymorphisms	24
2.1.2	Diseases and Disorders Associated with FMOs	24
2.1.3	Trimethylaminuria	25
2.1.4	Aim of the Study	31
2.2	Materials and Methods	32
2.2.1	Reagents	32
2.2.2	Genomic DNA Preparation and PCR Amplification	32
2.2.3	FMO3 Phenotyping by Urinary TMA and TMA- <i>N</i> -Oxide Analysis	33
2.2.4	Cloning and cDNA Expression	34
2.2.5	Purification of MBP-FMO3 Fusion Proteins	34
2.2.6	Determination of MBP-FMO3 Concentration	35
2.2.7	Enzyme Assays	35
2.2.8	Data Analysis	39
2.3	Results	39
2.3.1	Phenotyping and Genotyping Results	39

2.3.2	Cloning, Expression and Purification of Wild-type MBP-FMO3 and MBP-FMO3 Variants	40
2.3.3	Comparison of <i>N</i> - and <i>S</i> -Oxygenation Functional Activity of Wild-type MBP-FMO3 with MBP-FMO3 Variants	40
2.3.4	Kinetic Parameters for TMA <i>N</i> -Oxygenation by MBP-FMO3 and MBP-FMO3 Variants	41
2.3.5	Kinetic Parameters for MMI <i>S</i> -Oxygenation by MBP-FMO3 and MBP-FMO3 Variants	42
2.3.6	Stability of MBP-FMO3 and MBP-FMO3 Variants	43
2.4	Discussion	45
3	Expression, Purification, and Characterization of Human FMO5	50
3.1	Introduction and Aim of the Study	50
3.2	Materials and Methods	51
3.2.1	Reagents	51
3.2.2	Expression of MBP-hFMO5 and Optimization of the Affinity Chromatography Purification Method	51
3.2.3	Development of an Ion Exchange Chromatography Method	56
3.2.4	Characterization of Purified MBP-hFMO5	58
3.2.5	Data Analysis	60
3.3	Results	61
3.3.1	Expression and Purification of MBP-hFMO5 via Affinity Chromatography	61
3.3.2	Purification of MBP-hFMO5 via Ion Exchange Chromatography	66
3.3.3	Characterization of Purified MBP-hFMO5	70
3.4	Discussion	77
4	Crystallography Studies of Human FMO5	81
4.1	Introduction	81
4.1.1	FMO Model Structure	81
4.1.2	FMO Protein Structure, Binding Sites, and Interaction with the Membrane	83
4.1.3	Aim of the Study	84
4.2	Materials and Methods	84
4.2.1	Reagents	84
4.2.2	Cloning and Expression	84
4.2.3	MBP-hFMO5 Purification	85
4.2.4	Crystallization of MBP-hFMO5	85
4.2.5	Crystallography Studies of hFMO5 without MBP-tag	89
4.3	Results	92
4.3.1	Crystallization of MBP-hFMO5	92
4.3.2	Crystallography Studies of hFMO5 without MBP-tag	99

4.4	Discussion	105
5	pH Dependence of Human and Mouse FMO5	113
<hr/>		
5.1	Introduction	113
5.1.1	pH Dependence of FMO Isoforms	113
5.1.2	Aim of the Study	114
5.2	Materials and Methods	115
5.2.1	Reagents	115
5.2.2	Chimera-Design of hm159, mh159, hm435, and mh435	115
5.2.3	Chimera-Design of hm229, mh229, hm370, and mh370	117
5.2.4	Site-directed Mutagenesis of Human and Mouse FMO5 Variants	121
5.2.5	Expression and Purification of Human - Mouse FMO5 Chimera and Human or Mouse FMO5 and their Variants.	124
5.2.6	Determination of Protein Concentrations of FMO5 Chimera	124
5.2.7	Enzyme Assays	124
5.2.8	Data Analysis	125
5.3	Results	126
5.3.1	pH Dependence of Human and Mouse FMO5	126
5.3.2	pH Dependence of hm159, mh159, hm435, and mh435	126
5.3.3	pH Dependence of hm229, mh229, hm370, and mh370	127
5.3.4	Summary: pH Dependence of Human and Mouse FMO5 Chimeras	128
5.3.5	pH Dependence of Human and Mouse FMO5 Variants	129
5.4	Discussion	133
6	Substrate Selectivity and Screens of Potential FMO5 Substrates	137
<hr/>		
6.1	Introduction	137
6.1.1	FMO Substrates	137
6.1.2	Aim of the Study	139
6.2	Materials and Methods	140
6.2.1	Reagents	140
6.2.2	Cloning, Expression, and Purification of MBP-hFMO5	140
6.2.3	Determination of MBP-hFMO5 Concentration	141
6.2.4	Enzyme Assays	141
6.2.5	LC/MS Analysis	142
6.2.6	Development of a Photometric Activity Assay Method	143
6.2.7	Development of a Fluorimetric Activity Assay Method	144
6.2.8	Substrate Screens	145
6.3	Results	154
6.3.1	Comparison of Photometric and Fluorescent Activity Assay Methods	154

6.3.2	Substrate Screens	158
6.4	Discussion	160
7	Summary	162
<hr/>		
8	References	168
<hr/>		
9	Appendix	186
<hr/>		
9.1	Constructs	186
9.2	Buffers and Reagents	187
9.3	Equipment List	188

1 Introduction

1.1 Introduction to Flavin-containing Monooxygenases

The flavin-containing monooxygenases (FMOs) (EC 1.14.13.8) are a family of microsomal, NADPH dependent enzymes that catalyze the oxygenation of nucleophilic nitrogen-, sulfur-, phosphorus-, and other heteroatom-containing chemicals, drugs, and endogenous substrates [Cashman *et al.*, 2006; Ziegler, 1980]. They belong to the group of oxygenases. Oxygenases incorporate oxygen into their substrate and thus catalyze the most important oxidation reaction in the metabolism of xenobiotics. They are subdivided in monooxygenases and dioxygenases, depending whether one or two atoms of molecular oxygen are transferred into the substrate, respectively [Testa, 1995]. The most prominent of monooxygenases in regards of xenobiotic metabolism are the heme-coupled cytochrome P450 monooxygenases (P450s). In the early 1960s, it was believed that most, if not all NADPH dependent, heteroatom-containing compound oxidations were catalyzed by P450s. After the isolation, characterization, and purification of pig liver FMO by Ziegler and colleagues [Ziegler, 1980], it was clear that FMO could oxygenate many compounds previously thought to be exclusively oxidized by P450. It has been shown that the family of enzymes that collectively constitute mammalian FMOs contribute significantly to the oxygenation of nucleophilic xenobiotics, generally converting lipophilic heteroatom-containing compounds to polar, readily excreted, oxygenated metabolites [Cashman, 1995]. Of course, it should be recognized that FMO-mediated oxygenation is only one part of the myriad of biotransformation steps that can befall a xenobiotic, and the final disposition of a chemical will depend upon further metabolic processes, both oxidative and reductive.

Various names have been given to FMOs over the years. Initially the FMO enzyme was known as “Ziegler’s enzyme”, “dimethylaniline monooxygenase”, and “amine oxidase”. These terms were soon recognized to be a too restrictive description because at least some forms of the enzyme accept substrates as diverse as hydrazines, phosphines, boron-containing compounds, sulfides, selenides, iodide, in addition to primary, secondary, and tertiary amines. Later, the enzyme was more generally appreciated as a multi-substrate FMO [Ziegler, 1993].

In 1984 a new FMO was isolated from rabbit lung. This form possessed many properties that the well-studied pig liver FMO did not possess and it became apparent that FMO enzymes comprised a small family of enzymes [Tynes *et al.*, 1985; Williams *et al.*, 1984]. In the early 1990s three further FMO enzymes were described [Lawton *et al.*, 1993b] and today there is evidence for the existence of five forms of mammalian FMO enzymes with conserved amino acid sequences ranging between 50 % and 58 %. In addition, 6 *FMO* pseudogenes, i.e., genes that lost their ability to code for a functional protein [Vanin, 1985], have been described [Hernandez *et al.*, 2004; Hines *et al.*, 2002].

1.2 Nomenclature of FMO Enzymes

In 1994 a nomenclature was developed to provide a systematic guideline for the FMOs following the lead for the P450 enzymes [Lawton *et al.*, 1994]. The nomenclature is based on amino acid sequence comparison. To be considered a member of the mammalian FMO family, a sequence identity of 40 % or higher is required. Since other nonmammalian flavoenzymes have a lower sequence identity (e.g., the cyclohexane monooxygenase shares only 25 % amino acid sequence identity with other mammalian FMOs), they do not belong to this family. Within a subfamily, amino acid sequence identity of ≥ 80 % is required. Thus, the five human forms of FMO have 82 – 87 % sequence identity with their known orthologues in other mammals but only 50 – 58 % similarity to each other [Cashman, 2005; Phillips *et al.*, 1995]. The flavin-containing monooxygenase gene family is designated as “FMO”. Individual genes are distinguished by Arabic numbers (i.e., FMO1 through FMO5). Genes and cDNA designations are italicized while mRNA and protein designations are non-italicized [Lawton *et al.*, 1994]. Because all literature published before 1994 used several different methods naming FMO enzymes, Table 1.1 may serve as a guide to the nomenclature.

Table 1.1 Summary of mammalian flavin-containing monooxygenases.

Designation	Old name	Species	Accession number
FMO1	1A1	Rabbit	M32030
FMO1	Ziegler's enzyme	Pig	M32031
FMO1	FMO-1	Human	M64082
FMO2	1B1	Rabbit	M32029
FMO2	Lung enzyme	Rabbit	
FMO3	1D1	Rabbit	L10037
FMO3	HLFMO II	Human	M83772
FMO4	1E1	Rabbit	L10392
FMO4	FMO2	Human	Z11737
FMO5	1C1	Rabbit	L08449

Adapted from Hines *et al.* [Hines *et al.*, 1994] and Cashman *et al.* [Cashman *et al.*, manuscript in preparation].

1.3 FMO Gene Organization

It is thought that gene duplication of a common ancestral gene that took place long before the divergence of mammals led to all members of the *FMO* gene family [Phillips *et al.*, 1995]. Therefore, in all mammalian species, orthologues of each of the *FMO* forms should be found. Thus, the individual genes have remained on the same chromosomal arm, (i.e., the long arm of human chromosome 1) [Phillips *et al.*, 1995]. All *FMOs* share a similar pattern of intron/exon organization. *FMO2*, 3, and 5 contain eight coding exons (2 through 9), and the size and boundaries of these are highly conserved. They also contain at least one non-coding exon (numbered 1). In contrast, human *FMO1* and 4 contain an additional non-coding exon (numbered 0) [Dolphin *et al.*, 1997b; Ziegler, 1991].

In addition, six human *FMO* pseudogenes have been described (*FMOs* 6P, 7P, 8P, 9P, 10P and 11P) [Hernandez *et al.*, 2004; Hines *et al.*, 2002]. *FMOs* 1, 2, 3, 4, and 6 are located on the long arm of human chromosome 1, in a 220 kb cluster of region 1q23 – 25 [Hernandez *et al.*, 2004]. *FMO5* is located outside this cluster in region

1q21.1 [Gelb *et al.*, 1997; Hernandez *et al.*, 2004]. Approximately 4 Mb centromeric of the original *FMO* gene cluster is another cluster with five of the *FMO* pseudogenes [Hernandez *et al.*, 2004]. The pseudogene cluster presumably arose through a series of independent gene duplication events and not through complete duplication of the gene cluster because the nucleotide sequences of members of the human pseudogene cluster (*FMOs* 7*P*, 8*P*, 9*P*, 10*P* and 11*P*) are more similar to each other than to members of the known gene cluster (*FMOs* 1, 2, 3, 4 and 6) [Hernandez *et al.*, 2004].

1.4 Regulation

1.4.1 Regulation of FMO Gene Expression

FMO enzymes can be regulated by a number of different factors such as enzyme expression and physiological and dietary influences. FMO expression is dependent on the tissue, species, and developmental stage [Hines *et al.*, 1994; Ziegler, 1993]. These factors have been characterized in a number of animal species, such as humans [Cashman *et al.*, 2006; Zhang *et al.*, 2006], mice [Janmohamed *et al.*, 2004], rats [Lattard *et al.*, 2001; Lattard *et al.*, 2002a; Lattard *et al.*, 2003a; Lattard *et al.*, 2002b], pigs [Gasser *et al.*, 1990], and rabbits [Lawton *et al.*, 1990]. Results show that FMO expression profiles are quite distinct among different species. Therefore, studies concerning FMO in animal models (e.g., toxicology and metabolism studies on drugs) are not always easily translatable to humans. Thus, knowledge of FMO expression profiles and their regulation in small animals is essential to interpret data useful for establishing animal models correctly as well as predicting the data for use in studies of drug metabolism in humans.

1.4.2 Species-, Tissue-, Age-, and Gender-Dependence of FMO Expression

FMO1

In humans, all FMOs, with the exception of FMO1, are expressed at greater levels in adult liver and adult brain compared to fetal liver and fetal brain [Cashman *et al.*, 2006; Zhang *et al.*, 2006]. Human FMO1 is 83 % sequence identical with mouse FMO1 [Cherrington *et al.*, 1998] and 82 % sequence identical with rat FMO1. It shares the highest primary structure identity with rabbit (86 %) and pig FMO1 (88 %)

[Lawton *et al.*, 1994]. In humans, FMO1 is the most prevalent FMO in adult kidney. FMO1 expression in fetal liver, small intestine, and lung is only 10.4, 6.9, and 2.8 % of that in adult kidney, respectively [Cashman *et al.*, 2006; Zhang *et al.*, 2006]. While in adult liver FMO1 is almost non-existent (i.e., less than 1 % of that in adult kidney), other mammals, such as pigs, rabbits, rats, and mice, express FMO1 in a significant amount not only in kidney, but also in adult liver. Further, FMO1 was found in the lung of guinea pigs, hamsters, mice, and rats [Atta-Asafo-Adjei *et al.*, 1993] as well as in mouse brain [Janmohamed *et al.*, 2004].

FMO2

FMO2 is the dominant FMO form in adult human lung as well as in human heart [Nishimura *et al.*, 2006]. Also, it is the prominent FMO form expressed at high levels in lung of nonhuman primates and other mammals. However, due to a C→T transition in codon 472, it is not expressed as a full-length active enzyme in most humans [Dolphin *et al.*, 1998; Whetstine *et al.*, 2000; Yueh *et al.*, 1997]. Only a small portion of the population, mainly from African descent, has one normal allele and therefore expresses an active form of this enzyme [Krueger *et al.*, 2004]. FMO2 expression in kidney, small intestine, and adult liver is only 13.9, 2.3, and 1.8 % of that in lung, respectively [Cashman *et al.*, 2006; Zhang *et al.*, 2006]. FMO2 is found in the lung of rabbits, guinea pigs, and hamsters and in small amounts in the lung of mice [Atta-Asafo-Adjei *et al.*, 1993]. In contrast to other mammals, certain rat species only encode a non-functional protein as described for humans [Lattard *et al.*, 2002b].

FMO3

FMO3 is the major drug-metabolizing FMO form in adult human liver. It is expressed at a similar magnitude as P450 2C9 that represents around 20 % of total liver P450 [Klick *et al.*, 2007; Shimada *et al.*, 1994]. In lung, kidney, and fetal liver FMO3 is present at 4.5 %, 3.7 %, and 2.1 %, respectively, of the amount in adult liver. Small intestine and brain FMO3 constitute less than 1 % of adult liver FMO3 [Cashman *et al.*, 2006; Zhang *et al.*, 2006]. FMO3 expression is very low in fetal liver. Birth seems necessary, but not sufficient for the onset of FMO3 expression [Klick *et al.*, 2007]. During childhood, FMO3 expression increases to approximately 30 % of adult values. In contrast to mice, FMO3 expression increases further, in a gender-independent mechanism, approaching adult levels by 18 years of age. In some animals (e.g.,

mice, rats, and dogs), FMO3 expression is gender-dependent and with the exception of few species, all other mammals analyzed to date, including other primates, do not express FMO3 as the dominant adult hepatic form [Cashman, 1995; Janmohamed *et al.*, 2004]. Therefore most small animals represent poor models for human FMO3-mediated metabolism. Although there is no gender-difference in FMO3 levels in rabbits, rabbit liver contains slightly more FMO3 than human liver. Thus, rabbits do not represent good models because FMO3-contribution to human liver metabolism might be over-predicted [Cashman, 2000; Ripp *et al.*, 1999b]. One of the most common animals used in pharmacological and toxicological models to predict metabolism, toxicity, and effects in humans are rats that are about two months old and in a period of acquisition of sexual maturity. Rats only display gender dependence at a young age, but a significant gender difference is not observed in FMO3 expression in adult rats [Lattard *et al.*, 2002a] although it was reported that adult male rat liver contains slightly more FMO3 than adult female rat liver [Dannan *et al.*, 1986; Ripp *et al.*, 1999b]. Nevertheless, in rats, FMO3 levels are significantly lower than those in humans and thus metabolism in rats might under-predict the human situation. The liver of female mice and female dogs has much higher FMO3 activity than that of their male counterparts and relative FMO3 levels are comparable to those in human liver. Thus, these animals could serve as suitable models for human FMO3 activity. Nevertheless, it is important to keep in mind that both species, unlike humans, display gender specific FMO3 expression. Also, mice continue to express FMO1 in adult liver whereas the FMO1-content of adult human liver is almost non-existent [Janmohamed *et al.*, 2004].

FMO4

Compared to other FMO isoforms, FMO4 is detected in low amounts in several human tissues. It is most prevalent in adult liver and kidney, whereas fetal liver, small intestine, and lung contain about 10.9, 10.8, and 7 %, respectively, compared to FMO4 of adult liver [Cashman *et al.*, 2006; Zhang *et al.*, 2006]. In mice, FMO4 mRNA is also expressed in liver and kidney while very low amounts of FMO4 mRNA can be detected in lung and brain [Janmohamed *et al.*, 2004]. In rats, FMO4 was detected in kidney and brain [Lattard *et al.*, 2003a].

FMO5

In human as well as mouse liver, FMO5 mRNA is the most abundantly expressed FMO mRNA [Cashman *et al.*, 2006; Janmohamed *et al.*, 2004]. This is in contrast to the long held assumption that FMO3 is the major form in adult human liver. A considerable amount of FMO5 is also found in human fetal liver, small intestine, kidney, and lung (18.1 %, 12.8 %, 9.8 %, and 4 %, respectively, of the amount present in adult human liver) [Cashman *et al.*, 2006; Zhang *et al.*, 2006]. Human FMO5 is 84 % sequence identical with mouse FMO5 [Cherrington *et al.*, 1998]. In mice, FMO5 mRNA levels are also relatively prominent in male kidney (and to a lesser extent in female mouse kidney), lung, and brain [Janmohamed *et al.*, 2004]. FMO5 is also found in the liver and kidney of rabbits, rats, guinea pigs, and hamsters [Atta-Asafo-Adjei *et al.*, 1993]. Although FMO5 represents ≥ 50 % of the total FMO transcripts in adult human liver, the contribution of FMO5 enzyme functional activity has not been clearly established primarily due to a paucity of selective substrates.

1.4.3 Hormonal Regulation

The mechanisms controlling the expression of FMO have not been fully elucidated. However, the effects of hormones on FMO activity have been described in various animal models (e.g., rats [Coecke *et al.*, 1998; Dannan *et al.*, 1986; Lemoine *et al.*, 1991] and mice [Falls *et al.*, 1995; Falls *et al.*, 1997]). Female mice have a greater FMO activity than male mice. Testosterone decreases FMO1 activity and abolishes FMO3 activity in female mice and castrated male mice [Coecke *et al.*, 1998; Falls *et al.*, 1995]. Progesterone and estradiol do not seem to have an effect on FMO activity in mice [Coecke *et al.*, 1998; Falls *et al.*, 1995; Falls *et al.*, 1997].

In rats, hepatic FMO is apparently positively regulated by testosterone [Dannan *et al.*, 1986; Lemoine *et al.*, 1991] and repressed by 17β -estradiol [Coecke *et al.*, 1998; Dannan *et al.*, 1986]. Another study [Coecke *et al.*, 1998] suggested no involvement of testosterone in rat FMO, contradicting earlier reports. However, age-dependence was observed that supported the involvement of testosterone and 17β -estradiol regulation of FMO in rats [Lattard *et al.*, 2002a]. In male rat liver, FMO3 levels and functional activity increases significantly during puberty whereas FMO1 remains unchanged. However, the FMO3 levels in the liver of female rats stay stable while FMO1 undergoes an 85 % decrease as a function of age. The decrease in FMO1

might be due to an increase of 17β -estradiol during puberty [Coecke *et al.*, 1998; Dannan *et al.*, 1986; Lattard *et al.*, 2002a]. Overall, the age-dependent change results in almost no gender difference in rat hepatic FMO3 expression although a slightly higher FMO3 level in male rats than in female rats has been reported [Dannan *et al.*, 1986; Ripp *et al.*, 1999b].

Compared to liver, rat kidney displays a very different FMO expression pattern. In female and male rat kidney, FMO1 does not change with age. Levels of FMO3 mRNA increase significantly in female rat kidney. In male rat kidney FMO3 mRNA increases during puberty but decreases to the level of young rats thereafter [Lattard *et al.*, 2002a].

Other native and synthetic hormones that appear to influence FMO activity include cortisol, progesterone, and dexamethasone. Through its diurnal secretion, cortisol appears to control hepatic FMO activity in female mice [Dixit *et al.*, 1984]. Progesterone and the glucocorticoid dexamethasone increase FMO2 protein levels in rabbit lung [Lee *et al.*, 1995]. In the lung of pregnant rabbits FMO2 mRNA and protein expression correlate with the plasma peak of progesterone during mid- and late-gestation [Hines *et al.*, 1994; Lee *et al.*, 1995]. In rabbit kidney, only dexamethasone induces FMO2 protein levels and activity [Lee *et al.*, 1993; Lee *et al.*, 1995]. Rabbit liver FMO1 may also be regulated during gestation by progesterone or glucocorticoids because administration of these steroids resulted in a 4-fold enhancement of FMO1 mRNA levels [Lee *et al.*, 1995]. Up to a 20-fold variation of FMO activity has been observed in the corpora lutea of the pig during estrous [Heinze *et al.*, 1970].

Diet may also have an influence on FMO activity. In rats receiving total parenteral nutrition (TPN) with addition of choline, FMO activity was increased after 5 days [Cashman *et al.*, 2004]. The amount of FMO4 increased 1.6-fold when animals were given TPN and choline compared to rats receiving TPN alone [Cashman *et al.*, 2004].

In fish, osmoregulation was reported to play a role in FMO expression. In trout, FMO expression and activity in osmoregulatory organs like gills, kidney, and gut increase in a salinity-dependent manner [Larsen *et al.*, 2001]. When euryhaline fish were exposed to hypersaline environments, FMO was induced by trimethylamine *N*-oxide

(TMA *N*-oxide) and urea that acts as an organic osmolyte to counterbalance increases of osmotic pressure. Overall, much more work is needed to clarify the role of different hormones in the expression of FMO enzymes.

1.4.4 Transcriptional Regulation

Several transcriptional factors have been described that might influence FMO expression. In view of the developmental regulation of FMO3 and FMO1 in mice and humans, this is of importance. For example, nuclear transcription factor Y (NFY), upstream transcription factor 1 (USF1), an unidentified GC box binding element, and yin yang 1 (YY1) were found to be important for regulating *FMO3* transcription, but do not appear to have an impact on temporal or tissue-specific regulation of *FMO3* [Klick *et al.*, 2007]. A possible transcription factor that may participate in *FMO3* developmental- and tissue-specific regulation is pre-B-cell leukemia factor 2 (Pbx2), a heterodimer with an not yet identified homeodomain protein (Hox) isoform. Pbx2 appears to be widely expressed in many tissues during and after embryonic development [Selleri *et al.*, 2004]. However, Pbx2 DNA specificity and activity is dependent upon dimerization with one of the 39 human Hox isoforms that can be expressed at different times during development, in different tissues, and act as either an activator or repressor. Human *FMO3* hepatic expression is restricted to postnatal tissue [Koukouritaki *et al.*, 2002] and because it was shown that only eight of the 39 Hox isoforms, (i.e., A2, A4, A5, and B2 – B6), are expressed in human adult liver [Takahashi *et al.*, 2004], the Pbx2 partner involved in binding the *FMO3* promoter is possibly one or more of these eight Hox isoforms [Klick *et al.*, 2007].

Rabbit *FMO1* is apparently regulated by the homeodomain-containing hepatic nuclear factor HNF1 α and the orphan nuclear receptor HNF4 α [Luo *et al.*, 2001]. HNF1 α and HNF4 α might be responsible for the *FMO1* tissue-selective expression pattern because there is a good correlation between the tissue-selective expression patterns of HNF1 α , HNF4 α (i.e., expressed in liver, kidney, intestine, and stomach) [Kuo *et al.*, 1990; Sladek *et al.*, 1990] and *FMO1* (expressed in fetal liver, adult intestine, and kidney) [Luo *et al.*, 2001]. Also, it was suggested that HNF1 α and HNF4 α are likewise important in regulating human *FMO1* expression, because the regulatory elements identified for rabbit *FMO1* share high identity with human *FMO1* and, with the exception of one of the two HNF4 α sites, are also able to compete with

the rabbit sequences for specific nuclear protein binding [Klick *et al.*, 2007; Luo *et al.*, 2001]. It was reported that rabbit *FMO1* promoter activity might be negatively regulated by the YY1 transcription factor [Luo *et al.*, 2001]. However, a later study identified an upstream single-nucleotide polymorphism (SNP) (a C→A transversion) for human *FMO1* that lies within the conserved core binding sequence for the YY1 transcription factor. This SNP was shown to account for significant loss of *FMO1* promoter activity through elimination of YY1 binding. Genotype analysis showed individuals of Caucasian, African, and Hispanic descent possessed 11 %, 13 %, and 30 % frequency, respectively, leading to the proposal that this variant may account for the observed interindividual variation of *FMO1* expression. The study also showed, as has been described earlier [Thomas *et al.*, 1999], that YY1 may act as a negative as well as positive regulator for rabbit and human *FMO1*, respectively [Hines *et al.*, 2003].

1.4.5 Posttranscriptional Regulation

Posttranscriptional regulation of FMO enzymes requires additional studies. It is not known which factors affect FMO mRNA stability or transcript translation. *FMO1* was shown to be *N*-glycosylated at amino acid Asn 120 [Korsmeyer *et al.*, 1998]. This residue is well conserved suggesting that it may be important for enzyme structure and function. However, *FMO* expression in bacterial cultures showed that *N*-glycosylation is not required for functional enzyme activity. Expression of *FMO* enzymes as *N*-terminal maltose-binding fusion proteins in *E. coli* resulted in a more stable, active enzyme isolable in high purity [Brunelle *et al.*, 1997]. Coupling poly-His to the *C*-terminus of the protein also resulted in a very stable, readily purified enzyme [Lattard *et al.*, 2003b].

Nitric oxide (NO) appears to modify *FMO* posttranslationally. It was shown that NO suppresses *FMO1* activity directly and in a cGMP-independent manner by decreasing the half-life of *FMO1* mRNA rather than by decreasing its transcription. Under treatment with lipopolysaccharides and cytokines that result in conditions of NO-overproduction, mRNA levels of *FMO1* in cultured rat hepatocytes were decreased. Treatment with an NO-donor, spermine NONOate, also resulted in decreased *FMO* protein levels and functional activity [Ryu *et al.*, 2004].

1.5 Prominent FMO Polymorphisms

Although FMO1 is the major FMO form in the liver of most adult mammals, in adult humans it is more prominent in extra-hepatic drug metabolism. Some allelic variants (e.g., R502X, I303T) have been described, but most of them are rare [Furnes *et al.*, 2003; Hines *et al.*, 2003]. A relatively common variant is FMO1*6, a -9,536C→A transversion that lies within the binding sequence for the YY1 transcription factor and eliminates binding of YY1 resulting in a significant loss of *FMO1* promoter activity [Hines *et al.*, 2003].

The most common FMO2 mutation is a 1414C→T mutation that leads to a premature stop codon (Q472X). The expressed protein, designated hFMO2*2A, is truncated and non-functional. All Caucasians and Asians genotyped to date express this inactive protein. Only 26 % of individuals from African descent [Dolphin *et al.*, 1998; Whetstine *et al.*, 2000] and 5 % from Hispanic descent [Krueger *et al.*, 2004] possess at least 1 allele coding for the catalytically active full length FMO2 protein designated hFMO2*1. For the individuals carrying the hFMO2*1 allele this may have an impact on drug-metabolism and toxicity, because FMO2 is known to metabolize and preferentially bioactivate certain sulfur-containing chemicals such as substituted thioureas to reactive metabolites [Krueger *et al.*, 2002].

FMO3 represents the major drug-metabolizing FMO form in adult human liver and is responsible for the conversion of the strong neuro-olfactant TMA derived from certain foods, to its non-odorous *N*-oxide (TMA *N*-oxide). SNPs may lead to an FMO3 enzyme that is less active or inactive and therefore not capable of *N*-oxygenating TMA. The metabolic disorder in which the odorous unmetabolized TMA is excreted in body fluids is called trimethylaminuria (TMAu) and is likely the reason why FMO3 is the best-studied FMO isoform in regards to SNPs. Over 300 SNPs have been reported and deposited in the SNP database (<http://www.ncbi.nlm.nih.gov/projects/SNP/>). Many mutations have been found to decrease or even abolish FMO3 catalytic activity and lead to TMAu (e.g., E32K, A52T, N61S, N61K, M66I, P153L, I199T, R238Q, E305X, E314X, R387L, G475D, R500X, M82T, R223Q, and R492W). Most of these variants are rare and were found only in certain ethnic groups. The more common genetic variants (i.e., E158K, V257M, and E308G) are often linked to each other and can lead to decreased

catalytic activity and mild symptoms of TMAu. The polymorphic variant L360P, to date found only in individuals of African descent, is worth noting because it was found to increase FMO catalytic activity [Borbas *et al.*, 2006b]. Polymorphic variants that alter FMO3 activity may also effect an individual's drug metabolism as was shown for a number of drugs in several studies including benzydamine [Mayatepek *et al.*, 2004], ranitidine [Kang *et al.*, 2000], cimetidine [Cashman *et al.*, 1993a], tamoxifen [Krueger *et al.*, 2006; Shibutani *et al.*, 2003], and sulindac [Hisamuddin *et al.*, 2004; Hisamuddin *et al.*, 2005].

1.6 FMO Catalytic Mechanism

The catalytic steps of pig FMO1 are known in some detail and have been reported by the laboratories of Ballou [Beaty *et al.*, 1981a; Beaty *et al.*, 1981b; Jones *et al.*, 1986] and Ziegler [Poulsen *et al.*, 1979; Ziegler, 1988]. Presumably, the other FMO forms also follow a similar mechanism. The major steps in the FMO1 catalytic cycle are shown in Figure 1.1.

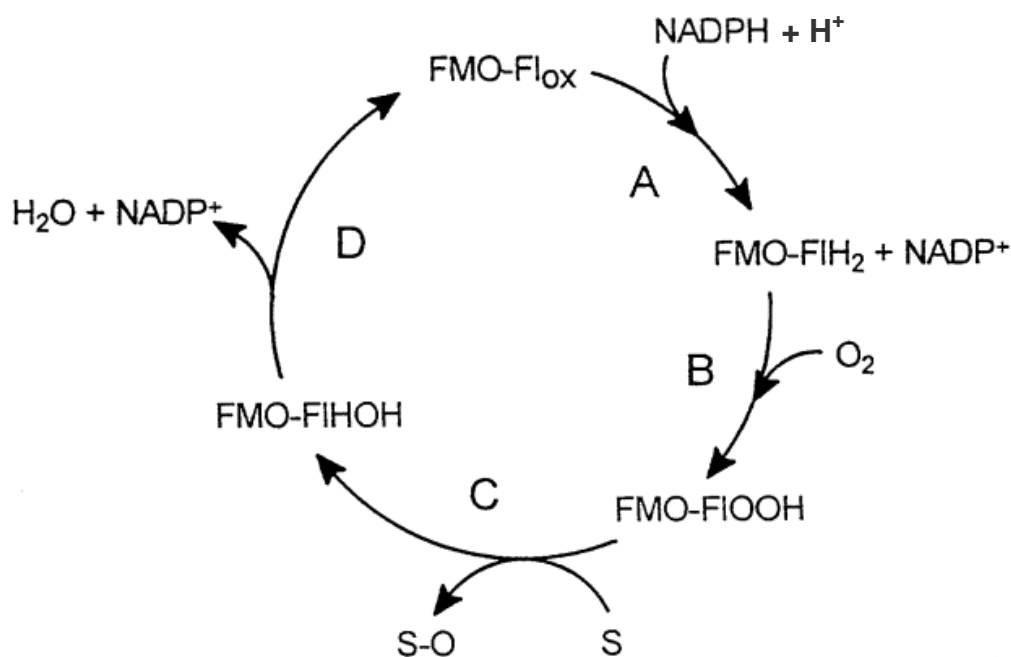


Figure 1.1 Schematic representation of the catalytic steps of pig FMO1.

S and *S-O* are the substrate and oxygenated substrate, respectively. Adapted from Cashman [Cashman, 1995].

In the first step of the enzyme reaction (step A), the fully oxidized flavoprotein (i.e., FMO-Fl_{ox}) reacts with NADPH in a fast step to give the enzyme in the reduced form

(i.e., FMO-FIH₂). The NADP⁺ produced remains at the active site of the enzyme. The reaction of the reduced enzyme with molecular oxygen (step B) is also rapid as shown in model studies, and generates the oxidant used in the enzyme reaction (i.e., the C4a-hydroperoxyflavin of FAD, FMO-FIOOH). The FMO structure stabilizes this hydroperoxyflavin intermediate and considerable spectral evidence is available that supports this stability, especially at low temperature [Beaty *et al.*, 1981a]. Its formation is remarkable because it is unusually resistant to decomposition, and it is remarkably long lived. These observations suggest that non-nucleophilic FMO active site amino acids are present to provide an appropriate lipophilic environment to preserve this highly reactive species. Unlike P450 that only forms oxidizing agents after substrate binding, the preloaded FMO active site oxidant, the C4a-hydroperoxyflavin, waits in a ready position to oxygenate substrate (S). The prediction is that FMO will oxygenate any nucleophilic heteroatom-containing substrate that can be readily oxidized by hydrogen peroxide or peracids. The exception are highly sterically hindered substrates that cannot reach the active site. Oxygenation of substrate again proceeds rapidly (step C) with attack on the terminal flavin peroxide oxygen to produce the oxygenated product (i.e., S-O) and the C4a-hydroxyflavin form of FAD (i.e., FMO-FIHOH). The next step is supposed to be rate-limiting and must involve either dehydration of the FMO-FIHOH or release of NADP⁺ (step D). Because NADP⁺ is a competitive inhibitor of the pig FMO1 cofactor NADPH, kinetic studies suggest that NADP⁺ leaves the flavoprotein last. Kinetic analysis of a good substrate such as dimethylaniline showed that the slow step in the overall catalytic cycle is not the release of oxygenated product which has important consequences for the kinetics of good substrates, because the rate-determining step occurs after product release. The mechanism of Figure 1.1 predicts that all good substrates possess similar and large V_{max} values. Solvent deuterium isotope effects on the kinetics of dimethylaniline *N*-oxygenation with pig FMO1 suggest participation of general acid catalysis [Fujimori *et al.*, 1986] that would tend to support dehydration as the rate-limiting step in the overall reaction. However, this point is controversial. NADP⁺ appears to play a "gate-keeper" role in that the FMO-FIH₂ that reacts with molecular oxygen in the absence of NADP⁺ produces significant amounts of H₂O₂ that is otherwise not normally formed [Beaty *et al.*, 1981a; Beaty *et al.*, 1981b]. FMO is generally tightly coupled and only minute amounts of H₂O₂ "leak" away from the monooxygenase under normal conditions. If this were not the case, FMO would

serve as an NADPH oxidase that would produce copious amounts of H_2O_2 in the absence of substrate, and expose the cell to the untoward effects of oxidative stress. The kinetics and proposed mechanism of FMO action is in accord with this suggestion, and such a paradigm does not violate principles of enzyme saturation (i.e., Michaelis-Menten) kinetics. However, a number of studies have shown that not all substrates precisely obey the above model. This is especially true when considering the stereoselectivity of FMO, where it appears that the nature of the substrate in some cases can have a significant effect on the velocity of the reaction.

1.7 Differences between P450 and FMO Enzymes

When discussing enzymes involved in xenobiotic metabolism and especially when discussing the group of monooxygenase enzymes, P450 enzymes come to mind immediately, being the most prominent enzyme family in this field. P450s represent typical characteristics of xenobiotic-metabolizing enzymes such as a mostly low substrate and product specificity and a susceptibility to being induced or inhibited by many xenobiotics, particularly by some of their own substrates. In general, this behavior is useful when it comes to the elimination of physiologically useless compounds, however it also leads to several problems including drug-drug interactions. Although both FMOs and P450s are able to catalyze similar and in some cases even the same biotransformation reactions, there are quite a few differences between the two monooxygenase families.

For example, the first step of the catalytic mechanism of P450 is substrate binding and only thereafter is P450 able to form oxidizing agents. In contrast, FMO pre-forms an oxygenating agent and is generally then ready to accept a substrate. The 4a-hydroperoxyflavin formed after addition of NADPH and molecular oxygen is very stable and only insignificant amounts of H_2O_2 are formed. P450 however, forms an unstable ferrous- O_2 complex that can decompose and lead to the generation of O_2^- or H_2O_2 . Another significant difference in the catalytic cycle is the apparent one- vs. two-electron nature of P450 and FMO, respectively, and a number of examples exists that show that FMO metabolites in many cases do not inactivate FMO but can leave the active site and migrate to other proteins nearby, and inhibit or covalently modify those proteins. This observation points out that the active site of FMO that generated

the highly reactive material is relatively immune to the electrophilic nature of the metabolite.

In contrast to the P450 catalyzed biotransformation reactions, FMO mediated metabolism may be utilized to the possibility of making future drugs safer through fewer adverse drug-drug interactions by utilization of alternative drug metabolism routes, i.e., FMO catalyzed drug metabolism.

Usually, the structure of the metabolite can be predicted with a great deal of certainty based on the products from treating a substrate of FMO with peracids or hydrogen peroxide. Although exceptions to this rule are known (i.e., *N*-oxide or *S*-oxide metabolites may undergo rearrangements or elimination reactions to give products that are not readily identifiable with FMO products), in general this chemical model provides an important way to predict ahead of time whether a reaction is catalyzed by FMO. Another advantage of FMO compared to P450 is that FMO enzymes are not readily inhibited or induced. Only few inhibitors of FMO enzymes (e.g., aminostilbene carboxylates) have been reported in the literature [Clement *et al.*, 1996]. Variation is mainly due to genetic differences and FMO inhibition is usually due to alternate substrate competitive inhibition. In contrast CYP is induced or inhibited by a wider variety of xenobiotics which in many cases leads to adverse drug-drug interactions. Therefore it is advantageous to develop drugs that are metabolized by FMO.

In summary FMO mediated metabolism is advantageous compared to P450 mediated reactions because firstly, FMO enzymes are not readily induced or inhibited and therefore metabolism of the compound is predictable. Secondly, the likelihood of adverse drug-drug interactions is decreased because CYP is less dominant and most drugs are metabolized by CYP and not FMO. Thus, even in combination with other drugs, medication will not lead to drug-drug interactions [Cashman, 2005].

1.8 Toxicity

In general, oxygenation of lipophilic xenobiotics by FMO enzymes leads to more polar, less toxic, and readily excreted metabolites. *N*-Oxygenation of tertiary amines, for example, leads to pharmacological inactivation. *N*-Oxygenation of (*S*)-nicotine to its *trans N*-oxide by liver FMO3 constitutes a detoxication route in animals and

humans, shunting alkaloid substrate from the metabolic pathway mediated by P450 that generate the electrophilic (S)-nicotine $\Delta^{1',5'}$ -iminium ion [Cashman *et al.*, 1992b; Damani *et al.*, 1988; Park *et al.*, 1993]. The neurotoxicant MPTP (1-methyl-4-phenyl-1,2,3,6-tetrahydropyridine) is a good substrate for FMO1 [Cashman, 1988; Cashman *et al.*, 1986] and tertiary amine *N*-oxygenation of MPTP affords a polar metabolite that represents a major route for detoxication [Chiba *et al.*, 1990; Chiba *et al.*, 1988]. In mice, MPTP *N*-oxide is the major metabolite observed in the urine of animals treated with MPTP. Presumably, monoamine oxidase-catalyzed oxidation of MPTP to the Parkinson-inducing neurotoxins MPDP⁺ (1-methyl-4-phenyl-2,3-dihydropyridinium cation) and MPP⁺ (1-methyl-4-phenylpyridinium cation) represent minor metabolic pathways. A study comparing metabolism of MPTP in rat brain with that in the brain of *Suncus murinus* (*S. murinus*) showed significant differences in MPTP metabolism. In contrast to rat brain, FMO activity was extremely low in *S. murinus* brain and therefore MPTP was able to penetrate into the brain to a higher extent. Presumably this leads to an accumulation of neurotoxic MPP⁺ in the brain of *S. murinus* [Mushiroda *et al.*, 2001]. Thus, MPTP metabolism is species dependent and the relative contribution of oxidative and reductive pathways may help determine the relative neurotoxicity of the compound [Chiba *et al.*, 1990; Chiba *et al.*, 1988; Di Monte *et al.*, 1991]. Other examples of metabolic detoxication mediated by an FMO enzyme include *N*-oxygenation of 1,1-dialkylhydrazines (some of the most toxic synthetic chemicals known to humans) or *S*-oxygenation of thiones [Prough *et al.*, 1981].

FMO enzymes also catalyze the *N*-oxygenation of a wide array of secondary and to some extent primary amines. In some cases, this leads to bioactivation of these compounds to more reactive metabolites [Cashman, 1989; Cashman *et al.*, 1992a; Cashman *et al.*, 1988; Cashman *et al.*, 1990b; Mani *et al.*, 1991; Vyas *et al.*, 1990]. For example, amphetamine and methamphetamine are oxidized by FMO3 to their *N*-hydroxylamines, but are not very efficiently *N*-oxygenated further to their oxime or nitron, respectively. Because these hydroxylamines are more cytotoxic than the parent compounds this metabolic route is considered a metabolic activation event [Cashman *et al.*, 1999b]. The *N*-desacetyl metabolite of the anti-fungal drug ketoconazole, a secondary amine, has been described to be a more potent cytotoxicant than the parent compound and is metabolized further by FMO to three

metabolites. Two of them were identified to be a secondary *N*-hydroxylamine and a nitron and may be capable of reacting with proteins or glutathione (GSH) [Rodriguez *et al.*, 1997a; Rodriguez *et al.*, 1997b; Rodriguez *et al.*, 2003; Rodriguez *et al.*, 2000; Rodriguez *et al.*, 1999]. Also, *N*-arylamines can be *N*-oxygenated by FMO to *N*-hydroxyarylamines and subsequent metabolic activation of these metabolites to reactive esters are implicated in the carcinogenic properties of arylamines in animals [Ziegler *et al.*, 1988]. An example for the bioactivation of arylamines is the *N*-oxygenation of dapsone and sulfamethoxazole by FMO3 to their arylhydroxylamines in human epidermal keratinocytes. These metabolites are further metabolized to the corresponding arylnitroso metabolites that can bind to cellular proteins [Vyas *et al.*, 2006].

The sulfur atom of sulfur-containing xenobiotics and drugs is the preferred site for FMO oxygenation, presumably because of the enhanced nucleophilicity of the heteroatom [Ziegler, 1980; Ziegler, 1988; Ziegler, 1990; Ziegler, 1993]. Thus, this class of compounds provides more examples of reactive metabolites produced by FMO. For example, thiols, thioamides, 2-mercaptoimidazoles, thiocarbamates, and thiocarbamides can be efficiently *S*-oxygenated by FMO to electrophilic reactive intermediates. These reactive metabolites do not inactivate FMO, but may covalently bind to other proteins. Thioamides are among the best substrates for FMO and sequentially form mono- and di-*S*-oxides [Hanzlik *et al.*, 1983]. Remarkably, even thiobenzamide *S,S*-dioxides do not inactivate FMO, but efficiently covalently modify other microsomal proteins, [Hanzlik, 1986] presumably by acylation of the amide carbon atom [Cashman *et al.*, 1983; Dyroff *et al.*, 1981; Hanzlik *et al.*, 1983]. Thioacetamide [Lee *et al.*, 2003], and thiobenzamide [Hanzlik *et al.*, 1983] are *S*-oxygenated to their hepatotoxic sulfines and sulfenes. The structurally related ethionamide, an agent used to treat tuberculosis, is a prodrug that is bioactivated by *S*-oxygenation in *Mycobacterium tuberculosis* [Vannelli *et al.*, 2002]. Thus, in this case the cytotoxicity is utilized to destroy the bacterium.

2-Mercaptoimidazoles are efficiently *S*-oxygenated to sulfenic acids by FMO as well as chemical oxidants that are subsequently *S*-oxygenated again to sulfinic acids [Decker *et al.*, 1992b; Miller *et al.*, 1988; Ziegler, 1980]. The intermediate sulfenic acid readily forms thiol adducts resulting in disulfides that serve as subsequent sites for disulfide exchange and net thiol oxidation and substrate regeneration [Krieter *et*

al., 1984]. Ziegler has shown that thiols that establish such a futile cycle catalyzing the oxidation of cellular thiols (i.e., GSH) and NADPH may render the cell susceptible to the toxic properties of other chemicals [Ziegler, 1993]. Thioureas are another class of nucleophilic compounds that are extremely efficiently S-oxygenated by FMO [Decker *et al.*, 1992b; Guo *et al.*, 1991; Kedderis *et al.*, 1985; Krieter *et al.*, 1984; Miller *et al.*, 1988]. Depending on the substituents on the nitrogen atom or whether the thiourea moiety is part of an aromatic ring system, sequential S-oxygenation by FMO may result in electrophilic sulfine metabolites. Sulfines are either rapidly hydrolyzed (and detoxicated) or sufficiently stable to react with biological macromolecules, and thus toxic [Decker *et al.*, 1992a; Hines *et al.*, 1994; Hui *et al.*, 1988]. In summary, the relative rate of sulfenic acid oxidation (i.e., to reactive electrophilic sulfines) compared with the propensity for attack by a thiol (or hydrolysis of the corresponding sulfines) probably determines the toxic potential of thioureido-containing chemicals and drugs. FMO2 is mainly responsible for the S-oxygenation of thioureas. Therefore, individuals carrying the catalytically active full length FMO2*1 enzyme are possibly at enhanced risk for toxicity stemming from thiourea-containing compounds [Henderson *et al.*, 2004b]. The thiourea-containing antitubercular prodrug thiacetazone acts in the same manner as the thioamide ethionamide, utilizing its toxicity against the bacterium. It was shown that human FMO1 and 3 catalyze the reaction to the reactive sulfenic acid species and subsequently to its sulfinic acid and carbodiimide that may lead to the reported hepatotoxicity [Qian *et al.*, 2006]. Nevertheless, there are also many examples of detoxication by FMO enzymes (e.g., the thioether-containing organophosphonate insecticides disulfoton and phorate) through S-oxygenation by the full-length FMO2. Again, the full length FMO2 enzyme is only expressed in certain mammals and a small portion of the human population and therefore only certain individuals may be at reduced risk of toxicity when exposed to these compounds [Henderson *et al.*, 2004a].

There are a few examples where FMO may promote the formation of electrophilic metabolites due to nonenzymatic rearrangement of enzymatically-generated tertiary amine *N*-oxides [Cashman *et al.*, 1988; Mani *et al.*, 1991]. For example, verapamil *N*-oxide is efficiently formed by FMO from the tertiary amine verapamil but the *N*-oxide is not indefinitely stable and undergoes decomposition to a hydroxylamine and 3,4-dimethoxystyrene [Cashman, 1989]. It is possible that formation of these

unanticipated metabolites of verapamil may contribute to the cardiotoxicity observed with the parent drug.

1.9 Clinical Significance

In adult humans, FMO serves a role in the metabolism of many tertiary amine-containing xenobiotics (e.g., trimethylamine [Ayesh *et al.*, 1993], (S)-nicotine [Park *et al.*, 1993], tamoxifen [Krueger *et al.*, 2006], ranitidine [Chung *et al.*, 2000], benzydamine [Mayatepek *et al.*, 2004], itopride [Mushiroda *et al.*, 2000], and olopatadine [Kajita *et al.*, 2002]) to polar, readily excreted tertiary amine *N*-oxides. Tamoxifen, a breast cancer therapeutic, is hydroxylated by P450 3A4 and subsequently sulfated producing a metabolite capable of binding to DNA whereas the *N*-oxygenation by FMO1 and to a lesser extent FMO3 represents a detoxification pathway [Krueger *et al.*, 2006; Mani *et al.*, 1991].

Heterocyclic amines metabolized by FMO enzymes include clozapine [Tugnait *et al.*, 1997], olanzapine [Ring *et al.*, 1996], and xanomeline [Ring *et al.*, 1999]. Xanomeline, a tetrahydropyridine and selective M1-muscarinic agonist, is metabolized to xanomeline *N*-oxide in kidney and liver by FMO1 and 3 although FMO3 has a much higher K_m than FMO1. The antipsychotic drug clozapine is *N*-oxygenated by FMO3 but also metabolized by P450 enzymes including P450 1A2 and 3A4 [Tugnait *et al.*, 1997]. In the brain of rats administered clozapine, clozapine *N*-oxide was found to be the major metabolite [Fang, 2000]. The structurally related antipsychotic olanzapine is metabolized by FMO to its *N*-oxide, but also by P450 enzymes 2D6 and 1A2 to its 2-hydroxymethyl and 4'-*N*-desmethyl metabolite, respectively [Ring *et al.*, 1996].

Sulphur-containing drugs metabolized by FMO enzymes include sulfides or thioethers that are *S*-oxygenated to their corresponding sulfoxides (e.g., albendazole [Molina *et al.*, 2007], cimetidine [Cashman *et al.*, 1993a], methionine [Duescher *et al.*, 1994; Ripp *et al.*, 1999a], sulindac sulfide [Hamman *et al.*, 2000; Hisamuddin *et al.*, 2004; Hisamuddin *et al.*, 2005], and tazarotenic acid [Attar *et al.*, 2003]), sulfoxides that are oxygenated to sulfones (e.g., ethionamide [Krueger *et al.*, 2005], flosequinan [Kashiyama *et al.*, 1994], *S*-methyl esonarimod [Ohmi *et al.*, 2003; Zhang *et al.*, 2007a], and other *S*-containing drugs such as methimazole and

S-methyl *N,N*-diethyldithiocarbamate [Pike *et al.*, 2001]. S-Methyl esonarimod, an active metabolite of the antirheumatic drug esonarimod, is mainly deactivated through FMO catalyzed *S*-oxygenation and P450 2C9-catalyzed 4-hydroxylation and excreted as sulfoxide and 4-hydroxy sulfoxide, respectively [Ohmi *et al.*, 2003]. FMO1 and FMO5 seem to be the major FMO forms involved in this oxygenation reaction. Studies with recombinant mouse FMO1, 3 and 5 showed that mFMO1 and mFMO5, but not mFMO3 catalyze *S*-oxygenation with a similar K_m value for both FMO1 and 5, but with a 3-fold higher V_{max} value for mFMO1 [Zhang *et al.*, 2007a]. Because recombinant FMO5 and human liver microsomes have the same K_m value and because FMO5 is the major FMO isoform in human liver, FMO5 is believed to be the major enzyme catalyzing this reaction in human liver [Ohmi *et al.*, 2003]. S-Methyl *N,N*-diethyldithiocarbamate (MeDDC), a metabolite of the alcohol deterrent disulfiram, is *S*-oxygenated in human kidney by FMO1 to MeDDC sulfine, a proposed necessary intermediate metabolite for the *in vivo* inhibition of aldehyde dehydrogenase by disulfiram, whereas in liver P450 is the major catalyst. Although the contribution of human kidney microsomal FMO1-mediated *S*-oxygenation of the S-methyl metabolite is 2- to 3-fold greater than P450, the clinical significance is not clear because the human kidney has at least 14-fold less metabolic capacity than the human liver [Pike *et al.*, 2001].

Many of these FMO substrates are stereoselectively metabolized and the stereoselectivity of the *S*-oxygenation by FMO is often distinct from that of P450 enzymes [Cashman *et al.*, 1993a; Cashman *et al.*, 1990a]. Also, for some substrates, a particular FMO could be highly stereoselective, and for other FMO orthologues the same substrate could be oxygenated with only modest stereoselectivity. Sulindac sulfide, the active metabolite of sulindac, is stereoselectively oxygenated by FMO1, 2, and 3 mainly to *R*-sulindac sulfoxide. This is consistent with the finding, that this enantiomer is enriched in human serum and urine [Hamman *et al.*, 2000]. (S)-Nicotine and cimetidine are probably the best studied *in vivo* stereoselective probes of FMO function. In the presence of (S)-nicotine, FMO2 and FMO3 exclusively form *trans*-(S)-nicotine *N*-1'-oxide [Cashman *et al.*, 1992b; Park *et al.*, 1993], whereas FMO1 as well as P450 enzymes form a mixture of *cis*- and *trans*-(S)-nicotine *N*-1'-oxide [Damani *et al.*, 1988; Park *et al.*, 1993]. Constraints on the binding channels of especially FMO2 and 3 as well as additional interactions could be at

work to produce the stereoselectivity observed. *In vitro* studies with adult human liver microsomes showed that *N*-oxygenation was solely dependent on FMO3 [Cashman *et al.*, 1992b] and exclusively resulted in *trans*-(*S*)-nicotine *N*-1'-oxide formation [Cashman *et al.*, 1992b; Cashman *et al.*, 1993b]. Thus, in adult male humans, (*S*)-nicotine is *N*-1'-oxygenated with absolute stereoselectivity to produce only *trans*-(*S*)-nicotine *N*-1'-oxide and formation of this metabolite is a selective functional marker of adult human liver FMO3. The fact that no *cis*-(*S*)-nicotine *N*-1'-oxide was observed suggests that neither extra-hepatic (i.e., kidney, intestine, or elsewhere) (*S*)-nicotine *N*-1'-oxygenation metabolism in humans (e.g., catalyzed by FMO1) nor autooxidation is occurring [Park *et al.*, 1993]. Cimetidine *S*-oxygenation represents another example in which FMO enzyme structural differences are manifested in functional differences in enzyme stereoselectivity [Cashman *et al.*, 1993a; Stevens *et al.*, 1993]. *In vitro* studies with adult human liver microsomes showed a clear stereopreference of FMO3 toward (-)-cimetidine *S*-oxide (i.e., (-):(+) 84:16) formation [Cashman *et al.*, 1995; Cashman *et al.*, 1993a] whereas FMO1 *S*-oxygenation resulted in almost equal amounts of (+)- and (-)-cimetidine *S*-oxide (i.e., (+):(-) 57:43) [Cashman *et al.*, 1993a]. In human urine samples cimetidine *S*-oxygenation stereopreference was (+):(-), 75:25. This is in relatively good agreement with the enantiomeric composition of cimetidine *S*-oxide found with human liver microsomes. The general conclusion is that stereoselective formation of cimetidine *S*-oxide (or formation of *trans*-(*S*)-nicotine *N*-1'-oxide) may be a useful bioindicator of the functional contribution of FMO3 in the human, or FMO1 and FMO3 in a particular species. In summary, knowledge of the stereoselective oxygenation of cimetidine and/or (*S*)-nicotine has been used as a diagnostic indicator of functional FMO activity in humans and animals.

1.10 Aim

The overall aim of this study was the characterization of structural and functional relations of FMO 3 and 5. The family of FMO enzymes consists of five isoforms (FMO1 – FMO5); the best studied of these are FMO1 and 3. In case of FMO1, the most prevalent FMO enzyme in adult kidney, this is due to its early purification from pig liver [Cashman *et al.*, 2006; Zhang *et al.*, 2006; Ziegler, 1980]. FMO3 is also well studied because of its association with the disorder TMAu and because of its high

expression in adult human liver. Nevertheless, there are still large gaps of knowledge in certain areas concerning FMO3. Although this isozyme has been studied to some extent and although TMAu is a disorder with a long history, many aspects need further investigation.

Self-reporting TMAu patients need to be examined because new polymorphic variants of the *FMO3* gene with unknown effect on metabolism may be found in these cases that need further investigation. Findings from these studies may provide important new information to our understanding of factors contributing to TMAu. In addition, it may help identify functionally important residues of human FMO3, and thus further our knowledge of the relationship between FMO enzyme structure and its function. Herein, a novel mutation observed from phenotyping and genotyping studies of self-reporting TMAu patients should be characterized.

For a long time FMO3 had been considered the major form in adult human liver. However, it has now been verified by more recent studies that FMO5 mRNA is the most abundantly expressed FMO mRNA in adult human liver [Cashman *et al.*, 2006; Janmohamed *et al.*, 2004]. Thus, besides FMO3, the largely understudied FMO5 is of special interest and investigations concerning its structure and function should be done within this thesis. Three main areas were of special interest: The first goal was to get an insight of the structure of FMO5. Since the underlying principle of function is structure, this will advance the knowledge of FMO5s catalytic mechanism as well as its substrate specificity and its general function. Solving the three-dimensional structure of FMO5 will in addition help advance our knowledge of FMO enzymes in general. Secondly, species differences of FMO5 and associated differences in pK_a values were of interest. This is also an important part when investigating the connection between structure and function of FMO enzymes. Although mouse and human FMO5 share a sequence identity of 84 % [Cherrington *et al.*, 1998], there are distinct differences in their pH dependent activity profile which should be compared in this study in order to identify and analyze the amino acids responsible for the difference. The third main area of interest was the development of a rapid and easy method to screen for possible FMO5 substrates. Although FMO5 is highly expressed, to date only very few substrates have been identified. Thus, the identification of new substrates will help further the knowledge of FMO5 and possibly help determine a physiological function of FMO5. In order to facilitate these studies, it was crucial to

have sufficient quantities of purified and well characterized enzyme. Thus, recombinant maltose-binding protein (MBP)-tagged FMO5 should be produced by expression in bacteria and subsequent purification and characterization.

The work will advance the knowledge of how SNPs and resulting amino acid changes may alter catalytic enzyme activity. It will provide additional knowledge regarding function of FMO enzymes through structure analysis and aid defining the substrate structure activity relationship for FMO enzymes further. Also, it will provide an understanding as to how the human family of FMOs work together to detoxicate drugs and chemicals.

2 Novel Variant of the Human FMO3 Gene Associated with Trimethylaminuria

2.1 Introduction

2.1.1 FMO3 Polymorphisms

More than 300 SNPs of FMO3 are deposited in the SNP database and/or reported elsewhere spanning the 26.92 kb human *FMO3* gene region. Only a small portion of those SNPs have been reported to be associated with interindividual differences in the expression and/or function of FMO enzymes that potentially contribute to an individual's susceptibility to toxicants and drug response. Further, *in vivo* studies of drugs like benzydamine [Mayatepek *et al.*, 2004], ranitidine [Kang *et al.*, 2000], cimetidine [Cashman *et al.*, 1993a], tamoxifen [Krueger *et al.*, 2006], and sulindac [Krueger *et al.*, 2005] showed a close connection between certain common FMO3 polymorphic variants and drug metabolism. The most prominent example of a direct causative relationship between mutations of the *FMO3* gene and disease is the disorder TMAu, which will be discussed in more detail below.

Some *FMO* gene variants appear to be restricted to certain ethnic populations. In most cases this is due to founder effects, meaning that a small number of individuals carrying only a fraction of the original population's genetic variation establishes a new population, with only a few exceptions where ethnic specific association has been demonstrated [Cashman *et al.*, 2003]. Overall, these interethnic differences contribute to the variability of FMO enzyme activity. Thus FMO-mediated drug metabolism and possible differences among ethnic groups are probably due to more common FMO3 genetic variants such as E158K, V257M, E308G and not rare polymorphic variants.

2.1.2 Diseases and Disorders Associated with FMOs

TMAu is the metabolic disorder most studied that has been associated with FMO enzymes. TMAu patients suffer from a strong body odor that is due to a decreased ability of the FMO3 enzyme to metabolize the odorous TMA to its non-odorous TMA

N-oxide. TMA is subsequently excreted in body fluids. The disorder will be discussed in more detail in section 2.1.3.

Changes in FMO functional activity have been associated with type I and II diabetes. Streptozotocin-induced diabetic (i.e., insulin deficient) rats and mice and congenital insulin resistant Ob/Ob mice were shown to express FMO with increased specific activity [Krueger *et al.*, 2005; Rouer *et al.*, 1988]. FMO3 mRNA increased dramatically in genetically modified male Db/Db mice with Type II diabetes compared with normal (Db/+) male mice, whereas female Db/Db mice showed lower mRNA-levels for FMO1, 3, 4, and 5 compared to female Db/+ mice. Thus, FMO3 is likely to be responsible for the previously reported increase in FMO activity. In diabetic rats, hepatic FMO1 activity increased and was restored after insulin-treatment [Borbás *et al.*, 2006a]. Also, hepatic FMO1 activity correlated with average blood glucose concentration. Thus, insulin appears to be involved in hepatic FMO1 regulation and blood glucose may serve as a good marker for FMO induction. In rats, FMO1 appears to be responsible for the observed increase in FMO activity.

Other diseases associated with FMOs include primary and secondary hemochromatosis [Barber *et al.*, 2000; Muckenthaler *et al.*, 2003] and hypertension [Cashman *et al.*, 2003; Cashman *et al.*, 2002; Dolan *et al.*, 2005; Larsen *et al.*, 2001], but much more work is needed in these fields.

2.1.3 Trimethylaminuria

TMAu is a metabolic disorder characterized by the inability of the affected individual to metabolize the odorous TMA to its non-odorous *N*-oxide (TMA *N*-oxide). Often individuals with TMAu have a fish-like body odor, therefore the disorder is also known as 'fish odor syndrome'.

2.1.3.1 History

Although there is no clinical report of TMAu until the 20th century, it is a disorder that can be found in numerous ancient anecdotal descriptions. The first time TMAu is mentioned was in 1000 BC in an epic of the Bharata Dynasty from India. In this story, a young woman named Satyavata is cast away from society to live a solitary life as a ferry woman because she stank like 'rotting fish'. The next entry of TMAu is from

around 1500 AD. Thai folklore of this time says that the fish odor syndrome was the major cause of suicide among concubines in the Sukhothai period. In William Shakespeare's 'The Tempest' from the 16th century the jester Trinculo speaks of the slave Caliban smelling strongly of old fish [Mitchell *et al.*, 2001]. In the early 17th century, the physician John Arbuthnot described in his 'Nature of Aliments' that certain individuals smelled rancid when their diet was mostly fish. Together with two other early papers published in the Lancet this was the first scientific description of the disorder [Cashman *et al.*, 2003]. In addition, several reports by physicians and chemists have also described patients with strong fish-like body odor, that could not be avoided just by paying more attention to cleanliness but instead seemed to decrease when omitting certain foods like fish [Mitchell *et al.*, 2001]. The first clinical report of TMAu was by Humbert and colleagues in 1970 who reported a case of a girl that had a fish-like odor. Biochemical studies showed that after a TMA challenge, the excretion of TMA increased and a subsequent biopsy of a liver sample revealed that the TMA *N*-oxidizing system was defective. Later reports showed that the disorder could affect children as well as adults and was associated with the excretion of an increased amount of TMA relative to TMA *N*-oxide [Mitchell *et al.*, 2001].

2.1.3.2 Cause and Severity

TMAu is due to excretion of TMA in body fluids such as sweat and urine. TMA is a strong neuro-olfactant that can be detected by the human nose in concentrations as low as 1 ppm. It is formed endogenously from the breakdown of precursors such as choline and carnitine or by reduction of TMA *N*-oxide through gut bacteria. Normally, over 95 % of TMA is metabolized in the liver by FMO3 to its non-odorous *N*-oxide. However, a number of genetic variants of the *FMO3* gene leads to enzymes not capable of oxygenating the odorous TMA. At least 40 genetic polymorphisms have been reported to cause TMAu, many of them associated with the incidence and severity of the disorder [Shimizu *et al.*, 2007a]. Some gene mutations lead to FMO enzymes that are still partly capable of oxygenating TMA. In these cases the individual has a mild form of TMAu and the disease is often only discovered by a choline challenge. Other genetic variants produce a totally inactive FMO3 leading to a severe form of TMAu where no or almost no TMA is *N*-oxidized. In general, an individual is recognized as not affected when more than 90 % of TMA is metabolized. When 10 – 39 % of the TMA remains unmetabolized, the disease is considered to be

mild. Individuals having over 40 % unmetabolized TMA or more than 10 mg/ml TMA in their urine are considered to be severely affected [Cashman *et al.*, 2003].

2.1.3.3 Incidence

The National Institute of Health (NIH) classifies this disease as rare, but the actual incidence is probably underreported because it is often mistaken for poor hygiene [Krueger *et al.*, 2005]. The incidence seems to be higher in females [Lambert *et al.*, 2001] and symptoms worsen for some but not all women during menstruation. Apparently, owing to a founder effect, the incidence is higher in areas that have populations derived from British, Scottish, and Irish descent like certain regions in the United States and Australia [Akerman *et al.*, 1999; Mitchell *et al.*, 2001]. Also, it has been stated that there is an elevated incidence of TMAu in tropical regions that possibly arises from the advantage of TMA as an anti-insect secretion [Mitchell *et al.*, 1997].

2.1.3.4 Clinical Manifestation

Clinically, TMAu is closely associated with several social and psychological problems no matter if adults or children are affected [Mitchell *et al.*, 2001]. Thus, it cannot simply be considered a 'social' or benign condition. The strong offensive body odor can be highly disruptive for an individual's personal life and work. Ayesh *et al.* [Ayesh *et al.*, 1993] described various psychological reactions noticed in a group of TMAu patients including shame, embarrassment, low self-esteem, and frustration. Associated social exclusion and isolation may further cause anxiety, paranoia, and depression. Also, suicidal personalities were described and it was noticed that many individuals had problems with addiction to cigarettes, alcohol, and drugs. Whether the depression that is seen in some cases is due to the social isolation or due to a dysfunctional metabolism of other endogenous substrates is not quite clear yet.

Besides the body odor it was reported that some male patients showed adverse reactions to choline loading, with fever and vomiting and that these symptoms were also observed on a number of occasions during periods of excessive malodor [Chalmers *et al.*, 2006]. McConnell *et al.* presented a boy with diagnosed TMAu whose TMA levels were associated to the seizures and behavioral disturbances he suffered from. This case suggests that not all of the psychiatric disturbances seen in

this disorder are necessarily related to a psychosocial reaction to the odor itself [McConnell *et al.*, 1997]. Another observation of this and other reports is that some individuals with TMAu are aware of their strong body odor while others remain unaware of the smell [Ayesh *et al.*, 1993].

2.1.3.5 Diagnosis

Accurate diagnosis is essential for appropriate genetic counseling and long-term management so that the affected individual can be treated as soon as possible [Chalmers *et al.*, 2006]. For diagnosis, the urinary ratios of TMA *N*-oxide to TMA should be measured. In healthy individuals the TMA *N*-oxide:TMA+TMA *N*-oxide ratio in the urine should be $\geq 95\%$. It is not always entirely satisfactory to test for TMAu if the person is on normal diet because the intake of TMA precursors may not be known. Therefore it was suggested that the urine should be investigated after a challenge dose of the TMA precursor choline [Murphy *et al.*, 2000]. In addition, genotyping the individuals and studying mutations in the *FMO3* gene that cause TMAu is also important.

2.1.3.6 Classification of TMAu

TMAu is generally divided into primary and secondary forms. The primary form is due to a dysfunction of the FMO3 enzyme that may be either a result of a mutation of the *FMO3* gene or due to hormonal or inhibitory chemical influences. The secondary form is the result of an overload of TMA precursor or TMA itself while the individual has normal or only slightly decreased FMO3 enzyme activity. Secondary TMAu may be observed in patients with chronic liver disease or in those individuals with bacterial overgrowth that results in an increased production of TMA from its dietary precursors [Cashman *et al.*, 2003; Fraser-Andrews *et al.*, 2003].

The primary form that accounts for the majority of TMAu reported cases is the genetic form. It is due to an autosomal recessively inherited gene defect that leads to FMO3 enzyme deficiency [Ayesh *et al.*, 1993; Mitchell, 1999]. Some of the polymorphic variants of FMO3 lead to enzymes that have abolished (severe TMAu) or decreased catalytic activity (mild TMAu). Combinations of common genetic polymorphisms may also lead to a mild form of TMAu [Akerman *et al.*, 1999; Cashman *et al.*, 2003; Zschocke *et al.*, 1999]. In case the disorder is present from

birth it becomes apparent as foods containing high amounts of choline or TMA *N*-oxide are introduced into the diet [Chalmers *et al.*, 2006; Mitchell *et al.*, 2001].

TMAu is further divided into various sub-forms, some of which are discussed below. The acquired form may emerge in adulthood without any genetic familial background [Cashman *et al.*, 2003; Mitchell, 1999; Mitchell *et al.*, 2001]. In several cases an incidence of hepatitis in adult life was reported that might have been responsible for the manifestation of the disorder. Possibly, viral DNA has been inserted into the genome affecting normal FMO expression [Cashman *et al.*, 2003; Mitchell *et al.*, 2001].

The transient childhood form may appear in early childhood when the child is fed a choline-containing diet. This form of TMAu is only temporary though. FMO3 is induced after birth (0 – 8 month), but is absent in fetal liver. The FMO3 expression levels increase afterwards, reaching significantly high levels at age 1 – 2 years and mature levels at age 11 – 18 years. TMAu disappears when FMO3 is fully expressed [Cashman *et al.*, 2003; Cashman *et al.*, 2002].

Another transient form of TMAu is associated with menstruation [Shimizu *et al.*, 2007a; Yamazaki *et al.*, 2004; Zhang *et al.*, 1996]. Further, it was proposed that even in otherwise healthy women, a mild form of TMAu may occur around time of menstruation that is due to a change in metabolic capacity. In those suffering from TMAu, the symptoms seem to intensify during menstruation. First observations for the decreased TMA metabolism were from self-reporting TMAu suffering patients. These were supported in studies on same individuals [Shimizu *et al.*, 2007a; Yamazaki *et al.*, 2004; Zhang *et al.*, 1996].

Another cause of TMAu may be an overload of precursors such as TMA *N*-oxide, choline, or carnitine [Zhang *et al.*, 1996]. The disorder may become apparent especially in individuals with certain FMO3 variants [Mitchell *et al.*, 2001]. Enzymatic oxidation capacity is usually not exceeded when on a normal diet [Zhang *et al.*, 1996], but it was reported that patients suffering from Huntington's disease who were treated with a daily oral dose of 8 – 20 g choline complained of a fishy odor in their urine, sweat, and breath [Growdon *et al.*, 1979]. Further, patients that suffer from impaired hepatocellular function have problems with the clearance of TMA as well as

those with bacterial overgrowth in the small intestine due to an increased TMA liberation from its precursors [Cashman *et al.*, 2003; Mitchell, 1999]. Indole-containing materials that may be formed in the gastrointestinal system after consuming Brussels sprouts are potent inhibitors of human FMO3. They decrease FMO3 activity [Cashman *et al.*, 1999a; Mitchell, 1999] and may exacerbate the TMAu condition.

The fact that TMA metabolism decreases in some but not all women at the onset of menstruation and the observation that the fishy odor is aggravated around puberty, after taking oral contraceptives, and around menopause [Zhou *et al.*, 2006] support the hypothesis that FMO activity may be modulated by hormones [Mitchell, 1996; Mitchell *et al.*, 2001; Shimizu *et al.*, 2007a] (see also chapter 1.4.3).

2.1.3.7 Treatment

Currently, there are only few ways to treat TMAu. On the one hand restriction of foods with a high content of TMA and its precursors such as TMA *N*-oxide (i.e., saltwater fish [Zhang *et al.*, 1999], cephalopods and crustaceans) and choline (eggs, liver, kidney, peas, beans, peanuts, soy products, and other legumes) is an option [Chalmers *et al.*, 2006; Mitchell, 1996]. It was reported though that dietary restriction primarily helped individuals that suffered from the mild form of TMAu. It was reported that breastfeeding infants after consumption of TMA precursors also had an effect on the baby [Mitchell, 1996]. Nevertheless, it is important not to over-restrict choline intake in young children and pregnant or nursing women because choline is crucial for the fetus' and young infant's nerve and brain development. For some individuals suffering from severe TMAu, adverse tyramine reactions have been described in the literature [Treacy *et al.*, 1998]. Therefore, individuals with a severe form of TMAu should also be careful with tyramine-containing foods such as aged cheese, red wine, meats, and yeast products [Cashman, 2002].

Also, temporary treatment with antibiotics like neomycin, metronidazole, or amoxicillin to inhibit the enterobacterial reduction of the TMA *N*-oxide in the intestine may help some patients. Antibiotics are able to decrease the production of TMA from choline to a limited extent and also slow the rate of TMA production, but antibiotics do not completely prevent formation of TMA from choline. Antibiotics should only be used in

exceptional cases and with caution. They should only be applied temporarily and as an adjunct to dietary treatment due to the risk of developing multi-antibiotic drug resistances. Temporary antibiotic treatment may be helpful if TMAu symptoms are exacerbated when the patient undergoes periods of great stress, emotional upset, exercise, or infection, or in women at the onset of menstruation, or whenever dietary restriction cannot be realized. To avoid resistance to antibiotics it is imperative to alternate the therapy of different antibiotics [Chalmers *et al.*, 2006; Mitchell *et al.*, 2001].

Treatment with charcoal or copper chlorophyllin may be effective to decrease free urinary TMA levels and increase TMA *N*-oxide levels to normal values. The effects of copper chlorophyllin appear to last longer [Yamazaki *et al.*, 2004]. Supplementation with folate is necessary because dietary choline restriction increases folate-requirements. To enhance residual hepatic FMO3 activity, addition of riboflavin (that might help stabilize FMO3 and increase its half-life) may be supplemented [Cashman *et al.*, 2003]. The use of soap with a pH value of 5.5 – 6.5 can remove traces of free TMA from the skin. At this pH odorous TMA (pK_a 9.8) is protonated and will be retained in a less volatile salt form and the salt can be washed off with water [Chalmers *et al.*, 2006; Mitchell, 1996].

2.1.4 Aim of the Study

TMAu often manifests itself in a body odor for individuals affected which is due to decreased metabolism of dietary-derived TMA. Several SNPs of the *FMO3* gene have been described and result in an enzyme with decreased or abolished functional activity for TMA *N*-oxygenation thus leading to TMAu. Herein, a novel mutation associated with TMAu that was observed from phenotyping and genotyping self-reporting individuals will be reported and characterized.

In a 33 year old woman, in addition to the common polymorphisms E158K and E308G, a SNP at position 187 (i.e., V187A) that had not been described to date and a truncation mutation E305X reported previously were observed. Examination of both biological parents showed that the biological mother carried the E158K/V187A/E308G allele, and the biological father carried the E305X allele. While it is known that E305X will abolish FMO3 function, the V187A mutation has not been

reported nor previously characterized. Aim of this study was to characterize this new and unusual variant. Thus, the V187A and the V187A/E158K variants of FMO3 should be cloned, expressed, and purified as maltose-binding fusion proteins. The triple mutant E158K/V187A/E308G reflecting the genotype of one allele of the affected individual examined was not studied because of difficulties in expression and characterization of the enzyme. The variants will be tested *in vitro* for the oxygenation of selective functional substrates for the FMO3 enzyme (i.e., 10-(*N,N*-dimethylamino pentyl)-2-trifluoromethyl)phenothiazine (5-DPT), 10-(*N,N*-dimethylamino octyl)-2-trifluoromethyl)phenothiazine (8-DPT), mercaptoimidazole (MMI), TMA, and sulindac sulfide). The thermal stability of the variant FMO3s will also be examined and compared to wild-type enzyme.

2.2 Materials and Methods

2.2.1 Reagents

Chemicals and reagents used in this study were purchased from Sigma-Aldrich Chemical Co. (St Louis, MO, USA) in appropriate purity. Buffers and other reagents were purchased from VWR Scientific, Inc. (San Diego, CA, USA). The synthesis of the phenothiazines 5-DPT and 8-DPT has been previously described [Lomri *et al.*, 1993b; Nagata *et al.*, 1990; Zhang *et al.*, 2007a] and was done by Dr. Karl Okolotowicz (HBRI, San Diego, USA).

2.2.2 Genomic DNA Preparation and PCR Amplification

Genomic DNA preparation and polymerase chain reaction (PCR) amplification had been done previously at the HBRI (San Diego, CA, USA) as described before [Zhang *et al.*, 2003]. Briefly, blood samples from individuals with self-reported TMAu symptoms were collected by their primary care physicians and sent to the HBRI laboratory for genotype analysis. All human samples were approved by the Independent Review Consultant Inc. (San Anselmo, CA, USA) institutional review board. The ethnicity of the individuals was defined by a self-report questionnaire that indicated the race of both biological parents. The individuals tested in this study were U.S. citizens from Northern European descent. Genomic DNA was prepared from whole blood using the Qiagen QIAmp Blood Kit (Valencia, CA, USA) following the manufacturer's protocol. Eight coding exons of *FMO3* and neighboring flanking

intronic regions were amplified from genomic DNA and sequenced using the primers listed in Table 2.1 and PCR conditions reported previously [Zhang *et al.*, 2003]. DNA sequences were analyzed with Sequencher Software (Gene Code Corporation, Ann Arbor, MI, USA) by procedures that could resolve heterozygotes under reliable quality-control conditions. Genbank sequence NT_004487 was used as the wild-type FMO3 reference sequence.

Table 2.1 Polymerase chain reaction and sequencing primers for coding exons of FMO3.

Exon	Length	Primer	Sequence (5'-3')
2	498 bp	forward	TCAAACCTCCTGGGCTCAAGT
		reverse	TTTCCAACCTGCTCTTGACA
3	581 bp	forward	CAGATTCAACCCACCATTGA
		reverse	TTCTTCAGCATTATGACAAGAGC
4/5	651 bp	forward	ATCTGCCAAAACCATTTGCT
		reverse	ACGAGAGTCACCCGAGTACC
6	408 bp	forward	GGGGTGCTCACCAGAATATC
		reverse	AAAAGCCAGCAGGCATATCA
7	429 bp	forward	TCCAATAATTGTCTCTGTTTTCCA
		reverse	TTCATCTTCGCAATCCATGA
8	473 bp	forward	GGAAAATTACAGGCTGGTCCT
		reverse	CATTCCAATGATGTCATTCAGG
9	475 bp	forward	GCGAGCCATTTTCTCTGTTC
		reverse	CCCCTGTCTGGGTATTGTCA

2.2.3 FMO3 Phenotyping by Urinary TMA and TMA-N-Oxide Analysis

FMO3 phenotyping by urinary TMA and TMA-N-oxide analysis had been done previously at the HBRI (San Diego, CA, USA). A selective functional method was used to characterize the FMO3 phenotype in humans by determining the amount of

TMA and TMA *N*-oxide from urine. After collection of first void morning urine sample the TMA and TMA *N*-oxide concentrations following a normal diet were determined. The urine was cooled to 4 °C with ice and acidified to pH 1 with 6 N HCl and immediately stored at -80 °C until thawing for assay. TMA and TMA *N*-oxide concentration was determined by electrospray ionization mass spectrometry with a deuterated TMA internal standard as previously described [Cashman *et al.*, 2001].

2.2.4 Cloning and cDNA Expression

The expression vector for *FMO* V187A and E158K/V187A constructs were cloned into pMAL-2c (New England BioLabs, Ipswich, MA, USA) by site directed mutagenesis methods as described previously [Brunelle *et al.*, 1997; Zhang *et al.*, 2003]. Cloning was done by Kiersten Riedler (HBRI, San Diego, CA, USA). Briefly, wild-type *FMO*3, *FMO*3 V187A, and *FMO*3 V187A/E158K were expressed as *N*-terminal maltose-binding fusion proteins (i.e., MBP-*FMO*3, MBP-*FMO*3 V187A, and MBP-*FMO*3 V187A/E158K). After transformation of *E. coli* DH1 α cells with pMAL-MBP-*FMO*3 plasmid, cells were grown at 37 °C in SOC medium to an absorbance of 0.4 - 0.5 at 600 nm and then 0.2 mM IPTG, 0.05 mM riboflavin, and 100 μ g/ml ampicillin were added and the cells were further shaken at room temperature overnight and harvested by centrifugation for 10 minutes at 6,000 *g*.

2.2.5 Purification of MBP-*FMO*3 Fusion Proteins

All of the following procedures including the purification process were carried out at 4 °C. The cell pellet was resuspended in lysis buffer as described previously [Lattard *et al.*, 2003b]. After stirring the cell suspension on ice for 30 minutes, the cells were disrupted by sonication (i.e., five 8-seconds bursts separated by periods of cooling) on a Sonics Vibracell ultrasonic processor (Sonics and Materials Inc., Newtown, CT, USA). The solution was centrifuged and the resulting supernatant was loaded onto an amylose column (New England BioLabs, Ipswich, MA). In order to obtain a higher yield of protein, the pellets were extracted a second time as described above and the resulting supernatant of the second extraction was also loaded onto the amylose column. Protein purification was carried out on a low pressure chromatography system, Biologic LP (Bio-Rad, Hercules, CA, USA). After loading the supernatants at 0.75 ml/min onto an amylose column that was equilibrated with 10 column volumes

of buffer A (i.e., 50 mM Na₂HPO₄ pH 8.4 and 0.5 % Triton[®] X-100 containing 15 µg/ml FAD) the column was washed with at least 10 column volumes of buffer A. Bound MBP-FMO3 protein was then eluted with a linear maltose gradient: 0 - 100 % 10 mM maltose in buffer A. Eluted fractions (5 ml each) were analyzed and the fractions with the highest enzyme activity were pooled and concentrated with a Centriprep centrifugal filter unit with Ultracel-30 membrane (Millipore, Billerica, MA, USA).

2.2.6 Determination of MBP-FMO3 Concentration

MBP-FMO3 and variants were quantified by SDS-PAGE and Coomassie Blue staining and compared with a bovine serum albumin (BSA) standard. Briefly, MBP-FMO3 proteins and different quantities of standard BSA (2, 1.5, 1.0, 0.5, and 0.1 µg per lane) were fractionated by electrophoresis on a 10 % polyacrylamide gel under denaturing conditions and stained with Coomassie Blue. After destaining, MBP-FMO quantification was done by densitometry analysis employing Kodak molecular imaging software (Eastman Kodak Company, Rochester, NY, USA).

2.2.7 Enzyme Assays

Oxygenation of mercaptoimidazole (MMI) was determined spectrophotometrically by measuring the rate of MMI S-oxygenation via the reaction of the oxidized product with nitro-5-thiobenzoate (TNB) to generate 5,5'-dithiobis(2-nitrobenzoate) (DTNB). The reaction is shown in Figure 2.1. The assay contained 50 mM sodium phosphate buffer, pH 8.5, 0.5 mM NADP⁺, 0.5 mM glucose-6-phosphate, 1.5 IU/ml glucose-6-phosphate dehydrogenase, 0.06 mM DTNB, 0.04 mM dithiothreitol (DTT), and depending on the variant 45 - 360 µg/ml MBP-FMO3. Reactions were initiated by the addition of 2 mM final concentration of substrate and the disappearance of the yellow color was followed spectrophotometrically at 412 nm. Kinetic parameters (i.e., V_{max} and K_m) for MBP-FMO3-mediated MMI S-oxygenation were determined by initiating the enzyme reaction with different amounts of substrate. The final substrate concentrations were 800, 400, 200, 100, 40, 10, and 1 µM for wild-type MBP-FMO3, 800, 200, 100, 40, 20, 10, 5, and 1 µM for the MBP-FMO3 V187A variant, and 200, 100, 40, 10, and 5 µM for the MBP-FMO3 V187A/E158K variant.

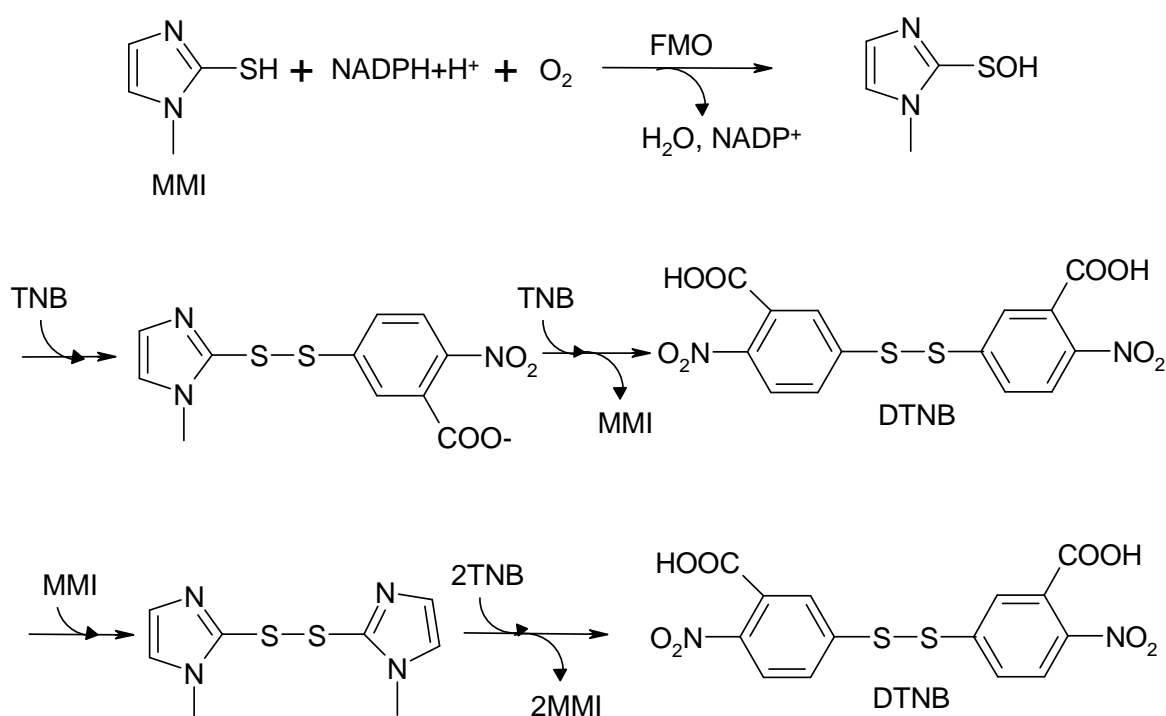


Figure 2.1 S-Oxygenation of MMI by FMO and reaction of the oxidized product with TNB to DTNB.

MMI, mercaptoimidazole; TNB, nitro-5-thiobenzoate; DTNB, 5,5'-dithiobis(2-nitrobenzoate). Adapted from Dixit *et al.* [Dixit *et al.*, 1984].

Kinetic parameters (i.e., V_{max} and K_m) for MBP-FMO3-mediated TMA *N*-oxygenation were determined by spectrophotometrically monitoring the oxidation of NADPH associated with TMA *N*-oxygenation. The assay medium contained 50 mM sodium phosphate buffer, pH 8.5, 0.5 mM diethylenetriaminepentaacetic acid (DETAPAC), 0.2 mM NADPH, and 160 - 640 μ g/ml MBP-FMO3. Incubations were initiated by the addition of different amounts of substrate and monitored at 340 nm for NADPH depletion. The final substrate concentration was 100, 40, 20, 10, and 5 μ M for wild-type MBP-FMO3 and the MBP-FMO3 V187A variant and 800, 400, 200, 100, and 40 μ M for MBP-FMO3 V187A/E158K.

N-Oxygenation of 5- and 8-DPT was determined by HPLC analysis as previously described [Lattard *et al.*, 2003b]. The reaction is shown in Figure 2.2. Both compounds are mainly *N*-oxygenated by FMO enzymes, but not *S*-oxygenated as described previously for phenothiazine drugs [Clement *et al.*, 1993] because of the electron withdrawing effect of the trifluoromethyl group inserted at the 2 position of the

phenothiazine ring system. Briefly, a standard incubation mixture of 250 μl final volume contained 50 mM potassium phosphate buffer, pH 8.4, 0.4 mM NADP^+ , 0.4 mM glucose-6-phosphate, 4 U glucose-6-phosphate dehydrogenase, 0.25 mM DETAPAC, and 40 $\mu\text{g/ml}$ wild-type MBP-FMO3 or its variant at 4 $^{\circ}\text{C}$. Incubations were initiated by the addition of substrate to a final concentration of 200 μM at 37 $^{\circ}\text{C}$. After incubation for 20 minutes shaking under aerobic conditions, enzyme reactions were stopped by the addition of 4 volumes of cold dichloromethane. About 20 mg of Na_2CO_3 was added and the incubations were mixed and centrifuged to partition metabolites and remaining substrate into the organic fraction. The organic phase was collected and evaporated under a stream of argon. Metabolites and remaining substrate were dissolved in methanol, mixed thoroughly, centrifuged and analyzed with a Hitachi HPLC system (Hitachi L-7200 autosampler and L-7100 pump interfaced to a Hitachi L-7400 UV detector). Chromatographic separation of analytes was done on an Axxi-Chrom normal phase analytical column (250 x 4.6 mm 5 μm , silica) with a mobile phase of 80 % MeOH/20 % isopropanol/0.025 % HClO_4 (v/v/v). The flow rate was 1.6 ml/min and the total run time was 10 minutes for 5-DPT and 8.5 minutes for 8-DPT. The wavelength for UV detection was set to 243 nm. The retention times for 5-DPT and 5-DPT *N*-oxide, and 8-DPT and 8-DPT *N*-oxide were 6.4, 4.6, 5.8, and 4.1 minutes, respectively.

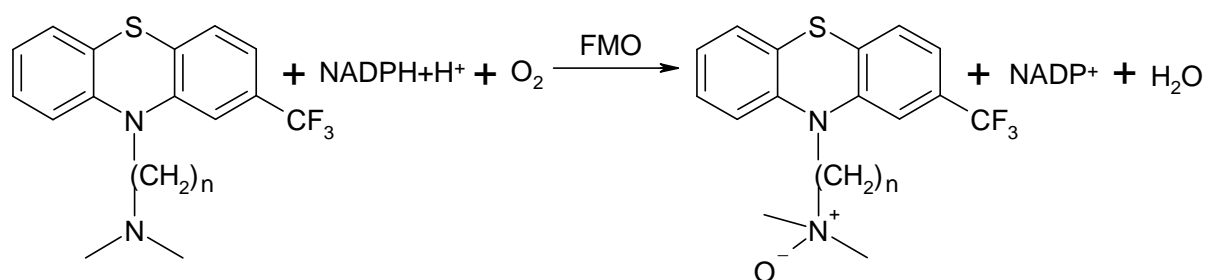


Figure 2.2 *N*-Oxygenation of 5- or 8-DPT by FMO.

n equals 5 or 8 for 5- and 8-DPT, respectively.

The *S*-oxygenation of sulindac sulfide was determined by HPLC analysis as previously described with slight modifications [Hamman *et al.*, 2000; Shimizu *et al.*, 2007b]. The reaction is shown in Figure 2.3. A standard incubation mixture of 250 μl final volume contained 50 mM potassium phosphate buffer, pH 8.4, 0.4 mM NADP^+ , 0.4 mM glucose-6-phosphate, 4 U glucose-6-phosphate dehydrogenase, 0.25 mM

DETAPAC, and 40 µg/ml wild-type MBP-FMO3 or MBP-FMO3 variant. Incubations were initiated by the addition of sulindac sulfide to a final concentration of 200 µM. After incubation for 20 minutes with continuous shaking under aerobic conditions at 37 °C, the incubation was stopped by addition of 20 µl cold 25 % phosphoric acid and 4 volumes of ethyl acetate. The incubations were mixed and centrifuged to partition metabolites and remaining substrate into the organic fraction. The organic fraction was collected and evaporated under a stream of argon. Metabolites and remaining substrate were dissolved in methanol, mixed thoroughly, centrifuged, and analyzed with a Hitachi HPLC system (Hitachi L-7200 autosampler and L-7100 pump interfaced to a Hitachi L-7400 UV detector). Chromatographic separation of analytes was performed on an Axxi-Chrom reverse phase analytical column (250 x 4.6 mm 5 µm, Supelco) with a mobile phase consisting of 70 % acetonitrile and 30 % phosphate buffer, pH 3. The flow rate was 1.0 ml/min and the total run time was 12 minutes. The wavelength for UV detection was set to 360 nm. The retention times for sulindac sulfide and sulindac S-oxide were 9.6 and 5.0 minutes, respectively.

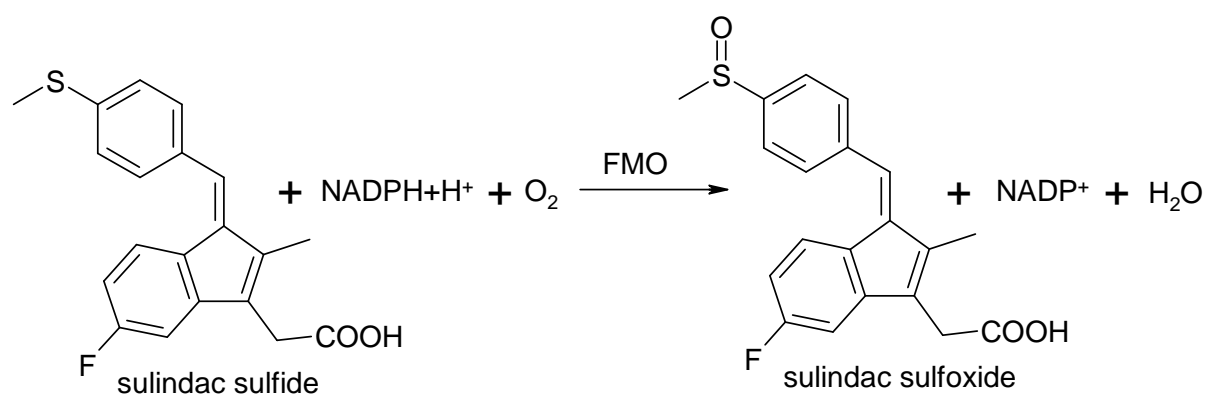


Figure 2.3 S-Oxygenation of sulindac sulfide by FMO.

To determine the thermal stability of wild-type MBP-FMO3, MBP-FMO3 V187A, and MBP-FMO3 V187A/E158K, all three FMO enzymes were incubated at 40 °C for 0, 1, and 5 minutes in the presence or absence of an NADPH-regenerating system prior to the addition of the completed reaction mixture. *N*-Oxygenation of 8-DPT was determined using the HPLC method described above. Mean velocity calculated for 0 minutes incubation at 40 °C was designated as 100 % for each recombinant enzyme, and the velocities for heat-treated enzymes were normalized accordingly.

2.2.8 Data Analysis

The kinetic parameters for TMA and MMI were determined by examining the data from incubation of at least five different substrate concentrations with MBP-FMO3 variants. Incubations were done in triplicate and for data analysis a nonlinear regression curve fit tool using a Michaelis-Menten model ($Y = (V_{max} \cdot X) / (K_m + X)$ with $V_{max} = Y_{max}$ and $K_m = X_{mid}$) in Graphpad software (Graphpad Prism, Version 3.00, San Diego, CA, USA) was utilized. Data obtained was presented as the best fit value \pm standard error. Statistical analysis was also done using Graphpad Prism software and statistical significance was judged at $P < 0.05$.

2.3 Results

2.3.1 Phenotyping and Genotyping Results

Diagnosis of TMAu included measurement of the urinary ratios of TMA *N*-oxide to TMA and genotyping of the affected individuals. A urine and blood sample from a young woman of Northern European descent with a history of unpleasant body odor was examined and the phenotype as well as genotype was determined. When determining TMA and TMA *N*-oxide levels in the urine of this sample, TMA could be detected whereas no TMA *N*-oxide was detectable indicating severely abnormal TMA metabolism.

Genotyping of the 33 year old female showed several mutations at a number of different loci. One heterozygous missense mutation identified was Val (GTT) to Ala (GCT) at position 187 in exon 4 of the *FMO3* gene. This is the first time this mutation was detected after genotyping over 100 individuals with self-reported body odor at HBRI. The V187A mutation has not been reported in the literature by any other group genotyping and phenotyping individuals for *FMO3*. The individual was also identified as heterozygous for E305X, a known mutation leading to TMAu due to abolished *FMO3* function. In addition, two common polymorphisms (i.e., E158K and E308G) were also identified and these SNPs have been shown to generally decrease *FMO3* activity when observed together [Cashman *et al.*, 2003; Dolan *et al.*, 2005; Zschocke *et al.*, 1999]. Sometimes, TMAu observed from individuals harboring the 158/308 mutations was modest and only observable under challenge situations such as

conditions of large dietary intake of TMA or TMA precursors. Other mutations were observed in the intronic regions with unknown biological significance and are not described here. Both biological parents of the young woman were also genotyped. The father was found to be heterozygous for E305X whereas the mother was heterozygous at three positions E158K/V187A/E308G. Thus, it was clear that E158K/V187A/E308G is on the same chromosome and inherited from the mother, and E305X is on the other chromosome inherited from the father. Unfortunately, the urine samples from the parents were not available for analysis.

2.3.2 Cloning, Expression and Purification of Wild-type MBP-FMO3 and MBP-FMO3 Variants

To study the effect of the novel V187A mutation on FMO3 enzyme function, and its effect on FMO3 enzyme activity in combination with the common E158K polymorphism, wild-type, V187A mutant, and V187A/E158K double-mutant *FMO3*s were expressed in *E. coli* as MBP-fusion proteins and assayed for their ability to catalyze the *N*- and *S*-oxygenation of various typical FMO substrates. When expressing the protein, we observed that the expression of both mutants (i.e., MBP-FMO3 V187A and MBP-FMO3 V187A/E158K) was less efficient than that of wild-type MBP-FMO3, yielding only about 20 % of the wild-type protein expressed. Due to the significant decrease in expression and enzyme activity for both, V187A/E158K and E158K/E308G, the triple mutant E158K/V187A/E308G reflecting the genotype of one allele of the affected individual examined was not studied because of the difficulty in expression and characterization of the enzyme.

2.3.3 Comparison of *N*- and *S*-Oxygenation Functional Activity of Wild-type MBP-FMO3 with MBP-FMO3 Variants

To compare the *N*- and *S*-oxygenation of wild-type MBP-FMO3 with MBP-FMO3 V187A and MBP-FMO3 V187A/E158K, selective functional substrates (i.e., 5- and 8-DPT) were used to examine *N*-oxygenation and sulindac sulfide was used as substrate to investigate differences in *S*-oxygenation. The results (Figure 2.1) showed that wild-type MBP-FMO3 had the highest *N*-oxygenation activity followed by MBP-FMO3 V187A with a specific activity of 69 % of wild-type *N*-oxygenation activity for 5- and 8-DPT. MBP-FMO3 V187A/E158K had the lowest specific activity with only

15 and 17 % of wild-type activity for 5- and 8-DPT, respectively. MBP-FMO3 V187A had an S-oxygenation activity of 102 % for sulindac sulfide compared to wild-type MBP-FMO3. For MBP-FMO3 V187A/E158K the S-oxygenation was decreased to only 31 % of wild-type values for sulindac sulfide S-oxygenation.

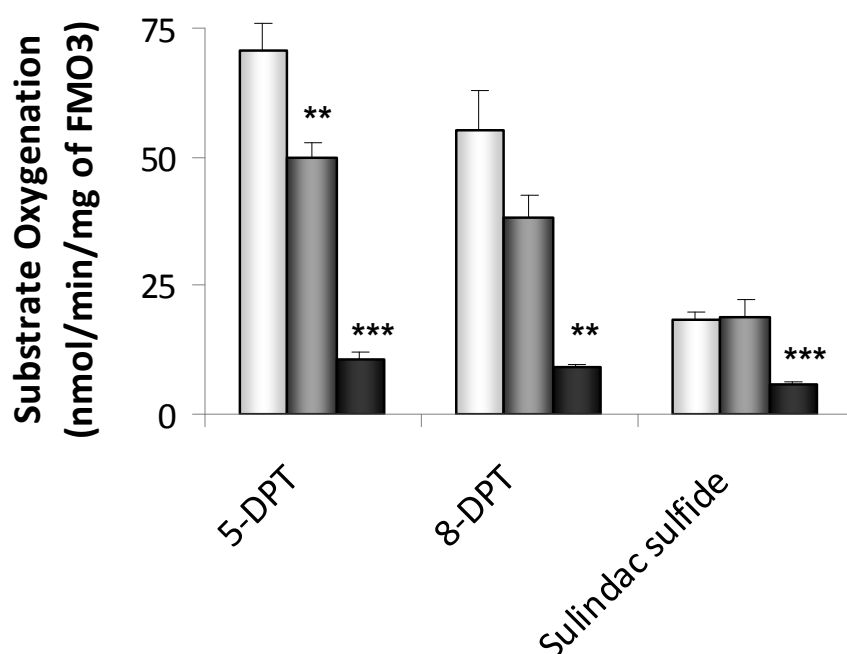


Figure 2.1 Specific activity for N-oxygenation of 5-DPT and 8-DPT and S-oxygenation of sulindac sulfide by wild-type MBP-FMO3 (white bars), MBP-FMO3 V187A (grey bars), and MBP-FMO3 V187A/E158K (black bars) in nmol/min/mg of FMO3 enzyme.

Statistically significant differences between wild-type MBP-FMO3 and MBP-FMO3 V187A or wild-type MBP-FMO3 and MBP-FMO3 V187A/E158K are identified with * for $P < 0.05$, ** for $P < 0.01$, and *** for $P < 0.001$.

2.3.4 Kinetic Parameters for TMA N-Oxygenation by MBP-FMO3 and MBP-FMO3 Variants

To determine the kinetic parameters for TMA N-oxygenation by MBP-FMO3 V187A and MBP-FMO3 V187A/E158K, the enzymes were incubated with different concentrations of TMA. The single mutant V187A had a similar V_{max} and K_m value as the wild-type enzyme. However, the double mutant MBP-FMO3 V187A/E158K had a much lower V_{max} value and a K_m that was 25-fold greater than that of MBP-FMO3

V187A or wild-type MBP-FMO3, causing a 65-fold decrease in catalytic efficiency for TMA (Table 2.2).

Table 2.2 *N*-Oxygenation of trimethylamine (TMA) by wild-type MBP-FMO3, MBP-FMO3 V187A, and MBP-FMO3 V187A/E158K.

	WT FMO3	FMO3 V187A	FMO3 V187A/E158K
K_m (μM)	15.3 \pm 5.1	17.5 \pm 5.3	430 \pm 150
V_{max} ($\text{nmol min}^{-1} \text{mg}^{-1}$)	11.9 \pm 1.3	19.3 \pm 2.0	6.3 \pm 1.1
V_{max}/K_m ($10^{-3} \text{min}^{-1} \text{mg}^{-1}$)	0.8 \pm 0.2	1.1 \pm 0.2	0.02 \pm 0.01

Data are best fit values \pm standard error. WT MBP-FMO3 data was calculated from one or two assays from two separate enzyme preparations. Data of MBP-FMO3 V187A was calculated from four assays from pooled enzyme of three enzyme preparations. MBP-FMO3 V187A/E158K data was calculated from two assays from pooled enzyme of four enzyme preparations.

2.3.5 Kinetic Parameters for MMI S-Oxygenation by MBP-FMO3 and MBP-FMO3 Variants

To determine the kinetic parameters for MMI S-oxygenation by MBP-FMO3 V187A and MBP-FMO3 V187A/E158K, the enzyme was incubated with different concentrations of MMI. All three enzymes had similar K_m values. The single mutant V187A also had a similar V_{max} value as the wild-type enzyme, but the V_{max} value of the double mutant MBP-FMO3 V187A/E158K was only 24 % of that of the wild-type enzyme (Table 2.3).

Table 2.3 S-Oxygenation of mercaptoimidazole (MMI) by wild-type MBP-FMO3, MBP-FMO3 V187A, and FMO3 V187A/E158K.

	WT FMO3	FMO3 V187A	FMO3 V187A/E158K
K_m (μM)	12.7 \pm 2.0	9.7 \pm 1.9	11.7 \pm 1.7
V_{max} ($\text{nmol min}^{-1} \text{mg}^{-1}$)	27.8 \pm 0.9	30.3 \pm 1.4	6.8 \pm 0.2
V_{max}/K_m ($10^{-3} \text{min}^{-1} \text{mg}^{-1}$)	2.2 \pm 0.3	3.1 \pm 0.5	0.6 \pm 0.1

Data are best fit values \pm standard error. WT MBP-FMO3 data was calculated from two enzyme preparations. Data of MBP-FMO3 V187A was calculated from two assays from pooled enzyme of three enzyme preparations. MBP-FMO3 V187A/E158K data was calculated from pooled enzyme of four enzyme preparations.

2.3.6 Stability of MBP-FMO3 and MBP-FMO3 Variants

The *N*-oxygenation of 5-DPT was determined by HPLC analysis as described under enzyme assays after incubation of the three FMO enzymes at 40 °C for 0, 1, 2, and 5 minutes in the presence or absence of an NADPH-regenerating system. In Figure 2.2 only wild-type MBP-FMO3 and MBP-FMO3 V187A are shown, because the functional activity of MBP-FMO3 V187A/E158K was non-detectable after incubation at 40 °C regardless of the presence or absence of a n NADPH regeneration system.

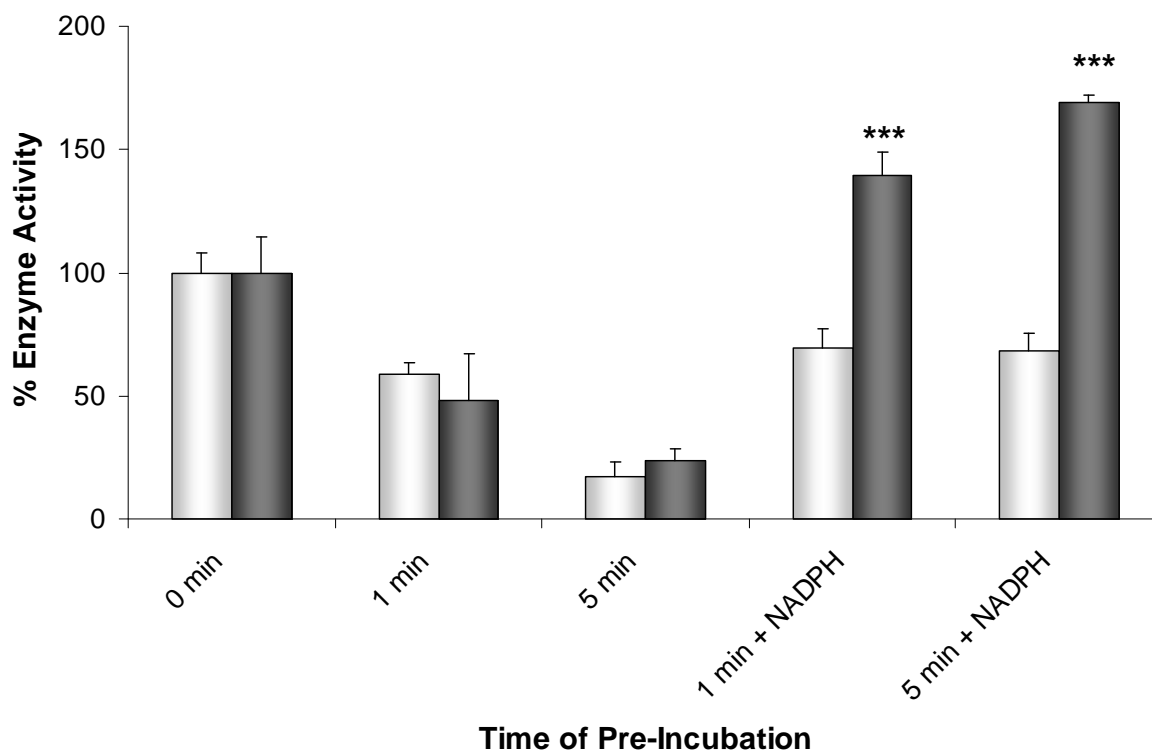


Figure 2.2 *N*-Oxygenation of 5-DPT by wild-type MBP-FMO3 (white bars) and MBP-FMO3 V187A (hatched bars) after incubation at 40 °C for 1 and 5 minutes with or without cofactor added expressed as % remaining activity.

The 0 minutes time point is set 100 % and equals 72 and 19 nmol/min/mg of FMO3 for wild-type MBP-FMO3 and MBP-FMO3 V187A, respectively. Statistically significant differences between wild-type MBP-FMO3 and MBP-FMO3 V187A are identified with * for $P < 0.05$, ** for $P < 0.01$, and *** for $P < 0.001$.

While no significant difference between the relative loss of activity for the wild-type enzyme compared to MBP-FMO3 V187A was observed after pre-incubation at 40 °C, a distinct difference was notable when both enzymes were pre-incubated at elevated temperature in the presence of NADPH for 1 and 5 minutes (Figure 2.2, $P < 0.001$). About 70 % of the wild-type MBP-FMO3 activity was retained whereas the enzyme activity of MBP-FMO3 V187A increased to 140 and 170 % of its original activity after 1 and 5 minutes preincubation with NADPH, respectively.

2.4 Discussion

Comprehensive biochemical characterization of recombinant variant FMO3 enzymes based on data from genotype and phenotype analysis of individuals with self-reported symptoms of TMAu can potentially reveal important new information about structure and function of human FMO3 [Akerman *et al.*, 1999; Cashman, 2002; Cashman *et al.*, 2002; Dolphin *et al.*, 1997a; Shimizu *et al.*, 2007b; Treacy *et al.*, 1998; Yeung *et al.*, 2007]. Findings from the studies herein provide important new information to our understanding of factors contributing to the primary genetic form of TMAu, and identify a functionally important residue of human FMO3. For the samples examined from the 33 year old woman, the novel mutation V187A in combination with the two common polymorphisms, E158K and E308G, were causative for decreased TMA metabolism and the resultant severe TMAu was confirmed by phenotyping studies.

Despite the subtlety of the V187A mutation, in combination with the E158K and E308G polymorphisms, a major impact on FMO3 enzyme functional activity could be observed that led to an enzyme with significantly decreased activity. To confirm this, not only the FMO3 V187A mutant enzyme, but also the double mutant, FMO3 V187A/E158K were expressed and purified and the enzyme function of both enzymes was characterized and compared with wild-type FMO3 using selective functional substrates. As shown in Figure 2.1, FMO3 enzyme activity observed from wild-type MBP-FMO3 confirmed that all substrates examined were efficiently oxygenated by human FMO3. The V187A mutation decreased the catalytic efficiency of the enzyme for 5-DPT and 8-DPT, and the double mutant V187A/E158K further decreased enzyme activity significantly for all substrates tested. Kinetic parameters for TMA *N*-oxygenation by MBP-FMO3 V187A and MBP-FMO3 V187A/E158K (Table 2.2) showed that although V_{max}/K_m for MBP-FMO3 V187A did not differ from wild-type MBP-FMO3, the V_{max}/K_m for MBP-FMO3 V187A/E158K was significantly decreased (65-fold). The kinetic parameters of MMI *S*-oxygenation by FMO3 (Table 2.3) showed similar V_{max}/K_m values for wild-type MBP-FMO3 and MBP-FMO3 V187A whereas the V_{max}/K_m for V187A/E158K for MMI *S*-oxygenation was about 4-fold lower than that of wild-type MBP-FMO3.

It has been reported previously that mutations that did not have a significant impact on specific activity of FMO3 by themselves decrease its oxygenation activity significantly in combination with other SNPs [Akerman *et al.*, 1999; Cashman *et al.*, 2003; Zschocke *et al.*, 1999]. Similarly, the effect of the V187A mutation on FMO3 functional activity is not very distinct, but in combination with the common mutation E158K the enzymes oxygenation activity is drastically decreased for all substrates tested.

As shown in 2.3 A, position V187 is a highly conserved residue within the *FMO* gene family (i.e., *FMO1* to 5) and across species (i.e., chimpanzee, rhesus monkey, dog, cattle, rabbit, chicken, rat, and mouse). From the primary sequence, the mutation is immediately upstream of the essential FMO3 NADPH binding domain (GXGXXG) (Figure 2.3). According to the human FMO3 homology structure model we developed based on four related proteins [Borbas *et al.*, 2006b], the residue V187 resides at the beginning part of a β -sheet leading to the NADPH binding domain. The residue is also conserved in FMO from *Schizosaccharomyces pombe* and *Methylophaga sp.* strain SK1, two FMO related enzymes with crystal structures recently solved [Alfieri *et al.*, 2008; Eswaramoorthy *et al.*, 2006], and phenylacetone monooxygenase from *Thermobifida fusca*, the first Baeyer-Villiger monooxygenase crystallized [Malito *et al.*, 2004] (Figure 2.3 B). Based on the crystal structure of these related enzymes, the hypothesis is that the Val resides in the second Rossmann fold involved in NADP⁺/NADPH binding. From the structure of *Methylophaga* FMO with NADP⁺, the Val side chain does not directly interact with NADP⁺. We hypothesize that the mutant amino acid of FMO3 V187A interferes with NADPH and NADP⁺ binding indirectly through affecting the Rossmann fold conformation. Alternatively, it is possible that the enzyme adopts large conformational changes during catalytic processes to accommodate substrate binding and hydroperoxyflavin formation [Alfieri *et al.*, 2008]. However, no crystal structure is available yet to illustrate those conformations. During such putative conformational changes, the Val could directly interact with NADPH and/or NADP⁺ binding, and therefore the V187A can possibly have direct interference with NADPH and/or NADP⁺ binding as well. As expected, the data from heat treatment (Figure 2.2) showed that wild-type MBP-FMO3 is not stable under elevated temperature when incubated in the absence of NADPH. Interestingly, a significantly higher activity was observed after pre-incubation of the V187A mutant

2 Novel Variant of the Human FMO3 Gene Associated with Trimethylaminuria

A

			187	NADPH-binding motiv:GXGXXG
			↓	
gi_6166183	FMO3_HUMAN	(179)	PGVFNGKRV	LVVGLGNSGCDIA
gi_57114053	FMO3_CHIMPANZEE	(179)	PGVFNGKRV	LVVGLGNSGCDIA
gi_74136341	FMO3_RHESUS MONKEY	(179)	PGVFKGKRV	LVVGLGNSGCDIA
gi_50978720	FMO3_DOG	(179)	PGIFKGKRV	LVI GLGNSGCDIA
gi_74355026	FMO3_CATTLE	(179)	PGIFKGKRV	LVI GLGNSGCDIA
gi_544325	FMO3_RABBIT	(179)	PGIFKGKRV	LVI GLGNSGCDIA
gi_45383027	FMO3_CHICKEN	(179)	PEKFRGKRV	LVVGLGNSGCDIA
gi_148539991	FMO3_RAT	(179)	PGTWKGKRV	LVI GLGNSGCDIA
gi_2494585	FMO3_MOUSE	(179)	PGIWKGKRV	LVI GLGNSGCDIA
gi_399505	FMO1_HUMAN	(179)	PDIFKDKRV	LVI GMGNSGTDIA
gi_6225373	FMO2_HUMAN	(179)	PDGFEGKRI	LVI GMGNSGSDIA
gi_399506	FMO4_HUMAN	(179)	PEGFQGKRV	LVI GLGNTGGDIA
gi_1346021	FMO5_HUMAN	(180)	PEGFTGKRV	II IGI GNSGGLA

B

			187	NADPH-binding motiv:GXGXXG
			↓	
gi_6166183	HUMAN FMO3	(179)	PGVFNGKRV	LVVGLGNSGCDIA
gi_185177618	BACTERIAL FMO	(197)	ALEFKDKTV	LLVVGSSYSAEDIG
gi_109158094	YEAST FMO	(207)	PELFGESV	LVVGGASSANDLV
gi_123629491	PAMO	(181)	PVDFSGQRV	GVIGTGSSGIQVS

Bacterial FMO, *Methylophaga* sp.; yeast FMO, *Schizosaccharomyces pombe*; PAMO, Phenylacetone monooxygenase (Baeyer-Villiger monooxygenase)

Figure 2.3 A Alignment of amino acids 179 to 200 for various FMOs.

V187 is highly conserved in FMO family members (FMO1, 3, 4, and 5) and across species lines. Amino acids adjacent to V187 including the nearby NADPH-binding domain (GxGxxG). Human FMO family members (FMO1 – 5) and FMO3 from different species including chimpanzee, rhesus monkey, dog, cattle, rabbit, chicken, rat, and mouse, are aligned based on homology. The GenBank accession number for each gene is indicated. The NADPH binding domain (GxGxxG) located downstream of V187 is marked. The V187 residue is conserved in all FMO genes listed except for human FMO2.

B Alignment of FMO3 amino acids 179 to 200 with the bacterial FMO from *Methylophaga* sp., a yeast FMO from *Schizosaccharomyces pombe* as well as a Baeyer-Villiger monooxygenase, PAMO (Phenylacetone monooxygenase).

V187 is highly conserved in all aligned flavoprotein monooxygenases. The GenBank accession number for each gene is indicated. The NADPH binding domain (GxGxxG) located downstream of V187 is marked.

enzyme with NADPH at 40 °C. This also points to a decreased or slower interaction with the enzyme's cofactor. Based on the literature, the departure of NADP⁺ is proposed to be the rate-limiting step in the catalytic cycle of FMO enzymes [Beaty *et al.*, 1981a; Beaty *et al.*, 1981b; Jones *et al.*, 1986; Poulsen *et al.*, 1979; Ziegler, 1988]. It is possible that the V187A mutation interferes with NADPH binding and the enzyme binds the NADPH less efficiently. To verify the possibility that wild-type FMO3 and FMO3 V187A kinetics differ from each other the effect of NADP⁺ on the selective functional activity of both enzymes was examined. NADP⁺ has been reported in the literature to be a non-competitive inhibitor of FMO1 against the xenobiotic substrate and a competitive inhibitor of NADPH binding to FMO1 [Beaty *et al.*, 1981b; Poulsen *et al.*, 1979]. The effect of NADP⁺ on the selective functional activity of wild-type MBP-FMO3 and MBP-FMO3 V187A was examined. For MBP-FMO3 V187A, increasing concentrations of NADP⁺ not only led to a decrease in V_{max} , but also resulted in a significant decrease in K_m (data not shown), suggesting that this variant follows an un-competitive model rather than a non-competitive model as proposed for pig-liver FMO1. Unfortunately, the photometric assay readouts in the presence of NADP⁺ reduced the range of assay detection limit and a conclusion of whether the inhibition mechanism is significantly different for the V187A variant compared to wild-type FMO3 cannot be reliably made. Alternative stopped-flow kinetic analysis will be necessary to clarify this issue. Thus, NADP⁺ could not be confirmed as a non-competitive inhibitor of MMI S-oxygenation in the presence of wild-type FMO3. Characterization of the V187A mutant in this report may prompt additional studies to test the hypothesis of cofactor interaction once additional FMO3 structural information becomes available and stopped-flow kinetic studies are performed.

It is also notable that enzyme expression for the recombinant protein is significantly lower for the V187A containing variants, suggesting that protein folding may not be as efficient as the wild-type enzyme. Whether this is occurring in the *in vivo* situation and results in lower overall FMO3 protein concentration in the adult human liver of affected individuals remains to be determined.

It has been reported previously that patients carrying heterozygotic FMO3 mutations show the TMAu phenotype, [Fujieda *et al.*, 2003; Zhang *et al.*, 2003; Zschocke *et al.*, 1999]. The possibility that other mutations in intronic regions of the allele that encode

for the functional enzyme can affect the enzyme expression level cannot be excluded. However, in the presence of different detergents formation of stable and catalytically active oligomeric forms of purified recombinant human FMO3 was observed (chapter 3) and similar observations were reported earlier [Ziegler *et al.*, 1972]. Whether FMO3 mutants can interfere with self oligomer-formation and/or hetero oligomer formation with wild-type enzymes and hence lead to lower overall enzyme activity is not known. The characterization of these effects in the *in vivo* setting that may affect oligomerization of FMO3 expressed from different alleles remains to be investigated.

In summary, a novel *FMO3* gene mutation associated with TMAu was recombinantly expressed and proved to influence substrate oxygenation characteristics. This novel mutation of human *FMO3*, V187A, in combination with the common polymorphism E158K leads to an enzyme that has less than 3 % TMA *N*-oxygenating activity compared with wild-type FMO3. Generally, the common polymorphisms E158K and E308G alter FMO3 enzyme activity only slightly [Cashman *et al.*, 2000], but often, if the two polymorphisms occur together, they can lead to an FMO3 enzyme with decreased activity [Cashman *et al.*, 2000; Cashman *et al.*, 2003; Dolan *et al.*, 2005; Zschocke *et al.*, 1999] and this has been reflected in *in vivo* functional activity leading to elevated unmetabolized TMA [Lambert *et al.*, 2001; Zschocke *et al.*, 1999]. Similarly, the novel V187A mutation in conjunction with the common polymorphisms E158K and E308G significantly impairs FMO3 resulting in an enzyme with drastically decreased function that manifests itself in severe TMAu.

3 Expression, Purification, and Characterization of Human FMO5

3.1 Introduction and Aim of the Study

FMOs are, after cytochromes P450, the most important monooxygenase system in humans and are involved in metabolism of many xenobiotics. Nevertheless, there is still a need to further the knowledge of this enzyme family, especially of to date neglected but possibly important isoforms such as FMO5.

In order to study structure and function of FMO5, the protein needs to be expressed and purified successfully. It is further important to characterize the purified FMO5. Detailed characterization becomes indispensable when attempting crystallography studies (chapter 4). The protein has to fulfill several requirements including sufficient purity and monodispersity. Also, it has to be functionally active and stable over a reasonable time period.

For future characterization studies of FMO5 the enzyme should be expressed as *N*-terminal maltose-binding fusion protein in *E. coli* (i.e., MBP-FMO5), solubilized from the bacterial membrane, and purified. The MBP-fusion construct has proven to be successful in expression of FMO enzymes yielding stable and highly active enzyme at greater purity than was readily possible before [Brunelle *et al.*, 1997]. Solubilization studies should be done to determine a suitable detergent for extraction of FMO5 from cells and subsequent purification utilizing different methods (i.e., affinity chromatography, ion exchange chromatography) to obtain highly pure FMO5. Further, the purified enzyme should be analyzed in various ways. Firstly, the expressed and purified recombinant produced MBP-tagged hFMO5 should be compared to commercially available hFMO5 (BD Gentest Supersomes, BD Biosciences, San Jose, CA, USA) in order to show that MBP-FMO5 may be used instead of commercially available FMO5 for kinetic and structural studies. Secondly, stability, oligomerization state as well as monodispersity of the purified FMO5 should be examined.

3.2 Materials and Methods

3.2.1 Reagents

Chemicals and reagents used in this study were purchased from Sigma-Aldrich Chemical Co. (St Louis, MO, USA) in appropriate purity. Buffers and other reagents were purchased from VWR Scientific, Inc. (San Diego, CA, USA). The synthesis of the phenothiazine 8-DPT has been previously described [Lomri *et al.*, 1993b; Nagata *et al.*, 1990; Zhang *et al.*, 2007a] and was done by Dr. Karl Okolotowicz (HBRI, San Diego, USA). Detergents were purchased from Anatrace (Maumee, OH, USA). MBP column material was purchased from New England BioLabs (Ipswich, MA, USA). Fast performance liquid chromatography (FPLC) columns were purchased from GE Healthcare (Uppsala, Sweden). Baculovirus-insect cell expressed FMO5 was purchased from BD Biosciences (BD Gentest Supersomes, BD Biosciences, San Jose, CA, USA).

3.2.2 Expression of MBP-hFMO5 and Optimization of the Affinity Chromatography Purification Method

3.2.2.1 Cloning and Expression

Human FMO5 was expressed as *N*-terminal maltose-binding fusion protein (MBP-FMO5). As described previously for mouse FMOs [Zhang *et al.*, 2007a], the hFMO5 gene was amplified at HBRI (San Diego, CA, USA) via reverse transcription (RT-) PCR from RNA using the following primers: 5'-hFMO5 GATCTCTAGAATGACTAAGAAAAGAATTGCTGTGA (XbaI site underlined) and 3'-FMO5 GATCCCTGCAGCCAATGAAAAACAGGGCAGT (PstI site underlined). The hFMO5 gene was then subcloned into the expression vector pMAL-c2 (New England BioLabs, Ipswich, MA, USA) through the corresponding cloning sites XbaI and PstI. The construct is shown in Figure 3.1.

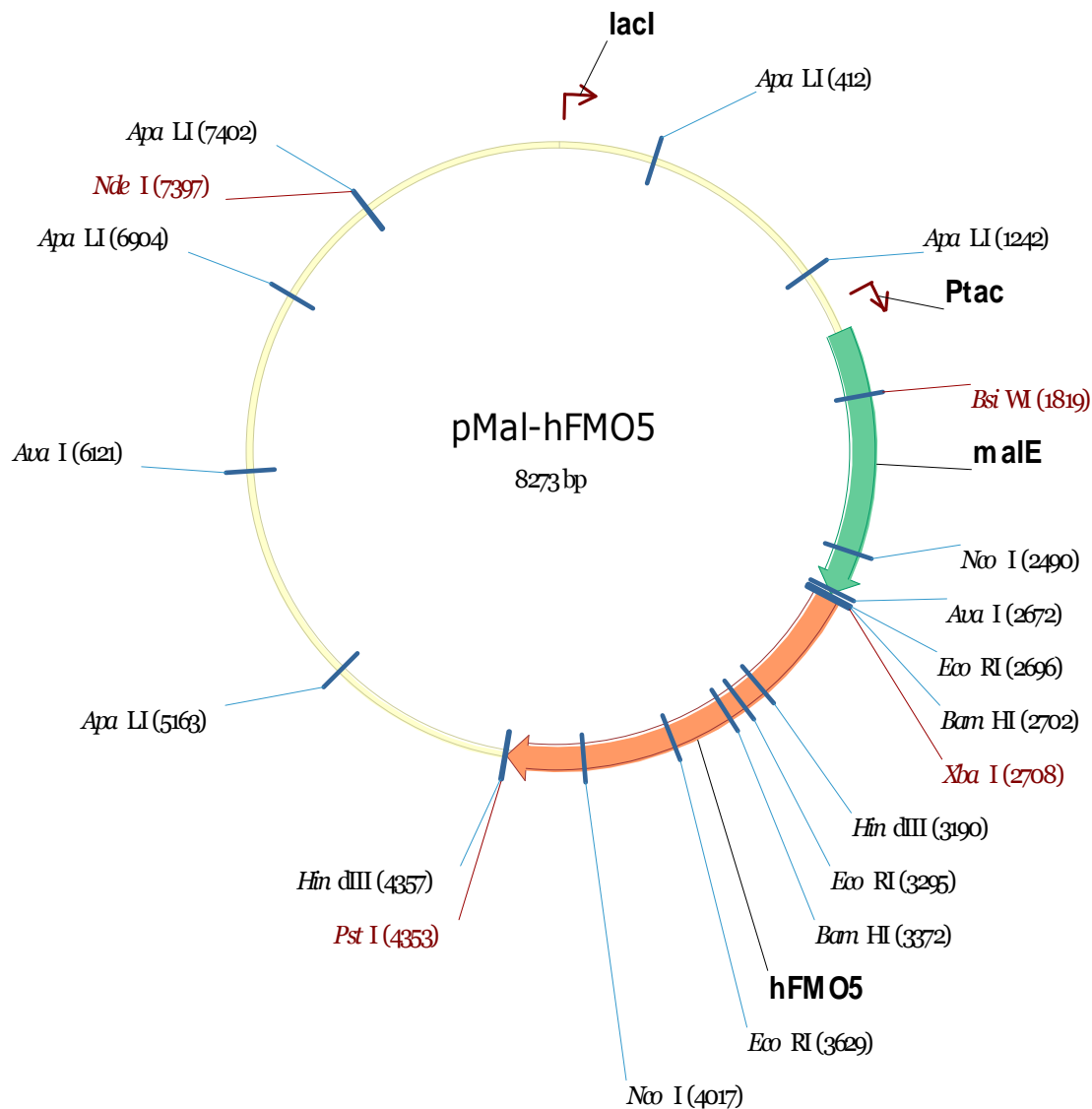


Figure 3.1 pMAL Vector with human FMO5.

The ampicillin-resistant site not shown in the Figure.

E. coli DH1 α cells transfected with pMAL-MBP-FMO5 plasmid were grown at 37 °C and 300 rpm in SOC medium containing 100 μ g/ml ampicillin to an absorbance of 0.4 – 0.5 at 600 nm. Induction solution (containing 0.2 mM isopropyl β -thiogalactopyranoside and 0.05 mM riboflavin) was added, flasks were covered with aluminum foil to keep riboflavin from light induced degradation, and the cells were further incubated shaking for 20 hours at room temperature. Cells were harvested by centrifugation at 6,000 *g* for 10 minutes. All of the following procedures were carried out at 4 °C. The cell pellet was resuspended in lysis buffer (consisting of 50 mM Na₂HPO₄, pH 8.4, containing 0.5 % Triton[®] X-100, 0.2 %

L- α -phosphatidylcholine, 0.5 mM phenylmethylsulfonylfluoride, and 100 mM FAD) as described previously [Lattard *et al.*, 2003b]. The resuspended cells were disrupted by sonication (i.e., five 8-seconds bursts separated by periods of cooling on a Sonics vibracell ultrasonic processor (Sonics and Materials Inc., Newtown, CT, USA)). The solution was centrifuged for 25 minutes at 18,000 *g* and 4 °C.

3.2.2.2 Extraction and Solubilization Studies

Effect of Different Detergents on *N*-Oxygenation Activity of MBP-hFMO5

The effects of a variety of detergents on *N*-oxygenation activity of FMO5 protein were tested by measuring enzyme activity of FMO5 after precipitation and re-solubilization with 8-DPT as substrate.

For precipitation polyethylene glycol (PEG) was used as previously described [Lomri *et al.*, 1993a]. An equal amount of 40 % PEG 8000 was added to the enzyme solution, mixed thoroughly, and centrifuged at 15,000 *g* in a bench top centrifuge for 20 minutes at 4 °C. Supernatant was discarded and the remaining pellet was resuspended in 50 mM potassium phosphate buffer, pH 8.4, containing 1 or 2 x critical micelle concentration (CMC) of one of the following detergents: the zwitterionic detergents CHAPS (3-[(3-Cholamidopropyl)dimethylammonio]-1-propanesulfonate) or FOS-CHOLINE[®]-12 (n-Dodecylphosphocholine, FC12), or the non-ionic detergents, n-decyl- β -D-maltoside (DM), n-dodecyl- β -D-maltoside (DDM), n-Octyl- β -D-glucoside (ODG), Cymal[®]-5, 6, and 7 (5-Cyclohexyl-1-pentyl- β -D-maltoside, C5), and Triton[®] X-100 (α -[4-(1,1,3,3-Tetramethylbutyl)phenyl]-hydroxy-poly(oxy-1,2-ethanediyl, TX100) (Table 3.1). The different batches were analyzed afterwards for 8-DPT *N*-oxygenation activity.

Table 3.1 Detergents tested in solubilization studies.

Detergent	CMC (H ₂ O) ¹	Structure
CHAPS	8 mM (0.49 %)	
FC12	1.5 mM (0.047 %)	
DM	1.8 mM (0.087 %)	
DDM	0.17 mM (0.0087 %)	
ODG	18-20 mM (0.53 %)	
C5-7	C5 = 2.4-5 mM (0.12 %) C6 = 0.56 mM (0.028 %) C7 = 0.19 mM (0.0099 %)	
TX 100	0.23 mM 0.010 - 0.016 %	

¹CMC values taken from supplier (Anatrace, Maumee, OH, USA); % given as (w/v). FOS-CHOLINE[®]-12, FC12; n-decyl-β-D-maltoside, DM; n-dodecyl-β-D-maltoside, DDM; n-Octyl-β-D-glucoside, ODG; Cymal[®]-5, 6 and 7, C5-7, and Triton[®] X-100, TX100.

Comparison of Extraction Efficiency of DDM and DM

E. coli with human pMAL-MBP-FMO5 was grown, induced, and pelleted. The pellets were then resuspended in lysis buffer containing either 0.1 – 0.2 % DM or 0.01 – 0.02 % DDM and disrupted by sonication. After addition of NADPH-regenerating system (see chapter 3.2.4.2) the solution was mixed thoroughly and centrifuged. To determine extraction efficiency, the supernatant was afterwards incubated with 8-DPT for 20 minutes for determination of enzyme activity (see chapter 3.2.4.2).

Extraction Efficiency of Triton® X-100 vs. DDM

E. coli with human pMAL MBP-FMO5 was grown, induced, and pelleted. The pellets were then resuspended in lysis buffer containing either 0.01 % DDM or 0.5 % Triton® X-100 and disrupted by sonication. As control, the pellet resulting from lysis with DDM was extracted a second time after centrifugation, this time with Triton® X-100. For batch-wise purification, 300 µl amylose column material equilibrated with 50 mM sodium phosphate buffer, pH 8.5, was added to all three supernatants (each 5 ml). After 3 hours incubation at 4 °C, the column material was washed with equilibration buffer and finally MBP-hFMO5 was eluted with 50 mM sodium phosphate buffer, pH 8.5, containing 10 mM maltose by incubation at 4 °C for 20 minutes and subsequent centrifugation. Afterwards, the supernatant was analyzed for enzyme activity as described in chapter 3.2.4.2.

3.2.2.3 Affinity Chromatography

The first purification step after cell lysis exploited the MBP-affinity tag connected to the FMO5 enzyme. Thus, after centrifugation of the lysed cells, the supernatant was loaded onto an amylose column (New England BioLabs, Ipswich, MA, USA). In order to improve the yield of protein, the pellets were extracted one more time as described above (chapter 3.2.2.1) and the resulting supernatant was also loaded onto the same amylose column. Protein purification was carried out on a low pressure chromatography system, Biologic LP (Bio-Rad, Hercules, CA, USA). For a 6 l bacterial culture, a 10 ml amylose column was used. After loading the supernatants at 1 ml/min onto a column equilibrated with ten column volumes of buffer A (i.e., 50 mM Na₂HPO₄, pH 8.4, and 0.5 % Triton® X-100 containing 15 µg/ml FAD) the column was washed with at least ten column volumes of buffer A. Bound MBP-hFMO5 protein was then eluted with 3 mM maltose in buffer A at 1 ml/min.

Eluted fractions were analyzed via absorption at 280 nm (Figure 3.5), SDS-PAGE (chapter 3.2.4.1), or HPLC-based enzyme activity assay (chapter 3.2.4.2). Fractions containing the fusion protein were concentrated with an Amicon Ultra-15 centrifugal filter unit with an Ultracel-50 filter (Millipore, Billerica, MA, USA).

3.2.3 Development of an Ion Exchange Chromatography Method

3.2.3.1 Buffer and Column Selection

A protocol for further protein purification utilizing ion exchange chromatography was developed. 700 mg of MBP-hFMO5 from 4 separate 6 l bacterial cultures was pooled after affinity chromatography and used to develop such a protocol. 2.5 mg of this protein was loaded at 1 ml/min onto a 1 ml DEAE, Q, or ANX column (HiTrap FF columns, GE Healthcare, Uppsala, Sweden) at four different pHs (i.e., pH 6, 7, 8, and 9). Elution profiles showing absorption at 280 nm and SDS gels of eluted fractions were evaluated regarding capture of MBP-hFMO5 protein.

3.2.3.2 Determination of a Salt Gradient

After choosing a column, an adequate salt gradient was determined. Affinity column purified MBP-hFMO5 was loaded onto a 1 ml HiTrap Q FF column at 1 ml/min and washed with 50 mM Bis-Tris, pH 6 (buffer B) containing 0.01 % DDM. A linear salt gradient of first 0 – 50 % and later 1 – 30 % 1 M NaCl in buffer B containing 0.01 % DDM was applied over 20 column volumes. Salt concentrations for a suitable step gradient for separation of contaminating protein and MBP-hFMO5 was roughly estimated from the first two linear gradients. The approximated step gradient was refined by repetitive ion exchange purification and SDS gel analysis of resulting fractions varying only the salt concentration of the different steps in the gradient.

3.2.3.3 Scale-Up Experiments

For larger amounts of purified protein the ion exchange chromatography method developed was transferred to a 5 ml Q HP column (GE Healthcare, Uppsala, Sweden). 30 mg of affinity purified MBP-hFMO5 was loaded onto a 5 ml Q HP column at 5 ml/min and eluted with a step gradient of 6.5 % and 25 % 1 M NaCl. Likewise, ion exchange purification could be adapted to 1 ml HiTrap Q HP columns

(GE Healthcare, Uppsala, Sweden) using a flow rate of 1 ml/min and a step gradient of 65 mM and 250 mM NaCl.

An overview of the purification process including columns, buffers, and flow rates is given in Table 3.2.

Table 3.2 Overview over the parameters in the purification process.

	Chromatography method			
	Affinity	Anion exchange		Size exclusion
Column	10 ml amylose column	1 ml HiTrap Q FF or HP	5 ml HiTrap Q HP	Superose 6 10/300 GL
Equilibration buffer	50 mM Na ₂ HPO ₄ pH 8.4, 15 µg/ml FAD, ± 0.5 % Triton [®] X-100	50 mM Bis-Tris pH 6 ± 0.01 % DDM	50 mM Bis-Tris pH 6 ± 0.01 % DDM	50 mM Bis-Tris pH 6, 0.01 % DDM
Elution buffer	50 mM Na ₂ HPO ₄ pH 8.4, 15 µg/ml FAD, 3 mM maltose, ± 0.5 % Triton [®] X-100	50 mM Bis-Tris pH 6 ± 0.01 % DDM, stepgradient: 0, 65, 250 and 1000 mM NaCl	50 mM Bis-Tris pH 6 ± 0.01 % DDM, stepgradient: 0, 65, 250 and 1000 mM NaCl	
Flow rate	1 ml/min	1 ml/min	5 ml/min	0.5 ml/min
Fraction size	5 ml	1 ml	5 ml	1 ml
Detection wavelength	280 nm	280 and 450 nm	280 and 450 nm	280 and 450 nm

3.2.4 Characterization of Purified MBP-hFMO5

3.2.4.1 Determination of MBP-hFMO5 Concentration

Concentration of purified MBP-hFMO5 was determined by SDS-PAGE and Coomassie Blue staining and compared with bovine serum albumin (BSA) standard. MBP-hFMO5 proteins and different quantities of standard BSA (i.e., 2, 1.5, 1.0, 0.5, and 0.1 μg per lane) were fractionated by electrophoresis on a 10 % polyacrylamide gel under denaturing conditions and stained with Coomassie Blue. After destaining, FMO5 quantification was done by densitometry analysis employing Kodak molecular imaging software (Eastman Kodak Company, Rochester, NY, USA) or Adobe Photoshop Elements (Version 7).

For protein concentration measurements of Q column purified fractions containing DDM instead of Triton[®] X-100 or no detergent at all, the absorbance at 280 nm was measured on a NanoDrop[™] ND-1000 UV/VIS Spectrophotometer (Thermo Fisher Scientific, Wilmington, DE, USA) using a calculated extinction coefficient of $121 \text{ M}^{-1}\text{cm}^{-1}$ estimated after the method of Gill and von Hippel [Gill *et al.*, 1989] using the online Protein Calculator v3.3.

3.2.4.2 8-DPT N-Oxygenation Activity and Stability of MBP-hFMO5

N-Oxygenation of 8-DPT HCl was determined by HPLC analysis as previously described [Lattard *et al.*, 2003b]. A standard incubation mixture of 250 μl final volume contained 50 mM potassium phosphate buffer at pH 8.5, 0.4 mM NADP⁺, 0.4 mM glucose-6-phosphate, 4 U glucose-6-phosphate dehydrogenase, 0.25 mM DETAPAC, and 40 μg MBP-hFMO5. Reactions were initiated by addition of substrate to a final concentration of 400 μM . After incubation for 20 minutes shaking under aerobic conditions at 37 $^{\circ}\text{C}$, enzyme reactions were stopped by addition of 4 volumes of cold dichloromethane. About 20 mg of sodium carbonate was added to incubations and they were mixed and centrifuged in order to partition metabolites and remaining substrate into the organic fraction. The organic phase was collected and evaporated under a stream of argon. Metabolites and remaining substrate were dissolved in methanol, mixed thoroughly, centrifuged, and analyzed with a Hitachi HPLC system (Hitachi L-7200 autosampler and L-7100 pump interfaced to a Hitachi L-7400 UV detector). Chromatographic separation of analytes was done on an Axxi-Chrom's

normal phase analytical column (250 x 4.6 mm 5 μ m, silica) with a mobile phase of 80 % methanol/ 20 % isopropanol/ 0.025 % perchloric acid (v/v/v). The flow rate was 1.6 ml/min and the total run time was 11 minutes. The wavelength for UV detection was set to 243 nm. Retention times for 8-DPT and 8-DPT *N*-oxide were 5.8, and 4.3 minutes, respectively, and the enzyme activity was determined by calculation of the ratio of 8-DPT to 8-DPT *N*-oxide peak.

Comparison of recombinant expressed MBP-hFMO5 and commercially available FMO5 (BD Gentest) was done by evaluating kinetic parameters and enzyme stability over 30 minutes at 37 $^{\circ}$ C for both enzymes. The kinetic parameters (i.e., V_{max} and K_m) for *N*-oxygenation of 8-DPT HCl by FMO5 was determined by HPLC analysis as described above. Incubations were initiated by the addition of different amounts of substrate. The final substrate concentrations were in the range of 10 μ M – 2 mM. Stability was determined by incubating the enzyme in presence of cofactor and 400 μ M 8-DPT HCl for 5, 10, 20, and 30 minutes. 8-DPT HCl and its *N*-oxide were then analyzed on a HPLC system as described above.

Stability of MBP-hFMO5 was determined by incubating 5 ml HP Q column-purified MBP-hFMO5 at 4 $^{\circ}$ C for 5 days. The 8-DPT *N*-oxygenation activity of MBP-hFMO5 was determined for three time-points (i.e., day 0, day 3, and day 5). 500 mM NADP⁺ and/or 20 % glycerol was added to determine whether these supplements improve the enzyme's stability.

3.2.4.3 Native Gel Electrophoreses

MBP-hFMO5 and five standard proteins (i.e., thyroglobulin (669 kDa), ferritin (440 kDa), aldolase (158 kDa), conalbumin (75 kDa), and ovalbumin (43 kDa)) were fractionated by electrophoresis on a NativePAGE Novex 3 – 12 % Bis-Tris Gel with Native-PAGE Running Buffer Kit (Invitrogen Corporation, Carlsbad, CA, USA) following the vendors instructions. After destaining, molecular weight determination of sample protein was done by comparison of MBP-hFMO5 bands with standard protein bands employing Kodak molecular imaging software (Eastman Kodak Company, Rochester, NY, USA).

3.2.4.4 Size Exclusion Chromatography

MBP-hFMO5 purified via affinity chromatography or ion exchange chromatography following affinity chromatography was also analyzed utilizing size exclusion chromatography. Peak fractions of the protein from either column were concentrated and loaded onto a Superose 6 10/300 GL size exclusion column equilibrated with 50 mM Bis-Tris, pH 6, containing 0.01 % DDM.

3.2.4.5 Dynamic Light Scattering

Protein was analyzed via dynamic light scattering (DLS) in order to determine the size distribution profile of the protein sample and ensure monodispersity before setting up crystallography experiments (chapter 4). For this purpose, 60 μ l protein solutions in different concentrations and with various additives were analyzed with a Zetasizer Nano-S (Malvern Instruments Ltd, Malvern, United Kingdom). DLS measurements were done at the Zentrum für Biochemie und Molekularbiologie (ZBM), University of Kiel. FMO5 fractions analyzed included affinity column purified MBP-hFMO5, Q-purified MBP-hFMO5 with and without 20 % glycerol. Some MBP-hFMO5 fractions were treated with Calbiosorb Adsorbent beads (Merck, Darmstadt, Germany) in order to evaluate the effect of removal of excess detergent on monodispersity. Also, Calbiosorb Adsorbent beads treated Q-purified FMO5 was examined in different concentrations (i.e., 25, 10, 5, 2.5, and 0.25 mg/ml).

3.2.5 Data Analysis

Kinetic parameters for 8-DPT *N*-oxygenation activity were determined by examining the data from incubations of seven different substrate concentrations with MBP-hFMO5 (i.e., 0, 10, 40, 100, 200, 400, 800 μ M, and 2 mM). Incubations were done in duplicates and for data analysis a nonlinear regression curve fit tool using a Michaelis-Menten model ($Y = (V_{max} \cdot X)/(K_m + X)$ with $V_{max} = Y_{max}$ and $K_m = X_{mid}$) in Graphpad software (Graphpad Prism, Version 3.00, San Diego, CA, USA) was utilized. Time dependence of MBP-hFMO5 was also done in duplicates and data was analyzed with linear regression using Graphpad software. Data obtained was presented as the best fit value \pm standard error. Statistical analysis was also done using Graphpad Prism software.

3.3 Results

3.3.1 Expression and Purification of MBP-hFMO5 via Affinity Chromatography

3.3.1.1 Extraction and Solubilization

Effect of Different Detergents on *N*-Oxygenation Activity of MBP-hFMO5

In order to determine a suitable detergent for MBP-hFMO5 solubilization and purification, the effect of nine different detergents (i.e., Triton[®] X-100, CHAPS, DM, DDM, ODG, FC12, and Cymal[®]-5, 6 and 7) on *N*-oxygenation activity of MBP-hFMO5 were tested.

In control experiments with MBP-hFMO5 solubilized in Triton[®] X-100 and MBP-hFMO5 after PEG precipitation and re-solubilization in Triton[®] X-100 no significant difference in enzyme activity between the two was observed (Figure 3.2). Overall, results showed that DM and DDM performed best even in concentrations of 2 x CMC. Thus, these detergents were chosen for further analyzation.

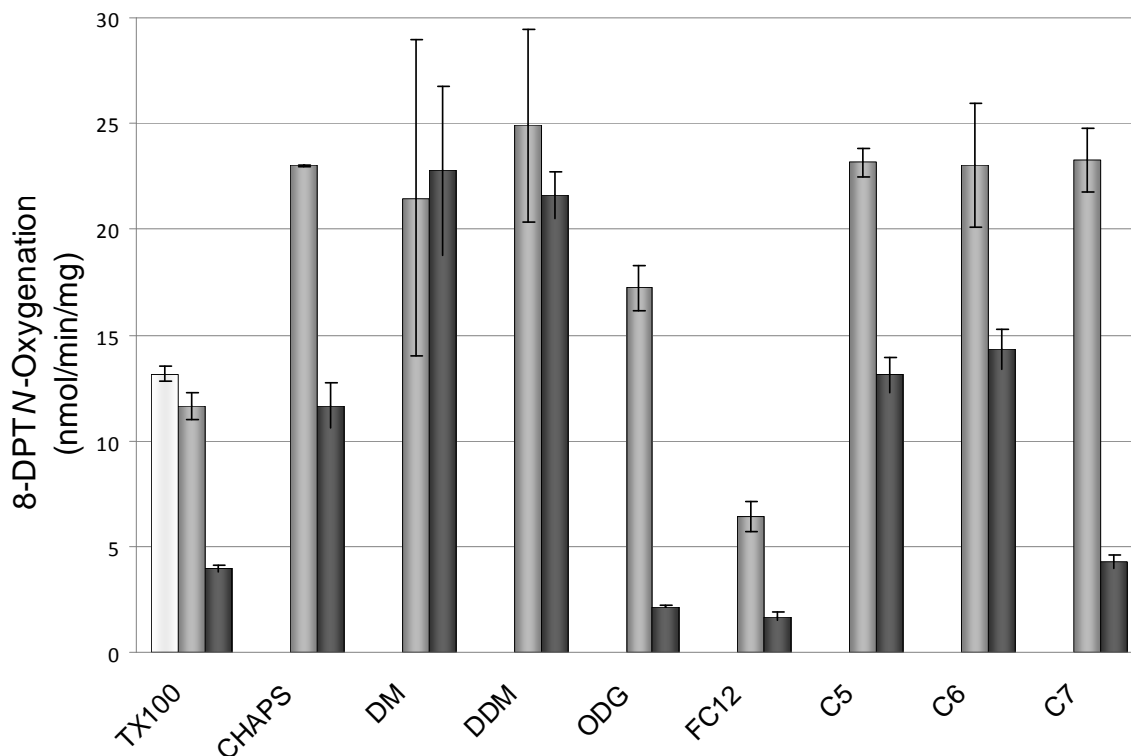


Figure 3.2 Effect of a variety of detergents on MBP-hFMO5 activity.

Amylose column purified MBP-hFMO5 was precipitated with 40 % PEG and resuspended in 50 mM phosphate buffer (pH 8.4) containing a variety of different detergents in two different concentrations: 1 x (grey bars) and 2 x CMC (black bars). 8-DPT N-oxygenation activity of the enzyme was determined. For comparison, regular amylose column-purified MBP-hFMO5 in buffer containing 0.5 % Triton[®] X-100 that was not precipitated with 40 % PEG is shown as a white bar. Triton[®] X-100, TX100; n-decyl- β -D-maltoside, DM; n-dodecyl- β -D-maltoside, DDM; n-Octyl- β -D-glucoside, ODG; FOS-CHOLINE[®]-12, FC12; Cymal[®]-5, 6 and 7, C5-7.

Extraction Efficiency of DDM and DM in Comparison

Comparison between DM and DDM showed a very slight advantage of DDM over DM (data not shown). Thus, extraction efficiency of DDM was afterwards compared to that of Triton[®] X-100 anticipating replacement of the latter.

Extraction Efficiency of Triton[®] X-100 and DDM

Comparison of MBP-hFMO5 extraction efficiencies from bacterial cell pellets with Triton[®] X-100 and DDM showed that although DDM seemed to have no negative influence on enzyme activity, it was not suitable for extraction (Figure 3.3). When

extracting the bacterial cells with lysis buffer containing Triton[®] X-100 a larger amount of MBP-hFMO5 was obtained after purification with amylose resin in comparison to bacterial cells extracted with lysis buffer containing DDM.

Only after the second extraction (i.e., with Triton[®] X-100 instead of DDM) of the bacterial pellet already extracted with DDM, an appropriate MBP-hFMO5 band could be observed on the SDS gel. Thus, Triton[®] X-100 was chosen for extraction of MBP-hFMO5 from bacterial cells and was used in the first purification step.

Triton[®] X-100 is rather heterogeneous and thus not suitable for crystallography studies. In order to remove it, a buffer exchange was done on the ion exchange column switching to DDM as detergent (see also Figure 3.15) because although DDM did not extract the protein very efficiently, it was superior with regards to enzyme activity (Figures 3.2 and 3.3).

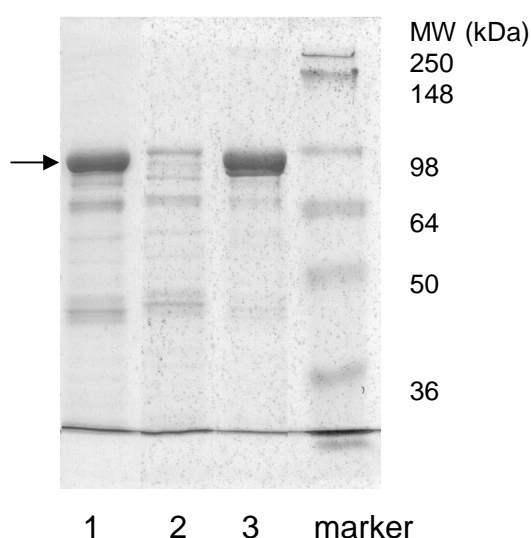


Figure 3.3 Extraction efficiency of Triton[®] X-100 and DDM.

Coomassie stained SDS gel of: 1, pellet extracted with Triton[®] X-100; 2, pellet extracted with DDM; 3, second extraction of already with DDM extracted pellet with Triton[®] X-100; molecular weight (MW) marker, SeeBlue[®] Plus2 (Invitrogen Corporation, Carlsbad, CA, USA). The arrow points to the MBP-hFMO5 band.

Later, after ensuring that no interference of DDM with the amylose column would occur, Triton[®] X-100 was replaced with DDM in the chromatography buffer in this first purification step (Figure 3.15). Subsequent studies showed that treatment of MBP-hFMO5 with an excess amount of polystyrene beads to remove residual detergents

from the protein sample did not result in precipitation of MBP-hFMO5 (chapters 4.2.4.3 and 4.3.1.3). Additional experiments also showed that MBP-hFMO5 could be purified in the absence of detergent. Thus, in the final purification protocol, Triton[®] X-100 was used to extract MBP-hFMO5 from *E. coli* cells, but all purification steps were done in the absence of detergent. An overview of the development and design of purification process including usage of detergents is given in Figure 3.15 at the end of this chapter.

3.3.1.2 Affinity Chromatography

In the first purification step utilizing an amylose column, a total of about 700 mg MBP-hFMO5 was obtained from four separate 6 l bacterial cultures (Figure 3.4). A representative elution chromatogram from this affinity purification step is shown in Figure 3.5. Protein concentration and the 8-DPT *N*-oxygenation activity were determined by HPLC analysis (Table 3.3). The obtained protein preparations were pooled and stored at -80 °C until used for ion exchange chromatography method development and initial crystallography screens.

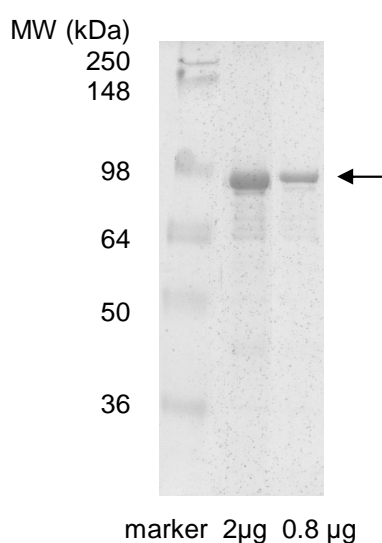


Figure 3.4 Representative Coomassie stained SDS gel with 2 and 0.8 µg of affinity chromatography purified MBP-hFMO5 protein.

SeeBlue[®] Plus2 (Invitrogen Corporation, Carlsbad, CA, USA) was used as MW protein marker. The arrow points to the MBP-hFMO5 band.

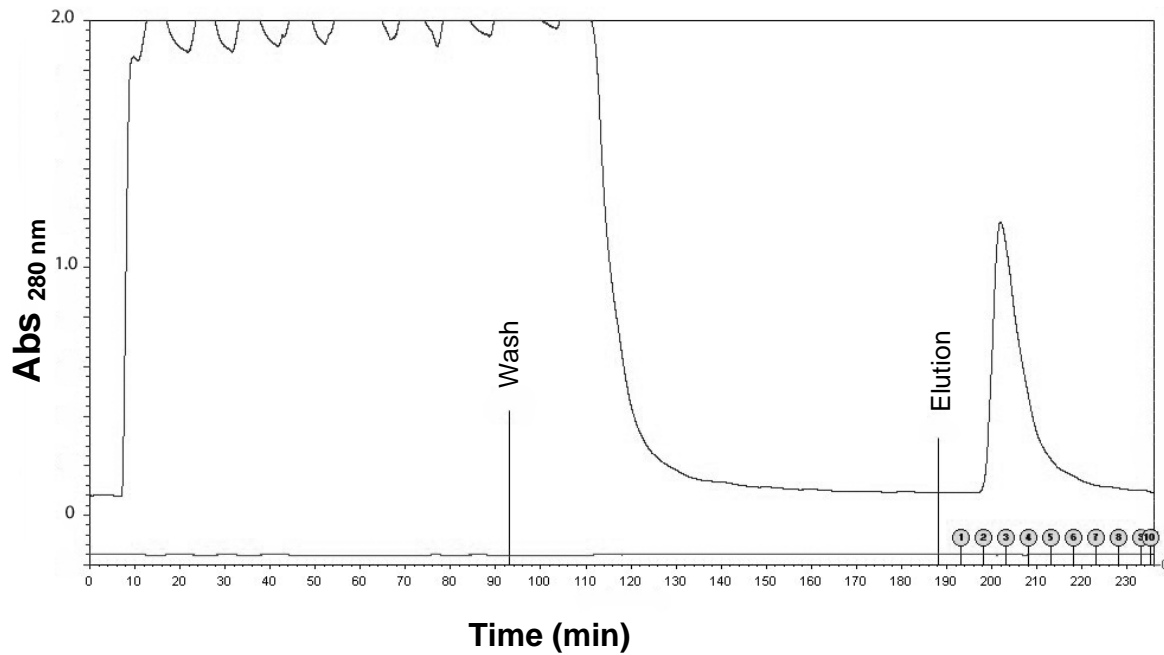


Figure 3.5 Representative elution profile of affinity chromatography of MBP-hFMO5.

0 – 93 minutes, loading of protein; 93 – 188 minutes, wash step; 188 – 236 minutes, elution step with 3 mM maltose.

Table 3.3 MBP-hFMO5 protein preparations of four separate 6 l bacterial cultures after affinity purification.

Batch	8-DPT assay		Yield	
	Specific activity (nmol/(min·mg))	Protein (mg/ml)	Total volume of fraction (ml)	Total amount of protein (mg)
1	12.5	54	2.7	146
2	5.0	39	3.2	126
3	7.2	69	3.6	249
4	7.1	57	3.5	199

3.3.2 Purification of MBP-hFMO5 via Ion Exchange Chromatography

3.3.2.1 Columns, Buffers, and pH

After affinity chromatography, a protocol for further protein purification utilizing ion exchange chromatography was developed using affinity column purified MBP-hFMO5 (section 3.2.2.3). The most promising conditions for further purification with an FPLC-system (Äkta-Purifier, GE Healthcare, Uppsala, Sweden) were determined by testing three different columns (i.e., DEAE, Q, and ANX) at different pHs (6 – 9). Most protein was captured at pH 6 on the ANX column followed by the Q column (Figure 3.6). For further purification, 1 ml or 5 ml HiTrap Q HP columns (GE Healthcare, Uppsala, Sweden) with Bis-Tris buffer at pH 6 were chosen because high performance columns are available for the Q column. Also, choosing a strong ion exchanger such as Q over a weak one (i.e., DEAE or ANX) is advantageous because it does not show variation in ion exchange capacity with change of pH.

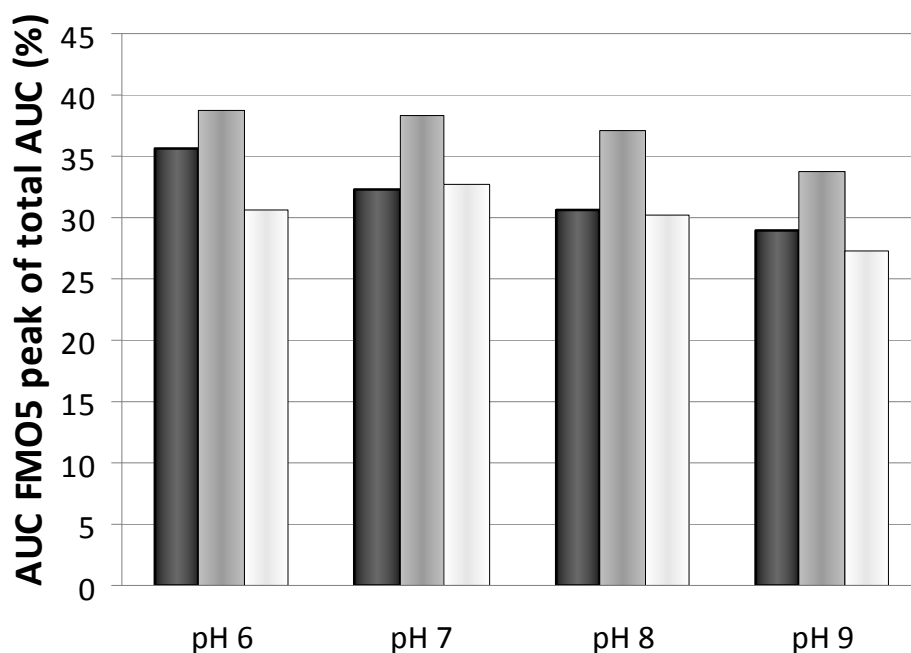


Figure 3.6 Determination of a suitable anion exchange column and pH.

% Area under the curve (AUC) of MBP-hFMO5 peaks in relation to AUC of all peaks eluted from the column (= 100 %) observed is shown for Q (black bars), ANX (grey bars), and DEAE (white bars) columns at pH 6, 7, 8, and 9.

3.3.2.2 Salt Gradient

To separate protein impurities from MBP-hFMO5, a step gradient was determined on 1 ml HiTrap Q FF column with affinity chromatography purified protein. Most impurities were eluted with 65 mM NaCl in buffer B. MBP-hFMO5 was then eluted with 250 mM NaCl in buffer B (Figure 3.7).

3.3.2.3 Scale-Up Experiments

For purification of larger amounts of MBP-hFMO5, a 5 ml HiTrap Q HP column was utilized. This column had been successfully used with 30 mg of affinity column purified MBP-hFMO5 and the previously determined step-gradient (elution of most impurities with 65 mM NaCl in buffer B followed by elution of MBP-hFMO5 with 250 mM NaCl in buffer B). The elution profile as well as the SDS gel of the fractions obtained (Figure 3.8) look similar to those obtained with the 1 ml HiTrap Q FF column.

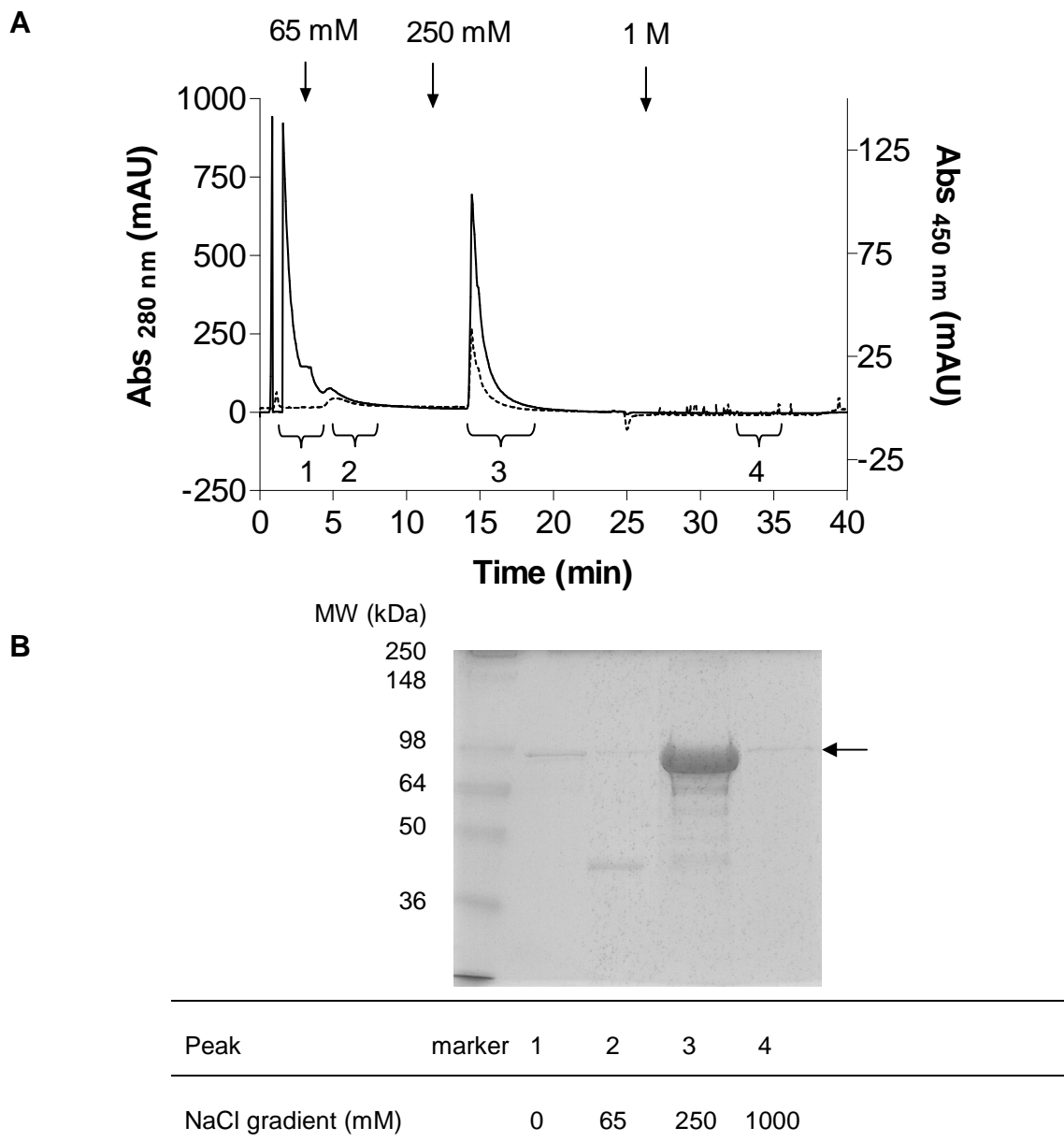


Figure 3.7 A Elution profile of MBP-hFMO5 purified on a 1 ml HiTrap Q FF column.

Absorbance at 280 nm is shown as solid line, absorbance at 450 nm as dashed line.

B Coomassie stained SDS gel of fractions from 1 ml HiTrap Q FF column eluted with a NaCl step-gradient as shown in A.

The column was loaded with 7 mg concentrated amylose column-purified MBP-hFMO5. The washing buffer consisted of 50 mM Bis-Tris buffer, pH 6, containing 0.01 % DDM. SeeBlue® Plus2 (Invitrogen Corporation, Carlsbad, CA) was used as MW protein marker. The arrow points to the MBP-hFMO5 band.

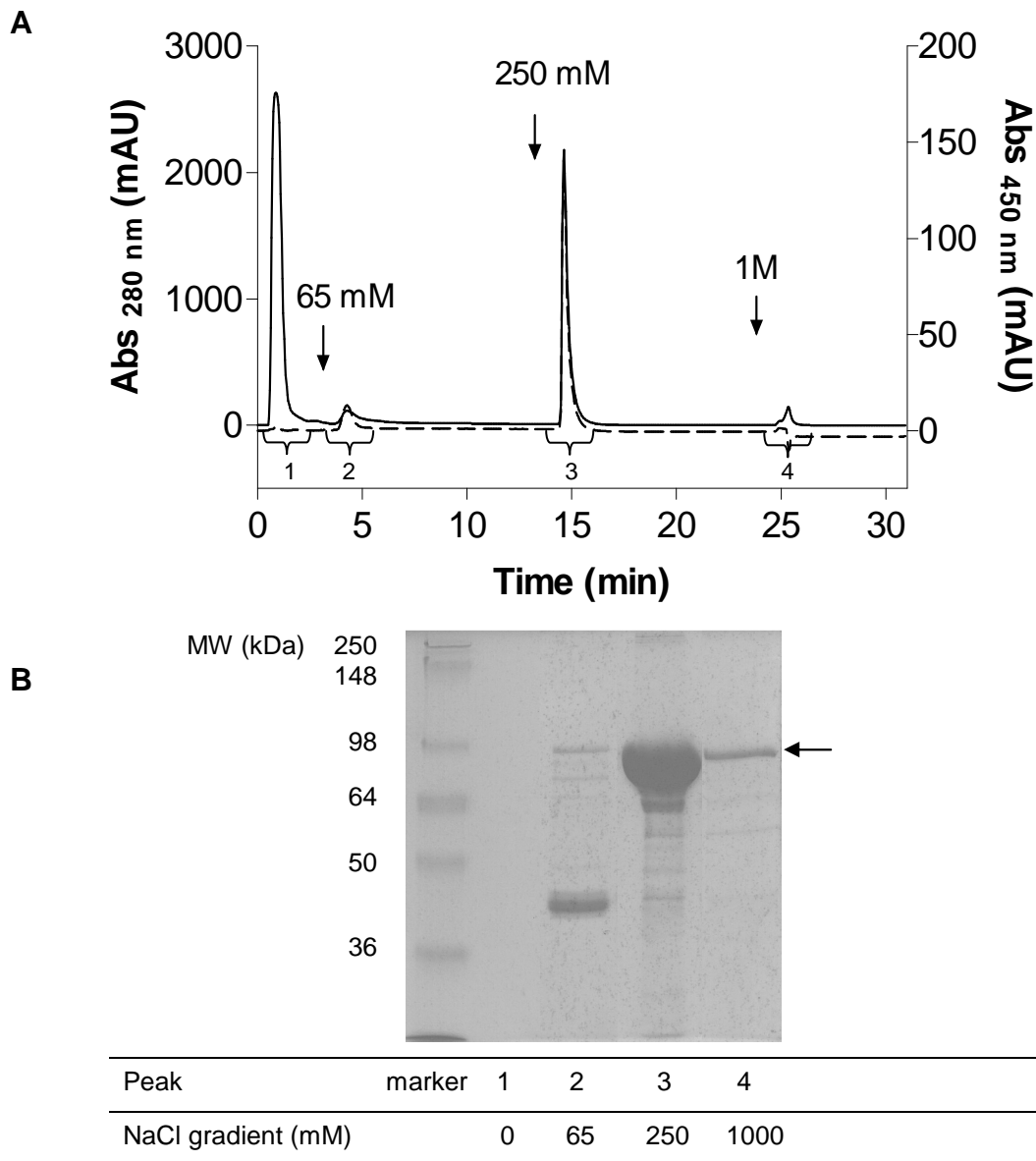


Figure 3.8 A Elution profile of MBP-hFMO5 purified on a 5 ml HiTrap Q HP column. Absorbance at 280 nm is shown as solid line, absorbance at 450 nm as dashed line.

B Coomassie stained SDS gel of fractions from 5 ml HiTrap Q HP column eluted with a NaCl step-gradient as shown in A.

The column was loaded with 30 mg concentrated amylose column-purified MBP-hFMO5. The washing buffer consisted of 50 mM Bis-Tris buffer, pH 6, containing 0.01 % DDM. SeeBlue[®] Plus2 (Invitrogen Corporation, Carlsbad, CA) was used as MW protein marker. The arrow points to the MBP-hFMO5 band.

3.3.3 Characterization of Purified MBP-hFMO5

3.3.3.1 Comparison between Recombinant Expressed MBP-hFMO5 and Commercially Available FMO5

8-DPT HCl Substrate Dependence

Kinetic parameters (i.e., V_{max} and K_m) for *N*-oxygenation of 8-DPT HCl by FMO5 were determined by HPLC analysis and the results are shown in Figure 3.9 and Table 3.4. Both enzymes had very similar K_m values (i.e., $120 \pm 21 \mu\text{M}$ for Gentest FMO5 and $117 \pm 21 \mu\text{M}$ for MBP-hFMO5). The V_{max} values were also similar, with a slightly higher value for MBP-hFMO5.

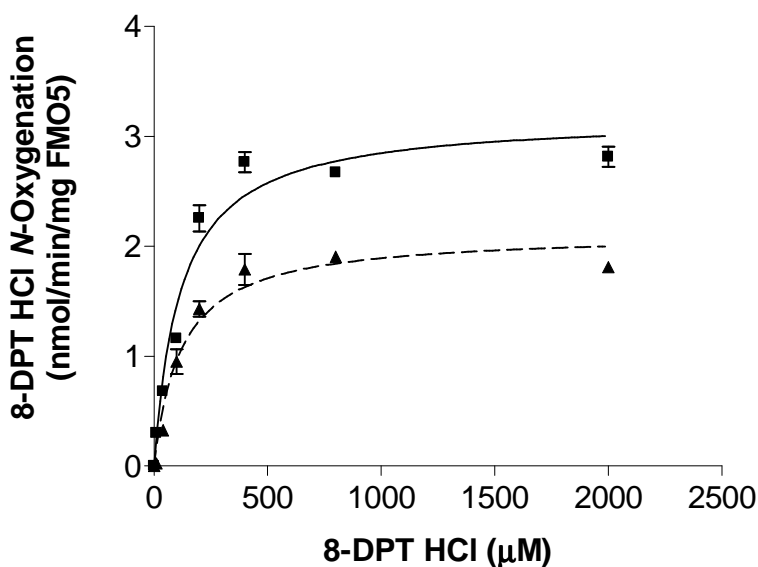


Figure 3.9 Determination of kinetic parameters for 8-DPT HCl *N*-oxygenation with MBP-hFMO5 and commercially available FMO5.

MBP-hFMO5 is shown as solid line (■), commercially available *FMO5* as dashed line (▲). r^2 Values are 0.96 and 0.97 for *MBP-hFMO5* and commercially available *FMO5*, respectively.

Table 3.4 Kinetic parameters for *N*-oxygenation of 8-DPT HCl with FMO5.

	V_{max} (nmol/min/mg FMO5)	K_m (μ M)	K_m / V_{max} (min ⁻¹ mg ⁻¹)
Commercially available FMO5	2.1 \pm 0.1	120 \pm 21	17.5 \pm 3.2
MBP-hFMO5	3.2 \pm 0.2	117 \pm 21	27.3 \pm 5.2

Data are presented as best fit values \pm standard error.

Time Dependence

FMO5 time dependence was determined by incubating the enzyme in presence of cofactor and 400 μ M 8-DPT HCl over 30 minutes. Time points were taken at 5, 10, 20, and 30 minutes. Results show linear increase of product formation over time for both enzymes. r^2 Values for linear regression with interception point set 0 were 0.97 and 0.99 for MBP-hFMO5 and FMO5 purchased from BD Gentest, respectively.

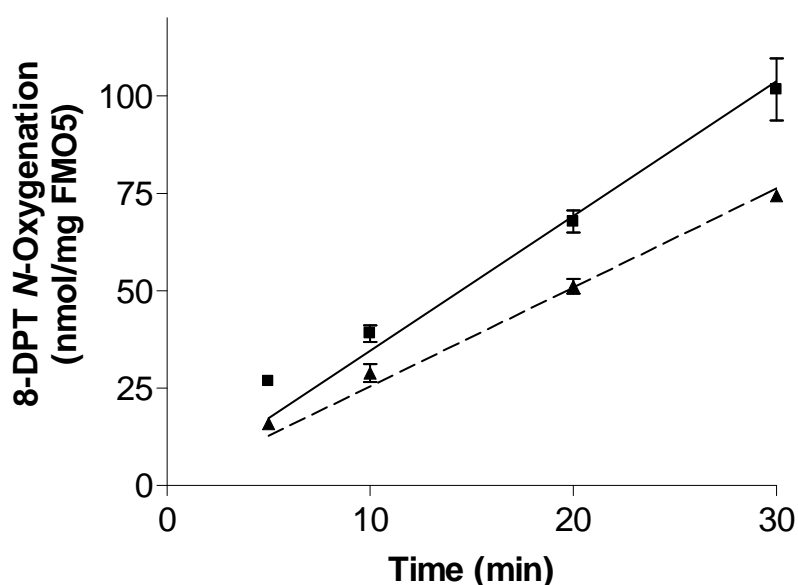


Figure 3.10 FMO5 time dependence was determined by measuring 8-DPT HCl *N*-oxygenation activity over 30 minutes.

MBP-hFMO5 is shown as solid line (■), commercially available FMO5 as dashed line (▲).

3.3.3.2 Stability of MBP-hFMO5 at 4 °C

The stability of MBP-hFMO5 at 4 °C was checked over 5 days and NADP⁺ and/or 20 % glycerol was added to determine whether these supplements improve the enzyme's stability. The addition of NADP⁺ and/or glycerol decreased loss of enzyme activity at 4 °C over 5 days. The specific activity of MBP-hFMO5 was still at 65 %, 73 %, and 80 % of that at day zero after addition of NADP⁺, glycerol, or both, respectively, whereas a 50 % loss in enzyme specific activity was observed when neither substance was added. Results are shown in Figure 3.11 and Table 3.5. Therefore, the NADP⁺ as well as 20 % glycerol was added to the enzyme to improve its stability in future crystallization studies (chapter 4). The observed increase of enzyme activity upon addition of glycerol at day 0 is probably due to the cryoprotective properties of glycerol.

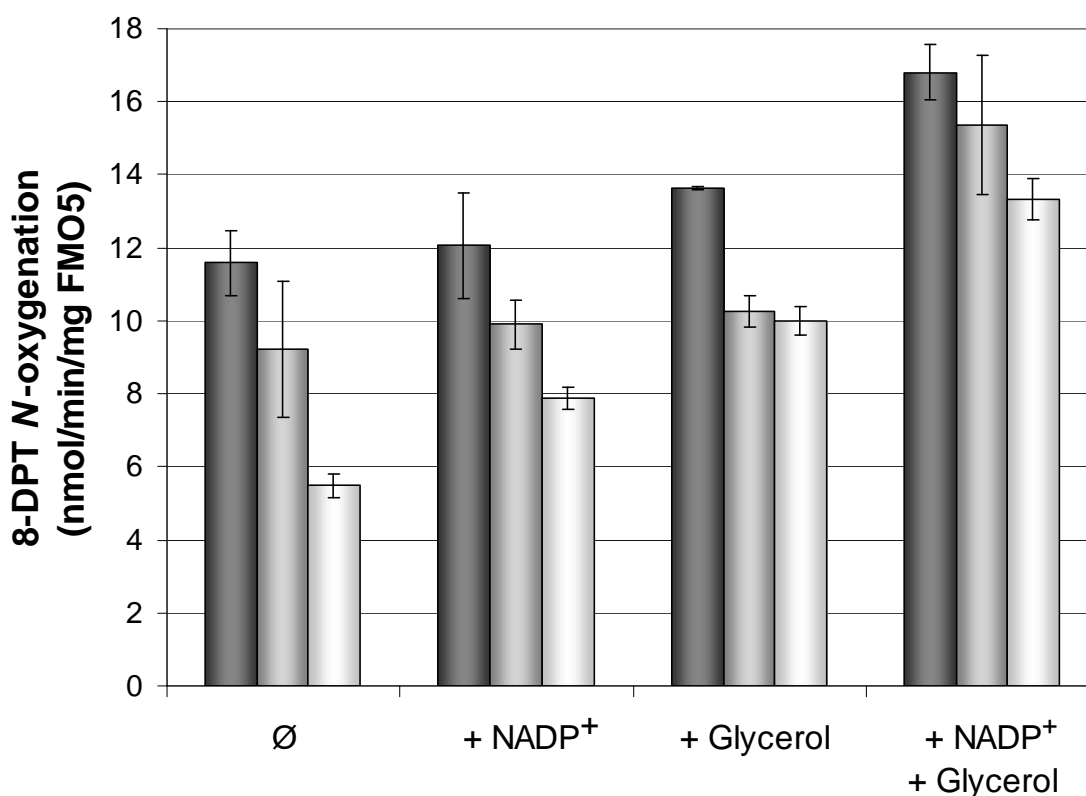


Figure 3.11 Stability of MBP-hFMO5 at 4 °C.

8-DPT N-oxygenation of MBP-hFMO5 at day 0 (black bars) and after incubation at 4 °C for 3 (grey bars) and 5 days (white bars) with and without addition of 500 mM NADP⁺ and/or 20 % glycerol.

Table 3.5 Stability of MBP-hFMO5 at 4 °C.

	∅	+ NADP ⁺	+ Glycerol	+ NADP ⁺ + Glycerol
Day 0	100.0 ± 7.7	100.0 ± 12.0	100.0 ± 0.4	100.0 ± 4.5
Day 3	79.6 ± 16.0	82.1 ± 5.5	75.1 ± 3.1	91.4 ± 11.2
Day 5	47.4 ± 2.8	65.3 ± 2.6	73.3 ± 2.8	79.2 ± 3.4

8-DPT N-oxygenation of hFMO5 at day 0 and after incubation at 4 °C for 3 and 5 days with and without addition of 500 mM NADP⁺ and/or 20 % glycerol are given in % with day 0 set 100 %.

3.3.3.3 Oligomerization State of MBP-hFMO5

The oligomerization state of MBP-hFMO5 was determined by native gel electrophoreses and gel filtration. After amylose column-purification, the enzyme existed mainly as mono-, tri-, and hexamer (Figure 3.12, lane 1) whereas it was primary found to be in a hexameric state after Q and SEC purification (Figure 3.12, lanes 2 and 3). After addition of 0.5 % Triton[®] X-100 (~30 x CMC) or 10 x CMC of DDM (0.1 %) to the Q and SEC-purified protein, the multimerization state changed towards coexistence of mono-, tri-, and hexamers (Figure 3.12, lanes 4-7).

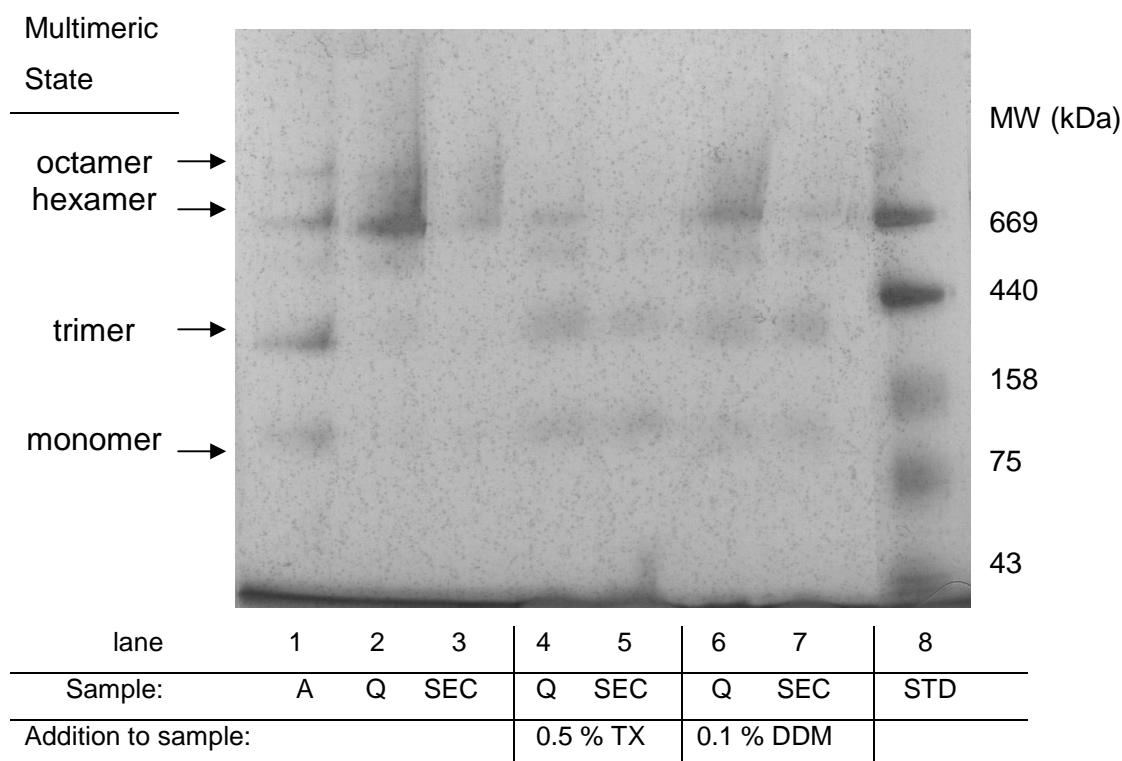


Figure 3.12 Native gel of MBP-hFMO5 in different purity.

Amylose-column purified MBP-hFMO5 (A, lane 1), HP Q column-purified MBP-hFMO5 (Q, lanes 2, 4, and 6), and MBP-hFMO5 purified on Superose 6 column after Q-purification (SEC, lanes 3, 5, and 7) with addition of 0.5 % Triton[®] X-100 (TX, lanes 4 and 5) or DDM (lanes 6 and 7). Standards (STD, i.e., thyroglobulin (669 kDa), ferritin (440 kDa), aldolase (158 kDa), conalbumin (75 kDa), and ovalbumin (43 kDa)) are loaded in lane 8. Molecular weight was determined employing Kodak molecular imaging software (Eastman Kodak Company, Rochester, NY, USA).

Also, size exclusion chromatography supports this assumption. The short retention time (Figure 3.13) suggests high aggregation state and after calculating the size utilizing various standard proteins (i.e., ovalbumin, conalbumin, aldolase, ferritin, and thyroglobulin) hexameric state of the protein seemed most likely.

Both MBP-hFMO5 from 1 ml HiTrap FF Q column or from amylose column were loaded onto a Sepharose 6 gel filtration column (Figure 3.13 A and B, respectively). In comparison to MBP-hFMO5 only purified via affinity chromatography where multiple protein species are still present, only one major peak could be observed after ion exchange purification.

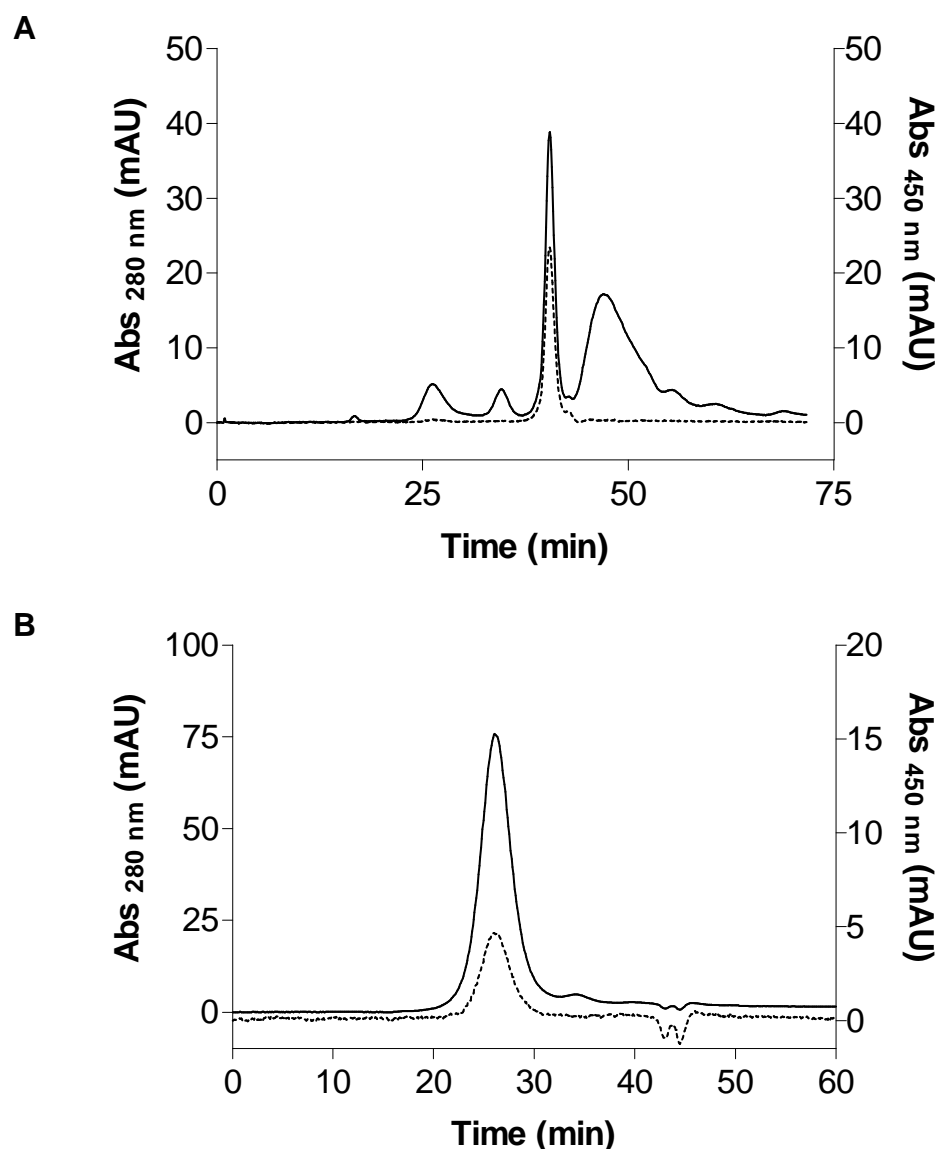


Figure 3.13 Elution profile of fractions from SEC column (Sephacrose 6) loaded with MBP-hFMO5.

Absorption at 280 nm is shown as solid line, absorption at 450 nm as dashed line.

A SEC elution profile of MBP-hFMO5 previously purified on an amylose column.

B SEC elution profile of MBP-hFMO5 previously purified on Q column.

3.3.3.4 Monodispersity of MBP-hFMO5

DLS analysis data of affinity purified MBP-hFMO5 is shown and either size (Figure 3.14 A) or volume (Figure 3.14 B) is plotted against intensity. When size is plotted against intensity two large peaks are observed, showing contamination or at least two species of proteins. However, when size is plotted against volume, it becomes apparent that the contamination is not as dominant as it seemed in Figure 3.14 A.

The polydispersity index (Pdl) values for amylose pure MBP-hFMO5 were 0.394 ± 0.006 .

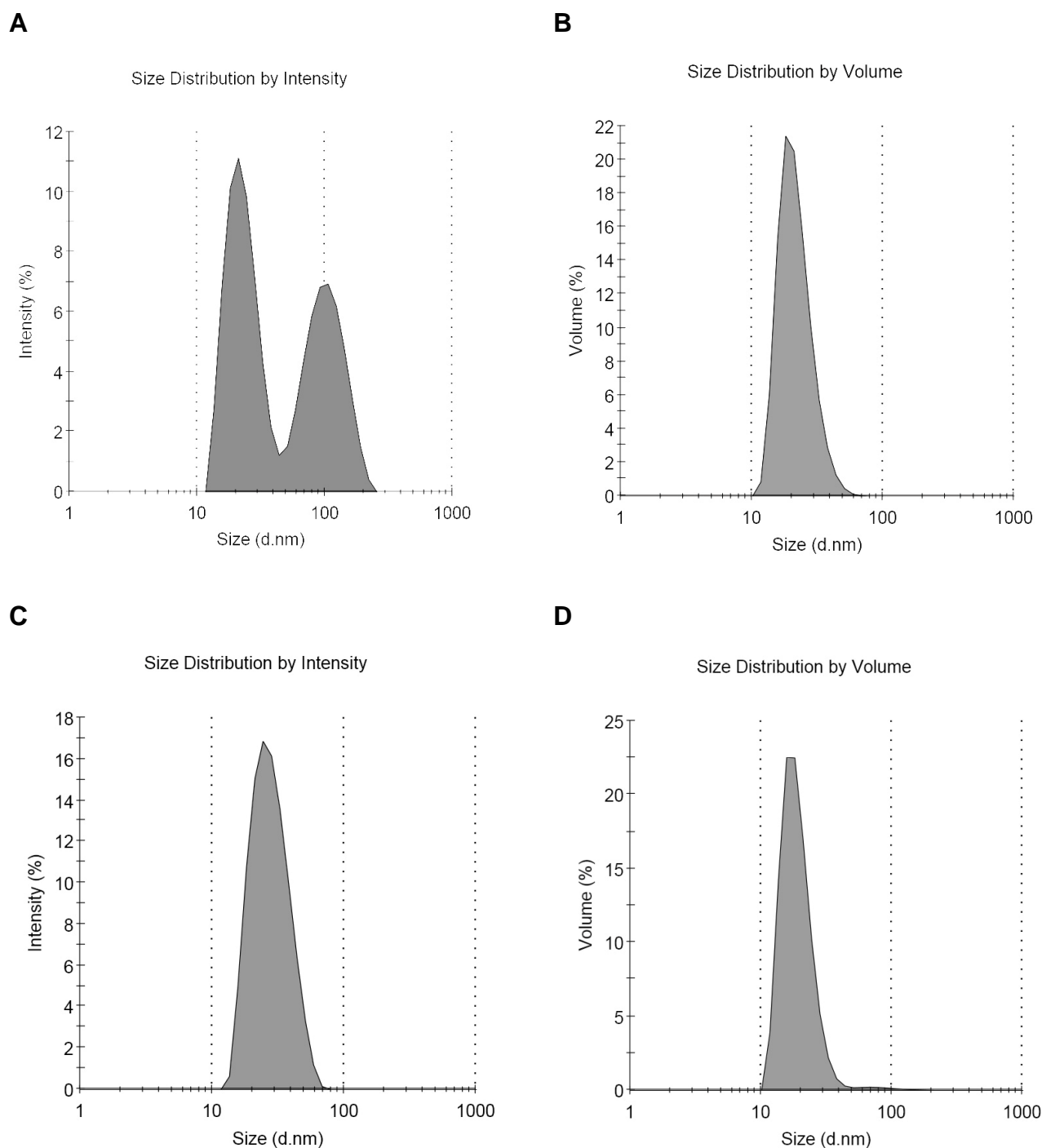


Figure 3.14 Dynamic light scattering of affinity (A, B) and ion exchange (C, D) purified MBP-hFMO5.

Dynamic light scattering of affinity purified and Q purified MBP-hFMO5 showed an increased monodispersity of the protein with only one peak visible in both graphs (Figure 3.14 C and D) and improved Pdl values of 0.134 ± 0.002 .

DLS analysis done with Q-purified MBP-hFMO5 where glycerol was added and Q-purified MBP-hFMO5 that was treated with Calbiosorb Adsorbent beads (Merck, Darmstadt, Germany) did not show significant differences. Further, Calbiosorb Adsorbent treated Q-purified MBP-hFMO5 was examined in various concentrations (i.e., 25, 10, 5, 2.5, and 0.25 mg/ml), but again no significant differences between the different concentrations could be observed (data not shown). For all Q-purified MBP-hFMO5 samples measured average Pdl values were 0.141 ± 0.037 .

3.4 Discussion

For structural and functional characterization of MBP-hFMO5, highly-purified and well characterized protein was needed. Especially crystallography experiments (chapter 4) require not only pure, but also monodispers and stable protein. Herein, a two-step purification method was developed and obtained protein was thoroughly characterized (Figure 3.15).

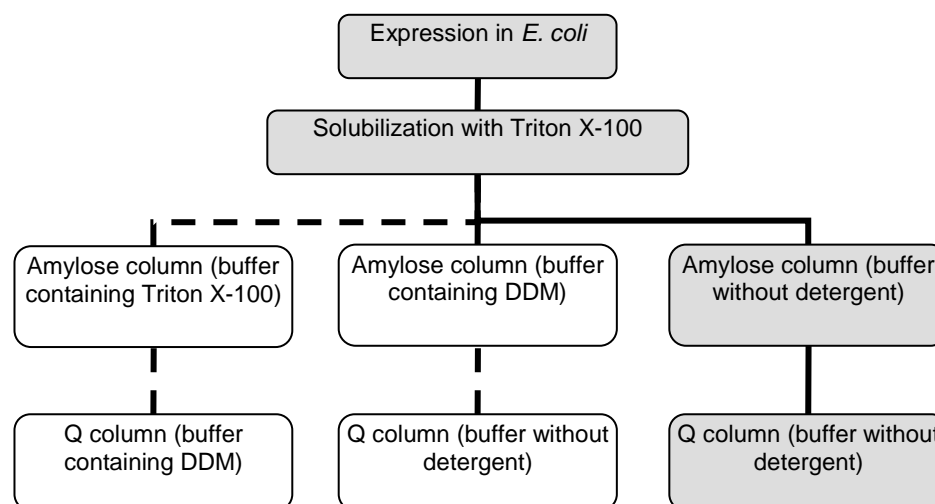


Figure 3.15 Overview of MBP-hFMO5 purification protocol development.

Dashed lines and white boxes stand for earlier steps in purification protocol development, solid lines and grey boxes represent final purification protocol as used for crystallography studies in chapter 4.

Human FMO5 was successfully expressed as *N*-terminal MBP-fusion protein (MBP-hFMO5) in *E. coli* DH1 α cells. After expression, a number of different detergents was tested for extraction of MBP-hFMO5, but only Triton[®] X-100 solubilized FMO5 sufficiently. The degree in which detergents are able to cross

membranes is said to be affecting the extent to which efficient solubilization occurs [le Maire *et al.*, 2000]. Triton[®] X-100 showed best solubilization ability. This might be due to the hydrophobic-hydrophilic properties of its polyethylene chains [Israelachvili, 1997] allowing Triton[®] X-100 to ‘flip-flop’ rapidly across membranes. In contrast, DDM has a strong hydrophilic head averting fast ‘flip flop’ across the membrane [Kragh-Hansen *et al.*, 1998; le Maire *et al.*, 2000] and thus proved unsuitable for extraction of MBP-hFMO5 as seen in this study. For subsequent studies, Triton[®] X-100 was chosen for extraction of MBP-hFMO5 from *E. coli*.

Affinity chromatography was used to purify the supernatant after cell lysis. This was done on an amylose column that binds to the MBP tagged to FMO5. Impurities could thus be eluted from the column during an extended washing step. Afterwards, the MBP and therefore the protein of interest was eluted with 3 mM maltose.

After this first purification step, a second step was added. MBP-hFMO5 was further purified on an ion exchange column. At pH 6, MBP-hFMO5 was bound to the resin of a 1 ml HiTrap Q column. Following a washing step with 65 mM NaCl in which impurities were removed, the protein of interest was eluted at a concentration of 250 mM NaCl.

Purified MBP-hFMO5 was characterized in order to confirm its suitability for kinetic and crystallization studies. Firstly, MBP-hFMO5 was supposed to be compared to commercially available hFMO5 (BD Gentest) in order to show that MBP-hFMO5 may be used for kinetic and structural studies instead of expensive purchasable FMO5. The kinetic parameters of recombinant expressed MBP-hFMO5 and commercially available FMO5 were determined and time dependence studies were carried out. These studies showed very similar kinetic behavior for both enzymes, with a K_m of roughly 120 μ M for both enzymes and a V_{max} of 2.1 and 3.2 for Gentest FMO5 and MBP-hFMO5, respectively. Time dependence studies also showed a linear behavior for both enzymes over 30 minutes validating the standard incubation time of 20 minutes. Thus, MBP-hFMO5 is very similar to commercially available FMO5 and may be used to study kinetic as well as structural parameters. In addition to lower costs, MBP-hFMO5 has the advantage that it can be purified easily utilizing its MBP-tag. Further, it can be produced in large quantities and higher purity may be achieved which is especially advantageous when attempting to crystallize the protein.

Enzyme stability was determined under various conditions at 4 °C. Results from this study showed that addition of glycerol and NADP⁺ to the sample improved MBP-hFMO5 stability 1.6-fold. Therefore, in subsequent crystallization studies these additives were added to the enzyme preparations.

For characterization of the protein, native gel electrophoresis and size exclusion chromatography were used to determine the oligomerization state of MBP-hFMO5. Compared to affinity purified MBP-hFMO5, the monodispersity improved significantly upon further purification via ion exchange chromatography. As shown on native gels, high detergent content seemed to separate protein molecules and MBP-hFMO5 that was primarily found to exist in a hexameric state after ion exchange chromatography and size exclusion chromatography changed its oligomerization state towards coexistence of mono-, tri-, and hexamers. Results from size exclusion chromatography of ion exchange purified MBP-hFMO5 also suggested hexameric state of the protein. The observation that FMO proteins possibly exist in higher ordered complexes has been made previously [Brunelle *et al.*, 1997] and a hexameric state of a native FMO enzyme was first presumed in 1972 by Ziegler and Mitchell [Ziegler *et al.*, 1972]. Although an MBP fusion could be affecting the oligomerization state of FMO, this was not the case for other MBP-tagged proteins like MBP-phenylalanin hydroxylase [Martinez *et al.*, 1995]. This was an important observation because multimerization could have a significant effect on crystallization.

Another important factor in crystallization studies is monodispersity of the protein. Thus, MBP-hFMO5 was characterized via DLS analysis. DLS is a method to determine particle size in solution and thus gives an estimate of the monodispersity of a given protein sample. It is a technique based on Brownian motion of particles. A laser beam is scattered by particles in solution and the time dependent change of the signal intensity compared to itself is used to determine the size of the particles. In case of small particles this change is fast whereas larger particles give 'speckle patterns' that fluctuate at a slower rate. Thus, the time gives an indication of the mean particle size. In addition, large particles will scatter more light than small ones and therefore, in case more than one peak is observed, the importance of the second peak will be represented more realistically if intensity is correlated to volume. This can also be observed with affinity column purified MBP-hFMO5 where two large peaks are visible when size is plotted against intensity whereas the second peak

(particles of larger size) decreases when size is plotted against volume. In comparison to only affinity-purified MBP-hFMO5 where impurities are obvious, DLS with Q-purified samples showed only a single peak. No significant difference could be observed between ion exchange purified MBP-hFMO5 and samples of the same purity that were treated with Calbiosorb Adsorbent beads added to remove residual detergent in the sample. Also, addition of 20 % glycerol and different concentrations of MBP-hFMO5 did not alter DLS results.

Studies showed that E6 oncoprotein from human Papillomavirus strain 16 fused to MBP formed soluble high molecular weight aggregates [Zanier *et al.*, 2007]. The size and amount of aggregated particles varied depending on expression conditions and *E. coli* strain, suggesting that aggregation took place *in vivo*. However, the aggregates were supposedly relatively monodispers and the E6 protein possessed a native-like fold. These features are advantageous in view of FMO5 crystallization attempts and seemed to be transferable to MBP-hFMO5. As shown for E6, MBP-hFMO5 seemed to be correctly folded, retaining its enzymatic activity. Also, DLS data suggested relatively monodispers protein, which is also in accordance with MBP-tagged E6 protein.

Overall, a cost-efficient way to obtain large quantities of highly purified MBP-hFMO5 for future structural and functional enzyme characterization studies was successfully developed and optimized.

4 Crystallography Studies of Human FMO5

4.1 Introduction

X-ray crystallography studies of proteins and enzymes are important tools to determine the 3D structure of a protein of interest. The three-dimensional structure is key to understanding the function of any protein. A crystal structure can give information about the location of the active site, substrate- and cofactor-binding domains, and about conformational changes a protein may undergo. This leads to a better understanding of the enzyme in respect of substrate binding, mechanism of action, as well as possible influence of different mutations. In case of FMO enzymes little is known about these properties because to date, the tertiary structure of the mammalian FMO enzymes is not known. Solving the three-dimensional structure of a mammalian FMO isozyme would help tremendously in the understanding of mammalian FMOs in general because they contain a large percentage of identical residues (50 – 58 % amino acid sequence identity in human FMO isozymes). Especially amino acids involved in FAD and NADPH binding are conserved throughout human FMOs and across species lines [Cashman, 1995].

4.1.1 FMO Model Structure

Although the tertiary structure of mammalian FMO enzymes has not been solved to date, model predictions by Cashman [Cashman, 2002] as well as Ziegler and Poulsen [Ziegler *et al.*, 1998] have been made for human FMO3. These were based on comparison with solved structures of other flavoproteins (Figure 4.1).

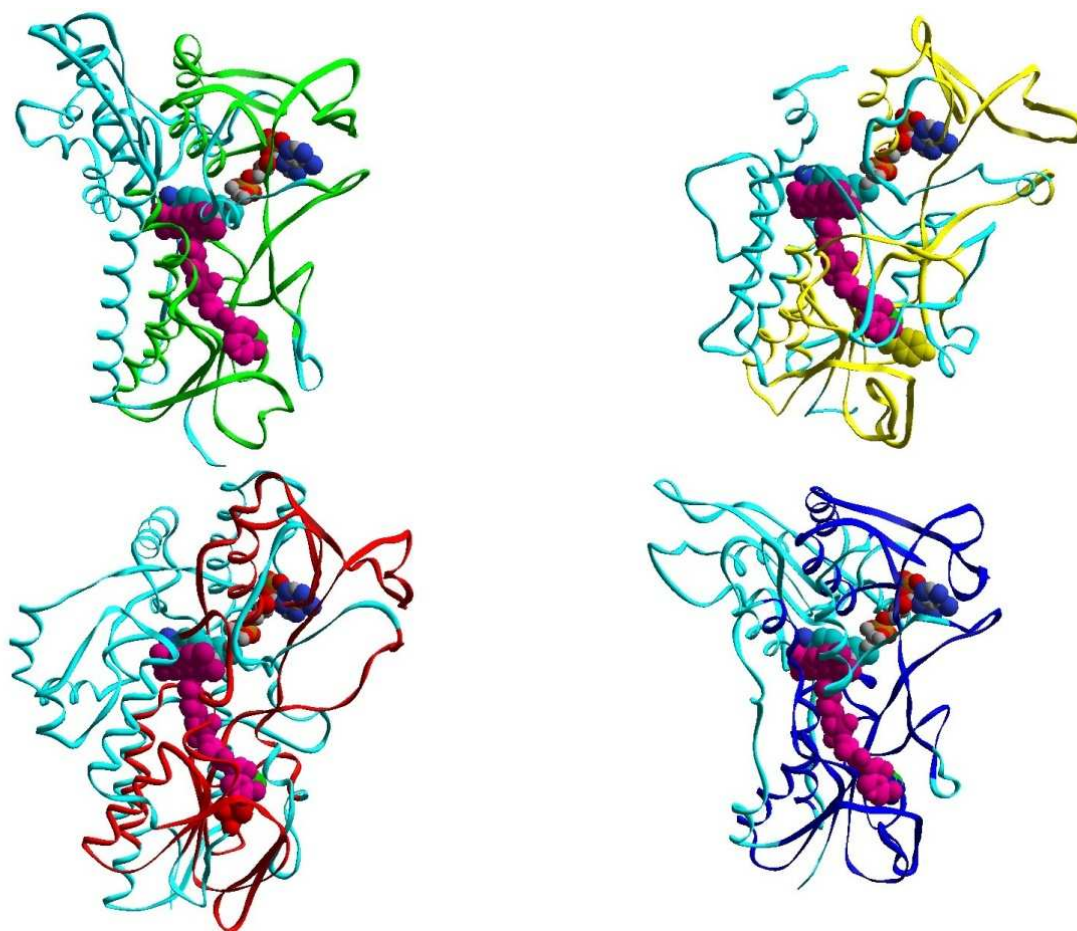


Figure 4.1 Proposed human FMO3 model.

The model is based on homology modeling with the protein structures 1get (green), 1vqw (yellow), 1w4x (red), and 1npx (blue). FAD (magenta) and NADPH are also shown. There are two domains in the structure, one being relevant for FAD, the other for NADPH binding. These two domains are relatively similar in all models whereas the rest of the structure is very divergent (cyan). Taken from [Cashman et al., manuscript in preparation].

In addition, the crystal structure of FMO from *Schizosaccharomyces pombe* (*S. pombe*) has been solved [Eswaramoorthy et al., 2006]. However, this information cannot be transferred to mammalian FMO enzymes without caution because *S. pombe* FMO consists of only 447 amino acids whereas human FMO1 – 5 are 532 to 558 amino acids in length and it shares only 21 to 23 % sequence identity with human FMOs.

4.1.2 FMO Protein Structure, Binding Sites, and Interaction with the Membrane

An overview of the different well conserved motives and their postulated functions was given by Krueger and Williams [Krueger *et al.*, 2005]. These functions were proposed based on the PRINTS database that catalogues protein fingerprints, conserved motives characterizing the protein family [Attwood *et al.*, 2003], and rabbit FMO2 as reference sequence for fingerprint analysis [Lawton *et al.*, 1990]. The main regions of interest for FMO3 are listed below and compared to the crystal structure of *S. pombe*.

4.1.2.1 FAD Binding

The FAD binding motif, GXGXXG, is supposed to be within the region of amino acids 3 – 26 and amino acids 27 – 51 are supposed to stabilize FAD binding through a EXXXXXGG motif [Krueger *et al.*, 2005]. Both regions seem essential and mutations in either one have been reported to result in loss of activity for FMO3 [Lawton *et al.*, 1993b]. Likewise, the nucleotide binding motif GXGXXG makes hydrogen-bonding contacts with the adenine nucleotide of FAD and the N3 of adenine binds to Arg 39 that is part of the EXXXXXGG motif in *S. pombe*.

4.1.2.2 NADPH Binding

The NADPH binding site is located in the region of residues 186 and 213. This proposal also seems consistent with the *S. pombe* structure, where NADPH is bound to the second nucleotide binding motif (GXGXX(G/A)). Here the nicotinamide is stacked with the isoalloxazine ring of the FAD so interaction between the bases of nicotinamide and flavin is possible [Eswaramoorthy *et al.*, 2006].

4.1.2.3 Substrate Binding

The substrate in the *S. pombe* structure (i.e., methimazole) is supposed to stack with the isoalloxazine ring of bound FAD and replace the NADPH in the structure. In case of mammalian FMO enzymes, this seems unlikely, because kinetic studies with FMO1 suggested that NADP⁺ does not leave the flavoprotein until after substrate oxygenation. Maybe a different binding mechanism applies here.

4.1.2.4 The FATGY-Motif and Membrane Interaction Sites

One other very prominent motif is the FATGY motif. It is a motif that is conserved in nearly all mammalian FMO enzymes and is located between amino acids 315 and 342 which represent the linkage between NADPH and the active site. Only FMO4 has a FTTGY and *S. pombe* FMO contains an YCTGY-motif.

The sites of membrane interaction are still unknown although considerable information about protein structure is already available [Krueger *et al.*, 2005; Lawton *et al.*, 1993a]. Maybe a crystal structure of a mammalian FMO enzyme will explain where FMO is bound to membranes.

4.1.3 Aim of the Study

The objective was to purify FMO5 in order to crystallize it and finally obtain a three-dimensional structure of a mammalian FMO enzyme. This would give answers to the location of binding sites for FAD, NADPH, and substrate and would lead to a better understanding of the mechanistic pathway of FMO mediated metabolism.

4.2 Materials and Methods

4.2.1 Reagents

Chemicals and reagents used in this study were purchased from Sigma-Aldrich Chemical Co. (St Louis, MO, USA) in appropriate purity. Buffers and other reagents were purchased from VWR Scientific, Inc. (San Diego, CA, USA). Polyethylene glycols (PEGs), crystallography screens, and crystallography plates (24 or 96 well sitting drop plates) were purchased from Hampton Research Corp. (Aliso Viejo, CA, USA).

4.2.2 Cloning and Expression

Human FMO5 was expressed as *N*-terminal maltose-binding fusion protein (MBP-hFMO5). Cloning and expression was done as described in section 3.2.2.1 with few changes. MBP-hFMO5 was expressed in *E. coli* DH1 α or *E. coli* BL21 cells. After induction, cells were incubated shaking either at room temperature for 20 hours or at 20 °C for 24 hours.

4.2.3 MBP-hFMO5 Purification

The purification procedure has already been described in chapter 3, but was optimized for crystallization trials.

After expression, *E. coli* cells were harvested by centrifugation at 6,000 *g* for 10 minutes and the cell pellet was frozen in order to increase yield. After resuspending the cell pellet in lysis buffer as described in section 3.2.2.1, cells were either disrupted via sonication as described above or by passage through a French press (Thermo Electron Corp., Needham Heights, MA, USA) operating at 20,000 psi depending on what method was available. For crystallization studies the cell pellet was only extracted once and after centrifugation the supernatant was loaded at 1 ml/min onto an amylose column (New England BioLabs, Ipswich, MA, USA) equilibrated with ten column volumes of buffer A' (i.e., 50 mM Na₂HPO₄, pH 8.4, containing 15 µg/ml FAD). The column was washed with at least ten column volumes of buffer A' and bound MBP-hFMO5 protein was eluted with 3 mM maltose in buffer A' at 1 ml/min. Eluted protein was concentrated with an Amicon Ultra-15 centrifugal filter unit with an Ultracel-50 filter (Millipore, Billerica, MA, USA).

Further protein purification was carried out on an FPLC system (Äkta-Purifier, GE Healthcare, Uppsala, Sweden) using a 1 ml Q HP column (GE Healthcare, Uppsala, Sweden) with a flow rate of 1 ml/min and a step gradient of 65 mM and 250 mM NaCl as described in chapter 3.3.2.

Refinement of the Lysis Protocol

The lysis buffer was changed to 50 mM phosphate buffer, pH 8.4, containing 0.5 % Triton[®] X-100, 0.1 % L- α -phosphatidylcholine, 0.5 mM phenylmethylsulfonylfluoride, 100 mM FAD, and 1 tablet /15 ml lysis buffer of Roche Mini Complete (EDTA-free) protease inhibitor mix (Roche, Indianapolis, IN, USA). This did not seem to improve crystallization and the original method was used for further MBP-hFMO5 purification.

4.2.4 Crystallization of MBP-hFMO5

4.2.4.1 Screening Kits

For Crystallization trials, laboratory space and equipment was generously provided by Prof. Dr. C. D. Stout at the Scripps Research Institute, La Jolla, CA, USA and

Prof. Dr. A. Scheidig at the ZBM, University of Kiel. Initial crystallization conditions for MBP-hFMO5 were screened using different commercially available 96-well screening kits with conditions ranging from pH 4.6 – 8.5, various precipitants including PEGs ranging from 200 to 20,000, and a wide variety of salts. Four 96-well crystal screening kits were set up in sitting drops using the vapor diffusion method: EasyXtal PEGs Suite (Qiagen Inc., Valencia, CA, USA), Crystal Strategy Screen I and II, and PACT premier (Molecular Dimensions, Apopka, FL, USA). The protein used was Q-purified MBP-hFMO5, in a concentration of 15 mg/ml containing 200 μ M NADP⁺ and 20 % glycerol. Protein solution was mixed with equal volumes of the reservoir solution.

4.2.4.2 Refinement Screens

The most promising results from initial 96-well screens were refined in terms of protein concentration as well as type and concentration of PEG and salt. 24-well plates were set up in sitting drops using the vapor diffusion technique.

Protein

In order to determine optimal protein concentration, plates were set up examining dependence of protein concentration vs. PEG concentration. Plates contained 0.3 M Na-acetate, 0.1 M Na-cacodylate, pH 6.5, PEG 2K monomethyl ether (PEG 2K MME). PEG concentrations screened were in the range of 20 – 30 %. Q-purified MBP-hFMO5 was mixed with an equal volume of reservoir solution in concentrations between 5 and 40 mg/ml.

PEG

Initial 96-well screens showed PEG to be the most successful precipitant. Thus, type and concentration was refined in further studies. Different concentrations of PEGs in the range of 400 – 20K were tested. Concentrations tested were 10 – 32 % for PEG 2K MME, 2 – 28 % for PEG 6K and 10K, and 2 – 22 % for PEG 20K. The plates were set up with 0.1 or 0.2 M sodium acetate as salt and 0.1 M Bis-Tris propane at pH 6.5. Protein solution in concentrations of 20 – 25 mg/ml was mixed with equal volumes of reservoir solution.

Salts

The best performing salts from the initial screens (i.e., Na-acetate, Na-formate, Na-tartrate, Na-phosphate, K-citrate, KSCN, MgCl₂, NH₄Cl, LiCl, and NaBr) were analyzed further. Conditions for salt screens were 0.1 M Na-cacodylate or 0.1 M Bis-Tris propane, pH 6.5, 22 – 26 % PEG 2K MME, and 0.1 or 0.2 M salt. Also, plates were set up containing 0.1 M Bis-Tris propane, pH 6.5, 24 – 28 % PEG 2K MME, and Na-acetate in the range of 0 - 1.5 M in order to determine the most advantageous salt concentration. Q-purified MBP-hFMO5 solution at 25 – 30 mg/ml was mixed with equal volumes of reservoir solution.

4.2.4.3 Influence of Detergents

Bio-Beads[®]-Treatment

In some cases, Q column-purified MBP-hFMO5 was treated with Bio-Beads[®] (Bio-Beads[®] SM Media, Bio-Rad, Hercules, CA, USA) in order to remove excess detergent (Triton[®] X-100 and/or DDM). Bio-Beads[®] were activated with methanol and washed thoroughly with 50 mM Bis-Tris buffer, pH 6.5. Afterwards, Bio-Beads[®] were slowly added to Q-purified protein.

For comparison between Bio-Beads[®]-treated and untreated MBP-hFMO5, plates were set up with 22 – 26 % PEG 2 K MME, 0.1 M Na-cacodylate or 0.1 M Bis-Tris propane at pH 6.5, and Na-formate, Na-acetate, MgCl₂, or NH₄Cl. Protein solution at a concentration of 30 mg/ml was left untreated or was treated with activated Bio-Beads[®] and crystallization drops were set up with either protein solution mixed with equal volumes of reservoir solution.

Detergent Refinement in the Purification Protocol

In order to remove Triton[®] X-100 quantitatively, the purification protocol was refined: The protein was still extracted in Triton[®] X-100, but after binding to amylose resin the protein was washed and further purified with buffer devoid of detergent.

Influence of Detergents

The influence of addition of a wide variety of detergents to crystallization drops was studied. Detergents tested are listed in Table 4.1. The reservoir solution consisted of 26 % PEG 2K MME, 0.2 M Na-acetate, and 0.1 M Bis-Tris propane, pH 6.5. Crystallization drops consisted of equal volumes of reservoir solution and Bio-

Table 4.1 Detergents used in crystal screens to determine influence of detergents on crystallization of MBP-hFMO5.

Detergent	Concentration	Detergent	Concentration
217 FA	1 and 2 x CMC	Cymal [®] -1	1 x CMC
231 FA	1 and 2 x CMC	Cymal [®] -2	1 x CMC
234 FA	1 and 2 x CMC	Cymal [®] -5	1 x CMC
235 FA	1 and 2 x CMC	Cymal [®] -6	1 x CMC
238 FA	1 and 2 x CMC	Cymal [®] -7	1 x CMC
C-HEGA [®] -10	1 and 2 x CMC	n-Nonyl- β -D-glucopyranoside	1 and 2 x CMC
Sucrose-monolaurate	1 x CMC	C ₈ E ₄	1 x CMC
CTAB	1 x CMC	C ₁₂ E ₈	1 x CMC
DDAO	1 x CMC	FOS-CHOLINE [®] -10	1 x CMC
n-Octanyl-sucrose	1 x CMC	FOS-CHOLINE [®] -12	2 x CMC
HECAMEG	1 and 2 x CMC	β -Octylglucoside	1 x CMC
n-Decanoyl-sucrose	1 x CMC	n-Octyl- β -D-glucopyranoside	1 and 2 x CMC
MEGA-8	1 x CMC	CHAPS	1 x CMC
ZWITTERGENT [®] 3-10	1 x CMC	n-Decyl-maltoside	1 x CMC
1-s-Nonyl- β -D-thio-glucoside	1 x CMC	n-Octyl-maltoside	1 x CMC
n-Nonyl- β -D-thio-maltoside	1 x CMC		

FA, facial amphiphile; C-HEGA[®]-10, Cyclohexylbutanoyl-N-hydroxyethylglucamide; CTAB, Cetyltrimethylammoniumbromid; DDAO, N,N-Dimethyl-1-dodecanamine-N-oxide; HECAMEG, Methyl-6-O-(N-heptylcarbamoil)- α -D-glucopyranoside; MEGA-8, Octanoyl-N-methylglucamide; ZWITTERGENT[®] 3-10, n-Decyl-N,N-dimethyl-3-ammonio-1-propanesulfonate; Cymal[®]-1-7, Cyclohexyl-alkyl- β -D-maltoside; C₈E₄, tetra(ethylene glycol) mono-octylether; C₁₂E₈, octa(ethylene glycol) dodecyl monoether; FOS-CHOLINE[®]-10, n-Decylphosphocholine; FOS-CHOLINE[®]-12, n-Dodecylphosphocholine; CHAPS, 3-[(3-Cholamidopropyl)-dimethylammonio]-1-propane sulfonate

Beads[®]-treated Q-pure MBP-hFMO5 (30 mg/ml) spiked with detergent to yield a final concentration of 1 or 2 times their CMC.

4.2.4.4 X-Ray Diffraction Measurement

X-ray diffraction measurement was done by Dr. Andrew Annalora (Scripps Research Institute, La Jolla, CA, USA). Several crystals were screened at the Stanford Synchrotron Radiation Laboratory (SSRL, Palo Alto, CA, USA) on Beamline 7-1 and 11-1. Prior to flash freezing and storage, several preparation conditions were tested: A quick (10 – 30 seconds) or long (30 seconds – 2 minutes) soak of the crystals in buffer identical to the reservoir condition but with addition of 20 % glycerol, and/or 17 % ethylene glycol was done for cryoprotection. Also, crystals were frozen directly from the drop with and without a quick soak in 100% paraffin oil.

4.2.5 Crystallography Studies of hFMO5 without MBP-tag

4.2.5.1 Cleavage of MBP-hFMO5 with Factor Xa

250 µg MBP-hFMO5 were incubated in a total volume of 100 µl 100 mM phosphate buffer, pH 7.6, containing 0.2 mM NADPH and 5 µg factor Xa (New England BioLabs, Ipswich, MA, USA) for 1.5 or 3 hours at 37 °C. In order to prevent potential precipitation of cleaved FMO5, incubations were also done in the presence of detergent (i.e., CHAPS). To compare rate of degradation or loss of activity during the 1.5 or 3 hour incubation period, 3-hour control incubations were done without factor Xa at 37 °C and at 4 °C. Again, control incubations were also done in the presence of CHAPS. The incubation scheme is shown in Table 4.2.

Table 4.2 Incubation scheme of factor Xa cleavage reaction.

Sample	Incubation conditions
A	incubation for 1.5 hrs at 37 °C + factor Xa
B	incubation for 3 hrs at 37 °C + factor Xa
C	incubation for 1.5 hrs at 37 °C + factor Xa + CHAPS
D	incubation for 3 hrs at 37 °C + factor Xa + CHAPS
E	incubation for 3 hrs at 37 °C
F	incubation for 3 hrs at 4 °C
G	incubation for 3 hrs at 37 °C + CHAPS
H	incubation for 3 hrs at 4 °C + CHAPS

After 1.5 or 3 hour incubation, samples were put on ice and immediately assayed for 8-DPT *N*-oxygenation activity as described in section 3.2.4.2 with minor changes. Briefly, a standard incubation mixture contained 100 mM potassium phosphate buffer, pH 8.4, 0.2 mM NADPH, 0.25 mM DETAPAC, and 75 µg/ml MBP-hFMO5. After extraction of metabolites and remaining substrate in dichloromethane, HPLC analysis was done on a Waters HPLC system (Waters 600E controller and Waters Autosampler 700 Satellite WISP interfaced to a Waters 486 Absorbance Detector). Chromatographic separation of analytes was done on a LiChrospher-Si 60 (250 x 4.6 mm, 5 µm; Merck, Darmstadt, Germany) with a mobile phase of 80 % methanol/20 % isopropanol/0.025 % HClO₄ (v/v/v). The flow rate was 1.5 ml/min and the total run time was 15 minutes. The wavelength for UV detection was set to 243 nm. The retention times for 8-DPT and 8-DPT *N*-oxide were 5.5 and 4.0 minutes, respectively.

In addition, immediately after incubation with factor Xa, samples were analyzed by SDS-PAGE and Coomassie Blue staining. 2 µl of protein samples were fractionated by electrophoresis on a 10 % polyacrylamide gel under denaturing conditions and stained with Coomassie Blue. Protein bands were analyzed by densitometry using Adobe Photoshop Elements (Version 7).

4.2.5.2 Purification of hFMO5 from MBP

After cleavage of MBP-hFMO5, hFMO5 had to be separated from remaining factor Xa, MBP-tag and non-cleaved MBP-hFMO5. This was attempted by various methods including ion exchange chromatography, affinity chromatography, and size exclusion chromatography.

Affinity Chromatography

MBP-hFMO5 was cleaved with factor Xa after affinity purification and subsequent ion exchange purification. The ion exchange purification step also served as buffer exchange to eliminate remaining maltose from the first affinity purification step.

A second affinity chromatography step was performed after cleaving the protein. 500 µl amylose resin (New England BioLabs, Ipswich, MA, USA) equilibrated with 50 mM phosphate buffer, pH 8.5, was incubated with 5 mg cleaved MBP-hFMO5 over night rotating at 4 °C. The next day, amylose resin was removed by filtration and bound protein was eluted with 3 mM maltose. Flow through (supposedly containing cleaved FMO5) and eluted protein (which should contain the MBP-tag) was then analyzed via SDS-PAGE and 8-DPT HCl *N*-oxygenation activity assay as described in section 3.2.4.2.

Ion Exchange Chromatography

Purification was carried out on an FPLC system (Äkta-Purifier, GE Healthcare, Uppsala, Sweden) at the ZBM, University of Kiel. Cleaved MBP-hFMO5 protein was loaded onto a HiTrap Q HP column equilibrated with 50 mM Bis-Tris buffer, pH 6, at 0.5 ml/min. The column was washed with at least ten column volumes of equilibration buffer. A linear salt gradient of 0 – 65 % 50 mM Bis-Tris buffer, pH 6 containing 1 M NaCl was applied to elute bound protein.

Size Exclusion Chromatography

Another attempt to purify hFMO5 from uncleaved MBP-hFMO5, MBP, and factor Xa was purification via size exclusion chromatography. Purification was carried out on a FPLC system (Äkta-Purifier, GE Healthcare, Uppsala, Sweden) at the ZBM, University of Kiel, Germany. Cleaved protein was loaded at 0.5 ml/min onto a Superdex 200 10/300GL size exclusion column (GE Healthcare, Uppsala, Sweden)

equilibrated with 50 mM Bis-Tris buffer, pH 6. Eluted fractions were concentrated with Microcon centrifugal filter units (Ultracel YM-30, Millipore, Billerica, MA, USA) and analyzed via SDS-PAGE.

4.3 Results

4.3.1 Crystallization of MBP-hFMO5

4.3.1.1 Screening Kits

Crystallization involves phase transition where an initially solubilized protein comes out of solution to form crystals as solution is slowly brought to supersaturation. Once nuclei have formed, protein concentration in the solution drops and no new crystals will form whereas already existing crystals one may grow [Chayen, 1998]. Vapor diffusion is the most widely used technique and involves a drop composed of a mixture of protein sample and crystallization reagent. The concentration within the drop is usually lower than that needed for crystallization. The drop is equilibrated against a liquid reservoir with higher concentrations. To achieve equilibrium, water vapor leaves the drop and the concentration within the drop will slowly increase [Chayen, 1998]. At best, crystals will form, but also amorphous precipitate or coadunate crystals may be observed.

The two most common set-ups for crystallization studies are hanging and sitting drop techniques. In the hanging drop technique, the drop of protein and reagent hangs from a coverslip above the reservoir solution. In case of the sitting drop technique, the protein-reservoir drop sits on a surface closer to the reservoir [Chayen, 1998].

The results of all screens showed that overall a lower pH, i.e., 6 - 6.5, seemed favorable. Also, PEGs were the preferred precipitant. A variety of salts was tested and those that performed best were: Na-acetate, Na-formate, Na-tartrate, Na-phosphate, K-citrate, KSCN, MgCl₂, NH₄Cl, LiCl, and NaBr. Especially chloride- and acetate-salts gave promising results.

4.3.1.2 Refinement Screens

The crystallization conditions were refined starting with the most promising conditions found in the 96-well screens. Optimal protein concentration as well as PEG type and concentration were determined and influence of salt concentration was evaluated.

Protein

Results from screens where protein concentration was screened against PEG 2K MME concentration showed that higher protein concentrations of 20 – 30 mg/ml gave better results than lower concentrations (Figure 4.2).

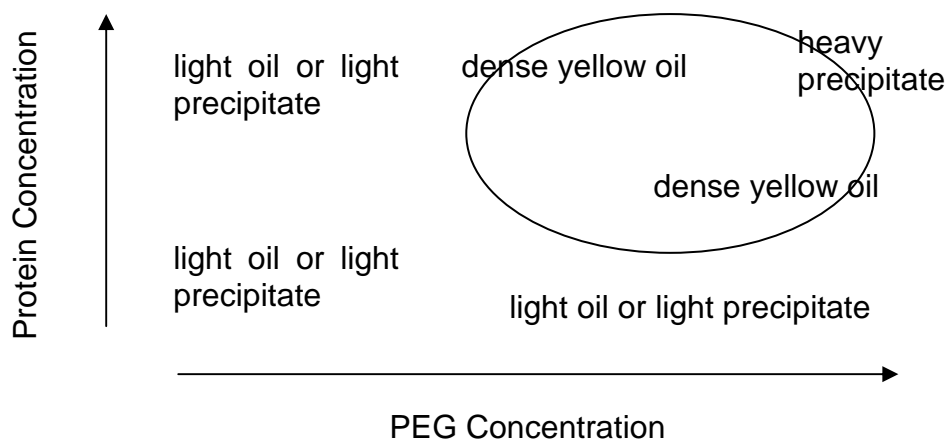


Figure 4.2 Protein concentration vs. PEG 2K MME concentration.

Crystallization conditions: 20 – 30 % PEG 2K MME, 0.3 M Na-acetate, and 0.1 M Na-cacodylate, pH 6.5. Drops consisted of equal volumes of reservoir solution and 5 – 40 mg/ml MBP-hFMO5.

PEG

The best results when evaluating various PEGs at different concentrations were obtained with PEG 2K MME, PEG 6K and PEG 10K. Lower molecular weight-PEGs as well as PEG 20K mostly led to heavy precipitation or no precipitation at all. For PEG 2K MME the preferred concentration range was 24 – 28 %, for PEG 6K it was 20 – 28 % and PEG 10K performed best at concentrations between 23 and 27 %. With these PEGs dense yellow oil-like phases as shown in Figure 4.3 were obtained.

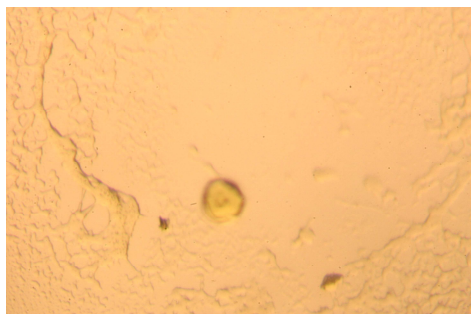


Figure 4.3 Picture of the yellow oil-like phase.

Crystallization condition: 0.1 M Bis-Tris propane, pH 6.5, 0.2 M Na-acetate, and 26 % PEG 2K MME. Drops consisted of equal volumes of reservoir solution and 30 mg/ml MBP-hFMO5.

Salts

The best performing salts from initial screens (Na-acetate, Na-formate, Na-tartrate, Na-phosphate, K-citrate, KSCN, MgCl₂, NH₄Cl, LiCl, and NaBr) were analyzed further and the most promising were Na-formate, MgCl₂, NH₄Cl, and Na-acetate. The latter was then used to set up further crystallography experiments. Evaluation of Na-acetate concentrations did not show an obvious trend of whether low or high salt concentrations are preferable.

Maltose

As previously reported, MBP may adopt distinct conformational states depending on presence or absence of maltose [Boos *et al.*, 1998; Spurlino *et al.*, 1991]. Thus, it is important to avoid partial occupancy of maltose that might result in mixed conformational states and interfere with crystallization by inhibiting formation of well-ordered crystals [Smyth *et al.*, 2003]. In general, addition of maltose to the protein solution gave more “dense yellow oil” (Figure 4.2). Thus, in addition to 200 μM NADP⁺ and 20 % glycerol, maltose was routinely added to protein preparations in a concentration of 100 μM.

4.3.1.3 Influence of Detergents

Bio-Beads[®]-Treatment

Crystallization trials showed that preparation of MBP-hFMO5 without detergent on Q column did not lead to crystals but rather resulted again in dense yellow oil phases

as shown in Figure 4.3. These were probably due to residual Triton[®] X-100 from the first purification step. Also, addition of different amounts (0.05 – 1 x CMC) of DDM to crystallization drops did not result in crystal growth.

It was found that Triton[®] X-100 is strongly adsorbed onto Bio-Beads[®] SM-2, a neutral porous polystyrene-divinylbenzene adsorbent [Holloway, 1973]. Thus, in order to remove excess Triton[®] X-100 from the sample, Bio-Beads[®] were added. It is remarkable, that even after addition of excess amounts of Bio-Beads[®], MBP-hFMO5 stayed in solution. From this experiment and the solubilization study it can be concluded that detergent (i.e., Triton[®] X-100) is necessary for protein extraction from *E. coli*, but that for subsequent purification procedures, no further addition of detergent is required.

A comparison was made between crystallization plates containing protein treated with Bio-Beads[®] and untreated protein. Overall, Bio-Beads[®]-treatment of MBP-hFMO5 resulted in more dense yellow oil phases and brown spheres (Figure 4.4).

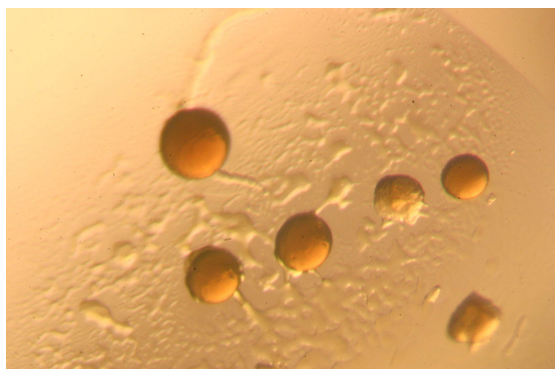


Figure 4.4 Example of dense yellow oil and brown spheres as seen after Bio-Beads[®]-treatment of purified MBP-hFMO5.

Crystallization condition: 0.1 M Bis-Tris propane, pH 6.5, 0.1 M Na-acetate, and 30 % PEG 2K MME. Drops consisted of equal volumes of reservoir solution and 25 mg/ml MBP-hFMO5 treated with Bio-Beads[®].

The brown spheres seem to be a pre-stage of crystals because they cracked when shattered producing sharp edges (Figure 4.5). Thus, MBP-hFMO5 is not only stable without detergent, it also seems that detergent removal is important for crystal growth.

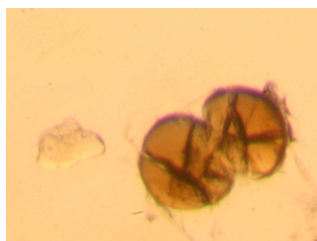


Figure 4.5 Picture showing a scattered sphere.

Crystallization condition: 0.1 M Bis-Tris propane, pH 6.5, 0.1 M Na-acetate, and 20 % PEG 20K. Drops consisted of equal volumes of reservoir solution and 25 mg/ml MBP-hFMO5 treated with Bio-Beads[®].

Detergent Refinement in the Purification Protocol

Earlier crystallization screens showed better results after addition of Bio-Beads[®] to MBP-hFMO5. Hence, it seems that complete removal of Triton[®] X-100 is necessary for crystal growth. In order to remove Triton[®] X-100 quantitatively, the purification protocol was refined.

Although, crystallization plates did not yield crystals, this study verified the earlier assumption that MBP-hFMO5 does not need detergent after extraction from the cells. Most likely, MBP-hFMO5 is not membrane bound but rather only associated with the membrane. In subsequent purification procedures Triton[®] X-100 was used solely for extraction purposes, but no detergent was used on either of the columns.

Influence of Detergents

The influence of a great variety of detergents on crystallization of MBP-hFMO5 was examined. Almost all wells gave good results yielding in previously observed dense yellow oil phases, spheres, or crystals. The phase transition of yellow oil to brown spheres and yellow crystals is shown in Figure 4.6.

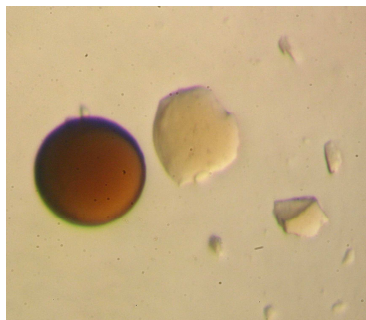
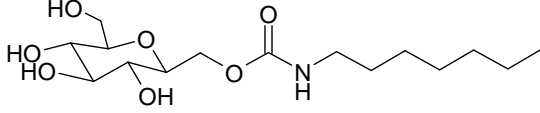

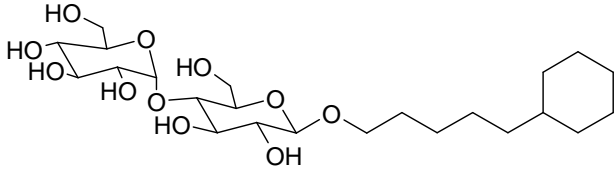

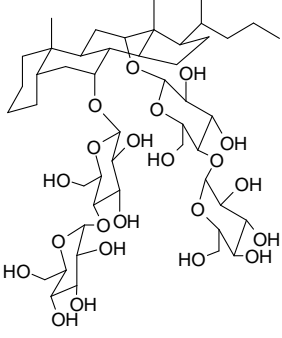

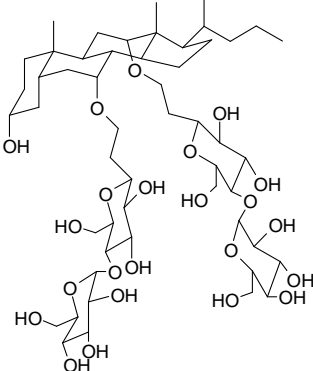
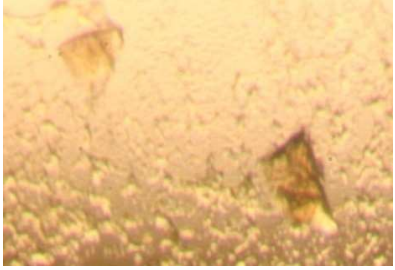


Figure 4.6 Picture showing the transition of yellow oil-like phase (in the center) to round spheres (on the left) and yellow crystals (on the right).

Crystallization condition: 0.1 M Bis-Tris propane, pH 6.5, 0.2 M Na-acetate, and 26 % PEG 2K MME. Q-purified MBP-hFMO5 solution at 30 mg/ml was mixed with an equal volume of reservoir solution and the crystallization drop was spiked with 1 x CMC Cymal[®]-6.

Addition of the following detergents led to best results: HECAMEG, Cymal[®]-5, and facial amphiphiles 217 and 231. Some examples are listed in Table 4.3.

Table 4.3 Examples of wells from screens with drops containing MBP-hFMO5 that were spiked with different detergents.

Detergent added	Picture of well
<p>HECAMEG</p> 	
<p>Cymal[®]-5</p> 	
<p>217 FA</p> 	
<p>231 FA</p> 	

Crystallization conditions were 26 % PEG 2K MME, 0.2 M Na-acetate, and 0.1 M Bis-Tris propane buffer at pH 6.5. Drops consisted of equal volumes of reservoir solution and 30 mg/ml Bio-Beads[®]-treated Q-pure MBP-hFMO5 spiked with detergent at 1 x (Cymal[®]-5, 217 FA and 231 FA) or 2 x (HECAMEG) their CMC. 231 FA (facial amphiphile), 3 α -hydroxy-7 α ,12 α -bis[(β -D-maltopyranosyl)ethoxy]cholane; 217 FA, 7 α ,12 α -bis[(β -D-maltopyranosyl)]cholane.

As shown in the SDS gel (Figure 4.7) the crystals proved to be MBP-tagged FMO5. Crystals dissolved in buffer were run on SDS gel and a band could be observed around 100 kDa. These results show that MBP-tagged human FMO5 is crystallizable.

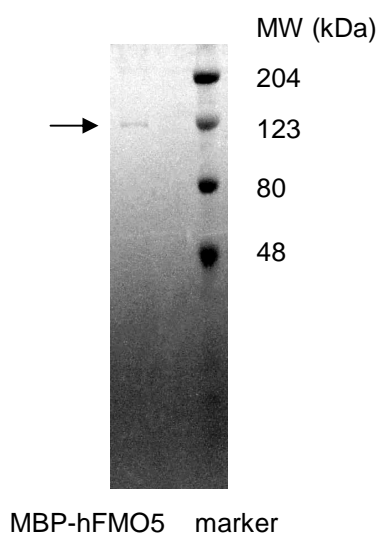


Figure 4.7 SDS gel of redissolved MBP-FMO5 crystal.

High Molecular Weight Prestained marker (Bio-Rad, Hercules, CA, USA) was used as MW protein marker. Arrow points to MBP-hFMO5.

However, these coadunate crystals did not yield satisfactory diffraction patterns and none of the preparation conditions prior to flash-freezing that were tested improved diffraction. The crystals obtained lacked in optical clarity, smooth faces and had only few sharp edges. Also, arrays were probably not ordered well enough to obtain evaluable diffraction patterns.

4.3.2 Crystallography Studies of hFMO5 without MBP-tag

Crystallization studies with purified MBP-hFMO5 led to a number of crystals in various conditions. Unfortunately, no satisfactory diffraction pattern could be obtained from these crystals. Thus, crystallization or purification conditions needed to be altered in order to improve crystal growth. Further refinement of purification conditions such as including additional protease inhibitors (Roche Mini Complete (EDTA-free) protease inhibitor mix) in the lysis buffer, usage of an extended linear NaCl gradient in the ion exchange purification step, addition of NADP⁺ after purification but before concentrating the protein, or air-fuging the protein before crystallization plates are set up, were tested but did not lead to improved crystallization.

Although expression and purification as MBP-fusion protein has numerous advantages, for crystallography experiments an MBP-tag might be problematic. It has been suggested that MBP hinders crystal growth by introducing conformational heterogeneity [Smyth *et al.*, 2003]. Since *FMO5* had been cloned into a pMAL-c2 vector that contains a protease sensitive site right after the MBP sequence (i.e., IEGR), the MBP-tag may be removed from FMO5 by proteolytic splicing of the fused protein from MBP with factor Xa. Consequently, FMO5 could be separated from its tag and crystallization studies with purified FMO5 could be attempted that might lead to good diffracting crystals.

4.3.2.1 Cleavage of MBP-hFMO5 with Factor Xa

After 1.5 or 3 hour incubation of MBP-hFMO5 with factor Xa, the samples were analyzed in regards to 8-DPT *N*-oxygenation activity and extent of cleavage. SDS-PAGE showed 67 % cleavage after 1.5 and 73 % after 3 hours incubation (Figure 4.8).

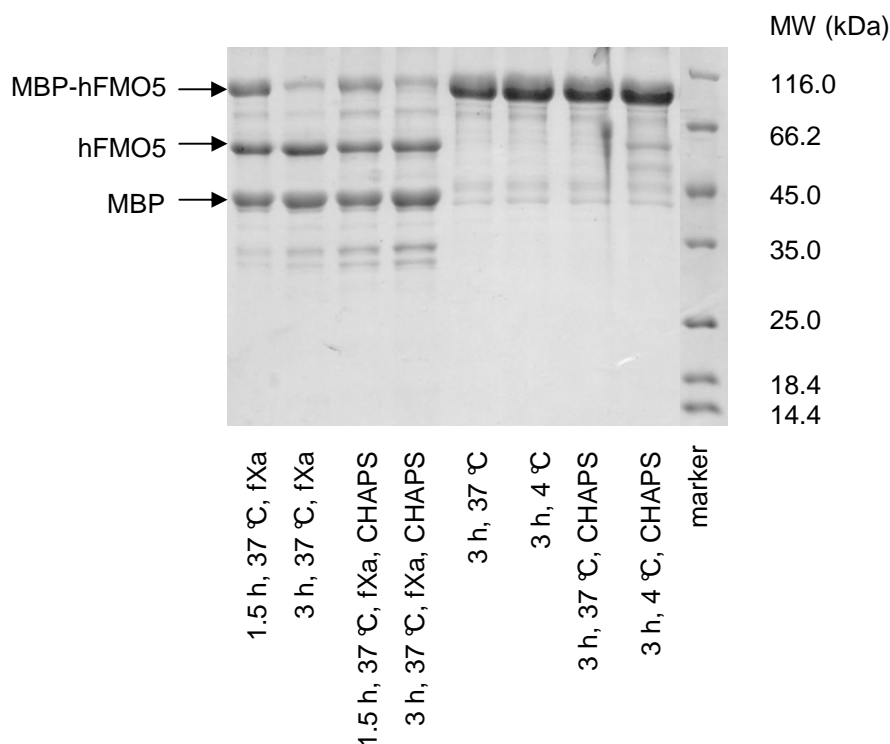


Figure 4.8 Coomassie stained SDS gel of fractions A-H (see also Table 4.2).

peqGOLD Protein-Marker I (Peqlab, Erlangen, Germany) was used as MW protein marker. Arrows point to MBP-hFMO5 and the cleaved products, hFMO5 and MBP.

In the presence of NADPH, hFMO5 retains almost 100 % of its 8-DPT *N*-oxygenation activity after 1.5 or 3 hour incubation at 37 °C compared to enzyme stored at 4 °C (Figure 4.9). Also, cleavage did not precipitate or inactivate the enzyme. Thus, including CHAPS in the incubation mixture was not necessary. It even seems disadvantageous to add CHAPS because 8-DPT *N*-oxygenation activity decreased about 65 % compared to MBP-hFMO5 stored at 4 °C (Figure 4.9).

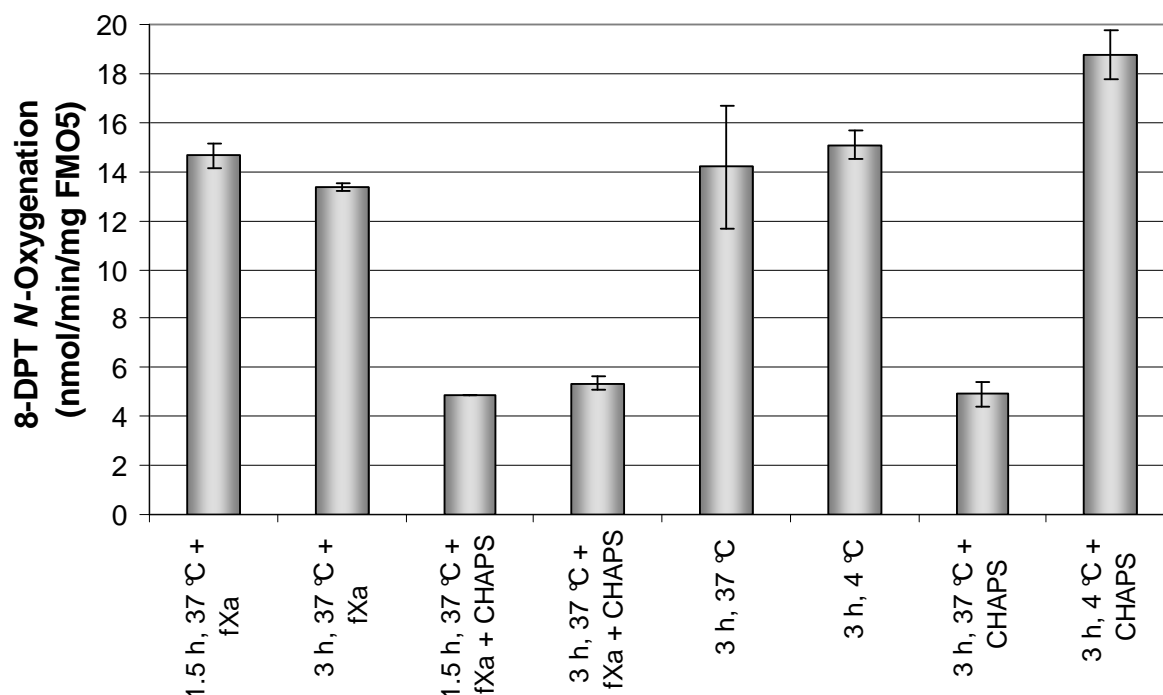


Figure 4.9 8-DPT *N*-oxygenation of fractions A – H (see also Table 4.2).

4.3.2.2 Purification of hFMO5 from MBP

Affinity Chromatography

Separation of hFMO5 from MBP was attempted via affinity chromatography on amylose resin. SDS-PAGE as well as HPLC based enzyme activity analysis showed no separation of hFMO5 and MBP (Figure 4.10). HPLC analysis showed the main activity in the eluate rather than the flow through which is in agreement with the SDS gel. It is possible that cleaved hFMO5 stays somewhat associated with the cleaved MBP-tag.

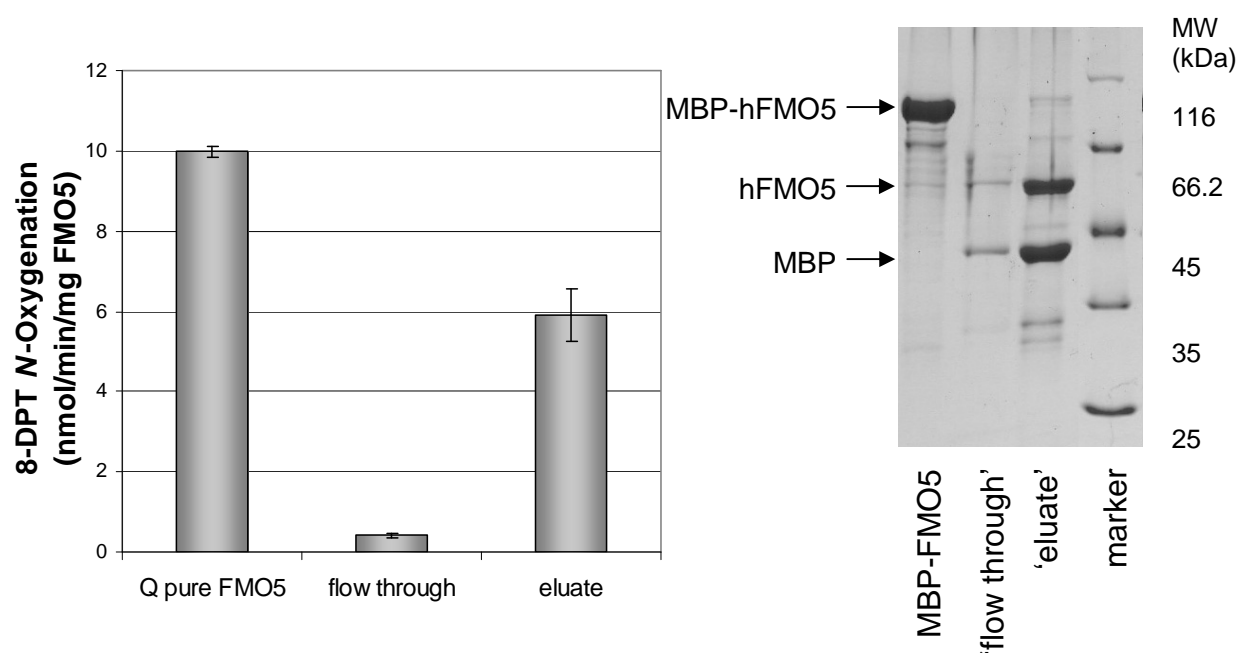


Figure 4.10 Results of 8-DPT *N*-oxygenation activity assays and Coomassie stained SDS gel of amylose purified, cleaved MBP-hFMO5.

peqGOLD Protein-Marker I (Peqlab, Erlangen, Germany) was used as MW protein marker. Arrows point to Q-pure MBP-hFMO5 and the cleaved products, hFMO5 and MBP.

Ion Exchange Chromatography

Another attempt to separate hFMO5 from MBP, MBP-hFMO5, and factor Xa was purification on a HiTrap Q HP anion exchange column. The resulting chromatogram is shown in Figure 4.11. The fractions were analyzed with SDS-PAGE (Figure 4.12). Both, chromatogram and SDS gel show good separation of MBP (peak 1) and FMO5 (peak 2), however, hFMO5 co-elutes with uncleaved MBP-hFMO5.

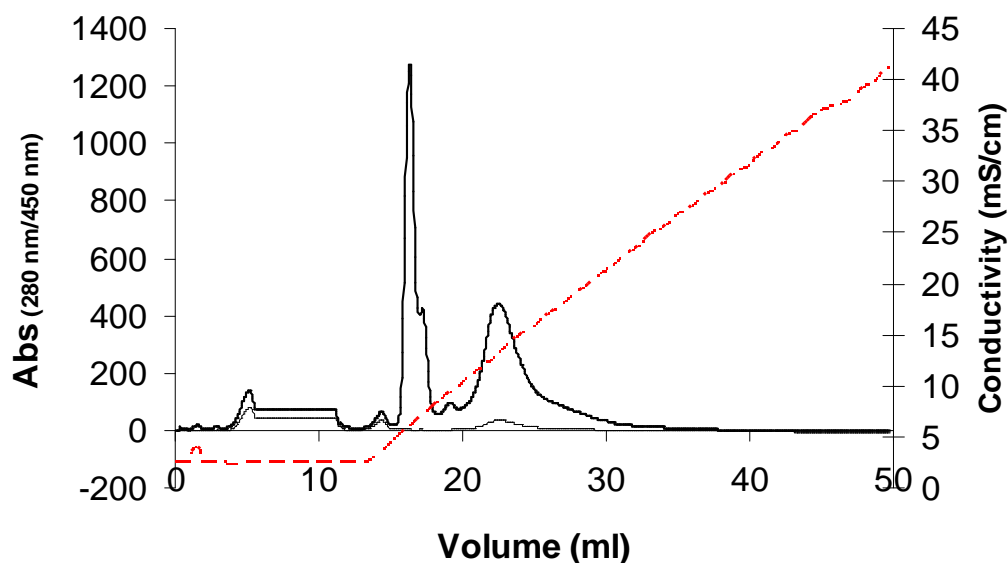


Figure 4.11 Chromatogram of Q-column purified cleaved MBP-hFMO5.

Absorbance at 280 nm is shown as solid line, absorbance at 450 nm as dotted line, and conductivity is shown as dashed line.

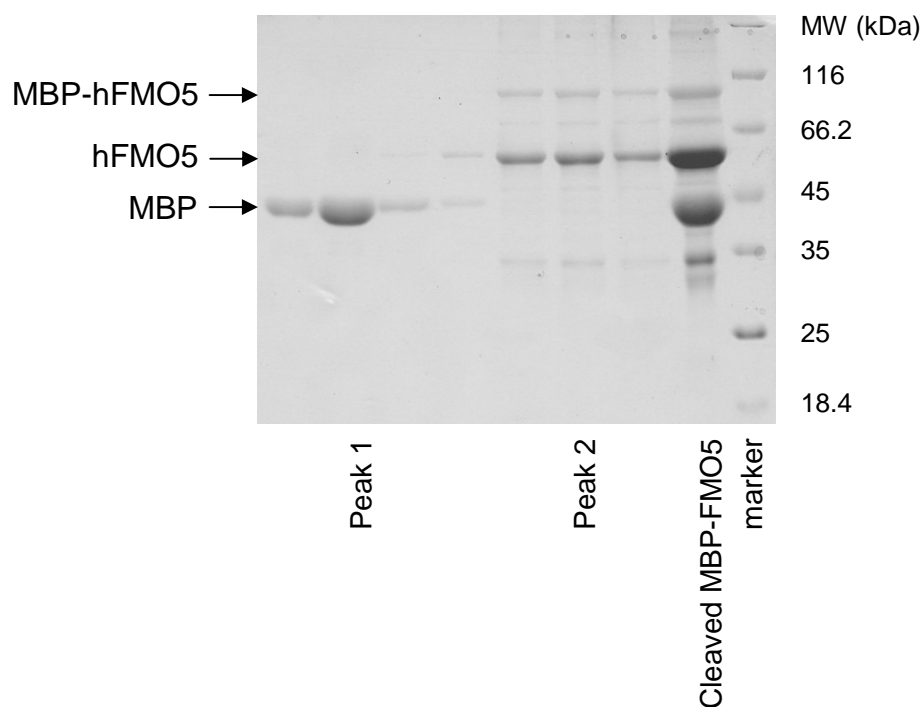


Figure 4.12 Coomassie stained SDS gel of fractions of Q column-purified cleaved MBP-hFMO5.

peqGOLD Protein-Marker I (Peqlab, Erlangen, Germany) was used as MW protein marker. Arrows point to Q-pure MBP-hFMO5 and the cleaved products, hFMO5 and MBP.

Size Exclusion Chromatography

As third method for FMO5 purification, size exclusion chromatography was tested. The chromatogram obtained from SEC is shown in Figure 4.13 and the SDS gel of the corresponding fractions is shown in Figure 4.14. In a first peak, hFMO5 elutes clearly visible with a band at ~ 60 kDa. In a second peak, MBP elutes giving a band at ~ 40 kDa in the SDS gel. However, as with anion exchange chromatography, hFMO5 co-elutes with MBP-hFMO5.

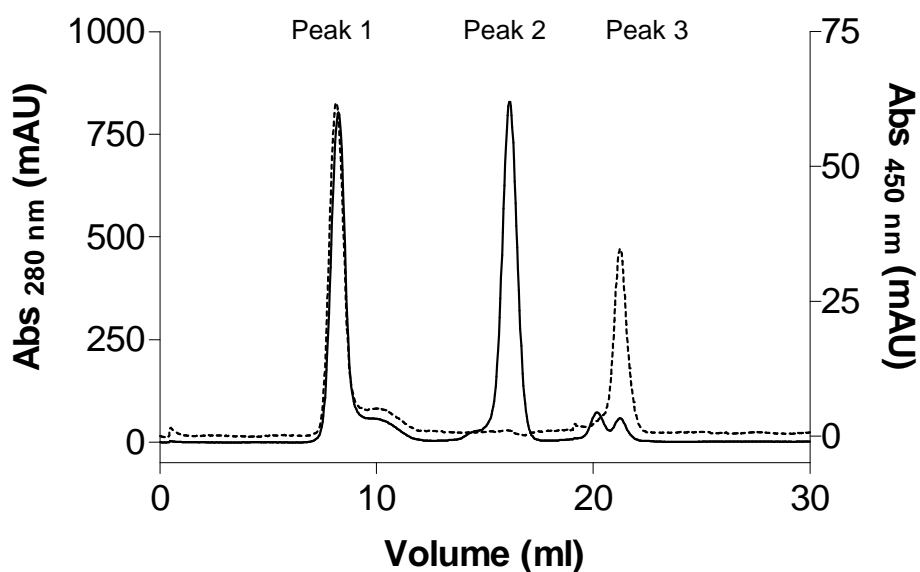


Figure 4.13 Elution profile of factor Xa cleaved MBP-hFMO5 on Sephadex 200 10/300GL size exclusion column.

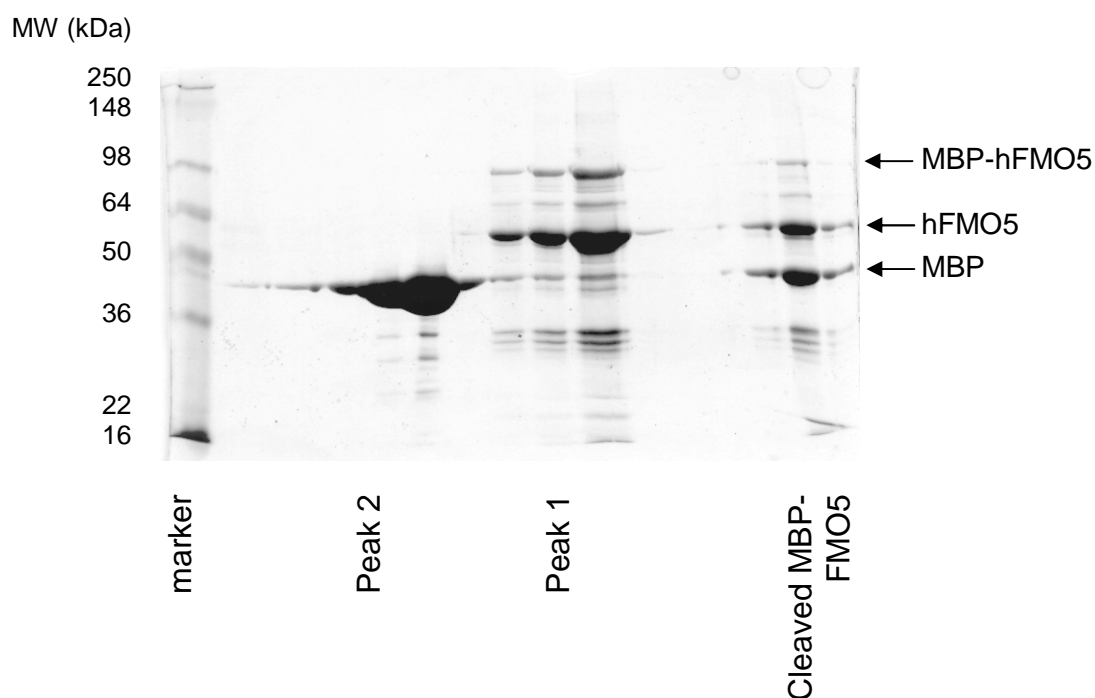


Figure 4.14 Coomassie stained SDS gel of fractions of cleaved MBP-hFMO5 purified on SEC column.

SeeBlue[®] Plus2 (Invitrogen Corporation, Carlsbad, CA, USA) was used as MW protein marker. Arrows point to Q-pure MBP-hFMO5 and the cleaved products, hFMO5 and MBP.

4.4 Discussion

It had been reported that fusion of a protein of interest to a large soluble affinity-tag such as MBP may improve several features of the protein like solubility [Donnelly *et al.*, 2006; Kapust *et al.*, 1999], yield [Butt *et al.*, 1989], and folding [Kapust *et al.*, 1999]. In addition, it could give protection from proteolysis and resulting fusion proteins may be easily purified via affinity chromatography [Smyth *et al.*, 2003]. Although less efficiently, even without the context of a fusion protein, MBP has been shown to interact preferentially with unfolded proteins and to promote their folding *in vitro* [Richarme *et al.*, 1997]. Further, it was proposed that MBP has chaperone-like qualities when fused to the *N*-terminus of a protein of interest assisting in correct protein folding and enhancing solubility [Kapust *et al.*, 1999; Sachdev *et al.*, 1998]. This might be partly due to its maltose binding site, a deep hydrophobic cleft that,

together with other hydrophobic sites located on the surface of the protein, could serve as binding sites to incompletely folded protein [Kapust *et al.*, 1999].

In accordance with these reported theories, a fusion of hFMO5 to MBP led to soluble, active, and stable protein as described in chapter 3. This protein was also obtained at a high yield and could easily be purified via affinity chromatography. Crystallization experiments were done screening various commercially available crystal screen kits for suitable crystallization conditions. These were refined further and the conditions that finally led to MBP-hFMO5 crystals were 26 % PEG 2K MME and 0.2 M sodium acetate in 0.1 M Bis-Tris propane buffer, pH 6.5. Interestingly, these crystallization conditions are analog to those reported for other MBP-tagged proteins that were successfully crystallized. Comparison of different crystals obtained as MBP-fusion proteins showed that, as for MBP-hFMO5, PEG and related molecules were most successful as precipitants and that the pH was generally low [Center *et al.*, 1998; Kukimoto *et al.*, 2000; Liu *et al.*, 2001; Smyth *et al.*, 2003].

When working with membrane associated proteins such as FMO enzymes use of detergents is unavoidable. As expected, surfactants play a dominant role in purification and crystallization of FMO5. Detergents are indispensable for solubilization of MBP-hFMO5 from *E. coli* (see chapter 3). Also in crystallography screens, surfactants play a major role, but the use of detergents introduces many problems. Detergent micelles have rough heterogeneous surfaces, their hydrophobic tails have considerable contact with the surrounding solution [Bogusz *et al.*, 2000], and they are fluid systems exchanging micellar components with the solvent [Garavito *et al.*, 2001; Wennerstrom *et al.*, 1979]. They have a major impact on protein crystallization, because detergent-detergent and detergent-protein interactions influence the behavior of membrane proteins. In addition, interactions with any remaining lipids have an effect on how a protein behaves [Garavito *et al.*, 2001]. In mixed systems (considering only detergents and lipids) phase behavior as well as changes in micelle shape, size, and CMC will be hard to predict because these systems never behave like solutions of the pure components [Wennerstrom *et al.*, 1979]. The behavior will be altered again when effects of solvent components like salts, PEG, or pH are considered [Arnold *et al.*, 2008; Garavito *et al.*, 2001].

Since usage of detergents introduces a completely new layer of unpredictability, a detergent used in crystallization studies preferably has a defined head group size and type. Especially mixtures like Triton[®] do not seem to work well [Arnold *et al.*, 2008]. In case of FMO5 where usage of Triton[®] X-100 was inevitable for extraction of the protein from *E. coli* (see chapter 3), complete removal of detergent and possibly substitution with other detergents before crystallization seemed necessary. Removal of detergent from protein samples previous to crystallography screens has been done by hydroxyl apatite column chromatography [Chen *et al.*, 1999] or by precipitation [Askolin *et al.*, 2004], dialysis, or dilution of the sample [Rigaud *et al.*, 1997]. Another method that proved to be successful in production of two-dimensional [Rigaud *et al.*, 1997] or three-dimensional crystals [Bron *et al.*, 1999] was surfactant removal utilizing Bio-Beads[®]. In 1973, Holloway *et al.* already described the successful removal of Triton[®] X-100 by adsorbance onto the polystyrene based Bio-Beads[®] [Holloway, 1973]. Interestingly, upon addition of excess amounts of Bio-Beads[®] to the protein solution, MBP-hFMO5 did not precipitate suggesting that FMO5 is not an integral membrane protein, but rather only associated with the membrane. As shown in the study, removal of Triton[®] X-100 with Bio-Beads[®] improved results from crystallization trials of MBP-hFMO5 leading to thick yellow oil phases and premature crystals with spherical shape (Figure 4.4).

Experiments in which a variety of different detergents was added after removal of Triton[®] X-100 led to further improvement of this first pre-stage of crystals (Table 4.3). The transition of the routinely obtained thick yellow oil to spherical shapes obtained after Triton[®] X-100 removal and to yellow crystals is shown in Figure 4.6.

In several wells that yielded crystals, detergents were added that belong to a new group of amphiphilic agents that is supposed to stabilize membrane proteins and lower the risk of denaturing or aggregation. The structure of these new types of amphiphilic molecules is based on cholic acid, but they exhibit facial amphiphilicity, meaning that their polar and nonpolar groups are located on opposite faces instead of at opposite ends as usual in other detergents [Zhang *et al.*, 2007b; Zhong *et al.*, 2005]. The terminal carboxylate of cholate was removed and uncharged polar groups were introduced at the parallel hydroxyl groups in the center of the cholic acid skeleton [Zhang *et al.*, 2007b]. The advantage of this structure is that these surfactants are supposed to self-assemble face-to-face. Thus the hydrophobic parts

of two molecules have similar dimensions as that of the lipid bilayer. In initial stability tests, the facial amphiphiles performed much better than previously used detergents, keeping the protein in solution and active for a longer time [Zhang *et al.*, 2007b]. Also in case of MBP-hFMO5, these detergents seemed to improve crystallization although others like HECAMEG and Cymals[®] also yielded crystals. Latter detergents have previously aided in crystallization studies, e.g., in case of hydrophobin HFBI from *Trichoderma reesei* that yielded crystals in the presence of Cymal[®]-5 [Askolin *et al.*, 2004]. In general, controlled addition of detergent and thus employing the concept of mixed micelles seems beneficial for MBP-hFMO5 crystal growth.

Unfortunately, no satisfactory diffraction pattern could be obtained from MBP-hFMO5 crystals. Several features of the MBP-hFMO5 construct could be argued to have been a cause for the poor condition of the crystals obtained. The MBP affinity tag itself might be problematic in crystallization experiments. Although expression and purification as MBP-fusion protein has numerous advantages, it has been suggested to hinder crystal growth by conformational heterogeneity introduced by the fusion tag [Smyth *et al.*, 2003]. Circumventing cleavage of MBP-hFMO5 and leaving the MBP-tag in place for crystallization studies has the advantage of avoiding potential problems often associated with proteolytic splicing including low yield, precipitation of target protein, cumbersome optimization of cleavage and subsequent purification conditions, high cost of proteases such as factor Xa, or potential loss of activity of the target protein during cleavage. However, leaving the tag attached to the protein of interest results in a multi-domain protein that might be less likely to form well-ordered, diffracting crystals, which is probably due to conformational heterogeneity allowed by the flexible linker region between MBP and the target protein [Smyth *et al.*, 2003]. In fact, most crystal structures of MBP-tagged proteins previously reported contained a shorter, more rigid linker between the affinity tag and the target protein [Center *et al.*, 1998; Ke *et al.*, 2003; Kukimoto *et al.*, 2000; Liu *et al.*, 2001]. These short, two to five amino acid long, mostly alanine containing linkers used instead of the typical longer linker in the MBP-hFMO5 fusion protein might be one reason for improved crystallization [Kapust *et al.*, 1999; Smyth *et al.*, 2003].

Also, in contrast to hFMO5, most proteins that led to crystals upon fusion with MBP were small in comparison with the rather large MBP-tag they were fused to. This could also play a role in successful crystallization as the ratio of MBP/protein might

be significant. Smaller proteins could be able to allow the larger MBP-tag to direct the construction of a crystal lattice whereas larger ones might be less susceptible to let MBP conduct crystal formation [Smyth *et al.*, 2003].

These potential problems implicated by leaving the large affinity tag fused to hFMO5 during crystallization trials have also been encountered in this study and although crystals could be grown from MBP-hFMO5, no satisfactory diffraction pattern could be obtained. Therefore, the next step was to cleave off the MBP-tag and perform crystallization experiments with only hFMO5. Successive experiments attempted proteolytic splicing of MBP from hFMO5 and subsequent purification of the latter. The separation of MBP and hFMO5 was done utilizing a previously inserted protease sensitive site right after the MBP sequence that may be cleaved by factor Xa. After incubation of three hours at 37 °C, cleavage was largely completed and addition of NADPH to the incubation mixture prevented the enzyme from being heat-inactivated. It is notable that similar experiments had been done with MBP-hFMO3 [Brunelle *et al.*, 1997]. However, after cleaving MBP from hFMO3, the latter showed intractable solubility and enhanced instabilities [Brunelle *et al.*, 1997] as previously described for a number of purified FMO enzymes [Cashman, 1995; Guan *et al.*, 1991]. In contrast to expectations, after proteolytical separation from MBP, human FMO5 stays in solution and is active.

After successful cleavage, the enzyme had to be separated from remaining factor Xa, MBP, and residual uncleaved MBP-hFMO5. A variety of methods to purify MBP from the target protein have been described including affinity purification [Riggs, 2000], ion exchange chromatography [de Pieri *et al.*, 2004; Guan *et al.*, 2002; Hao *et al.*, 2007; Riggs, 2000; Yan *et al.*, 2006], and size exclusion chromatography [Branco *et al.*, 2008]. Herein, these methods were carried out and evaluated.

Firstly, purification via amylose resin was attempted. In general, a disadvantage of this procedure is that although MBP can be removed from the cleavage mixture, the protease and other contaminants cannot be removed. Nevertheless, it has been described to be effective for MBP removal [Riggs, 2000]. After an ion exchange chromatography step to remove residual maltose from the elution of the first affinity column, the fusion protein (i.e., MBP-hFMO5) was cleaved and applied to the amylose resin. The target protein should be located in the flow through fractions and

freed of MBP. In this study however, MBP could not be separated from hFMO5. Both proteins were found mainly in the eluate after washing with 3 mM maltose but the flow through also contained both proteins to some degree. Potential difficulties might have arisen if MBP was denatured or otherwise damaged in the purification process, because then it presumably loses its affinity to the amylose resin [Riggs, 2000]. Maltose might also be more difficult to separate from the MBP than expected because it is buried in a deep groove almost inaccessible to solvent. Also, extensive hydrogen-bonding and van-der-Waals interactions keep the maltose in place [Spurlino *et al.*, 1991]. Thus, incomplete removal of maltose might have led to ineffective purification on amylose resin.

Secondly, separation of hFMO5 and the affinity tag was attempted by size exclusion chromatography. Successful purification of target protein from MBP after proteolytic splicing has been described for recombinant Lassa virus (LASV) proteins via SEC [Branco *et al.*, 2008]. hFMO5 could be successfully separated from MBP, however, it co-elutes with MBP-hFMO5.

Therefore, a third purification method to separate hFMO5 and MBP has been attempted, i.e., ion exchange chromatography. Especially anion exchange chromatography utilizing DEAE chromatography [de Pieri *et al.*, 2004; Guan *et al.*, 2002; Hao *et al.*, 2007; Riggs, 2000; Yan *et al.*, 2006] or Q columns [de Pieri *et al.*, 2004; Riggs, 2000] has been used several times. Purification of MBP from hFMO5 was successful using a 1ml HiTrap Q HP column, but as in case of SEC purification, hFMO5 co-eluted with uncleaved MBP-hFMO5.

Further studies are needed to succeed in purification of hFMO5 and subsequent crystallization experiments. Potential methods include cation exchange chromatography or antibody affinity chromatography. Theoretical calculation of the isoelectric point (pI) of MBP-hFMO5, MBP, and hFMO5 suggested that cation exchange purification on a HiTrap SP column (GE Healthcare, Uppsala, Sweden) at pH 7 could be successful (pI_{MBP} 5, pI_{FMO5} 8, and $pI_{\text{MBP-FMO5}}$ 6). To verify these calculated pI values, isoelectric focusing (IEF) could be performed. Afterwards, cation exchange should be used to purify hFMO5. Another approach to separate the MBP-tag from hFMO5 is the usage of MBP specific monoclonal antibodies that could be conjugated to Sepharose beads [Park *et al.*, 1998]. Also, a poly His site could be

introduced into the protein vector and protein could be purified via Ni²⁺-column affinity chromatography after proteolytic splicing of MBP from the target protein. This has been described previously for several other proteins [Feher *et al.*, 2004; Ramachandran *et al.*, 2007]. Using antibodies as well as using an additional His-tag have the disadvantage that they only remove MBP, but not the protease and other remaining contaminants. However, usage of biotin-labeled factor Xa has been reported to be advantageous because the protease can be removed after cleavage from the separated proteins by binding to streptavidin gel [Salek-Ardakani *et al.*, 2002].

Another approach to remove MBP from hFMO5 could exploit *in-situ* proteolysis. This is usually done by incubating trace amounts of protease with the protein of interest in crystallization trials [Dong *et al.*, 2007; Wernimont *et al.*, 2009]. The method was suggested to improve crystallization conditions because stable domains crystallize more readily and result in better diffracting crystals [Wernimont *et al.*, 2009] and might not be effective in case of MBP-hFMO5. However, for hFMO5, this *in-situ* proteolysis method might be applied to the cleavage of the large MBP-tag from hFMO5 to improve crystals by incubation with various amounts of factor Xa and screening at different conditions.

There are several of other suggestions to improve crystallization of either proteins that fail to crystallize or in case poorly ordered crystals are obtained. These improvements mainly aim at lowering molecular flexibility that may arise from motion of large domains, surface loops, or chain termini. Mostly, in these cases redesign of the protein construct is required. For instance, removal of a disoriented terminal extension has been successful. In case of FMOs though this may lead to a loss of function as has been shown for hFMO3 where even a truncation of only 22 amino acids led to a significant decrease in functional enzyme activity and further truncation (65 amino acids or more) resulted in abolished activity [Yamazaki *et al.*, 2007]. Thus, truncation of the hydrophobic C-terminus is not an option for crystallization studies of FMO enzymes.

Another approach is changing the surface properties of a protein. For example, methylation of lysine or site-directed mutagenesis of large charged residues that lie on the surface of the protein to smaller hydrophobic residues may be useful because

even small motions of these flexible, solvent-exposed amino acid side chains can be disruptive to a well-ordered crystal lattice [Walter *et al.*, 2006]. Controlled dehydration of poorly ordered crystals has been described to be successful [Heras *et al.*, 2003]. This method might afford an opportunity to improve the poor quality crystals already obtained.

In summary, this study showed that MBP-hFMO5 is crystallizable. However, further studies are needed to separate hFMO5 from MBP after factor Xa cleavage in order to start crystallization experiments with the tag-free protein and obtain better diffracting crystals.

5 pH Dependence of Human and Mouse FMO5

5.1 Introduction

5.1.1 pH Dependence of FMO Isoforms

FMO5 shows several unique features compared to other FMO enzymes. When comparing the pH dependence of three functional mouse FMOs (i.e., mFMO1, mFMO3, and mFMO5) and human FMO5 (hFMO5), it was found that the pH profile of FMO5 differed significantly from that of all other FMO isoforms examined in the study [Zhang *et al.*, 2007a] (Figure 5.1). The pH optima of FMO1 and 3 lie around

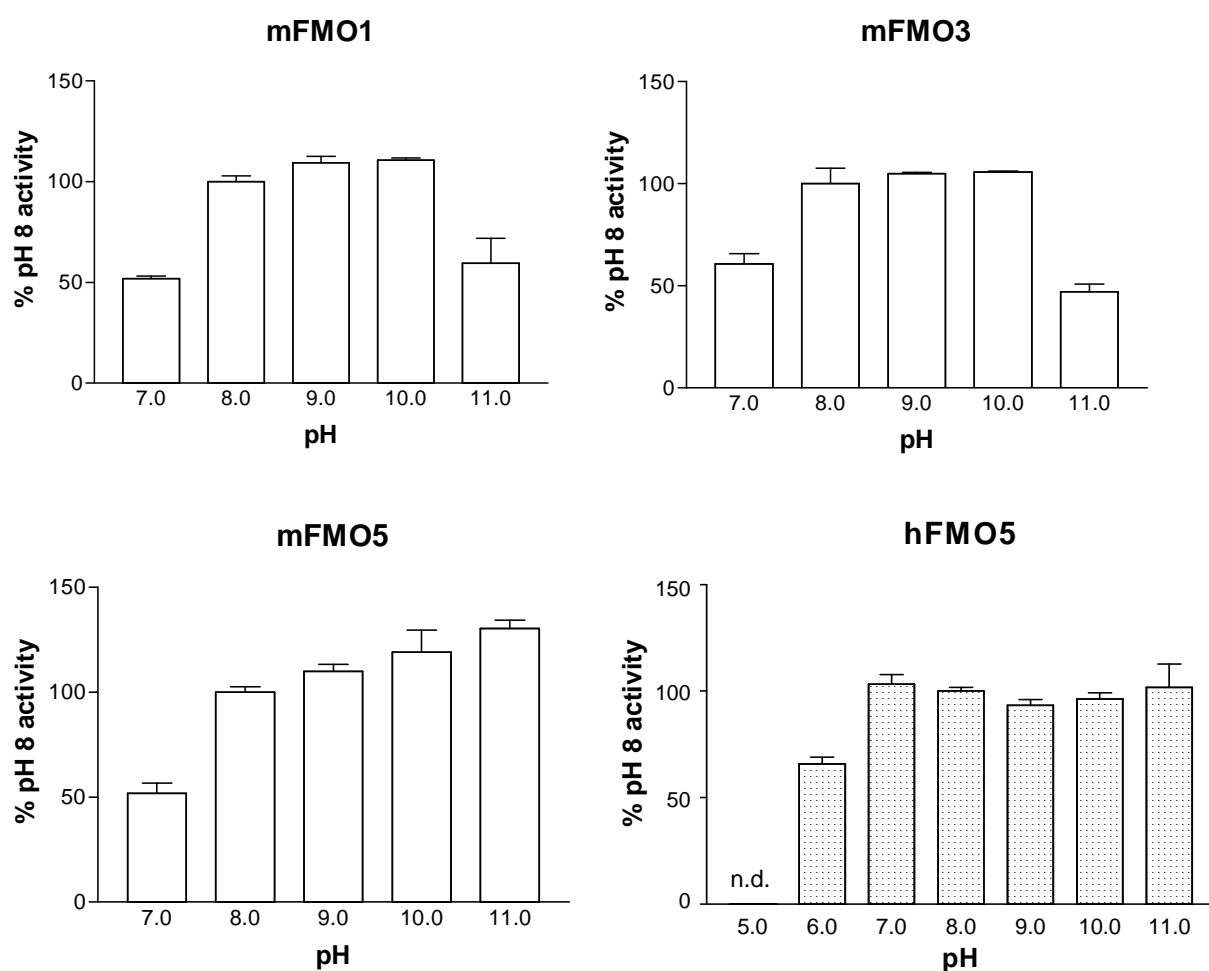


Figure 5.1 pH Dependence of mFMO1, mFMO3, mFMO5, and hFMO5.

Plots of mouse FMOs are shown as white bars, human plots as dotted bars. n.d., not detectable. Bar-graphs adapted from Zhang *et al.* [Zhang *et al.*, 2007a].

pH 8 through 10, whereas for FMO5 8-DPT *N*-oxygenation activity continues to increase from pH 7 to pH 11. Further, comparison of pH profiles from human and mouse FMO5 show significant differences in the lower pH range (Figure 5.1).

5.1.2 Aim of the Study

A comparison of FMOs showed that the pH dependent activity profile of FMO5 differed significantly from that of other FMO isoforms. The objective of this study was to examine the pH dependence of FMO5 to gain insight into the mechanism of action of FMO5 enzymes. Determination of pH dependent activity profiles and subsequent calculation of pK_a values for certain ionizable groups within the enzyme have been performed previously in order to reveal the roles of these amino acid residues in substrate binding and catalysis [Adachi *et al.*, 2010; Cook *et al.*, 1981; Grimshaw *et al.*, 1981; Viggiani *et al.*, 2004]. For the catalytic mechanism of FMO enzymes the theory is that the dehydration of the C4a-hydroxyflavin or the release of $NADP^+$, but not the release of oxygenated substrate represents the rate-limiting step (see also section 1.6). Thus, pK_a values calculated from pH dependent enzyme activity profiles of FMOs would have to attributed to titrable groups on amino acid residues involved in the rate-limiting step (e.g., $NADP^+$ release) or in conformational changes allowing $NADP^+$ release. Therefore these residues could be identified via pH studies. Functional recombinant human and mouse FMO5 were expressed as maltose-binding fusion proteins (i.e., MBP-hFMO5 and MBP-mFMO5) from *E. coli*, purified with affinity chromatography, and examined with 8-DPT as substrate for their *N*-oxygenation functional activity at different pH values. Results showed differences in enzyme activity at low pH between the two enzymes. In subsequent studies chimeras, i.e., enzymes composed of one part human and one part mouse sequence, should be expressed as MBP-fusion proteins and purified. To identify the region in that amino acid residues involved in an altered pH profile of hFMO5 and mFMO5 functional enzyme activity lie, pH dependent activity studies should be performed with these human-mouse chimeras. Once a manageable region of interest is located, human and mouse sequences will be aligned to locate amino acid differences between the two species within this region of interest. Amino acid/s involved in the pH shift between human and mouse FMO5 should be identified by swapping these amino acids utilizing site-directed mutagenesis. First, the amino acids will only be mutated in human FMO5 to those found in the mouse enzyme. To

verify initial results from this study, amino acid positions that seem to impact the pH profile in human FMO5 will also be mutated in the mouse enzyme. The results of these studies may help explain the mechanism of FMO function.

5.2 Materials and Methods

5.2.1 Reagents

All chemicals and reagents were purchased from Sigma-Aldrich Chemical Co. (St Louis, Missouri, USA) in appropriate purity. Buffers and other reagents were purchased from VWR Scientific, Inc. (San Diego, California, USA). The phenothiazine 8-DPT was synthesized by Dr. Karl Okolotowicz (HBRI, San Diego, USA) as previously described [Lomri *et al.*, 1993b; Nagata *et al.*, 1990; Zhang *et al.*, 2007a]. Plasmids pMAL-*hFMO5* and pMAL-*mFMO5* [Zhang *et al.*, 2007a] were prepared as previously described at HBRI.

5.2.2 Chimera-Design of hm159, mh159, hm435, and mh435

Chimeric *FMO5* hm159, mh159, hm435, and mh435 expression plasmids were created by swapping homologous restriction fragments of pMAL-*hFMO5* and pMAL-*mFMO5* plasmid DNAs. This had been previously done by Kiersten Riedler (HBRI, San Diego, CA, USA). Restriction enzymes used to cut both *hFMO5* and *mFMO5*, with the cut sites at the same positions within the *hFMO5* and *mFMO5* open reading frames, were HindIII and NcoI. HindIII cuts at position 3190 of both, the pMAL-*hFMO5* and pMAL-*mFMO5* plasmids, between codon 159 and codon 160 of *FMO5*, as well as a cut site downstream from the *FMO5* sequence. NcoI cuts at position 4017 of both plasmids, between codons 435 and 436 of *FMO5*, and at position 2490, upstream from the *FMO5* sequence (Figure 5.2).

USA) and chromatograms obtained from each sequencing reaction were analyzed using Sequencher software (Gene Codes Corporation, Ann Arbor, MI, USA).

5.2.3 Chimera-Design of hm229, mh229, hm370, and mh370

Due to the lack of convenient homologous restriction sites, the second set of chimeras was constructed by swapping homologous regions of pMAL-*hFMO5* and pMAL-*mFMO5* plasmid DNA through PCR amplification. The first swapping point was located at position 3399/3400 of the pMAL-*hFMO5* and pMAL-*mFMO5* plasmids, between codon 229 and codon 230 of *FMO5*. The other was located at position 3822/3823 of both plasmids, between codons 370 and 371 of *FMO5*. Chimeras were constructed in two steps of PCR reactions utilizing the FastStart High Fidelity PCR System, dNTPack (Roche Diagnostics GmbH, Mannheim, Germany): In a first PCR step, four human and four mouse *FMO5* parts were amplified separately, each with 25 extended bases of human and mouse *FMO*, respectively, at one end (Figure 5.3, PCR reaction 1). Primers used are listed in Table 5.1. PCR reactions were run using a Gene Amp PCR 9700 system (Perkin Elmer, Waltham, MA, USA). Each PCR reaction was prepared in a volume of 50 μ l and contained the following components: 5 μ l 10 x FastStart High Fidelity reaction buffer (Roche Diagnostics GmbH, Mannheim, Germany), 1 μ l template DNA (i.e., *mFMO5* or *hFMO5*), 2 μ l gene specific primer pair, 1 μ l dNTP mix (Roche Diagnostics GmbH, Mannheim, Germany), 0.5 μ l FastStart High Fidelity enzyme mix (Roche Diagnostics GmbH, Mannheim, Germany), and sterile water. The PCR was run at 95 $^{\circ}$ C for 2 minutes followed by 30 cycles at 95 $^{\circ}$ C for 30 seconds, 55 $^{\circ}$ C for 30 seconds, and 72 $^{\circ}$ C for 2 minutes. Afterwards a 10 minute-cycle was added at 72 $^{\circ}$ C.

PCR
reaction

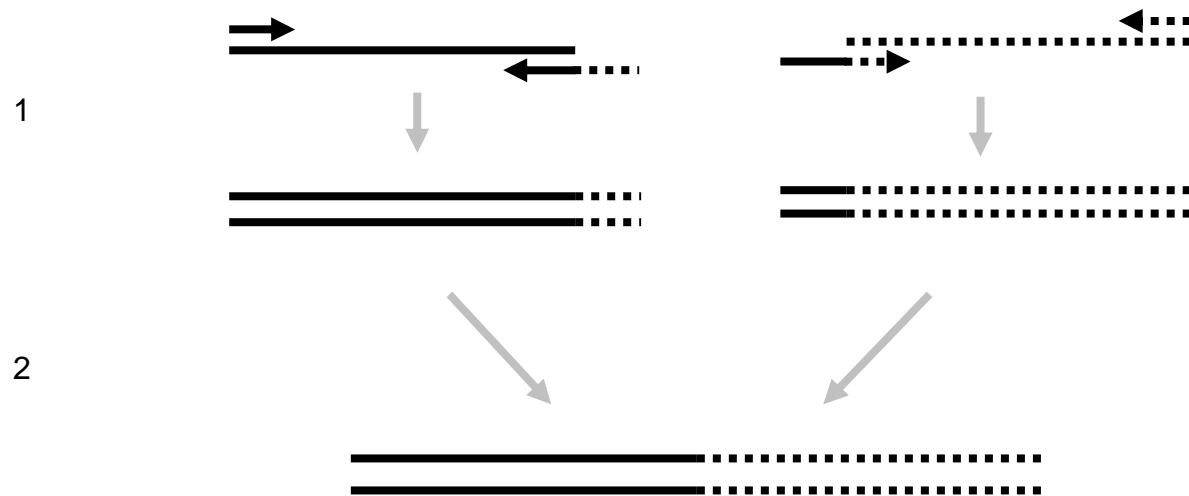


Figure 5.3 Scheme of PCR reactions for constructing human/mouse chimeras: hm229, mh229, hm370, and mh370.

Human parts are shown as solid lines, mouse parts as dashed lines. DNA is represented as lines, primers as solid black and dashed arrows.









Table 5.1 Polymerase chain reaction primers for human/mouse FMO5 chimeras.

FMO5 chimera	FMO5 part	Primer		
hm229	human, bp 1-687	hF5fXbal forward	5'- GAT CTC TAG AAT GAC TAA GAA AAG AAT TGC TGT GA -3'	
		reverse	5'- <u>AGA GAG TAG CAG GTC AAT AGG ATA TCC GTA GTC CCC TAC ACG ATT CAG</u> -3'	
	mouse, bp 688-1602	forward	5'- CTG AAT CGT GTA GGG GAC TAC GGA <u>TAT CCT ATT GAC CTG CTA CTC TCT</u> -3'	
		mF5rPstIn reverse	5'- <u>GAT CCT GCA GCT AAA AAT AAG CCA GGA TGA CAG C</u> -3'	
mh229	mouse, bp 1-687	mF5fXbal forward	5'- <u>GAT CTC TAG AAT GGC CAA AAA AAG GAT TGC T</u> -3'	
		reverse	5'- AGA GAA CAA CAC ATC AGC AGG ATA <u>TCC ATG CTT GCC TAC ACG GTT CAA</u> -3'	
	human, bp 688-1602	forward	5'- <u>TTG AAC CGT GTA GGC AAG CAT GGA</u> TAT CCT GCT GAT GTG TTG TTC TCT -3'	
		hF5rPstl reverse	5'- GAT CCT GCA GCC AAT GAA AAA CAG GGC AGT -3'	
	hm370	human, bp 1-1110	hF5fXbal forward	5'- GAT CTC TAG AAT GAC TAA GAA AAG AAT TGC TGT GA -3'
			reverse	5'- <u>AAT GGC TCC CAA GGG CTG AAT TAA</u> GCC TAT GAT TGC AAG AGT TGG CCT -3'
mouse, bp 1111-1602		forward	5'- AGG CCA ACT CTT GCA ATC ATA GGC <u>TTA ATT CAG CCC TTG GGA GCC ATT</u> -3'	
		mF5rPstIn reverse	5'- <u>GAT CCT GCA GCT AAA AAT AAG CCA GGA TGA CAG C</u> -3'	
mh370	mouse, bp 1-1110	mF5fXbal forward	5'- <u>GAT CTC TAG AAT GGC CAA AAA AAG GAT TGC T</u> -3'	
		reverse	5'- AAT GGC TCC TAA GGG CTG AAT CAA <u>GCC GAT GAT TGC AAG TGT TGG TTT</u> -3'	
	human, bp 1111-1602	forward	5'- <u>AAA CCA ACA CTT GCA ATC ATC GGC</u> TTG ATT CAG CCC TTA GGA GCC ATT -3'	
		hF5rPstl reverse	5'- GAT CCT GCA GCC AAT GAA AAA CAG GGC AGT -3'	

Mouse sequence parts are underlined.

After gel extraction and determination of DNA concentration of PCR products employing Kodak molecular imaging software (Eastman Kodak Company, Rochester, NY, USA), human and mouse parts were annealed with their counterparts and amplified in a second PCR reaction (Figure 5.3, PCR reaction 2). PCR reactions were run using a DNA Engine Peltier Thermal Cycler (Bio-Rad, Hercules, CA, USA) with FastStart High Fidelity PCR System, dNTPack (Roche Diagnostics GmbH, Mannheim, Germany). Each PCR reaction was prepared in a volume of 24 μ l and contained the following components: 2.5 μ l 10 x FastStart High Fidelity reaction buffer (Roche Diagnostics GmbH, Mannheim, Germany), 50 ng of each template DNA, 0.5 μ l dNTP mix (Roche Diagnostics GmbH, Mannheim, Germany), 0.5 μ l FastStart High Fidelity enzyme mix (Roche Diagnostics GmbH, Mannheim, Germany), and sterile water. The PCR was run at 95 $^{\circ}$ C for 2 minutes followed by 8 cycles at 95 $^{\circ}$ C for 30 seconds, 55 $^{\circ}$ C for 30 seconds, and 72 $^{\circ}$ C for 2 minutes to anneal human and mouse parts with their counterparts. Afterwards a 2 minute-cycle was inserted at 55 $^{\circ}$ C. During this cycle 1 μ l of corresponding end primers was added to each reaction (Table 5.2). The PCR was then run for an additional 30 cycles at 95 $^{\circ}$ C for 30 seconds, 55 $^{\circ}$ C for 30 seconds, and 72 $^{\circ}$ C for 2 minutes followed by a 7 minute-cycle at 72 $^{\circ}$ C to amplify chimera.

Table 5.2 Setup of 2nd PCR reaction.

FMO5 chimera	Template DNA from 1 st PCR reaction used in PCR reaction	Primer used in PCR reaction
hm229	human, bp 1-687 	hF5 f Xba I mF5 r Pst I
	mouse, bp 688-1602 	
mh229	mouse, bp 1-687 	mF5 f Xba I hF5 r Pst I
	human, bp 688-1602 	
hm370	human, bp 1-1110 	hF5 f Xba I mF5 r Pst I
	mouse, bp 1111-1602 	
mh370	mouse, bp 1-1110 	mF5 f Xba I hF5 r Pst I
	human, bp 1111-1602 	

Mouse parts are shown as dashed lines, human parts as solid lines.

The PCR products from this second PCR reaction were gel-purified and sequences of human-mouse chimera constructs were verified by sequencing analysis (Eton Bioscience Inc., San Diego, CA, USA). The chromatograms obtained from each sequencing reaction were analyzed with Sequencher software.

In order to ligate the chimera constructs into the pMAL vector, the vector was purified from overnight culture utilizing a QIAfilter Plasmid Midi Kit (Qiagen Inc., Valencia, CA, USA). 43 µl Backbone vector or 40 µl of each insert were double digested over night at 37 °C with each 1 µl PstI and 1 µl XbaI enzymes, and 5 µl 10 x buffer 3 (50 mM Tris-HCl pH 7.9, 100 mM NaCl, 10 mM MgCl₂, 1 mM DTT). 1 µl CIP enzyme was added to the vector DNA and incubated at 37 °C for one hour to minimize recircularization. After double digestion of both constructs and pMAL-backbone, both, vector DNA and inserts, were run on a 1 % agarose gel and purified. Ligation of inserts into the backbone vector was done by incubation of 2 µl ligase buffer with 2 µl backbone, 3 µl insert (or water as control), 1 µl ligase T4, and 2 µl of sterile water at 16 °C for 48 hours. Ligated DNA was then purified and concentrated by ethanol precipitation. To 10 µl ligation mix 25 µl ethanol was added. The mixture was vortexed and incubated at -80 °C for 4 hours followed by centrifugation and drying. Finally, ligation products were transformed into DH5α competent *E. coli* cells (easy shock 10B electro-competent cells, Bio-Rad, Hercules, CA, USA). These were cultured over night on ampicillin-resistant LB-agar plates. In order to unambiguously identify the sequence of each DNA insert, plasmids purified from single colonies of each construct transformed into *E. coli* were sequenced by Retrogen, Inc. (San Diego, CA, USA) and chromatograms obtained from each sequencing reaction were analyzed using the Sequencher program.

5.2.4 Site-directed Mutagenesis of Human and Mouse FMO5 Variants

Site-directed mutagenesis was done using the QuikChange Site-Directed Mutagenesis Kit (Stratagene, La Jolla, CA, USA) following the manufacturer's instructions. Primer designed for site-directed mutagenesis in mFMO5 and hFMO5 are listed in Table 5.3. Each PCR reaction was prepared in a volume of 50 µl and contained the following components: 5 µl 10 x reaction buffer for Pfu (Stratagene, La Jolla, CA, USA), 1 µl of each template DNA, 2 µl gene specific primer pair, 1 µl dNTP mix (Stratagene, La Jolla, CA, USA), 1 µl Pfu Turbo DNA polymerase (Stratagene,

La Jolla, CA, USA), and sterile water. The PCR was run at 95 °C for 30 seconds followed by 17 cycles at 95 °C for 30 seconds, 55 °C for 1 minute, and 68 °C for 9 minutes. Afterwards 2 µl DpnI was mixed into each reaction and incubated for at least 3 hours at 37 °C. PCR products were purified and concentrated by ethanol precipitation (in case of hFMO5 Q170K, E181V, G182V, D227K, and Y228R) or with QIAquick PCR Purification kit (Qiagen Inc., Valencia, CA, USA) following the manufacturers instructions (in case of mFMO5 K227D, H228Y and hFMO5 Y228F, Y228R, Y228K, and Y228A).

DNA was transformed into electro-competent cells (easy shock 10B electro-competent cells, Bio-Rad, Hercules, CA, USA, in case of mFMO5 H206Q and hFMO5 Q206H or DH5α electro-competent cells, New England BioLabs, Ipswich, MA, USA, in case of all other FMO5 variants), and cultured over night on ampicillin-resistant LB-agar plates. DNA, purified from selected colonies, was sent for sequencing (Eton Bioscience Inc., San Diego, CA, USA). The chromatograms obtained from each sequencing reaction were analyzed using the Sequencher program in order to verify the sequence of each DNA insert. If the sequence was correct, plasmids were transformed into DH1α cells. Afterwards the protein was expressed and purified as described in section 5.2.5.

Table 5.3 Polymerase chain reaction primers for human and mouse FMO5 variants.

FMO5 variant	Primer	Sequence
hFMO5 Q170K	forward	5'- GAG AAG TTC AAA GGG <u>AAG</u> TAC TTC CAC AGT CGA G -3'
	reverse	5'- CTC GAC TGT GGA AGT ACT <u>TCC</u> CTT TGA ACT TCT C -3'
hFMO5 E181V	forward	5'- GAC TAT AAG AAC CCA <u>GIG</u> GGA TTC ACT GGA AAG AG -3'
	reverse	5'- CTC TTT CCA GTG AAT CCC <u>ACT</u> GGG TTC TTA TAG TC -3'
hFMO5 G182E	forward	5'- CTA TAA GAA CCC AGA <u>GGA</u> ATT CAC TGG AAA GAG AGT C -3'
	reverse	5'- GAC TCT CTT TCC AGT GAA <u>TTC</u> CTC TGG GTT CTT ATA G -3'
hFMO5 Q206H	forward	5'- GGC TGT AGA GAT TAG CCA <u>CAC</u> AGC CAA GCA GGT TTT C -3'
	reverse	5'- GAA AAC CTG CTT GGC TGT <u>GTG</u> GCT AAT CTC TAC AGC C -3'
hFMO5 D227K	forward	5'- CCT GAA TCG TGT AGG <u>GAA</u> <u>GTA</u> CGG ATA TCC TGC TG -3'
	reverse	5'- CAG CAG GAT ATC CGT <u>ACT</u> <u>TCC</u> CTA CAC GAT TCA GG -3'
hFMO5 Y228H	forward	5'- GAA TCG TGT AGG GGA <u>CCA</u> <u>TGG</u> ATA TCC TGC TGA TGT G -3'
	reverse	5'- CAC ATC AGC AGG ATA TCC <u>ATG</u> GTC CCC TAC ACG ATT C -3'
hFMO5 Y228F	forward	5'- CGT GTA GGG GAC <u>TTC</u> GGA TAT CCT GCT -3'
	reverse	5'- AGC AGG ATA TCC <u>GAA</u> GTC CCC TAC ACG -3'
hFMO5 Y228R	forward	5'- CGT GTA GGG GAC <u>CGC</u> GGA TAT CCT GCT -3'
	reverse	5'- AGC AGG ATA TCC <u>GCG</u> GTC CCC TAC ACG -3'
hFMO5 Y228K	forward	5'- CGT GTA GGG GAC <u>AAG</u> GGA TAT CCT GCT -3'
	reverse	5'- AGC AGG ATA TCC <u>CTT</u> GTC CCC TAC ACG -3'
hFMO5 Y228A	forward	5'- CGT GTA GGG GAC <u>GCC</u> GGA TAT CCT GCT -3'
	reverse	5'- AGC AGG ATA TCC <u>GGC</u> GTC CCC TAC ACG -3'
mFMO5 K227D	forward	5'- GAA CCG TGT AGG <u>CGA</u> <u>CCA</u> TGG ATA TCC T -3'
	reverse	5'- AGG ATA TCC ATG <u>GTC</u> GCC TAC ACG GTT C -3'
mFMO5 H228Y	forward	5'- CCG TGT AGG CAA <u>GTA</u> <u>CGG</u> ATA TCC TAT TG -3'
	reverse	5'- CAA TAG GAT ATC <u>CGT</u> <u>ACT</u> TGC CTA CAC GG -3'

Mutant positions are underlined.

5.2.5 Expression and Purification of Human - Mouse FMO5 Chimera and Human or Mouse FMO5 and their Variants.

Expression vector for the eight FMO5 chimeras and hFMO5 and mFMO5 variants were cloned into pMAL-2c (New England BioLabs, Ipswich, MA, USA) with site-directed mutagenesis methods as described previously [Brunelle *et al.*, 1997; Zhang *et al.*, 2003]. Expression and purification was done as described in section 3.2.2 with minor changes. Briefly, the FMO5 enzymes were expressed as *N*-terminal maltose-binding fusion proteins (i.e., MBP-FMO5). After transformation of *E. coli* DH1 α cells with pMAL-MBP-FMO5 plasmid, cells were grown, induced and disrupted as described in section 3.2.2.1. The protein was then applied to a 10 – 15 ml amylose column at 0.75 ml/min or 1 ml/min. Bound MBP-FMO5 protein was eluted with 3 mM maltose or a linear maltose gradient: 0 – 100 % 10 mM maltose in buffer A over 100 minutes at 1 ml/min. Eluted fractions containing the fusion protein were pooled and concentrated with a Centriprep centrifugal filter unit with Ultracel-30 membrane or an Amicon Ultra-15 centrifugal filter unit with Ultracel-50 membrane (Millipore, Billerica, MA, USA).

5.2.6 Determination of Protein Concentrations of FMO5 Chimera

Concentration of purified MBP-FMO5 chimeras was determined by SDS-PAGE and Coomassie Blue staining and compared with BSA standard (see section 3.2.4.1).

5.2.7 Enzyme Assays

5.2.7.1 *N*-Oxygenation of 8-DPT by FMO5

N-Oxygenation of 8-DPT was determined by HPLC analysis as described in section 3.2.4.2 with incubation mixtures containing 100 mM potassium phosphate buffer at different pHs (i.e., pH 6.0, 6.3, 6.7, 7.0, 7.3, 7.7, and 8.0), 0.4 mM NADP⁺, 0.4 mM glucose-6-phosphate, 4 U glucose-6-phosphate dehydrogenase, 0.25 mM DETAPAC, and 80 μ g MBP-FMO5.

5.2.7.2 Optimization of Enzyme Assays

Assay conditions for 8-DPT *N*-oxygenation activity by FMOs have previously been described and successfully used for various studies [Brunelle *et al.*, 1997] and thus

were adapted with only minor changes for the pH study described herein. However, closer evaluation in terms of sensitivity to pH change and buffer strength showed that the previously used conditions can be optimized. Also, results from the determination of kinetic parameters (i.e., V_{max} and K_m) for FMO5-mediated 8-DPT HCl *N*-oxygenation suggested that a higher substrate concentration is favorable for routine analysis ($K_m = 117 \mu\text{M}$ and $V_{max} = 3.2 \text{ nmol/min/mg FMO5}$). However, although buffer strength and pH seem to play an important role, the K_m was not expected to be increased at different pHs and thus, a substrate concentration of $400 \mu\text{M}$ was considered saturation condition for all pHs examined. Therefore, for pH profile experiments of human and mouse FMO5 variants, a final 8-DPT HCl concentration of $400 \mu\text{M}$ was used. The revised assay protocol is stated hereafter. Nevertheless, pH profiles of human and mouse FMO5 were performed with both methods and comparison showed no significant changes. Thus, profiles generated with the original method were not repeated.

5.2.7.3 Optimized 8-DPT Assay

N-Oxygenation of 8-DPT was determined by HPLC analysis as described in section 3.2.4.2 with incubation mixtures containing a buffer mix consisting of 0.1 M ACES, 52 mM Tris, and 52 mM ethanolamine at different pHs (i.e., pH 6.0, 6.3, 6.7, 7.0, 7.3, 7.7, 8.0, and 9.0), 0.4 mM NADP^+ , 0.4 mM glucose-6-phosphate, 4 U glucose-6-phosphate dehydrogenase, 0.25 mM DETAPAC, and 40 μg MBP-FMO5. The advantage of this buffer system over phosphate buffer which was used earlier is that a) its ionic strength is virtually constant over a wide range of pHs and b) its buffer capacity is much better than that of phosphate buffer over the pH range tested [Ellis *et al.*, 1982]. Reactions were initiated by addition of substrate to a final concentration of $400 \mu\text{M}$. After 20-minute incubation the samples were processed and analyzed via HPLC as described in section 3.2.4.2.

5.2.8 Data Analysis

Results were analyzed with Graphpad software (Graphpad Prism, Version 2.00 or 3.00, San Diego, CA, USA). For pK_a determination, log-enzyme activities in nmol/min/mg FMO5 were plotted against pH and the following equation was applied: $Y = \log(V_{max}/(1+10^{\text{pK}_a-X}))$ with K_a representing the dissociation constant of an ionizable

group on the enzyme [Cook *et al.*, 1981]. Data obtained was presented as best fit value \pm standard error. Statistical analysis was also done using Graphpad Prism software and statistical significance was judged at $P < 0.05$.

5.3 Results

5.3.1 pH Dependence of Human and Mouse FMO5

The pH dependence of human and mouse FMO5 was studied and pK_a values were determined in the range of pH 6 – 8. As shown previously, the pK_a determined from pH dependent enzyme activity profiles with mouse FMO5 was significantly higher than that determined with human FMO5 (6.6 ± 0.1 and 7.2 ± 0.1 , respectively).

5.3.2 pH Dependence of hm159, mh159, hm435, and mh435

The pH dependent 8-DPT *N*-oxygenation activity of MBP-FMO5 chimeras hm159, mh159, hm435, and mh435 was analyzed and pH profiles were evaluated in regard to activity drop at low pH values. Comparing hm159 and mh159 FMO5, it can be concluded that the amino acid residues 1 – 159 of hFMO5 are not involved in the increased activity observed at lower pH for hFMO5 because the pH dependent activity profile of mh159 is close to that of human FMO5 whereas the pH drop of hm159 is steeper at low pH resembling the pH profile of mouse FMO5. Comparing the other two chimeras (i.e., hm435 and mh435), the difference in activity drop around pH 6 is not as pronounced. Nevertheless, the pH profile of hm435 seems closer to that of hm159 and thus to that of wild-type mouse FMO5, whereas the pH profile of mh435 seems to follow more the outline of mh159 (Figure 5.5). Therefore, the amino acid/s most likely to be responsible for the increased activity of hFMO5 at lower pH in comparison to mFMO5 lies between amino acid residues 160 and 434.

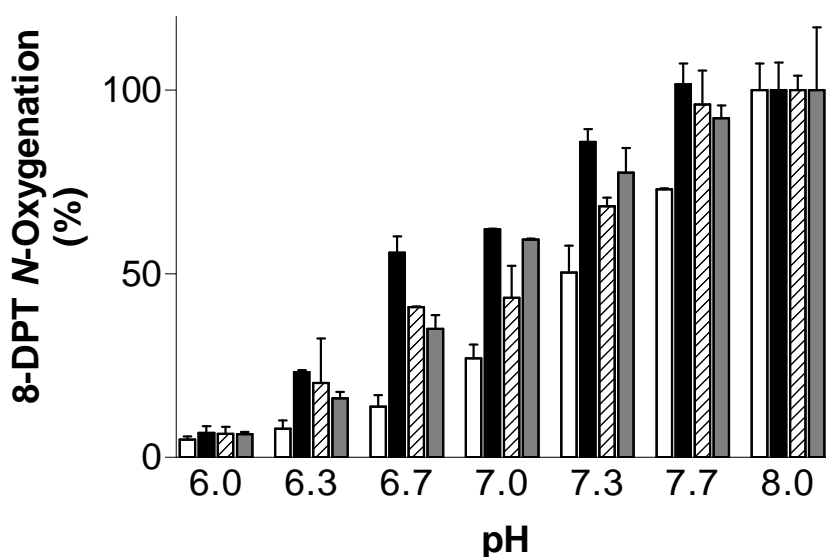


Figure 5.5 Human/mouse chimeras and their pH dependent activity profiles derived from 8-DPT *N*-oxygenation activity assays at pH 6 through 8.

hm159, white bars; *mh159*, black bars; *hm435*, hatched bars; *mh435*, grey bars.

5.3.3 pH Dependence of hm229, mh229, hm370, and mh370

With data from the first set of chimeras, the region of interest where the amino acid residue/s involved in the observed higher activity of hFMO5 below pH 7 are located could be narrowed down (i.e., aa 160 – 434). A set of four new chimeric FMO5 enzymes representing one part human FMO5 and one part mouse FMO5 were designed, expressed, and purified in order to determine their pH profiles and localize the amino acid/s of interest. The pH profile of hm229 FMO5 could not be determined due to very poor expression rates. The pH dependent FMO5 activity profiles for the other three chimeras analyzed do not differ significantly from each other and are shown in Figure 5.6.

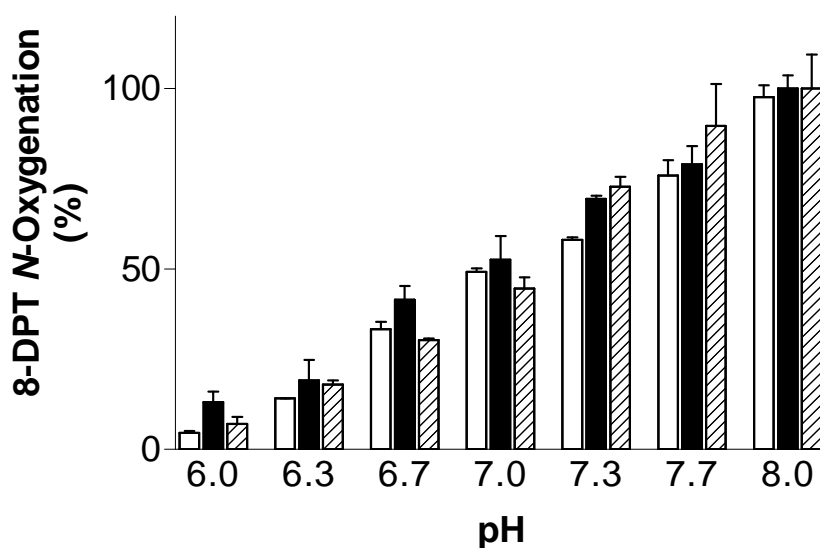


Figure 5.6 Human/mouse chimeras and their pH dependent activity profiles derived from 8-DPT *N*-oxygenation activity assays at pH 6 through 8. *mh229*, white bars; *hm370*, black bars; *mh370*, hatched bars.

5.3.4 Summary: pH Dependence of Human and Mouse FMO5 Chimeras

Chimeras of human and mouse FMO5 with swapping points at amino acids 229, 370, and 435 did not differ significantly in their pH dependent activity profiles (Figure 5.5 and 5.6). Thus, amino acid residue/s involved in the observed higher activity of hFMO5 below pH 7 is/are most likely located between amino acids 160 and 229 because only chimeras *mh159* and *hm159* showed significant differences from the wild-type enzymes whereas no significant differences could be observed with chimeras with cutting sites after codon 230.

Sequence alignment of human and mouse FMO5 showed that within this specific region, six amino acids of human FMO5 differ from mouse FMO5. Utilizing site-directed mutagenesis, these amino acids were changed in human FMO5 to the ones found in mouse FMO5, expressed, and purified. Their pH profile between pH 6 and 9 was determined in 8-DPT HCl *N*-oxygenation activity assays.

5.3.5 pH Dependence of Human and Mouse FMO5 Variants

The pH profile of wild-type hFMO5 and wild-type mFMO5 as well as hFMO5 variants purified was determined after optimization of assay conditions (section 5.2.7.3).

The results of wild-type human and mouse FMO5 are shown in Figure 5.7. The results are similar to those obtained with the original assay conditions with pK_a values of 7.7 ± 0.1 and 6.9 ± 0.1 calculated from the pH dependent activity profiles of mouse and human FMO5, respectively.

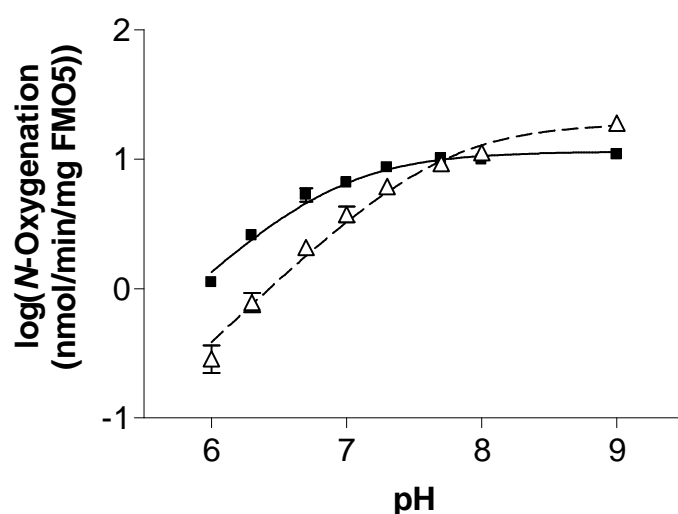


Figure 5.7 pH Dependence of wild-type human and mouse FMO5. *hFMO5 is shown as solid line (■), mFMO5 as dashed line (Δ).*

Five hFMO5 variants were successfully expressed, purified, and analyzed. Results for these variant hFMO5s are shown in Figure 5.8. The pK_a values determined with wild-type human and mouse FMO5 and variant hFMO5 are listed in Table 5.5.

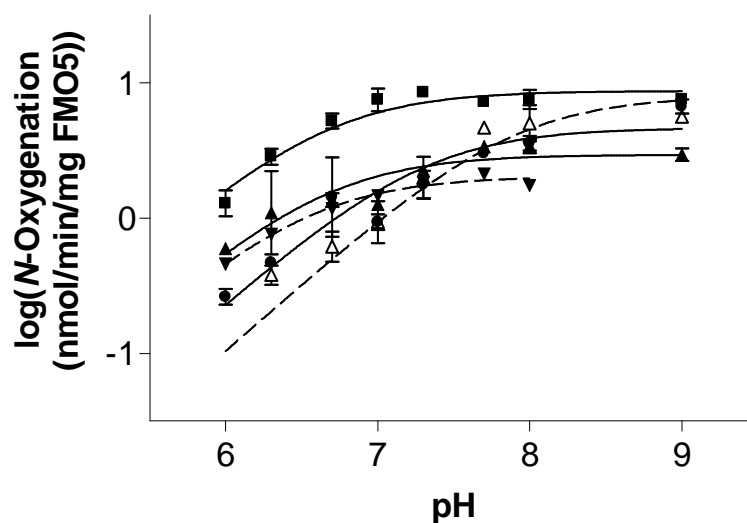


Figure 5.8 pH Dependence of human FMO5 variants.

■ *hFMO5* Q170K; ▲ *hFMO5* G182E; ▼ *hFMO5* Q206H; ● *hFMO5* D227K; △ *hFMO5* Y228H. *hFMO5* Q170K, *hFMO5* G182E, and *hFMO5* D227K are shown as solid lines, *hFMO5* Q206H and *hFMO5* Y228H are shown as dashed lines.

Table 5.5 pK_a Values calculated from pH dependence profiles of human FMO5 variants compared to those of wild-type human and mouse FMO5.

Variant	pK_a
wild-type hFMO5	6.9 ± 0.1
wild-type mFMO5	7.7 ± 0.1
<i>hFMO5</i> Q170K	6.6 ± 0.1
<i>hFMO5</i> G182E	6.6 ± 0.1
<i>hFMO5</i> Q206H	6.5 ± 0.05
<i>hFMO5</i> D227K	7.3 ± 0.1
<i>hFMO5</i> Y228H	7.9 ± 0.2

Data is presented as best fit value \pm standard error.

The data clearly show that replacement of the tyrosine at position 228 with histidine in *hFMO5* increases the pK_a and thus results in a pH profile similar to that observed

with the wild-type mouse enzyme, whereas hFMO5 Q170K, G182E, and Q206H mutations do not have a significant influence on pK_a . D227K showed a slightly increased pK_a in comparison to that calculated from pH dependence profiles of wild-type hFMO5, even though this increase was lower than hFMO5 Y228H. To confirm this result, the mouse counterparts with the amino acid of the corresponding human enzyme were made (i.e., mFMO5 K227D and H228Y) and as suspected, pH dependence studies with mouse FMO5 K227D as well as mouse FMO5 H228Y led to decreased pK_a values compared to that determined with wild-type mouse enzyme (Figure 5.9 and Table 5.6). Also, several variants of hFMO5 Y228 were made in order to evaluate the effect of different amino acids at position 228. The results are shown in Figure 5.10 and summarized in Table 5.6.

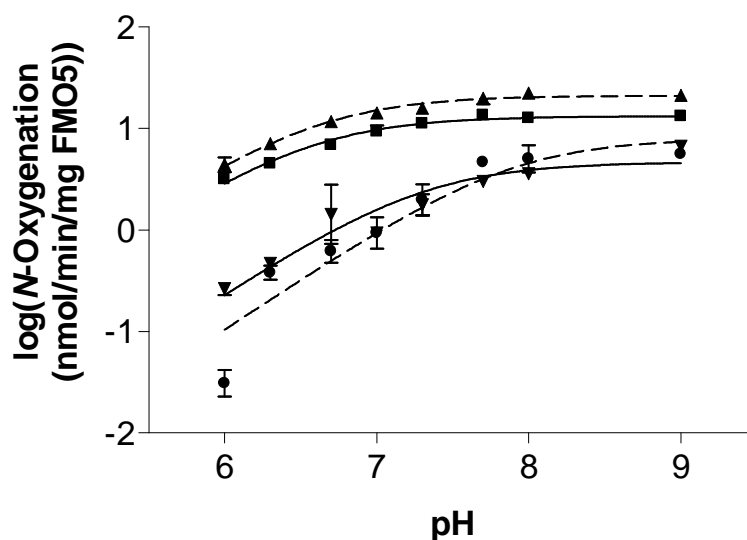


Figure 5.9 pH Dependence of human and mouse FMO5 variants.

▼ hFMO5 D227K; ■ mFMO5 K227D; ● hFMO5 Y228H; ▲ mFMO5 H228Y. hFMO5 D227K and mFMO5 K227D are shown as solid lines, hFMO5 Y228H and mFMO5 H228Y are shown as dashed lines.

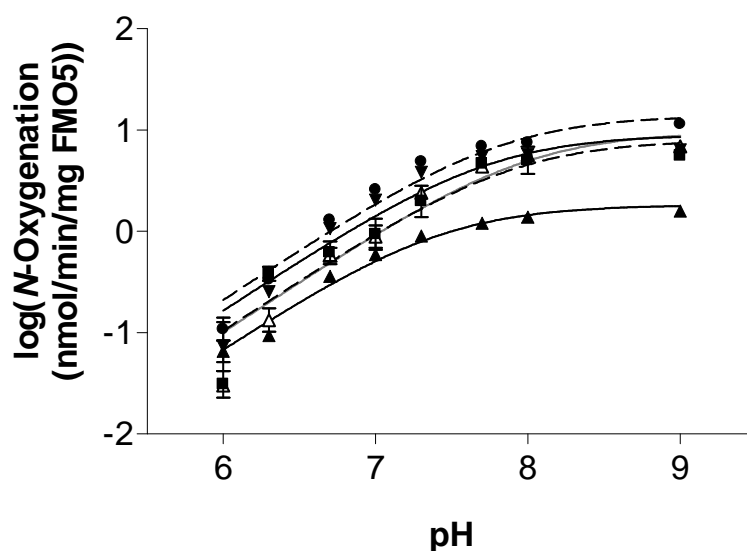


Figure 5.10 pH Dependence of human FMO5 Y228 variants.

■ *hFMO5 Y228H*; ▲ *hFMO5 Y228F*; ▼ *hFMO5 Y228R*; △ *hFMO5 Y228K*; ● *hFMO5 Y228A*. *hFMO5 Y228F*, *hFMO5 Y228R*, and *hFMO5 Y228K* are shown as solid lines, *hFMO5 Y228H* and *hFMO5 Y228A* are shown as dashed lines.

Table 5.6 pK_a Values calculated from pH dependence profiles of human and mouse FMO5 variants compared to those of the wild-type FMO5 enzymes.

Variant	pK_a
wild-type hFMO5	6.9 ± 0.1
wild-type mFMO5	7.7 ± 0.1
hFMO5 D227K	7.3 ± 0.1
mFMO5 K227D	6.6 ± 0.05
hFMO5 Y228H	7.9 ± 0.2
mFMO5 H228Y	6.5 ± 0.05
hFMO5 Y228K	8.0 ± 0.1
hFMO5 Y228A	7.8 ± 0.1
hFMO5 Y228F	6.7 ± 0.05
hFMO5 Y228R	7.7 ± 0.1

Data is presented as best fit value \pm standard error.

As expected, in mFMO5 replacement of a histidine at position 228 by tyrosine (mFMO5 H228Y) significantly decreased the calculated pK_a value in comparison to

wild-type mFMO5. The same observation was made for the K227D variant of mouse FMO5.

Changing the amino acid tyrosine in wild-type hFMO5 to three of the tested amino acids (i.e., lysine, alanine, or arginine) also increased the pK_a significantly. However, changing tyrosine to phenylalanine did not make a significant difference in pK_a value (pK_a of 6.9 and 6.7 determined with wild-type hFMO5 and hFMO5 Y228F, respectively). Overall, the low pK_a seemed to be due to the amino acids at position 227 and 228 in the human enzyme and thus they are at least in part responsible for the increased enzyme activity at low pH.

5.4 Discussion

Within this study, the observed pH dependent activity change of human FMO5 was compared to mouse FMO5. Interestingly, with the human enzyme a significantly lower pK_a was observed than with the mouse enzyme. Via chimera studies the region in which the amino acids that are responsible for this pK_a shift lie was determined. Alignment of human and mouse FMO5 sequences showed that this region is only distinguished by six amino acids. In additional site-directed mutagenesis studies these amino acids were changed and the pH dependent activity profiles of the resulting variants were determined. Resulting data clearly showed that the residues in question lie at positions 227 and 228 of the enzyme.

It has been reported previously that pH dependent activity of enzymes is set mainly by pK_a values of one or a few key ionizable groups within the enzyme, primarily in the active-site cleft [Joshi *et al.*, 2000]. According to the human FMO3 homology structure model developed based on four related proteins [Borbás *et al.*, 2006b] (see also chapter 4), the amino acid that influences the pH profile (i.e., Y228) lies on the surface of the protein close to the entrance of the back passage connected to the space between the two domains where NADPH binds. Therefore, in case of FMO5, it is more likely that NADPH-binding or $NADP^+$ release is altered rather than substrate binding.

It might have been expected that an amino acid change of tyrosine to histidine, which has a lower pK_a value on its own, would also lead to a decrease in the pK_a value measured. However, this could not be observed in this study. Instead, it is possible

that in wild-type human FMO5 the tyrosine at position 228 can make hydrogen bonding with NADP⁺. If tyrosine is replaced by a histidine, this interaction may be interrupted due to protonation at lower pH. The unpolar amino acids phenylalanine and alanine might not be able to interact because of the missing polar hydroxylic group. Indeed, with hFMO5 Y228A a significantly increased pK_a value was observed (7.8 ± 0.1). However, replacement of tyrosine by phenylalanine (hFMO5 Y228F) did not alter the pK_a significantly from that observed with the wild-type enzyme (6.7 ± 0.05). Also, a significantly increased pK_a for pH profiles of both hFMO5 Y228R and hFMO5 Y228K (i.e., 7.7 ± 0.1 and 8.0 ± 0.1 , respectively) in comparison to wild-type human FMO5 (6.9 ± 0.1) was observed showing that both lysine and arginine might affect NADP⁺ binding.

Conformational changes may also have an influence on titration behavior. Thus, the similar pK_a values observed for pH dependence profiles of hFMO5 Y228 and F228 could be explained by sterical similarity between the two amino acid side chains. It is possible that a benzene ring is needed in this position and that changing this might have an effect on neighboring residues such as D227. As the tyrosine at position 228, aspartic acid at position 227 could possibly form hydrogen bonds with NADP⁺ and changing Asp227 to lysine resulted in an increased pK_a (i.e., 7.3 ± 0.1). Shifting this residue by changing the size of the amino acid at position 228 might also prevent this interaction and lead to an altered pK_a.

Amino acid residues may be sensitive to both electrostatic and structural changes of others that are located in immediate vicinity. Thus, an amino acid change could have an effect on pK_a values of sterical neighboring residues as was described for the substitution of asparagine with aspartic acid at position 35 in *Bacillus circulans* xylanase [Joshi *et al.*, 2000]. In this enzyme, substitution of the basically neutral amino acid Asn with the acidic Asp (pK_a 3.7) also influenced the pK_a values of Glu78 and Glu172. Latter ones were elevated, probably due to charge repulsion. Overall, the pH optimum of the xylanase was shifted from 5.7 to 4.6 [Joshi *et al.*, 2000]. In addition, protonation or deprotonation of amino acids may also help stabilize other structurally close residues and substitution might lead to destabilization and an altered pH. For example, for a polyketide synthase, stabilization and promotion of a thiolate anion at cysteine 164 by histidine 303, as an imidazolium cation, was reported. Thus, upon substitution of this His303, in addition to reactivity, the pK_a

value of the Cys164 changed [Jez *et al.*, 2000]. It is possible that amino acid changes in FMO5 at position 227 and 228 may also alter pK_a values of surrounding residues or stabilize/destabilize these depending on the charge of the amino acid in these positions. Thus, although based on current three-dimensional models D227 and Y228 lie close to the surface of the protein, they could have an impact on amino acids that are closer to the substrate binding site or that influence NADPH binding or $NADP^+$ release. A crystal structure of a mammalian FMO may give more detailed answers as to how these amino acids influence residues in or close to the active site.

The pI of the enzyme could also affect its pH dependent activity profile. The theoretical pI of human and mouse MBP-FMO5 are 6.3 and 7.2, respectively (<http://www.expasy.ch/cgi-bin/protparam>). It is possible that the enzyme has to be negatively charged to function properly. Since human FMO5 has a lower pI than the mouse enzyme, it will keep its negative charge longer at lower pH. Thus, human FMO5 has a negative charge above pH 6 whereas mouse FMO5 is negatively charged above pH 7. Therefore, its activity decreases faster in comparison to human FMO5 below this pH as seen in the pH profiles in this study. Calculation of the variants' pI s shows an increase for human FMO5 D227K to 6.5 and a decrease for mouse FMO5 K227D to 6.8 supporting this theory. FMO5 is negatively charged at its pH optimum. Assuming the enzyme functions best when it is negatively charged, a substitution of Asn with Asp and the resulting change of pI could lead to altered charge of the enzyme at low pH. Also, the pI could simply be a requirement for stability in the surrounding environment rather than affecting substrate binding or turnover by determining the charge of the enzyme [Joshi *et al.*, 2000].

In conclusion, the pH dependent activity change of human and mouse FMO5 were compared and the amino acids responsible for an observed pK_a shift between the two were identified. Changing aspartic acid at position 227 to lysine or tyrosine at position 228 to histidine of human FMO5 elevated the pK_a observed in pH profiles from 6.9 to 7.3 and 7.9, respectively. Accordingly, an amino acid switch of Lys227 to Asp227 or His228 to Tyr228 in mouse FMO5 lowered the pK_a from 7.7 to 6.6 and 6.5, respectively. In order to address the question of how exactly the pH dependent activity profile is changed by these amino acids and whether the residues at position 227 and 228 interact with the cofactor directly or whether they affect neighboring residues will need further investigation. For example, crystallographic studies with

both wild-type and mutant enzymes at acidic pH value or determination of pK_a values for specific residues via NMR may lead to more comprehensive explanations of the mechanism of FMO5 catalysis and the influence of amino acids on pH dependent enzyme activity.

6 Substrate Selectivity and Screens of Potential FMO5 Substrates

6.1 Introduction

6.1.1 FMO Substrates

Generally, any compound containing a soft nucleophile can be a substrate to FMOs if it is able to gain access to the 4a-hydroperoxyflavin and the catalytic site of the FMO enzyme [Cashman, 1995; Krueger *et al.*, 2005]. This leads to differences in substrate specificity between the FMO isoforms because the substrate binding channel of different FMOs are clearly distinct [Lomri *et al.*, 1993b; Lomri *et al.*, 1993c; Nagata *et al.*, 1990]. FMO1 possesses the broadest and shallowest substrate binding channel of all mammalian FMOs. In contrast, FMO2 and FMO3 preferably *N*-oxygenate long-chain aliphatic amines (i.e., those possessing a nucleophilic tertiary amine at least six or seven carbon atoms away from a bulky moiety). The channel to the 4a-hydroperoxyflavin in pig FMO1 is about 3 Å deep and 12 Å wide [Cashman, 1995; Nagata *et al.*, 1990], but the binding site of human hepatic FMO1 is more restricted than that of animals and lies about 5 Å below the surface and is only 4.5 Å in diameter [Cashman *et al.*, 2006; Kim *et al.*, 2000; Krueger *et al.*, 2005; Ziegler, 2002]. Human FMO1 is efficient in *N*-oxygenating tertiary amines such as chlorpromazine, imipramine, and 10-[(*N,N*-dimethylamino)alkyl] phenothiazine derivatives (DPT), but does not readily catalyze *N*-oxygenation of primary amines, although aliphatic primary amines can act as positive effectors [Cashman, 1995; Cashman, 2000; Krueger *et al.*, 2005]. In contrast, the binding channel of rabbit and human FMO2 and human FMO3 rests at least 6 to 8 Å below the mouth of the substrate binding channel with a diameter of about 8 Å [Krueger *et al.*, 2005; Lomri *et al.*, 1993b; Nagata *et al.*, 1990]. FMO2 is the most size-restricted FMO isoform whereas FMO3 appears to be intermediate. FMO2 as well as FMO3 and 5 also *N*-oxygenate primary amines such as *n*-octylamine and the K_m decreases with an increasing length of the chain between C8 and C12. The resulting hydroxylamine is a better substrate for FMO2 and is usually *N*-oxygenated to the *cis*-isomer of the oxime [Poulsen *et al.*, 1986]. When examining rabbit, monkey, and human FMO2 for functional activity, it appears that generally sulfur-containing chemicals are better substrates for FMO2 than nitrogen-containing substrates [Dolphin *et al.*, 1998; Krueger *et al.*, 2004;

Krueger *et al.*, 2002; Whetstine *et al.*, 2000]. FMO3 enzymes generally prefer substrates that are slightly smaller than those accepted by FMO1, but are also able to *N*-oxygenate primary, secondary, and tertiary amines. Nitrogen atoms on longer side chains are more efficiently oxygenated than those on shorter side chains, apparently because the substrate binding site is buried deep within the enzyme. Typical substrates for FMO3 include benzydamine, methimazole, trimethylamine, and the probe substrate 5-DPT [Cashman, 2000; Cashman *et al.*, 2006].

Although not clearly understood to date, FMO4 and 5 supposedly have very restricted substrate specificities. FMO4 is very unstable and its cDNA expression is problematic affording poorly active enzyme [Lattard *et al.*, 2003a]. Thus, it has been difficult to establish extensive FMO4 substrate specificity relations [Cashman *et al.*, 2006]. FMO5 does not oxygenate the typical FMO substrates such as MMI and TMA [Overby *et al.*, 1995; Zhang *et al.*, 2007a]. In studies with a series of DPT-analogs an 8-fold increase in specific activity of mouse FMO5 was observed between 5-DPT and 8-DPT. Thus, it was suggested that the active site of mouse FMO5 lies about 6 Å below the surface [Zhang *et al.*, 2007a]. Known substrates of FMO5 are short-chain aliphatic primary amines such as *n*-octylamine, thioethers with proximal carboxylic acids (i.e., *S*-methyl esonarimod), and 5- and 8-DPT [Cashman *et al.*, 2006; Overby *et al.*, 1995; Zhang *et al.*, 2007a].

Endogenous substrates of FMOs include biogenic amines (i.e., tyramine and phenethylamine) [Cashman, 2000]. Tyramine is *N*-oxygenated by FMO1 and 3 to its *trans*-oxime, and FMO3 is predicted to be predominantly responsible for *trans*-oxime formation. Phenethylamine is also metabolized by human hepatic FMO3 and to a lesser extent by porcine liver FMO1. It is *N*-oxygenated to the phenethyl hydroxylamine and subsequently to its *trans*-oxime and this terminates biological activity [Lin *et al.*, 1997a; Lin *et al.*, 1997b]. FMO apparently precludes biologically important nucleophiles including many endogenous thiols and other heteroatom-containing compounds from the active site [Ziegler, 1990]. This is advantageous because if cellular nucleophiles were to be continuously oxidized, this would represent a tremendous drain on the ability of a cell to produce reducing equivalents (i.e., NADPH) for normal cell function. In addition, oxygenation of endogenous thiols by FMO would also produce a large amount of electrophilic metabolites that might overwhelm the cells ability to detoxicate them. FMO stabilizes the peroxyflavin and

does so with a molecular architecture that does not allow reactive metabolites generated to covalently modify the active site or substrate binding region. Thus, the substrate binding region is presumably composed of highly lipophilic and non-nucleophilic amino acid residues. Overall, substrate specificities of FMO1 – 3 have been examined thoroughly in the past. However, for FMO4 and FMO5 enzymes there is still a large gap in knowledge of substrate specificity and the substrate binding site dimensions.

6.1.2 Aim of the Study

As stated in 6.1.1, substrate specificity of FMO isozymes is mainly due to size restriction of the substrate binding channel of the enzyme. A three-dimensional structure of the FMO enzymes, as attempted in chapter 4 would certainly be useful to define substrate specificity since computational modeling studies could be performed. However, much can be learned about the size of the catalytic site from comparison of accepted substrates, as was already done for FMO1 – 3. In case of FMO5, however, the paucity of substrates prevents this approach.

A photometric HPLC based functional assay has been established for mouse and human FMO5 [Zhang *et al.*, 2007a]. In this HPLC analysis assay that has been previously described [Lattard *et al.*, 2003b] the ratio of a known FMO5 substrate (i.e., 8-DPT) to product (8-DPT *N*-oxide) after a 20 minute incubation period at 37 °C is determined. However, in order to screen and identify alternative substrates for FMO5, an easy and quick high-throughput (HT) capable kinetic activity assay should be developed to aid the search for new FMO5 substrates. This would help to gain a clearer understanding of the substrate specificity of human FMO5 and the structure and size of its catalytic site. Identification of structural groups oxygenated by FMO5 could suggest likely physiological substrates and contribute an explanation of the physiological role of FMO5 in mammalian tissue.

6.2 Materials and Methods

6.2.1 Reagents

Buffer reagents and substrates tested were purchased from Sigma-Aldrich Chemical Co. (St Louis, MO, USA) in appropriate purity. 8-DPT HCl was synthesized by Dr. Karl Okolotowicz (HBRI, San Diego, USA). 4'-(4-bromophenyl)- ω -dimethylaminobutyrophenon HCl (BDAB HCl) was originally developed in our research group as NO-inhibitor and was synthesized by Dr. Britta Gerig (Pharmaceutical Institute, CAU Kiel, Germany). 4'-(4"-bromophenyl)- ω -[4-chlorophenyl]-4-hydroxypiperidinyl]-butyrophenone (BCHP) as well as 4'-(4"-bromophenyl)- ω -(4-phenylpiperazinyl)butyrophenone (BPPB) were developed as antipsychotics and were synthesized by Nikola Klein (Pharmaceutical Institute, CAU Kiel, Germany). All compounds synthesized were of analytical grade and characterized in the usual way.

6.2.2 Cloning, Expression, and Purification of MBP-hFMO5

Recombinant human FMO5 was expressed as an *N*-terminal maltose-binding fusion protein (MBP-hFMO5) [Lattard *et al.*, 2003b] and purified as described in section 3.2.2 with minor changes. MBP-FMO5 was expressed in *E. coli* BL21 cells. After induction, cells were incubated shaking at 20 °C for 24 hours. After expression, *E. coli* cells were harvested by centrifugation at 6,000 *g* for 10 minutes and the cell pellet was frozen in order to increase yield. After resuspending the cell pellet in lysis buffer as described in section 3.2.2.1, cells were disrupted by passage through a French press (Thermo Electron Corp., Needham Heights, MA, USA) operating at 20,000 psi. The cell pellet was only extracted once and after centrifugation the supernatant was loaded at 1 ml/min onto an amylose column (New England BioLabs, Ipswich, MA, USA) equilibrated with ten column volumes of buffer A' (i.e., 50 mM Na₂HPO₄, pH 8.4, containing 15 µg/ml FAD). The column was washed with at least ten column volumes of buffer A' and bound MBP-hFMO5 protein was eluted with 3 mM maltose in buffer A' at 1 ml/min. Eluted protein was concentrated with an Amicon Ultra-15 centrifugal filter unit with an Ultracel-50 filter (Millipore, Billerica, MA, USA).

6.2.3 Determination of MBP-hFMO5 Concentration

Concentration of purified MBP-hFMO5 was determined by measuring the absorbance at 280 nm with a NanoDrop™ ND-1000 UV/VIS Spectrophotometer (Thermo Fisher Scientific, Wilmington, DE, USA) using a calculated extinction coefficient of $121 \text{ M}^{-1}\text{cm}^{-1}$ estimated after the method of Gill [Gill *et al.*, 1989].

6.2.4 Enzyme Assays

N-oxygenation of 8-DPT HCl by MBP-hFMO5 was determined by HPLC analysis as previously described (section 3.2.4.2).

As primary confirmatory assay for BDAB HCl as potential FMO5 substrate, *N*-oxygenation of 8-DPT HCl by MBP-hFMO5 was determined in the presence of BDAB HCl. A standard incubation mixture of 250 μl final volume contained 50 mM potassium phosphate buffer, pH 8.5, 0.2 mM NADPH, 0.25 mM DETAPAC, and 60 μg MBP-hFMO5. Reactions were initiated by addition of 8-DPT HCl or a mixture of 8-DPT HCl and BDAB HCl. For 8-DPT HCl, a final concentration of 400 μM was chosen, BDAB was added to a final concentration of 200 μM . After incubation for 20 minutes shaking under aerobic conditions at 37 °C, enzyme reactions were stopped and processed as described in section 3.2.4.2. HPLC analysis was done on a Waters Alliance™ HPLC-System (Waters e2695 XC Separations Modul, Waters 2998 Photodiode Array Detector and Empower™ 2 Software). Chromatographic separation of analytes was done on a LiChrospher-Si 60 (250 x 4.6 mm, 5 μm ; Merck, Darmstadt, Germany) with a mobile phase of 80 % methanol/20 % isopropanol/0.025 % HClO_4 (v/v/v). The flow rate was 1.5 ml/min and the total run time was 18 minutes. The wavelength for UV detection was set to 243 nm. The retention times for 8-DPT and 8-DPT *N*-oxide were 4.9 and 3.7 minutes, respectively. Statistical analysis was also done using Graphpad Prism software and statistical significance was judged at $P < 0.05$.

As secondary confirmatory assay, *N*-oxygenation of BDAB HCl was determined by HPLC analysis. A standard incubation mixture of 250 μl final volume contained 50 mM potassium phosphate buffer, pH 8.5, 0.2 mM NADPH, 0.25 mM DETAPAC, and 60 μg MBP-hFMO5. Reactions were initiated by addition of substrate to a final concentration of 200 μM . After incubation for 20 minutes shaking under aerobic

conditions at 37 °C, enzyme reactions were stopped by addition of 4 volumes of cold dichloromethane. About 20 mg of Na₂CO₃ was added and the incubations were mixed and centrifuged to partition metabolites and remaining substrate into the organic fraction. The organic phase was collected and evaporated. Metabolites and remaining substrate were dissolved in methanol, mixed thoroughly, centrifuged and analyzed with a Waters AllianceTM HPLC-System (Waters e2695 XC Separations Modul, Waters 2998 Photodiode Array Detector and EmpowerTM 2 Software). Chromatographic separation of analytes was done on a LiChrospher-Si 60 (250 x 4.6 mm, 5 µm; Merck, Darmstadt, Germany) with a mobile phase of 80 % methanol/20 % isopropanol/0.025 % HClO₄ (v/v/v). The flow rate was 1.5 ml/min and the total run time was 18 minutes. The wavelength for UV detection was set to 293 nm. The retention times for BDAB and BDAB *N*-oxide were 10.7 and 5.7 minutes, respectively.

6.2.5 LC/MS Analysis

In order to identify the metabolite produced by incubation of BDAB HCl with FMO5 in the presence of NADPH (section 6.2.4), an LC/MS-method was developed. After incubation, metabolites and remaining substrate were dissolved in methanol, mixed thoroughly, centrifuged and analyzed with an Esquire LC MS system (Bruker Daltonics, Bremen, Germany) after separation with an HP HPLC-System (HP Series 1100 Binary Pump G1312A, HP 1100 VWD UV/VIS Detector and Agilent ChemStation HPLC Software (Version A.09.01), and Esquire Control (Version 6.14) and Data Analysis (Version 3.0) MS Software). Chromatographic separation of analytes was done on a Symmetry C18 (250 x 4.6 mm, 5 µm; Waters) with a Guard Pak C18 precolumn (3 x 4 mm; Waters) and a mobile phase of 70 % of 0.1 % formic acid in acetonitrile, 15 % of 0.1 % acetic acid, and 15 % methanol (v/v/v). The flow rate was 1.5 ml/min and the total run time was 12 minutes. The wavelength for UV detection was set to 293 nm. The retention times for BDAB and BDAB *N*-oxide were 6.3 and 3.5 minutes, respectively. MS analysis was done using electrospray ionization (ESI) with a dry temperature of 340 °C, a dry gas flow rate of 7 l/min, and a spray pressure of 30 psi. The scan was done between 50 and 1000 m/z and peaks were detected at m/z 346 and 362 for BDAB and BDAB *N*-oxide, respectively.

6.2.6 Development of a Photometric Activity Assay Method

6.2.6.1 Assay Protocol Outline

The FMO5 activity assay was based on the photometric determination of NADPH consumption. During substrate oxygenation by FMO5, NADPH is oxidized to NADP⁺ and the disappearance of NADPH can be monitored photometrically over time at 340 nm. A typical reaction mixture consisted of 50 mM phosphate buffer, pH 8.4, 200 μ M NADPH, 250 μ M DETAPAC to inhibit autooxidation, and 200 μ g/ml MBP-hFMO5 in a final volume of 100 μ l. This mixture was prepared in advance and dispensed into 96-well flat-bottom UV-Star microplates (Greiner Bio-One, Frickenhausen, Germany). Afterwards, the reaction was initiated by addition of substrate. Kinetic decrease of NADPH was measured over 20 minutes and each well was read every 60 seconds using a Cary 50 Scan UV-Visible Spectrophotometer (Varian, Palo Alto, CA, USA). For initial assay optimization studies, the known substrate 8-DPT HCl was used to validate the high-throughput assay and the final 8-DPT HCl concentration in these initial studies was 400 μ M.

6.2.6.2 Optimization of Assay Conditions

Protein Concentration

Purified MBP-hFMO5 was evaluated over a range of enzyme concentrations in reactions containing 8-DPT HCl. The reaction mixture consisted of MBP-hFMO5 and 200 μ M NADPH in 50 mM potassium phosphate buffer, pH 8.4, containing 0.25 mM DETAPAC. The reactions were initiated by addition of 8-DPT HCl to a final concentration of 400 μ M. Slopes representing FMO activity generated by reactions containing 8-DPT HCl were normalized to slopes of control reactions without the substrate. Reactions were done in quadruplicates and enzyme was used in concentrations between 0.05 and 0.8 mg/ml.

Substrate Dependence

Kinetic parameters (V_{max} , K_m) of 8-DPT HCl were evaluated. The reaction mixture consisted of 200 μ g/ml MBP-hFMO5 and 200 μ M NADPH in 50 mM potassium phosphate buffer, pH 8.4, containing 0.25 mM DETAPAC. Reactions were initiated by addition of at least five varying concentrations of 8-DPT HCl between 5 and 400 μ M. Reactions were done in quadruplicates and slopes reflecting rates of

cofactor depletion were calculated by normalizing to slopes of reactions lacking protein.

6.2.7 Development of a Fluorimetric Activity Assay Method

6.2.7.1 Assay Protocol Outline

The FMO5 activity assay was based on the fluorimetric determination of NADPH consumption and was adapted from Simeonov *et al.* [Simeonov *et al.*, 2008] who established a fluorescence based NADPH depletion assay for inhibitor screening of the *Schistosoma mansoni* redox cascade. During substrate oxygenation by FMO5, NADPH is oxidized to NADP⁺ and the decrease of NADPH fluorescence can be monitored kinetically over 40 minutes, reading each well every 60 seconds at excitation/emission wavelengths of 365 nm/450 nm using a Perkin Elmer LS55 Fluorescence Spectrophotometer (Perkin Elmer, Waltham, MA, USA). A typical reaction mixture consisted of 50 mM phosphate buffer, pH 8.4, 200 μ M NADPH, 250 μ M DETAPAC, and 200 μ g/ml MBP-hFMO5. This mixture was prepared in advance and dispensed into white 96-well flat-bottom microplates (OptiPlate-96, Perkin Elmer, Waltham, MA, USA). Afterwards, the reaction was initiated by addition of substrate. For initial assay optimization studies, the known substrate 8-DPT HCl was used to validate the HT-assay and the final 8-DPT HCl concentration in these initial studies was 400 μ M.

6.2.7.2 Optimization of Assay Conditions

Protein Concentration

Purified MBP-hFMO5 was evaluated over a range of enzyme concentrations in reactions containing a final concentration of 400 μ M 8-DPT HCl. This was done measuring the decrease of NADPH fluorescence kinetically at excitation/emission wavelengths of 365 nm/450 nm over 50 minutes. Each well was read every 60 seconds. The reaction mixture consisted of MBP-hFMO5 in concentrations between 0.05 and 0.8 mg/ml and 200 μ M NADPH in 50 mM potassium phosphate buffer, pH 8.4, containing 0.25 mM DETAPAC. The reactions were initiated by addition of 8-DPT HCl to a final concentration of 400 μ M. Reactions were done in quadruplicates and slopes representing FMO5 activity generated by reactions

containing 8-DPT HCl were normalized to slopes of control reactions without substrate.

Substrate Dependence

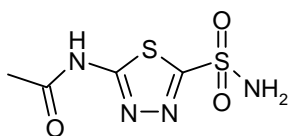
Kinetic parameters (V_{max} , K_m) of 8-DPT HCl were evaluated. Again, the decrease of NADPH fluorescence was measured kinetically at excitation/emission wavelengths of 365 nm/450 nm over 60 minutes and each well was read every 60 seconds. The reaction mixture consisted of 300 $\mu\text{g/ml}$ MBP-hFMO5 and 200 μM of its cofactor NADPH in 50 mM potassium phosphate buffer, pH 8.4, containing 0.25 mM DETAPAC. Reactions were initiated by addition of at least five varying concentrations of 8-DPT HCl between 20 and 1600 μM . Reactions were done in quadruplicates and slopes reflecting rates of cofactor NADPH depletion were calculated by normalizing to slopes of reactions lacking protein.

6.2.8 Substrate Screens

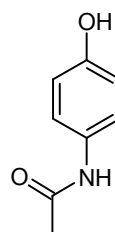
80 Compounds were tested with the developed photometric assay method for MBP-hFMO5 catalyzed oxygenation. These are listed in Table 6.1. Compounds were either dissolved in methanol or water and reactions were started by addition of these to yield final concentrations of 400 μM . Methanol concentrations in final incubations did not exceed 1 %. At this concentration, no significant change in enzyme activity was observed. Reactions were done in at least duplicates and slopes reflecting rates of NADPH depletion were calculated by normalizing to slopes of reactions lacking enzyme. In all plates at least one well contained 8-DPT HCl as positive control.

Table 6.1 Compounds tested with the developed photometric assay method.

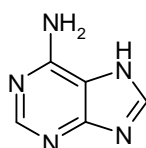
Acetazolamide



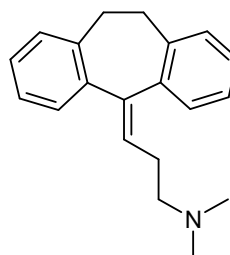
Acetaminophen



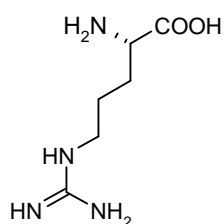
Adenine



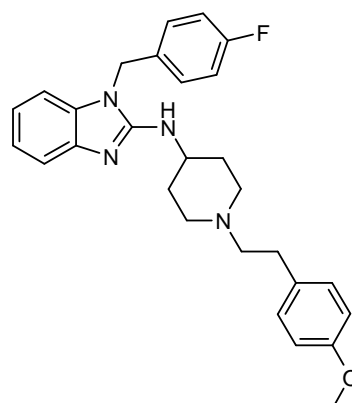
Amitriptyline



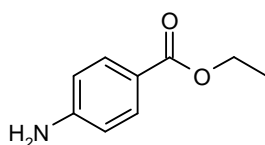
L-Arginine



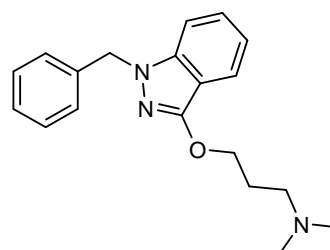
Astemizole



Benzocaine

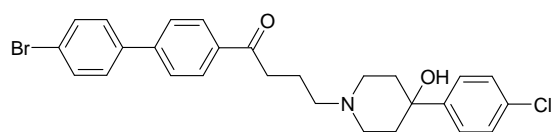


Benzydamine

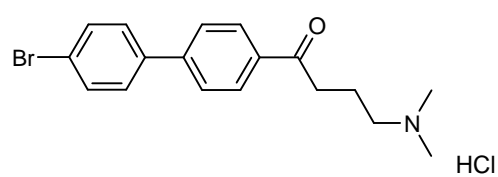


6 Substrate Selectivity and Screens of Potential FMO5 Substrates

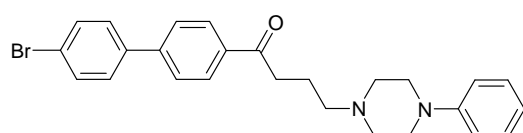
BCHP



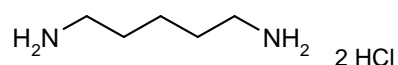
BDAB HCl



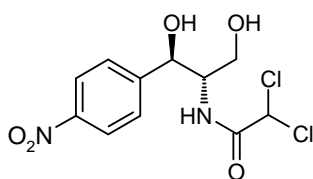
BPPB



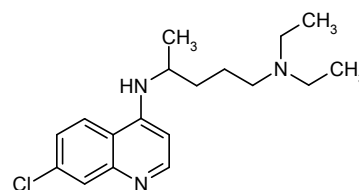
Cadaverine 2·HCl



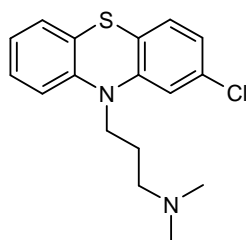
Chloramphenicol



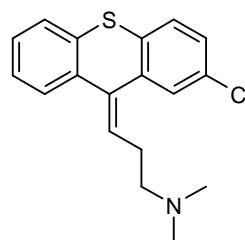
Chloroquine



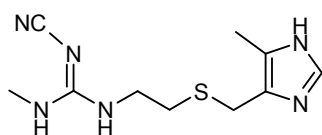
Chlorpromazine



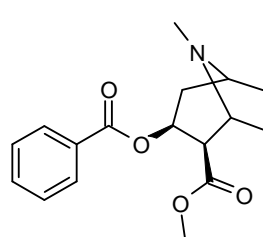
Chlorprothixene



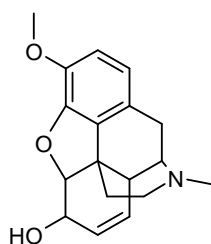
Cimetidine



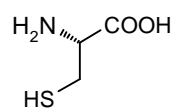
Cocaine



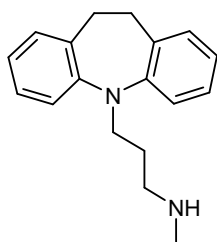
Codeine



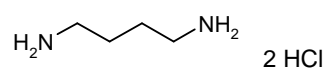
L-Cysteine



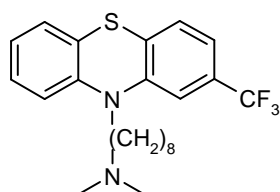
Desipramine



1,4-Diaminobutane 2·HCl



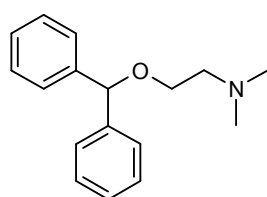
8-DPT HCl



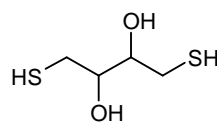
Dimethyl sulfoxide



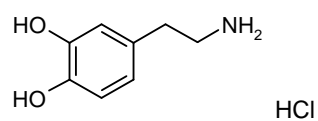
Diphenhydramine



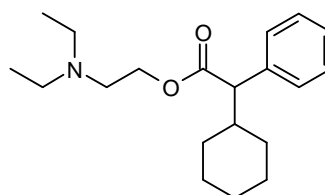
Dithiothreitol



Dopamine HCl

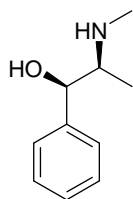


Drofenin

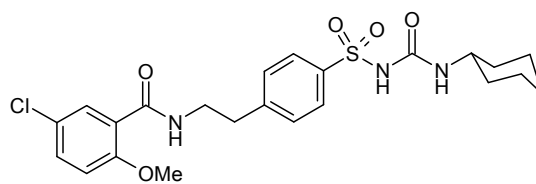


6 Substrate Selectivity and Screens of Potential FMO5 Substrates

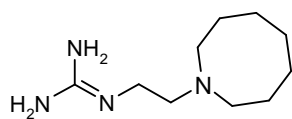
Ephedrine



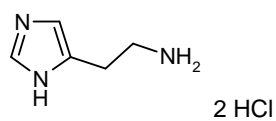
Glibenclamid



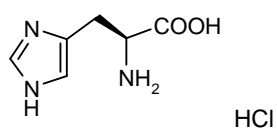
Guanethidine



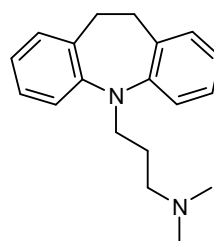
Histamine 2·HCl



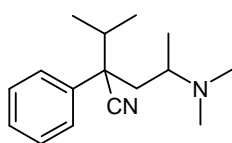
L-Histidine HCl



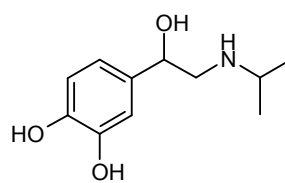
Imipramine



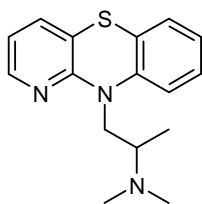
Isoaminile



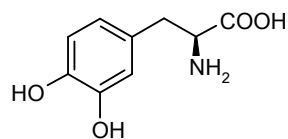
Isoprenalin



Isothipendyl

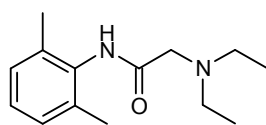


Levodopa

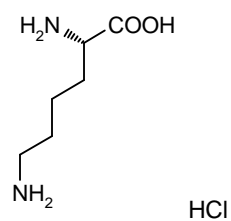


6 Substrate Selectivity and Screens of Potential FMO5 Substrates

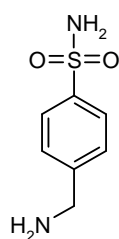
Lidocaine



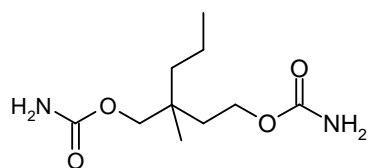
L-Lysine HCl



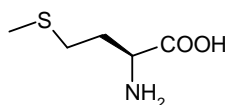
Mafenide



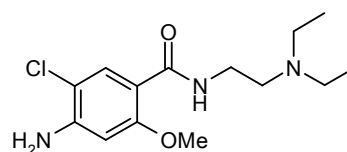
Meprobamate



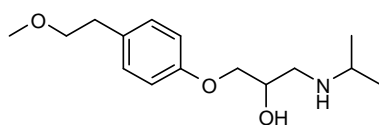
L-Methionine



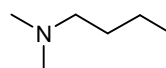
Metoclopramid



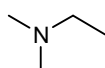
Metoprolol



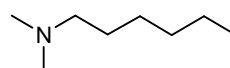
N,N-Dimethylbutylamine



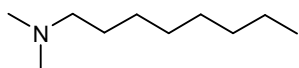
N,N-Dimethylethylamine



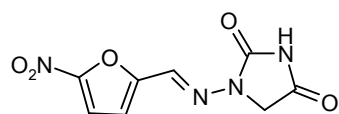
N,N-Dimethylhexylamine



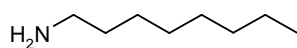
N,N-Dimethyloctylamine



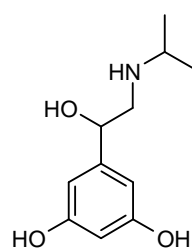
Nitrofurantoin



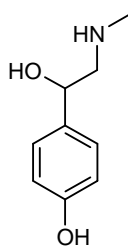
n-Octylamine



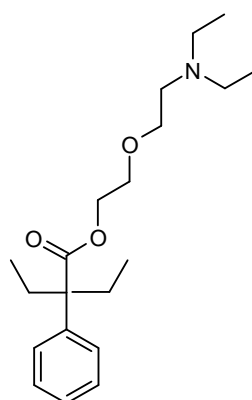
Orciprenaline



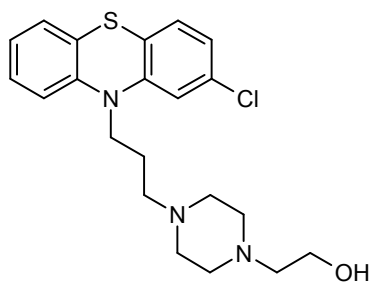
Oxedrin



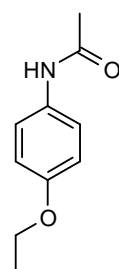
Oxeladin



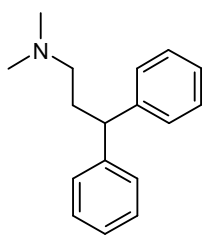
Perphenazin



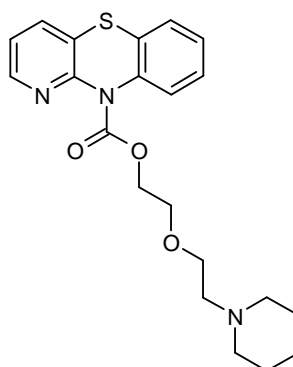
Phenacetin



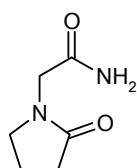
Pheniramine



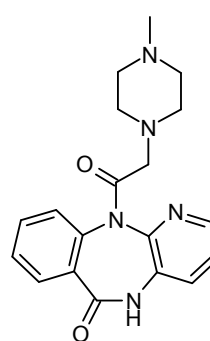
Pipazethate



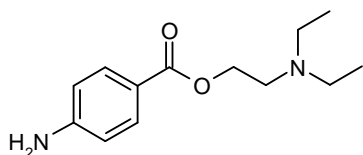
Piracetam



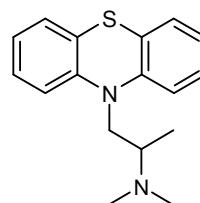
Pirenzipin



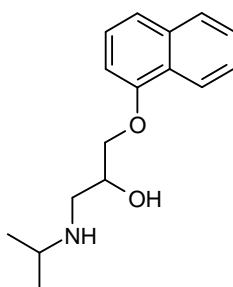
Procaine



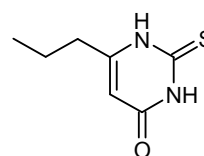
Promethazine



Propranolol

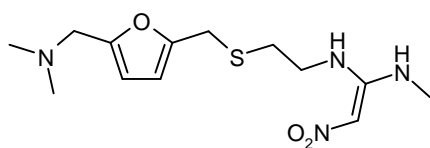


Propylthiouracil

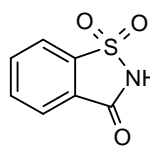


6 Substrate Selectivity and Screens of Potential FMO5 Substrates

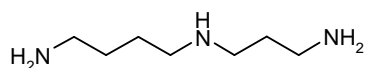
Ranitidine



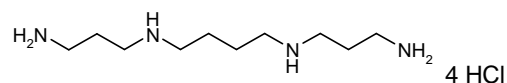
Saccharin



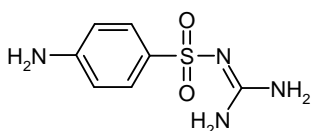
Spermidine



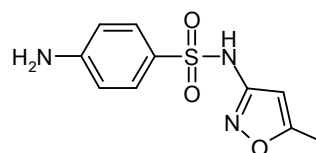
Spermine 4·HCl



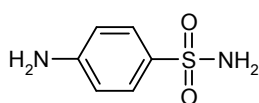
Sulfaguanidine



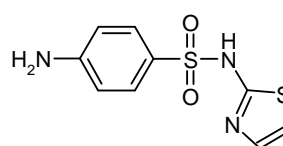
Sulfamethoxazol



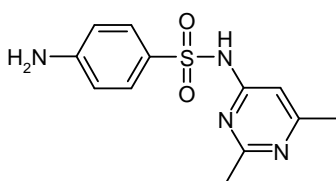
Sulfanilamide



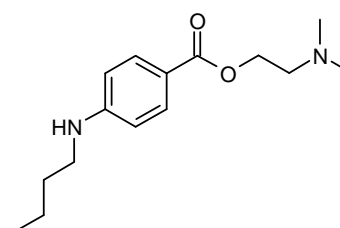
Sulfathiazole



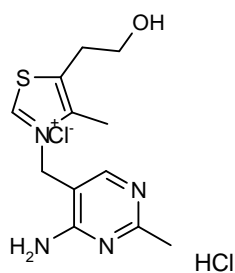
Sulfisomidin



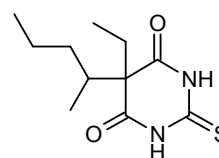
Tetracain



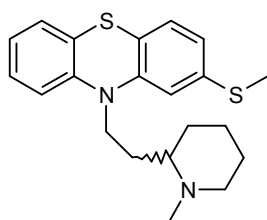
Thiamine chloride·HCl



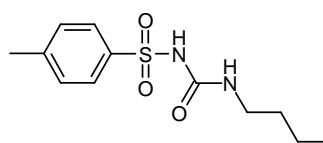
Thiopental



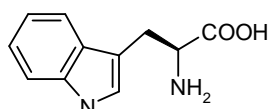
Thioridazine



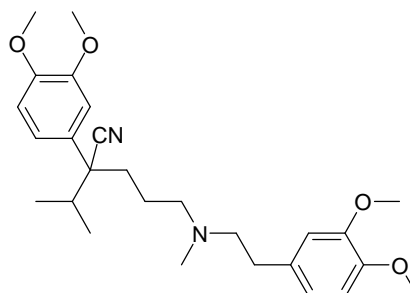
Tolbutamide



L-Tryptophan



Verapamil



6.3 Results

6.3.1 Comparison of Photometric and Fluorescent Activity Assay Methods

For the development of a suitable HT-adaptable FMO5 oxygenation activity assay, two approaches were carried out and evaluated. Both methods were based on NADPH consumption associated with FMO5 dependent oxygenation activity. However, one was a photometric approach whereas the other exploits the inherent fluorescence of NADPH.

6.3.1.1 Photometric Activity Assay Method

Time Dependence

Protein dependence as well as substrate dependence was measured over 20 minutes and graphs were plotted and evaluated in regards to signal stability over time. A stable slope for NADPH depletion at 340 nm could be observed for the whole time period measured.

Protein Concentration

Results of protein dependence studies are shown in Figure 6.1. The protein concentration dependent increase of activity is clearly visible. It is necessary to use enough enzyme to consume sufficient amounts of NADPH to generate detectable and reproducible slopes. However, at a concentration of 0.8 mg/ml enzyme the activity decreases. This might be due to nonspecific binding of MBP-hFMO5 to the substrate, leading to a decrease in effective concentration. For further studies, MBP-hFMO5 concentrations between 0.2 and 0.4 mg/ml were used.

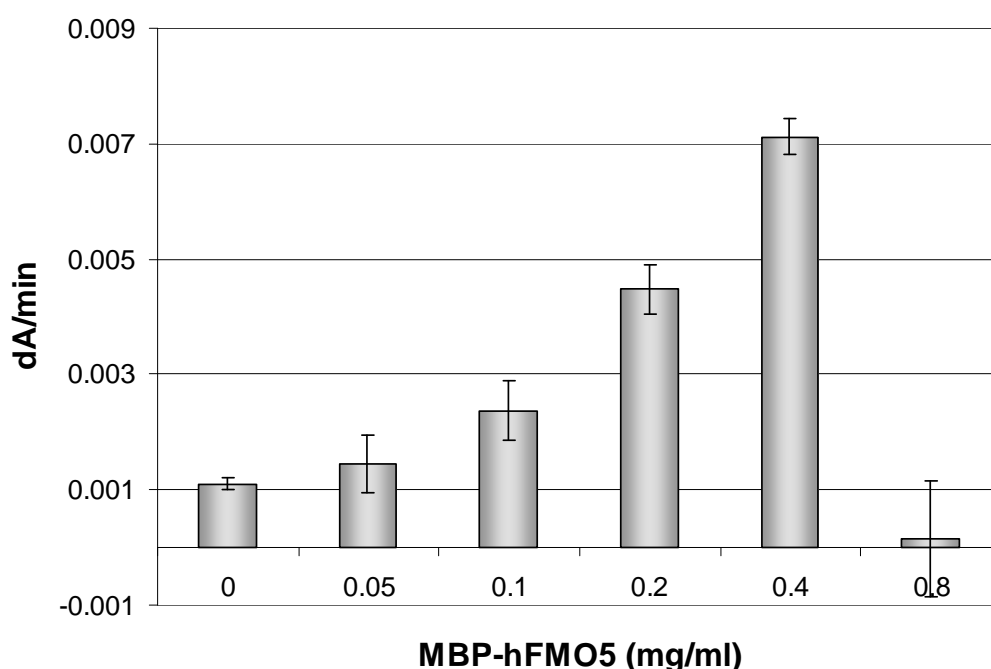


Figure 6.1 MBP-hFMO5 concentration dependence of the photometric plate-reader based NADPH depletion assay with 8-DPT HCl as substrate.

Substrate Dependence

Data obtained from incubation of MBP-hFMO5 with varying amounts of 8-DPT HCl was plotted as 8-DPT concentration vs. enzyme activity in nmol/min/mg FMO5 and a nonlinear regression curve fit tool using a Michaelis-Menten model ($Y = (V_{max} \cdot X) / (K_m + X)$ with $V_{max} = Y_{max}$ and $K_m = X_{mid}$) in Graphpad software (Graphpad Prism, Version 2.00, San Diego, CA, USA) was utilized to calculate the kinetic parameters. The obtained K_m was $12.3 \pm 1.0 \mu\text{M}$ and V_{max} was

6.4 ± 0.1 nmol/min/mg FMO5 (Figure 6.2). As positive control in screening assays, a concentration of 200 μ M 8-DPT HCl was selected.

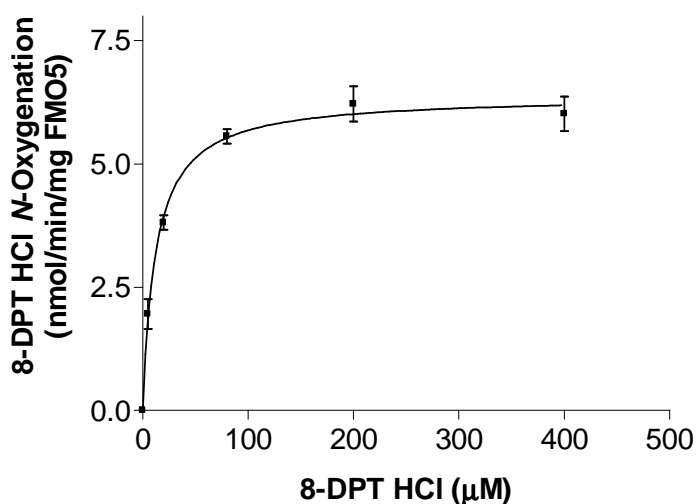


Figure 6.2 8-DPT HCl concentration dependence for photometric plate-reader based NADPH depletion assay with MBP-hFMO5.

6.3.1.2 Fluorimetric Activity Assay Method

Time Dependence

Protein dependence as well as substrate dependence was measured over 60 minutes and graphs were plotted and evaluated in regards to signal stability over time. Signal stability was dependent on protein concentration. A clear decrease of NADPH fluorescence could only be observed for 10 minutes at a MBP-hFMO5 concentration of 0.8 mg/ml. At 0.4 mg/ml, the signal was stable for 40 minutes and at protein concentrations below 0.4 mg/ml, the decrease was linear within the range tested (50 minutes) (data not shown).

Protein Concentration

Results of protein dependence studies are shown in Figure 6.3. The slopes were only evaluated in the range of 0 to 30 minutes because linearity was not given afterwards at higher enzyme concentrations (see also time dependence). The protein concentration dependent increase of activity is clearly visible. However, although it is necessary to use enough enzyme to consume sufficient amounts of NADPH to

generate detectable and reproducible slopes, large amounts of enzyme will consume substrate too quickly and the slope will decrease. Also, protein may nonspecifically bind to a substrate, leading to a decrease in effective concentration. The optimal concentration for further studies lies in the range of 0.2 and 0.4 mg/ml MBP-hFMO5.

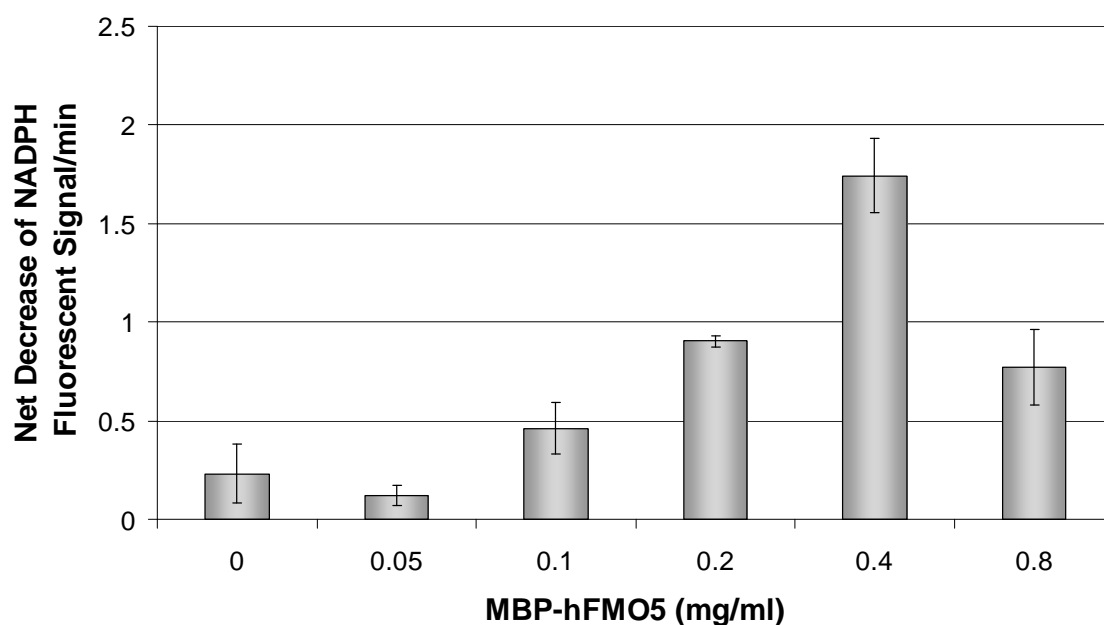


Figure 6.3 MBP-hFMO5 concentration dependence of the fluorimetric plate-reader based NADPH depletion assay with 8-DPT HCl as substrate.

Substrate Dependence

Data from substrate dependence studies fit to Michaelis-Menten kinetic in the range of 20 – 400 μM . However, higher concentrations of substrate led to decreased netto fluorescence signal. This could be due to an inhibitory effect of substrate on the enzyme. Thus, data obtained from incubation of MBP-hFMO5 was plotted in the range of 20 - 400 μM as 8-DPT HCl concentration vs. netto decrease of NADPH fluorescent signal and a nonlinear regression curve fit tool using a Michaelis-Menten model ($Y = (V_{max} \cdot X)/(K_m + X)$ with $V_{max} = Y_{max}$ and $K_m = X_{mid}$) in Graphpad software (Graphpad Prism, Version 2.00, San Diego, CA, USA) was utilized to calculate kinetic parameters. The obtained K_m was $30.3 \pm 4.5 \mu\text{M}$ and V_{max} was $6.4 \pm 0.2 \text{ nmol/min/mg}$ (Figure 6.4). As positive control in subsequent assays, a concentration of 200 μM 8-DPT HCl should be used.

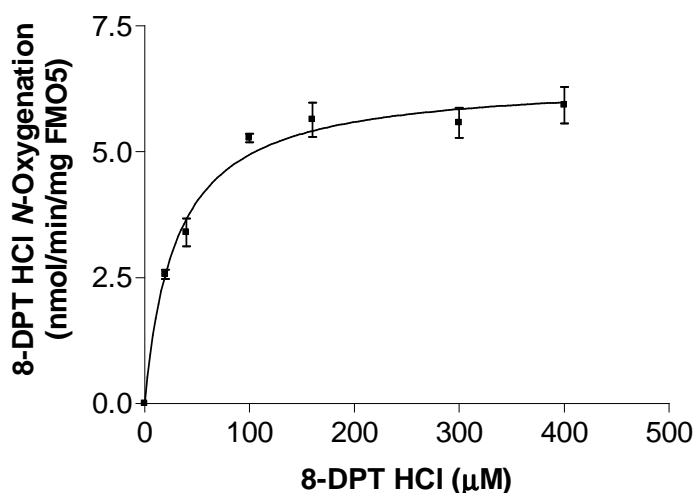


Figure 6.4 8-DPT HCl concentration dependence of fluorescence plate-reader based NADPH depletion assay with MBP-hFMO5.

6.3.2 Substrate Screens

No significant differences in terms of protein and substrate concentration needed could be observed between photometric and fluorescence enzyme activity assay. For substrate screens, the photometric assay was chosen. Besides the positive control substrate 8-DPT HCl, only 4'-(4-bromophenyl)- ω -dimethylaminobutyrophenone HCl (BDAB HCl) showed considerable decrease in absorbance at 340 nm. For all other compounds tested, no decrease in absorbance could be observed at the substrate concentrations used in the assay. A few other substrates including chlorpromazine, chlorprothixene, drofenin HCl, promethazine HCl, thioridazine, and phenacetin appeared to be potential hits after the primary screen and were re-screened to eliminate false-positives. None of these compounds proved to be a substrate for FMO5 and thus only BDAB HCl was examined further. BDAB *N*-oxygenation activity of FMO5 was supposed to be confirmed with an independent assay. Within this assay, 8-DPT HCl was incubated with MBP-hFMO5 in the presence and absence of BDAB HCl. As shown in Figure 6.5, conversion of 8-DPT was significantly inhibited by addition of BDAB to the incubation mixture. This inhibition was possibly due to BDAB HCl being a competitive substrate for MBP-hFMO5. Thus, in a secondary confirmatory assay, an HPLC-based method was developed to separate BDAB HCl from its metabolite/s after incubation with FMO5.

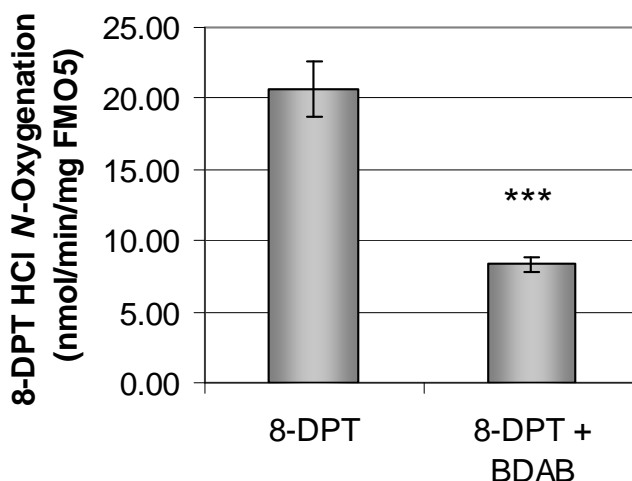


Figure 6.5 8-DPT HCl *N*-oxygenation by MBP-hFMO5 with and without BDAB.

*Statistically significant differences between incubation with 8-DPT HCl and incubation with a combination of 8-DPT HCl and BDAB HCl are identified with *** for $P < 0.001$.*

Only one additional peak was observed in HPLC analysis after incubation of BDAB with MBP-hFMO5. This peak was analyzed via LC-MS and proved to be BDAB *N*-oxide with m/z 362 (Figure 6.6).

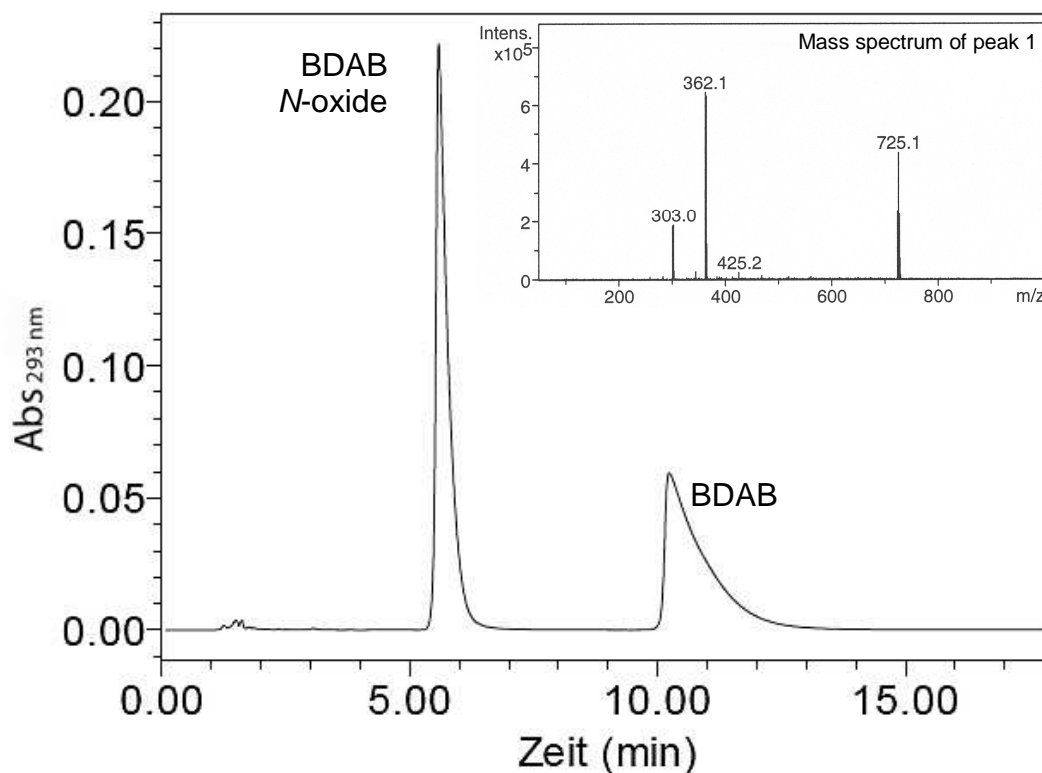


Figure 6.6 HPLC Chromatogram of BDAB HCl and BDAB *N*-oxide.

6.4 Discussion

Two different HT-compatible screening methods that are based on NADPH consumption during enzyme catalysis have been developed and were compared. No significant difference in terms of necessary protein and substrate concentrations could be observed. The photometric assay was chosen to screen several potential FMO5 substrates. Besides the control substrate 8-DPT HCl and BDAB HCl, none of the compounds tested showed considerable decrease in 340 nm absorbance. Further evaluation of BDAB HCl proved this compound to be a substrate for FMO5.

Several substrates have already been tested for oxygenation activity catalyzed by FMO5 from various species (i.e., mouse, human, and rabbit FMO5) including methimazole [Atta-Asafo-Adjei *et al.*, 1993; Overby *et al.*, 1995; Zhang *et al.*, 2007a], ranitidine and cimetidine [Overby *et al.*, 1997], phorate [Cherrington *et al.*, 1998], trimethylamine [Atta-Asafo-Adjei *et al.*, 1993; Zhang *et al.*, 2007a], chlorpromazine, perchlorperazine, imipramine, *N,N*-dimethylaniline, cysteamine, trimethylamine and *n*-decylamine [Atta-Asafo-Adjei *et al.*, 1993], L-arginine and *N*^δ-Methyl-D,L-arginine [Kotthaus, 2008], *n*-octylamine [Atta-Asafo-Adjei *et al.*, 1993; Cherrington *et al.*, 1998; Overby *et al.*, 1995], *n*-nonylamine [Atta-Asafo-Adjei *et al.*, 1993], *S*-methylesonarimod [Ohmi *et al.*, 2003; Zhang *et al.*, 2007a] and 8-DPT [Zhang *et al.*, 2007a]. However, only the last four compounds were actually oxygenated by the enzyme. Of these four known FMO5 substrates, besides 8-DPT, *n*-octylamine was examined within this study. It is notable that upon incubation with *n*-octylamine no decrease of NADPH dependent absorption at 340 nm could be observed in the photometric assay although this compound had previously been reported by one group [Overby *et al.*, 1995] to be a substrate for human FMO5. This could not be confirmed in this study.

Overall, the assay methods developed may be used to screen for further potential substrates. Screening a library of several thousands of compounds in a HT-format may help find additional FMO5 substrates and may lead to identification of structural groups oxygenated by FMO5 that will suggest likely physiological substrates and contribute an explanation of the role of FMO5.

A potential problem of both screening methods is the requirement of high substrate concentrations that might make it difficult to find a suitable library. An alternative approach could be an inhibitor screen for competition against 8-DPT as FMO5 substrate. Lower compound concentrations would be needed for this approach and the method may still identify groups capable of binding to the enzyme's active site, providing an indirect perspective on true substrate structure features. In general, the assay protocol would be similar to that of the direct FMO5 substrate screen and the inhibitor approach could also be combined with HPLC analysis of 8-DPT *N*-oxygenation as a basis for secondary confirmatory assays.

A completely different approach to test the significance of FMO5 would be the development of a knock-out or knock-in mouse model of FMO5 or the usage of short interfering RNA (si-RNA) in order to suppress *FMO5* expression. Such studies could also give more information about the physiological role and importance of FMO5.

7 Summary

In this work, the structural and functional relations of flavin-containing monooxygenases (FMOs) 3 and 5 were investigated. The family of FMO enzymes represents, after the cytochromes P450, the most important monooxygenases in humans. It consists of five isozymes (FMO1 – 5) which catalyze mainly the oxygenation of nucleophilic *N*- and *S*-containing xenobiotics [Cashman *et al.*, 2006; Ziegler, 1980]. In the main drug-metabolizing organ, the adult human liver, FMO3 and FMO5 mRNA are the most abundantly expressed FMO mRNAs [Cashman *et al.*, 2006; Janmohamed *et al.*, 2004]. Thus special interest was paid to these two isoforms.

In the past, FMO3 gained considerable importance because of its association with trimethylamineuria (TMAu). TMAu is a disorder that often manifests itself in a body odor for individuals affected. It is due to decreased metabolism of dietary-derived trimethylamine (TMA). In a healthy individual, 95 % or more of TMA is converted by the FMO3 to non-odorous TMA *N*-oxide. Several SNPs of the *FMO3* gene have been described and result in an enzyme with decreased or abolished functional activity for TMA *N*-oxygenation thus leading to TMAu.

The disorder may be diagnosed by genotyping or by measuring urinary ratios of TMA *N*-oxide to TMA. Accurate diagnosis is essential for the affected individuals so that they can be treated appropriately. Treatment comprises restriction of certain foods, supplementation of folate, riboflavin, and, in very severe cases administration of antibiotics to decrease TMA formation due to gut bacteria [Akerman *et al.*, 1999; Ayesh *et al.*, 1993; Cashman *et al.*, 2002; Mitchell, 1996; Mitchell *et al.*, 2001].

Biochemical characterization of recombinant expressed variant FMO3 observed from genotyping and phenotyping aids to reveal important information about structure and function of human FMO3 [Akerman *et al.*, 1999; Cashman, 2002; Cashman *et al.*, 2002; Dolphin *et al.*, 1997b; Shimizu *et al.*, 2007b; Treacy *et al.*, 1998; Yeung *et al.*, 2007].

Herein, a novel mutation observed from phenotyping and genotyping of self-reporting individuals was examined. This novel mutation was heterozygous at position 187

(V187A) and occurred in combination with mutations at position 158 (E158K), 308 (E308G), and 305 (E305X). Familial genetic analysis showed that the E158K/V187A/E308G derived from the same allele from the mother, and the E305X was derived from the father. Wild-type human FMO3 and its variants V187A and V187A/E158K were expressed as maltose-binding fusion proteins (MBP-FMO3), purified, and characterized for oxygenation of several common FMO3 substrates (i.e., 5- and 8-DPT, mercaptoimidazole (MMI), TMA, and sulindac sulfide) and for their thermal stability. The novel mutation in combination with the common polymorphism E158K led to severely decreased enzyme activity. Similarly, although by itself, the common polymorphisms E158K and E308G only slightly alter FMO3 activity, in combination they may lead to decreased activity [Cashman, 2000; Cashman *et al.*, 2003; Dolan *et al.*, 2005; Zschocke *et al.*, 1999]. This has also been reflected *in vivo* leading to TMAu [Lambert *et al.*, 2001; Zschocke *et al.*, 1999]. Likewise, the novel V187A mutation in conjunction with the common polymorphisms E158K and E308G significantly impairs FMO3 resulting in an enzyme with drastically decreased function that manifests itself in severe TMAu.

Although FMO5 mRNA is most abundantly expressed in human adult liver, it is a largely understudied enzyme. Therefore, besides FMO3, FMO5 was of particular interest and was characterized structurally and functionally within this thesis.

To facilitate these studies, highly-purified and well characterized FMO5 enzyme was produced. Human FMO5 was successfully expressed as maltose-binding fusion protein (MBP-hFMO5). Solubilization studies showed Triton[®] X-100 to be superior in extracting MBP-hFMO5 from *E. coli*. After cell lysis, protein was purified exploiting the MBP-tag for amylose-column chromatography. Further purification was done on an anion-exchange column and remaining impurities could be removed utilizing a NaCl salt gradient. Comparison to commercially available FMO5 showed no significant differences in kinetic behavior and since MBP-hFMO5 could be readily purified at low cost and in high quantities, it was chosen for further studies. Also MBP-hFMO5 could be obtained in high purity and was thus also suitable for crystallography studies. Further, MBP-hFMO5 was characterized in terms of enzyme activity and purity, stability at 4 °C, and oligomerization state and monodispersity. Especially for crystallography studies these characterization studies are substantial. They showed that addition of glycerol and NADP⁺ to the sample improved MBP-hFMO5 stability

1.6-fold and in subsequent crystallization studies these additives were added to enzyme preparations. Results from size exclusion chromatography of ion exchange purified MBP-hFMO5 suggested hexameric state for the protein which is in accordance with previous publications [Brunelle *et al.*, 1997; Ziegler *et al.*, 1972]. Dynamic light scattering (DLS) data of ion exchange purified FMO5 samples showed a single peak, suggesting pure, monodispers protein suitable for crystallography studies.

When working with membrane associated proteins such as FMO enzymes use of detergents is unavoidable. As expected, surfactants play a dominant role in purification and crystallization of FMO5. Unfortunately, usage of detergents introduces a high level of unpredictability, especially if detergents are used that are heterogenic by themselves, such as Triton[®] X-100. However, the usage of this detergent was inevitable for the extraction of MBP-hFMO5 from *E. coli* and complete removal of Triton[®] X-100 and possibly substitution with other detergents seemed necessary prior to crystallization trials. Removal was done using polystyrene based beads (e.g., Bio-Beads[®]) and interestingly, upon addition of excess amounts of Bio-Beads[®] to the protein solution, MBP-hFMO5 did not precipitate. This result suggests that FMO5 is not an integral membrane protein, but rather only associated with the membrane. Also, removal of Triton[®] X-100 with Bio-Beads[®] improved results from crystallization trials of MBP-hFMO5 leading to thick yellow oil phases and premature crystals with spherical shapes.

Crystallography experiments were done by initially screening various commercially available 96-well plate crystal screen kits for suitable crystallization conditions. The most promising conditions were refined further in 24-well plates evaluating protein concentration, salts and buffers as well as precipitant type and concentration. Conditions that finally led to MBP-hFMO5 crystals were 26 % PEG 2K MME and 0.2 M sodium acetate in 0.1 M Bis-Tris propane buffer, pH 6.5.

Experiments in which a variety of different detergents was added after removal of Triton[®] X-100 led to further improvement of these first spherical shaped pre-stages of crystals. Detergents that yielded best results mainly belonged to a new group of amphiphilic agents that is supposed to stabilize membrane proteins and lower the risk of denaturing or aggregation. These surfactants are based on cholic acid and

exhibit facial amphiphilicity [Zhang *et al.*, 2007b; Zhong *et al.*, 2005]. In addition, detergents such as HECAMEG and the Cymal[®] series also yielded crystals. In general, employing the concept of mixed micelles by controlled addition of detergent seemed beneficial for FMO5 crystal growth.

Unfortunately, no satisfactory diffraction pattern could be obtained from MBP-hFMO5 crystals. This might be due to the flexible linker region between MBP-tag and FMO5 that possibly introduces conformational heterogeneity [Smyth *et al.*, 2003]. Therefore, MBP-hFMO5 was cleaved to perform crystallization experiments with only hFMO5. Splicing of MBP from hFMO5 was done utilizing a previously inserted protease sensitive site right after the MBP sequence that may be cleaved by factor Xa. After incubation for three hours at 37 °C, cleavage was largely completed and addition of NADPH to the incubation mixture prevented the enzyme from being heat-inactivated. It is notable that similar experiments had been done with MBP-hFMO3 [Brunelle *et al.*, 1997]. However, after cleaving MBP from hFMO3, the latter showed intractable solubility and enhanced instabilities [Brunelle *et al.*, 1997] as previously described for a number of purified native FMO enzymes [Cashman, 1995; Guan *et al.*, 1991]. In contrast to expectations, after proteolytical separation from MBP, human FMO5 stayed in solution and retained the same level of enzyme activity as the tagged protein. However, subsequent purification of hFMO5 from remaining factor Xa, MBP, and residual uncleaved MBP-hFMO5 using a variety of previously described methods including affinity purification [Riggs, 2000], ion exchange chromatography [de Pieri *et al.*, 2004; Guan *et al.*, 2002; Hao *et al.*, 2007; Riggs, 2000; Yan *et al.*, 2006], and size exclusion chromatography [Branco *et al.*, 2008] failed.

In summary, this study showed that MBP-hFMO5 is crystallizable. However, further studies are needed to purify hFMO5 from MBP in order to start crystallization experiments with the tag-free protein and obtain well diffracting crystals.

FMO5 displays a significantly different pH dependent activity profile than the other FMO isoforms [Zhang *et al.*, 2007a]. While pH optima of mouse FMO1 and 3 (mFMO1 and 3) display normal bell shape curves peaking around pH 8 to 10, with human FMO5 (hFMO5) and mFMO5, 8-DPT *N*-oxygenation activity continues to increase from pH 7 to pH 11 [Zhang *et al.*, 2007a]. A possible reason for the different pH profile found in FMO5 could be a slower overall turnover rate indicating a possibly

different rate-limiting step in the catalytic cycle of FMO5. To date, the catalytic steps of pig FMO1 are known in some detail [Beaty *et al.*, 1981a; Beaty *et al.*, 1981b; Jones *et al.*, 1986; Poulsen *et al.*, 1979; Ziegler *et al.*, 1988] and presumably, the other FMO isoforms follow a similar mechanism. However, this might not be the case for all FMO isoenzymes and the assumption is that FMO5 catalytical mechanism is distinct from that of other FMO enzymes.

The objective of this study was to determine the pH dependence of FMO5 to gain an insight into the mechanism of action of FMO5 enzymes. Therefore, functional recombinant hFMO5 and mFMO5 were expressed as MBP-fusion proteins from *E. coli*, purified with affinity chromatography, and examined for their 8-DPT *N*-oxygenation activity at different pH values. MBP-hFMO5 showed a broader range and greater functional activity from pH 6 to 11 compared to mFMO5. mFMO5 lost nearly all functional activity at pH 6, while hFMO5 maintained almost normal enzyme activity. In order to identify the amino acid residues involved in the effects of pH on hFMO5 and mFMO5 functional enzyme activity, pH-studies in the range of pH 6 through 9 were done with MBP-tagged chimeras of recombinant human and mouse FMO5 and variants of both. Results of this study showed that the residues responsible for the pH profile distinction between MBP-hFMO5 and MBP-mFMO5 are located at positions 227 and 228 of the enzyme. Further mutants were made to investigate the role of these amino acids. Combined with additional structural, functional and kinetic information, this study may add to provide insight into the mechanism of FMO5 revealing important interactions between substrate or cofactors of FMO and specific amino acid residues of the enzyme. In addition, results may be relevant for other FMO enzymes as well if the catalytic mechanism of all FMOs proves to be identical.

The last objective within this thesis was the development of a high-throughput (HT) compatible enzyme activity assay in order to screen for new FMO5 substrates. Two different HT-compatible screening methods that are based on a decrease of NADPH during enzyme catalysis have been developed and were compared. One was based on fluorescence whereas the other was a photometric assay. Since no significant difference in terms of protein and substrate concentrations needed or sensitivity could be observed, the photometric assay was chosen to screen 80 compounds as possible FMO5 substrates. Potential hits from this first screen were re-screened in

order to eliminate false-positives. Besides the control substrate 8-DPT HCl only 4'-(4-bromophenyl)- ω -dimethylaminobutyrophenone (BDAB) HCl showed considerable decrease in 340 nm absorbance. Thus, only this compound was examined further. An HPLC method was developed to separate substrate from its metabolite/s after incubation with MBP-hFMO5. The resulting BDAB metabolite observed after incubation was analyzed via LC-MS and proved to be BDAB *N*-oxide. Thus, results from the primary photometric assay could be confirmed. This compound fits well into the proposed selectivity range of FMO5, having a tertiary amine group on a long carbon side-chain away from a bulky moiety. It is still surprising that compounds with very similar structures such as benzydamine or tetracaine did not prove to be substrates of FMO5. Overall, further compound screens will be needed to identify additional FMO5 substrates and gain more knowledge of substrate specificity and thus the relationship between structure and function.

8 References

- Adachi, M.S., Juarez, P.R., Fitzpatrick, P.F. 2010. Mechanistic studies of human spermine oxidase: kinetic mechanism and pH effects. *Biochemistry* **49**:386-92
- Akerman, B.R., Lemass, H., Chow, L.M., Lambert, D.M., Greenberg, C., Bibeau, C., Mamer, O.A., Treacy, E.P. 1999. Trimethylaminuria is caused by mutations of the FMO3 gene in a North American cohort. *Mol Genet Metab* **68**:24-31
- Alfieri, A., Malito, E., Orru, R., Fraaije, M.W., Mattevi, A. 2008. Revealing the moonlighting role of NADP in the structure of a flavin-containing monooxygenase. *Proc Natl Acad Sci U S A* **105**:6572-7
- Arnold, T., Linke, D. 2008. The use of detergents to purify membrane proteins. *Curr Protoc Protein Sci* **Chapter 4**:Unit 4 8 1-4 8 30
- Askolin, S., Turkenburg, J.P., Tenkanen, M., Uotila, S., Wilson, K.S., Penttila, M., Visuri, K. 2004. Purification, crystallization and preliminary X-ray diffraction analysis of the *Trichoderma reesei* hydrophobin HFBI. *Acta Crystallographica Section D-Biological Crystallography* **60**:1903-1905
- Atta-Asafo-Adjei, E., Lawton, M.P., Philpot, R.M. 1993. Cloning, sequencing, distribution, and expression in *Escherichia coli* of flavin-containing monooxygenase 1C1. Evidence for a third gene subfamily in rabbits. *J Biol Chem* **268**:9681-9
- Attar, M., Dong, D., Ling, K.H., Tang-Liu, D.D. 2003. Cytochrome P450 2C8 and flavin-containing monooxygenases are involved in the metabolism of tazarotenic acid in humans. *Drug Metab Dispos* **31**:476-81
- Attwood, T.K., Bradley, P., Flower, D.R., Gaulton, A., Maudling, N., Mitchell, A.L., Moulton, G., Nordle, A., Paine, K., Taylor, P., Uddin, A., Zygouri, C. 2003. PRINTS and its automatic supplement, prePRINTS. *Nucleic Acids Res* **31**:400-2
- Ayesh, R., Mitchell, S.C., Zhang, A., Smith, R.L. 1993. The fish odour syndrome: biochemical, familial, and clinical aspects. *Bmj* **307**:655-7
- Barber, M., Conrad, M.E., Umbreit, J.N., Barton, J.C., Moore, E.G. 2000. Abnormalities of flavin monooxygenase as an etiology for sideroblastic anemia. *Am J Hematol* **65**:149-53
- Beaty, N.B., Ballou, D.P. 1981a. The oxidative half-reaction of liver microsomal FAD-containing monooxygenase. *J Biol Chem* **256**:4619-25
- Beaty, N.B., Ballou, D.P. 1981b. The reductive half-reaction of liver microsomal FAD-containing monooxygenase. *J Biol Chem* **256**:4611-8
- Bogusz, S., Venable, R.M., Pastor, R.W. 2000. Molecular dynamics simulations of octyl glucoside micelles: Structural properties. *Journal of Physical Chemistry B* **104**:5462-5470
- Boos, W., Shuman, H. 1998. Maltose/maltodextrin system of *Escherichia coli*: transport, metabolism, and regulation. *Microbiol Mol Biol Rev* **62**:204-29

- Borbas, T., Benko, B., Dalmadi, B., Szabo, I., Tihanyi, K. 2006a. Insulin in flavin-containing monooxygenase regulation. Flavin-containing monooxygenase and cytochrome P450 activities in experimental diabetes. *Eur J Pharm Sci* **28**:51-8
- Borbas, T., Zhang, J., Cerny, M.A., Liko, I., Cashman, J.R. 2006b. Investigation of structure and function of a catalytically efficient variant of the human flavin-containing monooxygenase form 3. *Drug Metab Dispos* **34**:1995-2002
- Branco, L.M., Matschiner, A., Fair, J.N., Goba, A., Sampey, D.B., Ferro, P.J., Cashman, K.A., Schoepp, R.J., Tesh, R.B., Bausch, D.G., Garry, R.F., Guttieri, M.C. 2008. Bacterial-based systems for expression and purification of recombinant Lassa virus proteins of immunological relevance. *Virology* **5**:74
- Bron, P., Lacapere, J.J., Breyton, C., Mosser, G. 1999. The 9 Å projection structure of cytochrome b₆f complex determined by electron crystallography. *J Mol Biol* **287**:117-26
- Brunelle, A., Bi, Y.A., Lin, J., Russell, B., Luy, L., Berkman, C., Cashman, J. 1997. Characterization of two human flavin-containing monooxygenase (form 3) enzymes expressed in *Escherichia coli* as maltose binding protein fusions. *Drug Metab Dispos* **25**:1001-7
- Butt, T.R., Jonnalagadda, S., Monia, B.P., Sternberg, E.J., Marsh, J.A., Stadel, J.M., Ecker, D.J., Crooke, S.T. 1989. Ubiquitin fusion augments the yield of cloned gene products in *Escherichia coli*. *Proc Natl Acad Sci U S A* **86**:2540-4
- Cashman, J.R. 1988. Facile N-oxygenation of 1-methyl-4-phenyl-1,2,3,6-tetrahydropyridine by the flavin-containing monooxygenase. A convenient synthesis of tritiated [methyl-3H]-4-phenyl-2,3-dihydropyridinium species. *J Med Chem* **31**:1258-61
- Cashman, J.R. 1989. Enantioselective N-oxygenation of verapamil by the hepatic flavin-containing monooxygenase. *Mol Pharmacol* **36**:497-503
- Cashman, J.R. 1995. Structural and catalytic properties of the mammalian flavin-containing monooxygenase. *Chem Res Toxicol* **8**:166-81
- Cashman, J.R. 2000. Human flavin-containing monooxygenase: substrate specificity and role in drug metabolism. *Curr Drug Metab* **1**:181-91
- Cashman, J.R. 2002. Human flavin-containing monooxygenase (form 3): polymorphisms and variations in chemical metabolism. *Pharmacogenomics* **3**:325-39
- Cashman, J.R. 2005. Some distinctions between flavin-containing and cytochrome P450 monooxygenases. *Biochem Biophys Res Commun* **338**:599-604
- Cashman, J.R., Akerman, B.R., Forrest, S.M., Treacy, E.P. 2000. Population-specific polymorphisms of the human FMO3 gene: significance for detoxication. *Drug Metab Dispos* **28**:169-73
- Cashman, J.R., Camp, K., Fakharzadeh, S.S., Fennessey, P.V., Hines, R.N., Mamer, O.A., Mitchell, S.C., Nguyen, G.P., Schlenk, D., Smith, R.L., Tjoa, S.S., Williams, D.E., Yannicelli, S. 2003. Biochemical and clinical aspects of the human flavin-containing monooxygenase form 3 (FMO3) related to trimethylaminuria. *Curr Drug Metab* **4**:151-70

- Cashman, J.R., Celestial, J.R., Leach, A.R. 1992a. Enantioselective N-oxygenation of chlorpheniramine by the flavin-containing monooxygenase from hog liver. *Xenobiotica* **22**:459-69
- Cashman, J.R., Lattard, V., Lin, J. 2004. Effect of total parenteral nutrition and choline on hepatic flavin-containing and cytochrome P-450 monooxygenase activity in rats. *Drug Metab Dispos* **32**:222-9
- Cashman, J.R., Motika, M.S. manuscript in preparation. Monoamine Oxidases and Flavin-Containing Monooxygenases. *In: Comprehensive Toxicology C*. McQueen, editor. ELSEVIER, Kidlington, United Kingdom
- Cashman, J.R., Parikh, K.K., Traiger, G.J., Hanzlik, R.P. 1983. Relative hepatotoxicity of ortho and meta mono substituted thiobenzamides in the rat. *Chem Biol Interact* **45**:341-7
- Cashman, J.R., Park, S.B., Berkman, C.E., Cashman, L.E. 1995. Role of hepatic flavin-containing monooxygenase 3 in drug and chemical metabolism in adult humans. *Chem Biol Interact* **96**:33-46
- Cashman, J.R., Park, S.B., Yang, Z.C., Washington, C.B., Gomez, D.Y., Giacomini, K.M., Brett, C.M. 1993a. Chemical, enzymatic, and human enantioselective S-oxygenation of cimetidine. *Drug Metab Dispos* **21**:587-97
- Cashman, J.R., Park, S.B., Yang, Z.C., Wrighton, S.A., Jacob, P., 3rd, Benowitz, N.L. 1992b. Metabolism of nicotine by human liver microsomes: stereoselective formation of trans-nicotine N'-oxide. *Chem Res Toxicol* **5**:639-46
- Cashman, J.R., Proudfoot, J., Pate, D.W., Hogberg, T. 1988. Stereoselective N-oxygenation of zimeldine and homozimeldine by the flavin-containing monooxygenase. *Drug Metab Dispos* **16**:616-22
- Cashman, J.R., Williams, D.E. 1990a. Enantioselective S-oxygenation of 2-aryl-1,3-dithiolanes by rabbit lung enzyme preparations. *Mol Pharmacol* **37**:333-9
- Cashman, J.R., Xiong, Y., Lin, J., Verhagen, H., van Poppel, G., van Bladeren, P.J., Larsen-Su, S., Williams, D.E. 1999a. In vitro and in vivo inhibition of human flavin-containing monooxygenase form 3 (FMO3) in the presence of dietary indoles. *Biochem Pharmacol* **58**:1047-55
- Cashman, J.R., Xiong, Y.N., Xu, L., Janowsky, A. 1999b. N-oxygenation of amphetamine and methamphetamine by the human flavin-containing monooxygenase (form 3): role in bioactivation and detoxication. *J Pharmacol Exp Ther* **288**:1251-60
- Cashman, J.R., Yang, Z., Yang, L., Wrighton, S.A. 1993b. Stereo- and regioselective N- and S-oxidation of tertiary amines and sulfides in the presence of adult human liver microsomes. *Drug Metab Dispos* **21**:492-501
- Cashman, J.R., Yang, Z.C., Hogberg, T. 1990b. Oxidation of N-hydroxynorzimeldine to a stable nitron by hepatic monooxygenases. *Chem Res Toxicol* **3**:428-32
- Cashman, J.R., Zhang, J. 2002. Interindividual differences of human flavin-containing monooxygenase 3: genetic polymorphisms and functional variation. *Drug Metab Dispos* **30**:1043-52
- Cashman, J.R., Zhang, J. 2006. Human flavin-containing monooxygenases. *Annu Rev Pharmacol Toxicol* **46**:65-100

- Cashman, J.R., Zhang, J., Leushner, J., Braun, A. 2001. Population distribution of human flavin-containing monooxygenase form 3: gene polymorphisms. *Drug Metab Dispos* **29**:1629-37
- Cashman, J.R., Ziegler, D.M. 1986. Contribution of N-oxygenation to the metabolism of MPTP (1-methyl-4-phenyl-1,2,3,6-tetrahydropyridine) by various liver preparations. *Mol Pharmacol* **29**:163-7
- Center, R.J., Kobe, B., Wilson, K.A., Teh, T., Howlett, G.J., Kemp, B.E., Poubourios, P. 1998. Crystallization of a trimeric human T cell leukemia virus type 1 gp21 ectodomain fragment as a chimera with maltose-binding protein. *Protein Sci* **7**:1612-9
- Chalmers, R.A., Bain, M.D., Michelakakis, H., Zschocke, J., Iles, R.A. 2006. Diagnosis and management of trimethylaminuria (FMO3 deficiency) in children. *J Inherit Metab Dis* **29**:162-72
- Chayen, N.E. 1998. Comparative studies of protein crystallization by vapour-diffusion and microbatch techniques. *Acta Crystallogr D Biol Crystallogr* **54**:8-15
- Chen, Z.W., Baruch, P., Mathews, F.S., Matsushita, K., Yamashita, T., Toyama, H., Adachi, O. 1999. Crystallization and preliminary diffraction studies of two quinoprotein alcohol dehydrogenases (ADHs): a soluble monomeric ADH from *Pseudomonas putida* HK5 (ADH-IIB) and a heterotrimeric membrane-bound ADH from *Gluconobacter suboxydans* (ADH-GS). *Acta Crystallographica Section D-Biological Crystallography* **55**:1933-1936
- Cherrington, N.J., Falls, J.G., Rose, R.L., Clements, K.M., Philpot, R.M., Levi, P.E., Hodgson, E. 1998. Molecular cloning, sequence, and expression of mouse flavin-containing monooxygenases 1 and 5 (FMO1 and FMO5). *J Biochem Mol Toxicol* **12**:205-12
- Chiba, K., Horii, H., Kubota, E., Ishizaki, T., Kato, Y. 1990. Effects of N-methylmercaptoimidazole on the disposition of MPTP and its metabolites in mice. *Eur J Pharmacol* **180**:59-67
- Chiba, K., Kubota, E., Miyakawa, T., Kato, Y., Ishizaki, T. 1988. Characterization of hepatic microsomal metabolism as an in vivo detoxication pathway of 1-methyl-4-phenyl-1,2,3,6-tetrahydropyridine in mice. *J Pharmacol Exp Ther* **246**:1108-15
- Chung, W.G., Park, C.S., Roh, H.K., Lee, W.K., Cha, Y.N. 2000. Oxidation of ranitidine by isozymes of flavin-containing monooxygenase and cytochrome P450. *Jpn J Pharmacol* **84**:213-20
- Clement, B., Lustig, K.L., Ziegler, D.M. 1993. Oxidation of desmethylpromethazine catalyzed by pig liver flavin-containing monooxygenase. Number and nature of metabolites. *Drug Metab Dispos* **21**:24-9
- Clement, B., Weide, M., Ziegler, D.M. 1996. Inhibition of purified and membrane-bound flavin-containing monooxygenase 1 by (N,N-dimethylamino)stilbene carboxylates. *Chem Res Toxicol* **9**:599-604
- Coecke, S., Debast, G., Phillips, I.R., Vercruyssen, A., Shephard, E.A., Rogiers, V. 1998. Hormonal regulation of microsomal flavin-containing monooxygenase activity by sex steroids and growth hormone in co-cultured adult male rat hepatocytes. *Biochem Pharmacol* **56**:1047-51

- Cook, P.F., Kenyon, G.L., Cleland, W.W. 1981. Use of pH studies to elucidate the catalytic mechanism of rabbit muscle creatine kinase. *Biochemistry* **20**:1204-10
- Damani, L.A., Pool, W.F., Crooks, P.A., Kaderlik, R.K., Ziegler, D.M. 1988. Stereoselectivity in the N'-oxidation of nicotine isomers by flavin-containing monooxygenase. *Mol Pharmacol* **33**:702-5
- Dannan, G.A., Guengerich, F.P., Waxman, D.J. 1986. Hormonal regulation of rat liver microsomal enzymes. Role of gonadal steroids in programming, maintenance, and suppression of delta 4-steroid 5 alpha-reductase, flavin-containing monooxygenase, and sex-specific cytochromes P-450. *J Biol Chem* **261**:10728-35
- de Pieri, C., Beltramini, L.M., Selistre-de-Araujo, H.S., Vettore, A.L., da Silva, F.R., Arruda, P., Oliva, G., de Souza, D.H. 2004. Overexpression, purification, and biochemical characterization of GumC, an enzyme involved in the biosynthesis of exopolysaccharide by *Xylella fastidiosa*. *Protein Expr Purif* **34**:223-8
- Decker, C.J., Doerge, D.R. 1992a. Covalent binding of 14C- and 35S-labeled thiocarbamides in rat hepatic microsomes. *Biochem Pharmacol* **43**:881-8
- Decker, C.J., Doerge, D.R., Cashman, J.R. 1992b. Metabolism of benzimidazoline-2-thiones by rat hepatic microsomes and hog liver flavin-containing monooxygenase. *Chem Res Toxicol* **5**:726-33
- Di Monte, D.A., Wu, E.Y., Irwin, I., Delanney, L.E., Langston, J.W. 1991. Biotransformation of 1-methyl-4-phenyl-1,2,3,6-tetrahydropyridine in primary cultures of mouse astrocytes. *J Pharmacol Exp Ther* **258**:594-600
- Dixit, A., Roche, T.E. 1984. Spectrophotometric assay of the flavin-containing monooxygenase and changes in its activity in female mouse liver with nutritional and diurnal conditions. *Arch Biochem Biophys* **233**:50-63
- Dolan, C., Shields, D.C., Stanton, A., O'Brien, E., Lambert, D.M., O'Brien, J.K., Treacy, E.P. 2005. Polymorphisms of the Flavin containing monooxygenase 3 (FMO3) gene do not predispose to essential hypertension in Caucasians. *BMC Med Genet* **6**:41
- Dolphin, C.T., Beckett, D.J., Janmohamed, A., Cullingford, T.E., Smith, R.L., Shephard, E.A., Phillips, I.R. 1998. The flavin-containing monooxygenase 2 gene (FMO2) of humans, but not of other primates, encodes a truncated, nonfunctional protein. *J Biol Chem* **273**:30599-607
- Dolphin, C.T., Janmohamed, A., Smith, R.L., Shephard, E.A., Phillips, I.R. 1997a. Missense mutation in flavin-containing mono-oxygenase 3 gene, FMO3, underlies fish-odour syndrome. *Nat Genet* **17**:491-4
- Dolphin, C.T., Riley, J.H., Smith, R.L., Shephard, E.A., Phillips, I.R. 1997b. Structural organization of the human flavin-containing monooxygenase 3 gene (FMO3), the favored candidate for fish-odor syndrome, determined directly from genomic DNA. *Genomics* **46**:260-7
- Dong, A., Xu, X., Edwards, A.M., Chang, C., Chruszcz, M., Cuff, M., Cymborowski, M., Di Leo, R., Egorova, O., Evdokimova, E., Filippova, E., Gu, J., Guthrie, J., Ignatchenko, A., Joachimiak, A., Klostermann, N., Kim, Y., Korniyenko, Y., Minor, W., Que, Q., Savchenko, A., Skarina, T., Tan, K., Yakunin, A., Yee, A.,

- Yim, V., Zhang, R., Zheng, H., Akutsu, M., Arrowsmith, C., Avvakumov, G.V., Bochkarev, A., Dahlgren, L.G., Dhe-Paganon, S., Dimov, S., Dombrovski, L., Finerty, P., Jr., Flodin, S., Flores, A., Graslund, S., Hammerstrom, M., Herman, M.D., Hong, B.S., Hui, R., Johansson, I., Liu, Y., Nilsson, M., Nedyalkova, L., Nordlund, P., Nyman, T., Min, J., Ouyang, H., Park, H.W., Qi, C., Rabeh, W., Shen, L., Shen, Y., Sukumard, D., Tempel, W., Tong, Y., Tresagues, L., Vedadi, M., Walker, J.R., Weigelt, J., Welin, M., Wu, H., Xiao, T., Zeng, H., Zhu, H. 2007. In situ proteolysis for protein crystallization and structure determination. *Nat Methods* **4**:1019-21
- Donnelly, M.I., Zhou, M., Millard, C.S., Clancy, S., Stols, L., Eschenfeldt, W.H., Collart, F.R., Joachimiak, A. 2006. An expression vector tailored for large-scale, high-throughput purification of recombinant proteins. *Protein Expr Purif* **47**:446-54
- Duescher, R.J., Lawton, M.P., Philpot, R.M., Elfarra, A.A. 1994. Flavin-containing monooxygenase (FMO)-dependent metabolism of methionine and evidence for FMO3 being the major FMO involved in methionine sulfoxidation in rabbit liver and kidney microsomes. *J Biol Chem* **269**:17525-30
- Dyroff, M.C., Neal, R.A. 1981. Identification of the major protein adduct formed in rat liver after thioacetamide administration. *Cancer Res* **41**:3430-5
- Ellis, K.J., Morrison, J.F. 1982. Buffers of constant ionic strength for studying pH-dependent processes. *Methods Enzymol* **87**:405-26
- Eswaramoorthy, S., Bonanno, J.B., Burley, S.K., Swaminathan, S. 2006. Mechanism of action of a flavin-containing monooxygenase. *Proc Natl Acad Sci U S A* **103**:9832-7
- Falls, J.G., Blake, B.L., Cao, Y., Levi, P.E., Hodgson, E. 1995. Gender differences in hepatic expression of flavin-containing monooxygenase isoforms (FMO1, FMO3, and FMO5) in mice. *J Biochem Toxicol* **10**:171-7
- Falls, J.G., Ryu, D.Y., Cao, Y., Levi, P.E., Hodgson, E. 1997. Regulation of mouse liver flavin-containing monooxygenases 1 and 3 by sex steroids. *Arch Biochem Biophys* **342**:212-23
- Fang, J. 2000. Metabolism of clozapine by rat brain: the role of flavin-containing monooxygenase (FMO) and cytochrome P450 enzymes. *Eur J Drug Metab Pharmacokinet* **25**:109-14
- Feher, A., Boross, P., Sperka, T., Oroszlan, S., Tozser, J. 2004. Expression of the murine leukemia virus protease in fusion with maltose-binding protein in *Escherichia coli*. *Protein Expr Purif* **35**:62-8
- Fraser-Andrews, E.A., Manning, N.J., Ashton, G.H., Eldridge, P., McGrath, J., Menage Hdu, P. 2003. Fish odour syndrome with features of both primary and secondary trimethylaminuria. *Clin Exp Dermatol* **28**:203-5
- Fujieda, M., Yamazaki, H., Togashi, M., Saito, T., Kamataki, T. 2003. Two novel single nucleotide polymorphisms (SNPs) of the FMO3 gene in Japanese. *Drug Metab Pharmacokinet* **18**:333-5
- Fujimori, K., Yaguchi, M., Mikami, A., Matsuura, T., Furukawa, N., Oae, S., Iyanagi, T. 1986. Kinetic Solvent Deuterium-Isotope Effect on the Oxygenation of N,N-

- Dimethylaniline with the Pig-Liver Microsomal Fad-Containing Monooxygenase. *Tetrahedron Letters* **27**:1179-1182
- Furnes, B., Feng, J., Sommer, S.S., Schlenk, D. 2003. Identification of novel variants of the flavin-containing monooxygenase gene family in African Americans. *Drug Metab Dispos* **31**:187-93
- Garavito, R.M., Ferguson-Miller, S. 2001. Detergents as tools in membrane biochemistry. *J Biol Chem* **276**:32403-6
- Gasser, R., Tynes, R.E., Lawton, M.P., Korsmeyer, K.K., Ziegler, D.M., Philpot, R.M. 1990. The flavin-containing monooxygenase expressed in pig liver: primary sequence, distribution, and evidence for a single gene. *Biochemistry* **29**:119-24
- Gelb, B.D., Zhang, J., Cotter, P.D., Gershin, I.F., Desnick, R.J. 1997. Physical mapping of the human connexin 40 (GJA5), flavin-containing monooxygenase 5, and natriuretic peptide receptor a genes on 1q21. *Genomics* **39**:409-11
- Gill, S.C., von Hippel, P.H. 1989. Calculation of protein extinction coefficients from amino acid sequence data. *Anal Biochem* **182**:319-26
- Grimshaw, C.E., Cook, P.F., Cleland, W.W. 1981. Use of isotope effects and pH studies to determine the chemical mechanism of *Bacillus subtilis* L-alanine dehydrogenase. *Biochemistry* **20**:5655-61
- Growdon, J.H., Wurtman, R.J. 1979. Oral Choline Administration to Patients with Huntington's Disease. *Advances in Neurology* **23**:765-776
- Guan, M., Su, B., Ye, C., Lu, Y. 2002. Production of extracellular domain of human tissue factor using maltose-binding protein fusion system. *Protein Expr Purif* **26**:229-34
- Guan, S.H., Falick, A.M., Williams, D.E., Cashman, J.R. 1991. Evidence for complex formation between rabbit lung flavin-containing monooxygenase and calreticulin. *Biochemistry* **30**:9892-900
- Guo, W.X., Ziegler, D.M. 1991. Estimation of flavin-containing monooxygenase activities in crude tissue preparations by thiourea-dependent oxidation of thiocholine. *Anal Biochem* **198**:143-8
- Hamman, M.A., Haehner-Daniels, B.D., Wrighton, S.A., Rettie, A.E., Hall, S.D. 2000. Stereoselective sulfoxidation of sulindac sulfide by flavin-containing monooxygenases. Comparison of human liver and kidney microsomes and mammalian enzymes. *Biochem Pharmacol* **60**:7-17
- Hanzlik, R.P. 1986. Chemistry of covalent binding: studies with bromobenzene and thiobenzamide. *Adv Exp Med Biol* **197**:31-40
- Hanzlik, R.P., Cashman, J.R. 1983. Microsomal metabolism of thiobenzamide and thiobenzamide S-oxide. *Drug Metab Dispos* **11**:201-5
- Hao, H.F., Li, X.S., Gao, F.S., Wu, W.X., Xia, C. 2007. Secondary structure and 3D homology modeling of grass carp (*Ctenopharyngodon idellus*) major histocompatibility complex class I molecules. *Protein Expr Purif* **51**:120-5
- Heinze, E., Hlavica, P., Kiese, M., Lipowsky, G. 1970. N-oxygenation of arylamines in microsomes prepared from corpora lutea of the cycle and other tissues of the pig. *Biochem Pharmacol* **19**:641-9

- Henderson, M.C., Krueger, S.K., Siddens, L.K., Stevens, J.F., Williams, D.E. 2004a. S-oxygenation of the thioether organophosphate insecticides phorate and disulfoton by human lung flavin-containing monooxygenase 2. *Biochem Pharmacol* **68**:959-67
- Henderson, M.C., Krueger, S.K., Stevens, J.F., Williams, D.E. 2004b. Human flavin-containing monooxygenase form 2 S-oxygenation: sulfenic acid formation from thioureas and oxidation of glutathione. *Chem Res Toxicol* **17**:633-40
- Heras, B., Edeling, M.A., Byriel, K.A., Jones, A., Raina, S., Martin, J.L. 2003. Dehydration converts DsbG crystal diffraction from low to high resolution. *Structure* **11**:139-45
- Hernandez, D., Janmohamed, A., Chandan, P., Phillips, I.R., Shephard, E.A. 2004. Organization and evolution of the flavin-containing monooxygenase genes of human and mouse: identification of novel gene and pseudogene clusters. *Pharmacogenetics* **14**:117-30
- Hines, R.N., Cashman, J.R., Philpot, R.M., Williams, D.E., Ziegler, D.M. 1994. The mammalian flavin-containing monooxygenases: molecular characterization and regulation of expression. *Toxicol Appl Pharmacol* **125**:1-6
- Hines, R.N., Hopp, K.A., Franco, J., Saeian, K., Begun, F.P. 2002. Alternative processing of the human FMO6 gene renders transcripts incapable of encoding a functional flavin-containing monooxygenase. *Mol Pharmacol* **62**:320-5
- Hines, R.N., Luo, Z., Hopp, K.A., Cabacungan, E.T., Koukouritaki, S.B., McCarver, D.G. 2003. Genetic variability at the human FMO1 locus: significance of a basal promoter yin yang 1 element polymorphism (FMO1*6). *J Pharmacol Exp Ther* **306**:1210-8
- Hisamuddin, I.M., Wehbi, M.A., Chao, A., Wyre, H.W., Hylind, L.M., Giardiello, F.M., Yang, V.W. 2004. Genetic polymorphisms of human flavin monooxygenase 3 in sulindac-mediated primary chemoprevention of familial adenomatous polyposis. *Clin Cancer Res* **10**:8357-62
- Hisamuddin, I.M., Wehbi, M.A., Schmotzer, B., Easley, K.A., Hylind, L.M., Giardiello, F.M., Yang, V.W. 2005. Genetic polymorphisms of flavin monooxygenase 3 in sulindac-induced regression of colorectal adenomas in familial adenomatous polyposis. *Cancer Epidemiol Biomarkers Prev* **14**:2366-9
- Holloway, P.W. 1973. A simple procedure for removal of Triton X-100 from protein samples. *Anal Biochem* **53**:304-8
- Hui, Q.Y., Armstrong, C., Laver, G., Iverson, F. 1988. Monooxygenase-mediated metabolism and binding of ethylene thiourea to mouse liver microsomal protein. *Toxicol Lett* **41**:231-7
- Israelachvili, J. 1997. The different faces of poly(ethylene glycol). *Proc Natl Acad Sci U S A* **94**:8378-9
- Janmohamed, A., Hernandez, D., Phillips, I.R., Shephard, E.A. 2004. Cell-, tissue-, sex- and developmental stage-specific expression of mouse flavin-containing monooxygenases (Fmos). *Biochem Pharmacol* **68**:73-83

- Jez, J.M., Noel, J.P. 2000. Mechanism of chalcone synthase. pKa of the catalytic cysteine and the role of the conserved histidine in a plant polyketide synthase. *J Biol Chem* **275**:39640-6
- Jones, K.C., Ballou, D.P. 1986. Reactions of the 4a-hydroperoxide of liver microsomal flavin-containing monooxygenase with nucleophilic and electrophilic substrates. *J Biol Chem* **261**:2553-9
- Joshi, M.D., Sidhu, G., Pot, I., Brayer, G.D., Withers, S.G., McIntosh, L.P. 2000. Hydrogen bonding and catalysis: a novel explanation for how a single amino acid substitution can change the pH optimum of a glycosidase. *J Mol Biol* **299**:255-79
- Kajita, J., Inano, K., Fuse, E., Kuwabara, T., Kobayashi, H. 2002. Effects of olopatadine, a new antiallergic agent, on human liver microsomal cytochrome P450 activities. *Drug Metab Dispos* **30**:1504-11
- Kang, J.H., Chung, W.G., Lee, K.H., Park, C.S., Kang, J.S., Shin, I.C., Roh, H.K., Dong, M.S., Baek, H.M., Cha, Y.N. 2000. Phenotypes of flavin-containing monooxygenase activity determined by ranitidine N-oxidation are positively correlated with genotypes of linked FM03 gene mutations in a Korean population. *Pharmacogenetics* **10**:67-78
- Kapust, R.B., Waugh, D.S. 1999. Escherichia coli maltose-binding protein is uncommonly effective at promoting the solubility of polypeptides to which it is fused. *Protein Sci* **8**:1668-74
- Kashiyama, E., Yokoi, T., Itoh, K., Itoh, S., Odomi, M., Kamataki, T. 1994. Stereoselective S-oxidation of flosequinan sulfide by rat hepatic flavin-containing monooxygenase 1A1 expressed in yeast. *Biochem Pharmacol* **47**:1357-63
- Ke, A., Wolberger, C. 2003. Insights into binding cooperativity of MATa1/MATalpha2 from the crystal structure of a MATa1 homeodomain-maltose binding protein chimera. *Protein Sci* **12**:306-12
- Kedderis, G.L., Rickert, D.E. 1985. Loss of rat liver microsomal cytochrome P-450 during methimazole metabolism. Role of flavin-containing monooxygenase. *Drug Metab Dispos* **13**:58-61
- Kim, Y.M., Ziegler, D.M. 2000. Size limits of thiocarbamides accepted as substrates by human flavin-containing monooxygenase 1. *Drug Metab Dispos* **28**:1003-6
- Klick, D.E., Hines, R.N. 2007. Mechanisms regulating human FMO3 transcription. *Drug Metab Rev* **39**:419-42
- Korsmeyer, K.K., Guan, S., Yang, Z.C., Falick, A.M., Ziegler, D.M., Cashman, J.R. 1998. N-Glycosylation of pig flavin-containing monooxygenase form 1: determination of the site of protein modification by mass spectrometry. *Chem Res Toxicol* **11**:1145-53
- Kotthaus, J. 2008. Substituierte L-Arginin-Derivate als Modulatoren des Stickstoffmonoxid-generierenden Systems. *In: Pharmaceutical Chemistry*. University of Kiel, Kiel
- Koukouritaki, S.B., Simpson, P., Yeung, C.K., Rettie, A.E., Hines, R.N. 2002. Human hepatic flavin-containing monooxygenases 1 (FMO1) and 3 (FMO3) developmental expression. *Pediatr Res* **51**:236-43

- Kragh-Hansen, U., le Maire, M., Moller, J.V. 1998. The mechanism of detergent solubilization of liposomes and protein-containing membranes. *Biophys J* **75**:2932-46
- Krieter, P.A., Ziegler, D.M., Hill, K.E., Burk, R.F. 1984. Increased biliary GSSG efflux from rat livers perfused with thiocarbamide substrates for the flavin-containing monooxygenase. *Mol Pharmacol* **26**:122-7
- Krueger, S.K., Siddens, L.K., Martin, S.R., Yu, Z., Pereira, C.B., Cabacungan, E.T., Hines, R.N., Ardlie, K.G., Raucy, J.L., Williams, D.E. 2004. Differences in FMO2*1 allelic frequency between Hispanics of Puerto Rican and Mexican descent. *Drug Metab Dispos* **32**:1337-40
- Krueger, S.K., Vandyke, J.E., Williams, D.E., Hines, R.N. 2006. The role of flavin-containing monooxygenase (FMO) in the metabolism of tamoxifen and other tertiary amines. *Drug Metab Rev* **38**:139-47
- Krueger, S.K., Williams, D.E. 2005. Mammalian flavin-containing monooxygenases: structure/function, genetic polymorphisms and role in drug metabolism. *Pharmacol Ther* **106**:357-87
- Krueger, S.K., Williams, D.E., Yueh, M.F., Martin, S.R., Hines, R.N., Raucy, J.L., Dolphin, C.T., Shephard, E.A., Phillips, I.R. 2002. Genetic polymorphisms of flavin-containing monooxygenase (FMO). *Drug Metab Rev* **34**:523-32
- Kukimoto, M., Nureki, O., Shirouzu, M., Katada, T., Hirabayashi, Y., Sugiyama, H., Furuyama, S., Yokoyama, S., Hara-Yokoyama, M. 2000. Crystallization and preliminary X-ray diffraction analysis of the extracellular domain of the cell surface antigen CD38 complexed with ganglioside. *J Biochem* **127**:181-4
- Kuo, C.J., Conley, P.B., Hsieh, C.L., Francke, U., Crabtree, G.R. 1990. Molecular cloning, functional expression, and chromosomal localization of mouse hepatocyte nuclear factor 1. *Proc Natl Acad Sci U S A* **87**:9838-42
- Lambert, D.M., Mamer, O.A., Akerman, B.R., Choiniere, L., Gaudet, D., Hamet, P., Treacy, E.P. 2001. In vivo variability of TMA oxidation is partially mediated by polymorphisms of the FMO3 gene. *Mol Genet Metab* **73**:224-9
- Larsen, B.K., Schlenk, D. 2001. Effect of salinity on flavin-containing monooxygenase expression and activity in rainbow trout (*Oncorhynchus mykiss*). *J Comp Physiol [B]* **171**:421-9
- Lattard, V., Buronfosse, T., Lachuer, J., Longin-Sauvageon, C., Moulin, C., Benoit, E. 2001. Cloning, sequencing, tissue distribution, and heterologous expression of rat flavin-containing monooxygenase 3. *Arch Biochem Biophys* **391**:30-40
- Lattard, V., Lachuer, J., Buronfosse, T., Garnier, F., Benoit, E. 2002a. Physiological factors affecting the expression of FMO1 and FMO3 in the rat liver and kidney. *Biochem Pharmacol* **63**:1453-64
- Lattard, V., Longin-Sauvageon, C., Benoit, E. 2003a. Cloning, sequencing and tissue distribution of rat flavin-containing monooxygenase 4: two different forms are produced by tissue-specific alternative splicing. *Mol Pharmacol* **63**:253-61
- Lattard, V., Longin-Sauvageon, C., Krueger, S.K., Williams, D.E., Benoit, E. 2002b. The FMO2 gene of laboratory rats, as in most humans, encodes a truncated protein. *Biochem Biophys Res Commun* **292**:558-63

- Lattard, V., Zhang, J., Tran, Q., Furnes, B., Schlenk, D., Cashman, J.R. 2003b. Two new polymorphisms of the FMO3 gene in Caucasian and African-American populations: comparative genetic and functional studies. *Drug Metab Dispos* **31**:854-60
- Lawton, M.P., Cashman, J.R., Cresteil, T., Dolphin, C.T., Elfarra, A.A., Hines, R.N., Hodgson, E., Kimura, T., Ozols, J., Phillips, I.R., et al. 1994. A nomenclature for the mammalian flavin-containing monooxygenase gene family based on amino acid sequence identities. *Arch Biochem Biophys* **308**:254-7
- Lawton, M.P., Gasser, R., Tynes, R.E., Hodgson, E., Philpot, R.M. 1990. The flavin-containing monooxygenase enzymes expressed in rabbit liver and lung are products of related but distinctly different genes. *J Biol Chem* **265**:5855-61
- Lawton, M.P., Philpot, R.M. 1993a. Functional characterization of flavin-containing monooxygenase 1B1 expressed in *Saccharomyces cerevisiae* and *Escherichia coli* and analysis of proposed FAD- and membrane-binding domains. *J Biol Chem* **268**:5728-34
- Lawton, M.P., Philpot, R.M. 1993b. Molecular genetics of the flavin-dependent monooxygenases. *Pharmacogenetics* **3**:40-4
- le Maire, M., Champeil, P., Moller, J.V. 2000. Interaction of membrane proteins and lipids with solubilizing detergents. *Biochim Biophys Acta* **1508**:86-111
- Lee, J.W., Shin, K.D., Lee, M., Kim, E.J., Han, S.S., Han, M.Y., Ha, H., Jeong, T.C., Koh, W.S. 2003. Role of metabolism by flavin-containing monooxygenase in thioacetamide-induced immunosuppression. *Toxicol Lett* **136**:163-72
- Lee, M.Y., Clark, J.E., Williams, D.E. 1993. Induction of flavin-containing monooxygenase (FMO B) in rabbit lung and kidney by sex steroids and glucocorticoids. *Arch Biochem Biophys* **302**:332-6
- Lee, M.Y., Smiley, S., Kadkhodayan, S., Hines, R.N., Williams, D.E. 1995. Developmental regulation of flavin-containing monooxygenase (FMO) isoforms 1 and 2 in pregnant rabbit. *Chem Biol Interact* **96**:75-85
- Lemoine, A., Williams, D.E., Cresteil, T., Leroux, J.P. 1991. Hormonal regulation of microsomal flavin-containing monooxygenase: tissue-dependent expression and substrate specificity. *Mol Pharmacol* **40**:211-7
- Lin, J., Cashman, J.R. 1997a. Detoxication of tyramine by the flavin-containing monooxygenase: stereoselective formation of the trans oxime. *Chem Res Toxicol* **10**:842-52
- Lin, J., Cashman, J.R. 1997b. N-oxygenation of phenethylamine to the trans-oxime by adult human liver flavin-containing monooxygenase and retroreduction of phenethylamine hydroxylamine by human liver microsomes. *J Pharmacol Exp Ther* **282**:1269-79
- Liu, Y., Manna, A., Li, R., Martin, W.E., Murphy, R.C., Cheung, A.L., Zhang, G. 2001. Crystal structure of the SarR protein from *Staphylococcus aureus*. *Proc Natl Acad Sci U S A* **98**:6877-82
- Lomri, N., Thomas, J., Cashman, J.R. 1993a. Expression in *Escherichia coli* of the cloned flavin-containing monooxygenase from pig liver. *J Biol Chem* **268**:5048-54

- Lomri, N., Yang, Z., Cashman, J.R. 1993b. Expression in *Escherichia coli* of the flavin-containing monooxygenase D (form II) from adult human liver: determination of a distinct tertiary amine substrate specificity. *Chem Res Toxicol* **6**:425-9
- Lomri, N., Yang, Z., Cashman, J.R. 1993c. Regio- and stereoselective oxygenations by adult human liver flavin-containing monooxygenase 3. Comparison with forms 1 and 2. *Chem Res Toxicol* **6**:800-7
- Luo, Z., Hines, R.N. 2001. Regulation of flavin-containing monooxygenase 1 expression by ying yang 1 and hepatic nuclear factors 1 and 4. *Mol Pharmacol* **60**:1421-30
- Malito, E., Alfieri, A., Fraaije, M.W., Mattevi, A. 2004. Crystal structure of a Baeyer-Villiger monooxygenase. *Proc Natl Acad Sci U S A* **101**:13157-62
- Mani, C., Kupfer, D. 1991. Cytochrome P-450-mediated activation and irreversible binding of the antiestrogen tamoxifen to proteins in rat and human liver: possible involvement of flavin-containing monooxygenases in tamoxifen activation. *Cancer Res* **51**:6052-8
- Martinez, A., Knappskog, P.M., Olafsdottir, S., Doskeland, A.P., Eiken, H.G., Svebak, R.M., Bozzini, M., Apold, J., Flatmark, T. 1995. Expression of recombinant human phenylalanine hydroxylase as fusion protein in *Escherichia coli* circumvents proteolytic degradation by host cell proteases. Isolation and characterization of the wild-type enzyme. *Biochem J* **306 (Pt 2)**:589-97
- Mayatepek, E., Flock, B., Zschocke, J. 2004. Benzylamine metabolism in vivo is impaired in patients with deficiency of flavin-containing monooxygenase 3. *Pharmacogenetics* **14**:775-7
- McConnell, H.W., Mitchell, S.C., Smith, R.L., Brewster, M. 1997. Trimethylaminuria associated with seizures and behavioural disturbance: a case report. *Seizure* **6**:317-21
- Miller, A.E., Bischoff, J.J., Pae, K. 1988. Chemistry of aminoiminomethanesulfinic and -sulfonic acids related to the toxicity of thioureas. *Chem Res Toxicol* **1**:169-74
- Mitchell, S.C. 1996. The fish-odor syndrome. *Perspect Biol Med* **39**:514-26
- Mitchell, S.C. 1999. Trimethylaminuria: susceptibility of heterozygotes. *Lancet* **354**:2164-5
- Mitchell, S.C., Smith, R.L. 2001. Trimethylaminuria: the fish malodor syndrome. *Drug Metab Dispos* **29**:517-21
- Mitchell, S.C., Zhang, A.Q., Barrett, T., Ayesh, R., Smith, R.L. 1997. Studies on the discontinuous N-oxidation of trimethylamine among Jordanian, Ecuadorian and New Guinean populations. *Pharmacogenetics* **7**:45-50
- Molina, A.J., Merino, G., Prieto, J.G., Real, R., Mendoza, G., Alvarez, A.I. 2007. Absorption and metabolism of albendazole after intestinal ischemia/reperfusion. *Eur J Pharm Sci* **31**:16-24
- Muckenthaler, M., Roy, C.N., Custodio, A.O., Minana, B., deGraaf, J., Montross, L.K., Andrews, N.C., Hentze, M.W. 2003. Regulatory defects in liver and intestine

- implicate abnormal hepcidin and Cybrd1 expression in mouse hemochromatosis. *Nat Genet* **34**:102-7
- Murphy, H.C., Dolphin, C.T., Janmohamed, A., Holmes, H.C., Michelakakis, H., Shephard, E.A., Chalmers, R.A., Phillips, I.R., Iles, R.A. 2000. A novel mutation in the flavin-containing monooxygenase 3 gene, FM03, that causes fish-odour syndrome: activity of the mutant enzyme assessed by proton NMR spectroscopy. *Pharmacogenetics* **10**:439-51
- Mushiroda, T., Ariyoshi, N., Yokoi, T., Takahara, E., Nagata, O., Kato, H., Kamataki, T. 2001. Accumulation of the 1-methyl-4-phenylpyridinium ion in suncus (*Suncus murinus*) brain: implication for flavin-containing monooxygenase activity in brain microvessels. *Chem Res Toxicol* **14**:228-32
- Mushiroda, T., Douya, R., Takahara, E., Nagata, O. 2000. The involvement of flavin-containing monooxygenase but not CYP3A4 in metabolism of itopride hydrochloride, a gastroprokinetic agent: comparison with cisapride and mosapride citrate. *Drug Metab Dispos* **28**:1231-7
- Nagata, T., Williams, D.E., Ziegler, D.M. 1990. Substrate specificities of rabbit lung and porcine liver flavin-containing monooxygenases: differences due to substrate size. *Chem Res Toxicol* **3**:372-6
- Nishimura, M., Naito, S. 2006. Tissue-specific mRNA expression profiles of human phase I metabolizing enzymes except for cytochrome P450 and phase II metabolizing enzymes. *Drug Metab Pharmacokinet* **21**:357-74
- Ohmi, N., Yoshida, H., Endo, H., Hasegawa, M., Akimoto, M., Higuchi, S. 2003. S-oxidation of S-methyl-esonarimod by flavin-containing monooxygenases in human liver microsomes. *Xenobiotica* **33**:1221-31
- Overby, L.H., Buckpitt, A.R., Lawton, M.P., Atta-Asafo-Adjei, E., Schulze, J., Philpot, R.M. 1995. Characterization of flavin-containing monooxygenase 5 (FMO5) cloned from human and guinea pig: evidence that the unique catalytic properties of FMO5 are not confined to the rabbit ortholog. *Arch Biochem Biophys* **317**:275-84
- Overby, L.H., Carver, G.C., Philpot, R.M. 1997. Quantitation and kinetic properties of hepatic microsomal and recombinant flavin-containing monooxygenases 3 and 5 from humans. *Chem Biol Interact* **106**:29-45
- Park, J.H., Choi, E.A., Cho, E.W., Hahm, K.S., Kim, K.L. 1998. Maltose binding protein (MBP) fusion proteins with low or no affinity to amylose resins can be single-step purified using a novel anti-MBP monoclonal antibody. *Mol Cells* **8**:709-16
- Park, S.B., Jacob, P., 3rd, Benowitz, N.L., Cashman, J.R. 1993. Stereoselective metabolism of (S)-(-)-nicotine in humans: formation of trans-(S)-(-)-nicotine N-1'-oxide. *Chem Res Toxicol* **6**:880-8
- Phillips, I.R., Dolphin, C.T., Clair, P., Hadley, M.R., Hutt, A.J., McCombie, R.R., Smith, R.L., Shephard, E.A. 1995. The molecular biology of the flavin-containing monooxygenases of man. *Chem Biol Interact* **96**:17-32
- Pike, M.G., Mays, D.C., Macomber, D.W., Lipsky, J.J. 2001. Metabolism of a disulfiram metabolite, S-methyl N,N-diethyldithiocarbamate, by flavin monooxygenase in human renal microsomes. *Drug Metab Dispos* **29**:127-32

- Poulsen, L.L., Taylor, K., Williams, D.E., Masters, B.S., Ziegler, D.M. 1986. Substrate specificity of the rabbit lung flavin-containing monooxygenase for amines: oxidation products of primary alkylamines. *Mol Pharmacol* **30**:680-5
- Poulsen, L.L., Ziegler, D.M. 1979. The liver microsomal FAD-containing monooxygenase. Spectral characterization and kinetic studies. *J Biol Chem* **254**:6449-55
- Prough, R.A., Freeman, P.C., Hines, R.N. 1981. The oxidation of hydrazine derivatives catalyzed by the purified liver microsomal FAD-containing monooxygenase. *J Biol Chem* **256**:4178-84
- Qian, L., Ortiz de Montellano, P.R. 2006. Oxidative activation of thiacetazone by the Mycobacterium tuberculosis flavin monooxygenase EtaA and human FMO1 and FMO3. *Chem Res Toxicol* **19**:443-9
- Ramachandran, S., Lu, H., Prabhu, U., Ruoho, A.E. 2007. Purification and characterization of the guinea pig sigma-1 receptor functionally expressed in Escherichia coli. *Protein Expr Purif* **51**:283-92
- Richarme, G., Caldas, T.D. 1997. Chaperone properties of the bacterial periplasmic substrate-binding proteins. *J Biol Chem* **272**:15607-12
- Rigaud, J.L., Mosser, G., Lacapere, J.J., Olofsson, A., Levy, D., Ranck, J.L. 1997. Bio-Beads: an efficient strategy for two-dimensional crystallization of membrane proteins. *J Struct Biol* **118**:226-35
- Riggs, P. 2000. Expression and purification of recombinant proteins by fusion to maltose-binding protein. *Mol Biotechnol* **15**:51-63
- Ring, B.J., Catlow, J., Lindsay, T.J., Gillespie, T., Roskos, L.K., Cerimele, B.J., Swanson, S.P., Hamman, M.A., Wrighton, S.A. 1996. Identification of the human cytochromes P450 responsible for the in vitro formation of the major oxidative metabolites of the antipsychotic agent olanzapine. *J Pharmacol Exp Ther* **276**:658-66
- Ring, B.J., Wrighton, S.A., Aldridge, S.L., Hansen, K., Haehner, B., Shipley, L.A. 1999. Flavin-containing monooxygenase-mediated N-oxidation of the M(1)-muscarinic agonist xanomeline. *Drug Metab Dispos* **27**:1099-103
- Ripp, S.L., Itagaki, K., Philpot, R.M., Elfarra, A.A. 1999a. Methionine S-oxidation in human and rabbit liver microsomes: evidence for a high-affinity methionine S-oxidase activity that is distinct from flavin-containing monooxygenase 3. *Arch Biochem Biophys* **367**:322-32
- Ripp, S.L., Itagaki, K., Philpot, R.M., Elfarra, A.A. 1999b. Species and sex differences in expression of flavin-containing monooxygenase form 3 in liver and kidney microsomes. *Drug Metab Dispos* **27**:46-52
- Rodriguez, R.J., Acosta, D., Jr. 1997a. Metabolism of ketoconazole and deacetylated ketoconazole by rat hepatic microsomes and flavin-containing monooxygenases. *Drug Metab Dispos* **25**:772-7
- Rodriguez, R.J., Acosta, D., Jr. 1997b. N-deacetyl ketoconazole-induced hepatotoxicity in a primary culture system of rat hepatocytes. *Toxicology* **117**:123-31

- Rodriguez, R.J., Buckholz, C.J. 2003. Hepatotoxicity of ketoconazole in Sprague-Dawley rats: glutathione depletion, flavin-containing monooxygenases-mediated bioactivation and hepatic covalent binding. *Xenobiotica* **33**:429-41
- Rodriguez, R.J., Miranda, C.L. 2000. Isoform specificity of N-deacetyl ketoconazole by human and rabbit flavin-containing monooxygenases. *Drug Metab Dispos* **28**:1083-6
- Rodriguez, R.J., Proteau, P.J., Marquez, B.L., Hetherington, C.L., Buckholz, C.J., O'Connell, K.L. 1999. Flavin-containing monooxygenase-mediated metabolism of N-deacetyl ketoconazole by rat hepatic microsomes. *Drug Metab Dispos* **27**:880-6
- Rouer, E., Rouet, P., Delpech, M., Leroux, J.P. 1988. Purification and comparison of liver microsomal flavin-containing monooxygenase from normal and streptozotocin-diabetic rats. *Biochem Pharmacol* **37**:3455-9
- Ryu, S.D., Kang, J.H., Yi, H.G., Nahm, C.H., Park, C.S. 2004. Hepatic flavin-containing monooxygenase activity attenuated by cGMP-independent nitric oxide-mediated mRNA destabilization. *Biochem Biophys Res Commun* **324**:409-16
- Sachdev, D., Chirgwin, J.M. 1998. Order of fusions between bacterial and mammalian proteins can determine solubility in Escherichia coli. *Biochem Biophys Res Commun* **244**:933-7
- Salek-Ardakani, S., Stuart, A.D., Arrand, J.E., Lyons, S., Arrand, J.R., Mackett, M. 2002. High level expression and purification of the Epstein-Barr virus encoded cytokine viral interleukin 10: efficient removal of endotoxin. *Cytokine* **17**:1-13
- Selleri, L., DiMartino, J., van Deursen, J., Brendolan, A., Sanyal, M., Boon, E., Capellini, T., Smith, K.S., Rhee, J., Popperl, H., Grosveld, G., Cleary, M.L. 2004. The TALE homeodomain protein Pbx2 is not essential for development and long-term survival. *Mol Cell Biol* **24**:5324-31
- Shibutani, S., Suzuki, N., Laxmi, Y.R., Schild, L.J., Divi, R.L., Grollman, A.P., Poirier, M.C. 2003. Identification of tamoxifen-DNA adducts in monkeys treated with tamoxifen. *Cancer Res* **63**:4402-6
- Shimada, T., Yamazaki, H., Mimura, M., Inui, Y., Guengerich, F.P. 1994. Interindividual variations in human liver cytochrome P-450 enzymes involved in the oxidation of drugs, carcinogens and toxic chemicals: studies with liver microsomes of 30 Japanese and 30 Caucasians. *J Pharmacol Exp Ther* **270**:414-23
- Shimizu, M., Cashman, J.R., Yamazaki, H. 2007a. Transient trimethylaminuria related to menstruation. *BMC Med Genet* **8**:2
- Shimizu, M., Yano, H., Nagashima, S., Murayama, N., Zhang, J., Cashman, J.R., Yamazaki, H. 2007b. Effect of genetic variants of the human flavin-containing monooxygenase 3 on N- and S-oxygenation activities. *Drug Metab Dispos* **35**:328-30
- Simeonov, A., Jadhav, A., Sayed, A.A., Wang, Y., Nelson, M.E., Thomas, C.J., Inglese, J., Williams, D.L., Austin, C.P. 2008. Quantitative High-Throughput Screen Identifies Inhibitors of the Schistosoma mansoni Redox Cascade. *PLoS Negl Trop Dis* **2**:e127

- Sladek, F.M., Zhong, W.M., Lai, E., Darnell, J.E., Jr. 1990. Liver-enriched transcription factor HNF-4 is a novel member of the steroid hormone receptor superfamily. *Genes Dev* **4**:2353-65
- Smyth, D.R., Mrozkievicz, M.K., McGrath, W.J., Listwan, P., Kobe, B. 2003. Crystal structures of fusion proteins with large-affinity tags. *Protein Sci* **12**:1313-22
- Spurlino, J.C., Lu, G.Y., Quiocho, F.A. 1991. The 2.3-A resolution structure of the maltose- or maltodextrin-binding protein, a primary receptor of bacterial active transport and chemotaxis. *J Biol Chem* **266**:5202-19
- Stevens, J.C., Shipley, L.A., Cashman, J.R., Vandenbranden, M., Wrighton, S.A. 1993. Comparison of human and rhesus monkey in vitro phase I and phase II hepatic drug metabolism activities. *Drug Metab Dispos* **21**:753-60
- Takahashi, Y., Hamada, J., Murakawa, K., Takada, M., Tada, M., Nogami, I., Hayashi, N., Nakamori, S., Monden, M., Miyamoto, M., Katoh, H., Moriuchi, T. 2004. Expression profiles of 39 HOX genes in normal human adult organs and anaplastic thyroid cancer cell lines by quantitative real-time RT-PCR system. *Exp Cell Res* **293**:144-53
- Testa, B. 1995. Biochemistry of Redox Reactions. Academic Press, London
- Thomas, M.J., Seto, E. 1999. Unlocking the mechanisms of transcription factor YY1: are chromatin modifying enzymes the key? *Gene* **236**:197-208
- Treacy, E.P., Akerman, B.R., Chow, L.M., Youil, R., Bibeau, C., Lin, J., Bruce, A.G., Knight, M., Danks, D.M., Cashman, J.R., Forrest, S.M. 1998. Mutations of the flavin-containing monooxygenase gene (FMO3) cause trimethylaminuria, a defect in detoxication. *Hum Mol Genet* **7**:839-45
- Tugnait, M., Hawes, E.M., McKay, G., Rettie, A.E., Haining, R.L., Midha, K.K. 1997. N-oxygenation of clozapine by flavin-containing monooxygenase. *Drug Metab Dispos* **25**:524-7
- Tynes, R.E., Sabourin, P.J., Hodgson, E. 1985. Identification of distinct hepatic and pulmonary forms of microsomal flavin-containing monooxygenase in the mouse and rabbit. *Biochem Biophys Res Commun* **126**:1069-75
- Vanin, E.F. 1985. Processed pseudogenes: characteristics and evolution. *Annu Rev Genet* **19**:253-72
- Vannelli, T.A., Dykman, A., Ortiz de Montellano, P.R. 2002. The antituberculosis drug ethionamide is activated by a flavoprotein monooxygenase. *J Biol Chem* **277**:12824-9
- Viggiani, A., Siani, L., Notomista, E., Birolo, L., Pucci, P., Di Donato, A. 2004. The role of the conserved residues His-246, His-199, and Tyr-255 in the catalysis of catechol 2,3-dioxygenase from *Pseudomonas stutzeri* OX1. *J Biol Chem* **279**:48630-9
- Vyas, K.P., Kari, P.H., Ramjit, H.G., Pitzemberger, S.M., Hichens, M. 1990. Metabolism of antiparkinson agent dopazinol by rat liver microsomes. *Drug Metab Dispos* **18**:1025-30
- Vyas, P.M., Roychowdhury, S., Koukouritaki, S.B., Hines, R.N., Krueger, S.K., Williams, D.E., Nauseef, W.M., Svensson, C.K. 2006. Enzyme-mediated protein haptentation of dapsone and sulfamethoxazole in human keratinocytes:

- II. Expression and role of flavin-containing monooxygenases and peroxidases. *J Pharmacol Exp Ther* **319**:497-505
- Walter, T.S., Meier, C., Assenberg, R., Au, K.F., Ren, J., Verma, A., Nettleship, J.E., Owens, R.J., Stuart, D.I., Grimes, J.M. 2006. Lysine methylation as a routine rescue strategy for protein crystallization. *Structure* **14**:1617-22
- Wennerstrom, H., Lindman, B. 1979. Micelles - Physical-Chemistry of Surfactant Association. *Physics Reports-Review Section of Physics Letters* **52**:1-86
- Wernimont, A., Edwards, A. 2009. In situ proteolysis to generate crystals for structure determination: an update. *PLoS One* **4**:e5094
- Whetstine, J.R., Yueh, M.F., McCarver, D.G., Williams, D.E., Park, C.S., Kang, J.H., Cha, Y.N., Dolphin, C.T., Shephard, E.A., Phillips, I.R., Hines, R.N. 2000. Ethnic differences in human flavin-containing monooxygenase 2 (FMO2) polymorphisms: detection of expressed protein in African-Americans. *Toxicol Appl Pharmacol* **168**:216-24
- Williams, D.E., Ziegler, D.M., Nordin, D.J., Hale, S.E., Masters, B.S. 1984. Rabbit lung flavin-containing monooxygenase is immunochemically and catalytically distinct from the liver enzyme. *Biochem Biophys Res Commun* **125**:116-22
- Yamazaki, H., Fujieda, M., Togashi, M., Saito, T., Preti, G., Cashman, J.R., Kamataki, T. 2004. Effects of the dietary supplements, activated charcoal and copper chlorophyllin, on urinary excretion of trimethylamine in Japanese trimethylaminuria patients. *Life Sci* **74**:2739-47
- Yamazaki, H., Fujita, H., Gunji, T., Zhang, J., Kamataki, T., Cashman, J.R., Shimizu, M. 2007. Stop codon mutations in the flavin-containing monooxygenase 3 (FMO3) gene responsible for trimethylaminuria in a Japanese population. *Mol Genet Metab* **90**:58-63
- Yan, R.Q., Li, X.S., Yang, T.Y., Xia, C. 2006. Structures and homology modeling of chicken major histocompatibility complex protein class I (BF2 and beta2m). *Mol Immunol* **43**:1040-6
- Yeung, C.K., Adman, E.T., Rettie, A.E. 2007. Functional characterization of genetic variants of human FMO3 associated with trimethylaminuria. *Arch Biochem Biophys*
- Yueh, M.F., Krueger, S.K., Williams, D.E. 1997. Pulmonary flavin-containing monooxygenase (FMO) in rhesus macaque: expression of FMO2 protein, mRNA and analysis of the cDNA. *Biochim Biophys Acta* **1350**:267-71
- Zanier, K., Nomine, Y., Charbonnier, S., Ruhlmann, C., Schultz, P., Schweizer, J., Trave, G. 2007. Formation of well-defined soluble aggregates upon fusion to MBP is a generic property of E6 proteins from various human papillomavirus species. *Protein Expr Purif* **51**:59-70
- Zhang, A.Q., Mitchell, S.C., Smith, R.L. 1996. Exacerbation of symptoms of fish-odour syndrome during menstruation. *Lancet* **348**:1740-1
- Zhang, A.Q., Mitchell, S.C., Smith, R.L. 1999. Dietary precursors of trimethylamine in man: a pilot study. *Food Chem Toxicol* **37**:515-20
- Zhang, J., Cashman, J.R. 2006. Quantitative analysis of FMO gene mRNA levels in human tissues. *Drug Metab Dispos* **34**:19-26

- Zhang, J., Cerny, M.A., Lawson, M., Mosadeghi, R., Cashman, J.R. 2007a. Functional activity of the mouse flavin-containing monooxygenase forms 1, 3, and 5. *J Biochem Mol Toxicol* **21**:206-15
- Zhang, J., Tran, Q., Lattard, V., Cashman, J.R. 2003. Deleterious mutations in the flavin-containing monooxygenase 3 (FMO3) gene causing trimethylaminuria. *Pharmacogenetics* **13**:495-500
- Zhang, Q., Ma, X., Ward, A., Hong, W.X., Jaakola, V.P., Stevens, R.C., Finn, M.G., Chang, G. 2007b. Designing facial amphiphiles for the stabilization of integral membrane proteins. *Angew Chem Int Ed Engl* **46**:7023-5
- Zhong, Z., Yan, J., Zhao, Y. 2005. Cholic acid-derived facial amphiphiles with different ionic characteristics. *Langmuir* **21**:6235-9
- Zhou, J., Shephard, E.A. 2006. Mutation, polymorphism and perspectives for the future of human flavin-containing monooxygenase 3. *Mutat Res* **612**:165-71
- Ziegler, D.M. 1980. Microsomal flavin-containing monooxygenase: Oxygenation of nucleophilic nitrogen and sulfur compounds. *In: Enzymatic Basis of Detoxification*. W.B. Jakoby, editor. pp. 201-227. Academic Press, New York
- Ziegler, D.M. 1988. Flavin-containing monooxygenases: catalytic mechanism and substrate specificities. *Drug Metab Rev* **19**:1-32
- Ziegler, D.M. 1990. Flavin-containing monooxygenases: enzymes adapted for multisubstrate specificity. *Trends Pharmacol Sci* **11**:321-4
- Ziegler, D.M. 1991. The 1990 Bernard B. Brodie Award Lecture. Unique properties of the enzymes of detoxication. *Drug Metab Dispos* **19**:847-52
- Ziegler, D.M. 1993. Recent studies on the structure and function of multisubstrate flavin-containing monooxygenases. *Annu Rev Pharmacol Toxicol* **33**:179-99
- Ziegler, D.M. 2002. An overview of the mechanism, substrate specificities, and structure of FMOs. *Drug Metab Rev* **34**:503-11
- Ziegler, D.M., Ansher, S.S., Nagata, T., Kadlubar, F.F., Jakoby, W.B. 1988. N-methylation: potential mechanism for metabolic activation of carcinogenic primary arylamines. *Proc Natl Acad Sci U S A* **85**:2514-7
- Ziegler, D.M., Mitchell, C.H. 1972. Microsomal oxidase. IV. Properties of a mixed-function amine oxidase isolated from pig liver microsomes. *Arch Biochem Biophys* **150**:116-25
- Ziegler, D.M., Poulsen, L.L. 1998. Catalytic mechanism of FMO catalyzed N- and S-oxidations. *In: Drug Metabolism. Towards the next Millennium*. N. Gooderham, editor. pp. 30-38. IOS Press, Amsterdam
- Zschocke, J., Kohlmüller, D., Quak, E., Meissner, T., Hoffmann, G.F., Mayatepek, E. 1999. Mild trimethylaminuria caused by common variants in FMO3 gene. *Lancet* **354**:834-5

9 Appendix

9.1 Constructs

Amino acid sequences of all wild-type constructs are listed below. All constructs were cloned into pMAL-vector.

MBP-hFMO3

MKIEEGKLVIIWINGDKGYNGLAEVGGKFEKDTGIKVTVEHPDKLEEKFPQVAATGDGPDIIFWAHDRFGGYAQSGLLAEITPDKAFQDKLYPFTWDAVRYNGKLIAYPIAVEALSIIYNKDLLPNPPKTWEEIPALDKELKAKGKSALMFLNLQEPYFTWPLIAADGGYAFKYENGGYDIKDVGVNAGAKAGLTFLVDLIKNKHMNADTDYSIAEAAFNKGETAMTINGPWAWSNIDTSKVNYGVTVLPTFKGQPSKPFVGVLSAGINAASPNKELAKEFLENYLLTDEGLEAVNKDKPLGAVALKSYEEELAKDPRIAATMENAQKGEIMPNI PQMSAFWYAVRTAVINAASGRQTVDEALKDAQTNSSSNNNNNNNNNNLGIIEGRGKVAIIIGAGVSGLASIRSCLEEGLEPTCFEKSNDIGGLWKFSDHAEGRASIIKSVFSNSSKEMMCFPDFPDDFNFPMHNSKIQEYIIAFAKEKNLLKYIQFKTFVSSVNKHPDFATTGQWDVTTTERDGKKE SAVFDAMVCSGHVYVNLPKESFPGLNHFKGKCFHSRDYKEPGVFNGKRVLVVGLGNSGCDIATELSRTAEQVMISSRSGSWVMSRVWDNGYPWDMLLVTRFGTFLKNNLPTAISDWLYVKQMNARFKHENYGLMPLNGVLRKEPVFNDEL PASILCGIVSVKPNVKEFTETSIFEDGTIFEGIDCVIFATGYSFAYPFLDESIKSRNNEIILFKGVFPPLLEKSTIAVIGFVQSLGAAIPTVDLQSRWAAQVIKGTCTLP SMEDMMNDINEKMEKKRKWF GKSETIQTDYIVYMDELSSFIGAKPNIPWFLFTDPKLAMEVYFGPCSPYQFRLVGPQWPGARNAILTQWDRSLKPMQTRVVGRLLQKPCFFFWHLKLF AIPILLIAVFLVLT

MBP-hFMO5

MKIEEGKLVIIWINGDKGYNGLAEVGGKFEKDTGIKVTVEHPDKLEEKFPQVAATGDGPDIIFWAHDRFGGYAQSGLLAEITPDKAFQDKLYPFTWDAVRYNGKLIAYPIAVEALSIIYNKDLLPNPPKTWEEIPALDKELKAKGKSALMFLNLQEPYFTWPLIAADGGYAFKYENGGYDIKDVGVNAGAKAGLTFLVDLIKNKHMNADTDYSIAEAAFNKGETAMTINGPWAWSNIDTSKVNYGVTVLPTFKGQPSKPFVGVLSAGINAASPNKELAKEFLENYLLTDEGLEAVNKDKPLGAVALKSYEEELAKDPRIAATMENAQKGEIMPNI PQMSAFWYAVRTAVINAASGRQTVDEALKDAQTNSSSNNNNNNNNNNLGIIEGRISSEFGSSRMTKKRIAVIIGGGVSGLSSIKCCVEEGLEPVCFERTDDIGGLWRFQENPEEGRASIIKSVIINTSKEMMCFSDYPIPDHYPNFMHNAQVLEYFRMYAKEFDLLKYIRFKTTVCSVKKQPDFATSGQWEVVTESEGGKEMNVFDGVMVCTGHHTNAHLPLESFPPIEKFQYFHSRDYKNPEGFTGKRVIIGIGNSGGDLAVEISQTAKQVFLSTRRGAWILNRVGDYGYPADVLFSSRLTHFIWKICGQSLANKYLEKKINQRFDHEMFGLKPKHRALSQHPTLNDDLPNRIISGLVKVKGNVKEFTETAIFEDGSREDDIDAVIFATGYSFDFPFLEDSVKVVKNKIPLYKKVFPNLERPTLAIIGLIQPLGAIMPISSELQGRWATQVFKGLKTLPSQSEMMAEISKAQEEIDKRYVESQRHTIQGDYIDTMEELADLVGVRPNLLSLAFTDPKLALHLLLPCTPIHYRVQGPQWPGARKAILTDDRIRKPLMTRVVERSSSMTSTMTIGKFMLALAFFAII IAYF

MBP-mFMO5

MKIEEGKLVIIWINGDKGYNGLAEVGGKFEKDTGIKVTVEHPDKLEEKFPQVAATGDGPDIIFWAHDRFGGYAQSGLLAEITPDKAFQDKLYPFTWDAVRYNGKLIAYPIAVEALSIIYNKDLLPNPPKTWEEIPALDKELKAKGKSALMFLNLQEPYFTWPLIAADGGYAFKYENGGYDIKDVGVNAGAKAGLTFLVDLIKNKHMNADTDYSIAEAAFNKGETAMTINGPWAWSNIDTSKVNYGVTVLPTFKGQPSKPFVGVLSAGINAASPNKELAKEFLENYLLTDEGLEAVNKDKPLGAVALKSYEEELAKDPRIAATMENAQKGEIMPNI PQMSAFWYAVRTAVINAASGRQTVDEALKDAQTNSSSNNNNNNNNNNLGIIEGRISSEFGSSRMTKKRIAVIIGGGVSGLSSIKCCVEEGLEPVCFERTDDIGGLWRFQENPEEGRASIIKSVIINTSKEMMCFSDYPIPDHYPNFMHNAQVLEYFRMYAKEFDLLKYIRFKTTVCSVKKQPDFATSGQWEVVTESEGGKEMNVFDGVMVCTGHHTNAHLPLESFPPIEKFQYFHSRDYKNPEGFTGKRVIIGIGNSGGDLAVEISQTAKQVFLSTRRGAWILNRVGDYGYPADVLFSSRLTHFIWKICGQSLANKYLEKKINQRFDHEMFGLKPKHRALSQHPTLNDDLPNRIISGLVKVKGNVKEFTETAIFEDGSREDDIDAVIFATGYSFDFPFLEDSVKVVKNKIPLYKKVFPNLERPTLAIIGLIQPLGAIMPISSELQGRWATQVFKGLKTLPSQSEMMAEISKAQEEIDKRYVESQRHTIQGDYIDTMEELADLVGVRPNLLSLAFTDPKLALHLLLPCTPIHYRVQGPQWPGARKAILTDDRIRKPLMTRVVERSSSMTSTMTIGKFMLALAFFAII IAYF

9.2 Buffers and Reagents

LB-Agar	LB-medium (10 g tryptone, 5 g yeast, 5 g NaCl, H ₂ O ad 1 l) + 1.5 % (w/v) agar. Autoclave and add antibiotic after cooling to ~ 50 °C.
SOC	20g peptone 5 g yeast 0.5 g NaCl 2.5 ml 1 M KCl 5 ml MgCl ₂ 20 ml 1 M glucose H ₂ O ad 1 l Autoclave.
Induction solution	0.048 g riboflavin 1.2 ml 1 M IPTG sterile H ₂ O ad 20 ml
Lysis buffer	600 µl FAD (10 mg/ml) 0.36 g L- α -phosphatidylcholine 1 ml 0.1 M PMSF 0.5 % Triton [®] X-100 50 mM K ₂ HPO ₄ buffer, pH 8.4, ad 200 ml
10 % SDS resolving gel	9.2 ml H ₂ O 8.3 ml 30 % acrylamide mix 6.3 ml 1.5 M Tris pH 8.8 250 µl 10 % (w/v) SDS 250 µl 10 % (w/v) APS 10 µl TEMED
5 % SDS stacking gel	6.8 ml H ₂ O 1.7 ml 30 % acrylamide mix 1.25 ml 1.0 M Tris pH 6.8 100 µl 10 % (w/v) SDS 100 µl 10 % (w/v) APS 10 µl TEMED
5 x Tris glycine electrophoresis buffer	15.1 g Tris base 94 g glycine 50 ml 10 % (w/v) SDS H ₂ O ad 1 l
4 x SDS gel-loading buffer	0.25 M Tris HCl pH 8.5 8 % SDS 1.6 mM EDTA 0.04 % bromophenol blue 40 % glycerol add 20 x reducing agent (2 M DTT) right before use.
SDS gel destain	500 ml methanol 400 ml H ₂ O 100 ml glacial acetic acid

Coomassie staining solution	0.35 g Coomassie Brilliant Blue R250 100 ml ,SDS gel destain'
Amylsoe column wash buffer (buffer A)	50 mM K ₂ HPO ₄ , pH 8.4 0.5 % Triton [®] X-100 15 µg/ml FAD
Amylsoe column wash buffer (buffer A')	50 mM K ₂ HPO ₄ , pH 8.4 15 µg/ml FAD
Amylsoe column elution buffer	50 mM K ₂ HPO ₄ , pH 8.4 15 µg/ml FAD 3 mM maltose in some cases 0.5 % Triton [®] X-100 was included
Q column wash buffer (buffer B)	50 mM Bis-Tris buffer, pH 6 in some cases 0.01 % DDM was included
Q column elution buffer	50 mM Bis-Tris buffer, pH 6 1 M NaCl in some cases 0.01 % DDM was included

9.3 Equipment List

Instrument	Manufacturer
Minitron incubator shaker	INFORS HT, Bottmingen, Switzerland
Centrifuge J2-21M , Rotor JA-20 and JA-10	Beckman Coulter, Inc., Brea, CA, USA
Optima MAX-E Ultra Centrifuge MAX (100K)	Beckman Coulter, Inc., Brea, CA, USA
Biofuge pico	Heraeus, Newport Pagnell, United Kingdom
Eppendorf centrifuge 5415R	Eppendorf AG, Hamburg, Germany
Megafuge 1.0R	Heraeus, Newport Pagnell, United Kingdom
Sonicator Sonics Vibracell (VC130)	Sonics and Materials Inc., Newtown, CT, USA
French press	Thermo Electron Corp., Needham Heights, MA, USA
Bio-Rad Biologic LP System & Software	Bio-Rad, Hercules, CA, USA

Econo-Column Chromatography Columns, 1.5 x 5 cm	Bio-Rad, Hercules, CA, USA
Fraction collector Redi frac	Amersham Biosciences Europe GmbH, Freiburg, Germany
ISMATEC tubing pump (MCP ISM 726)	ISMATEC Labortechnik GmbH, Wertheim-Mondfeld, Germany
UVS/Vis Spectrophotometer Cary 300 Bio	Varian Inc., Palo Alto, CA, USA
UVS/Vis Spectrophotometer Cary 50 Bio	Varian GmbH, Darmstadt, Germany
Lambda 25 UV Vis Spectromer	Perkin Elmer, Waltham, MA, USA
Perkin Elmer LS55 fluorescence spectrophotometer	Perkin Elmer, Waltham, MA, USA
Zetasizer Nano-S	Malvern Instruments Ltd, Malvern, United Kingdom
Mini-PROTEAN gel electrophoresis system	Bio-Rad, Hercules, CA, USA
PowerPac Basic power supply	Bio-Rad, Hercules, CA, USA
NanoDrop™ ND-1000 UV/VIS Spectrophotometer	Thermo Fisher Scientific, Wilmington, DE, USA
Kodak Gel Logic 200 Imaging System	Eastman Kodak Company, Rochester, NY , USA
Hitachi HPLC system: Hitachi L-7200 autosampler and L-7100 pump with a Hitachi L-7400 UV detector	Hitachi, Peoria, IL, USA
Waters HPLC system: Waters 600E controller and Waters Autosampler 700 Satellite WISP with a Waters 486 Absorbance Detector	Waters, Eschborn, Germany
Waters Alliance™ HPLC-System: Waters e2695 XC Separations Modul with a Waters 2998 Photodiode Array Detector and Empower™ 2 Software	Waters, Eschborn, Germany
Esquire LC with Atmospheric Pressure Chemical Ionisation	Bruker Daltonics, Bremen, Germany
HP Series 1100 Binary Pump G1312A with HP 1100 VWD UV/VIS Detektor	Hewlett Packard, Waldbronn, Germany

Water bath GFL 1087	Gesellschaft für Labortechnik, Burgwedel, Germany
pH Meter inoLab pH level1	Wissenschaftlich-Technische Werkstätten GmbH, Wetheim, Germany
Corning 440 pH Meter	Corning, Electrochemistry Products, Woburn, MA, USA
Ultrasonic bath, Sonorex, Super RK 510H	Bandelin, Berlin, Germany
Vortex VF2	Janke & Kunkel GmbH & Co KG, Staufen, Germany
Balance MC1, Laboratori LC 620S	Satorius, Göttingen, Germany
Balance MC1, Research RC 210P	Satorius, Göttingen, Germany
MicroPulser Elektroporator	Bio-Rad, Hercules, CA, USA
Gene Amp PCR 9700 system	Perkin Elmer, Waltham, MA, USA
DNA Engine Peltier Thermal Cycler	Bio-Rad, Hercules, CA, USA
Pipettes Reference Eppendorf	Eppendorf AG, Hamburg, Germany
RAININ Classic Pipettes	Rainin Instrument LLC, Oakland, CA, USA
Polystyrene (PS) Cuvettes; 1.5–3.0; Semi-Micro	VWR International, West Chester, PA, USA
Crychem Plate, HR3-160	Hampton Research Corp., Aliso Viejo, CA, USA
96-well flat-bottom UV-Star microplates	Greiner Bio-One, Frickenhausen, Germany
OptiPlate-96 (white) 96-well flat-bottom microplates	Perkin Elmer, Waltham, MA, USA

Erklärung zu § 9 Abs. 2 Nr. 2 der Promotionsordnung

Der Inhalt dieser Arbeit wurde – abgesehen von der Beratung durch meine Betreuer – selbstständig von mir erarbeitet und in dieser Form zusammengestellt.

Die Arbeit hat an keiner anderen Stelle im Rahmen eines Prüfungsverfahrens vorgelegen. Teilergebnisse dieser Arbeit wurden in folgenden Beiträgen vorab veröffentlicht:

Motika, M.S., Zhang, J., Cashman, J.R. 2007. Flavin-containing monooxygenase 3 and human disease. *Expert Opin Drug Metab Toxicol* **3**:831-45

Zhang, J., Chaluvadi, M.R., Reddy, R., Motika, M.S., Richardson, T.A., Cashman, J.R., Morgan, E.T. 2009. Hepatic flavin-containing monooxygenase gene regulation in different mouse inflammation models. *Drug Metab Dispos* **37**:462-8

Motika, M.S., Zhang, J., Zheng, X., Riedler, K., Cashman, J.R. 2009. Novel variants of the human flavin-containing monooxygenase 3 (FMO3) gene associated with trimethylaminuria. *Mol Genet Metab* **97**:128-35

Cashman, J.R., Motika, M.S. manuscript in preparation. Monoamine Oxidases and Flavin-Containing Monooxygenases. *In: Comprehensive Toxicology* C. McQueen, editor. ELSEVIER, Kidlington, United Kingdom

Motika, M.S., Zhang, J., Zheng, X., Riedler, K., Cashman, J.R. 2008. Novel Variants of the Human Flavin-Containing Monooxygenase 3 (FMO3) Gene Associated with Trimethylaminuria. *In: 15th North American ISSX Regional Meeting, San Diego USA*

Zhang, J., Chaluvadi, M., Reddy, R., Motika, M.S., Cashman, J.R., Morgan, E.T. 2008. Hepatic flavin-containing monooxygenase gene regulation in different mouse inflammation models. *In: ASBMB Annual Meeting, San Diego, USA*

Motika, M.S., Zheng, X., Zhang, J., Riedler, K., Cashman, J.R. 2009. pH-Dependence of Mouse and Human Flavin-containing Monooxygenase 5 *In: 3rd Asian Pacific ISSX Meeting, Bangkok, Thailand*

Reddy, R.R., Ralph, E., Motika, M.S., Zhang, J., Cashman, J.R. 2009. Oligomeric and kinetic characterization of purified human FMO3 and FMO5 expressed as maltose binding protein fusions. *In: 16th North American ISSX Regional Meeting, Baltimore, USA*

Die Arbeit ist unter Einhaltung der Regeln guter wissenschaftlicher Praxis der Deutschen Forschungsgemeinschaft entstanden.

Kiel, im März 2010

Meike Motika

Danksagung

Die vorliegende Arbeit entstand am Pharmazeutischen Institut der Christian-Albrechts-Universität zu Kiel sowie am Human BioMolecular Research Institut in San Diego auf Anregung und unter der Leitung von

Prof. Dr. Bernd Clement und Prof. Dr. John R. Cashman.

Für die freundliche Aufnahme in den Arbeitskreis, die Überlassung des interessanten Promotionsthemas und des damit verbundenen Auslandsaufenthaltes sowie der steten Diskussionsbereitschaft und Unterstützung möchte ich mich bei meinem Doktorvater, Prof. Dr. B. Clement, sehr herzlich bedanken.

Mein besonderer Dank gilt auch Prof. Dr. J. Cashman, der mich an seinem Institut aufgenommen und betreut hat und Dr. Jun Zhang für die stets vorhandene Diskussions- und Hilfsbereitschaft bei molekularbiologischen und biochemischen Fragen.

Prof. Dr. Axel Scheidig und Prof. Dr. David C. Stout danke ich vor allem für die ständige Bereitschaft zu Diskussionen und die vielen hilfreichen Tipps bei molekular- und strukturbioologischen Problemstellungen sowie für die Bereitstellung eines Laborplatzes.

Weiterhin möchte ich mich bei Karl Okolotowicz, Britta Gerig und Nikola Klein für die Durchführung der Synthesen einiger FMO5 Substrate, bei Jane Xueying Zheng und Joscha Kotthaus für die Hilfe bei der HPLC-Analytik und bei Sven Wichman für die Durchführung der massenspektrometischen Analysen herzlich bedanken.

Für das zügige Korrekturlesen der Arbeit sowie die konstruktiven und hilfreichen Hinweise bedanke ich mich bei Dorothea Wree, Joscha Kotthaus, Nikola Klein, Helen Hungeling, Antje Havemeyer und Annette Faust.

Außerdem möchte ich mich bei Andy Annalora, Mitch Luna, Rich Wilson, Annette Faust, Ulrich Zander, Dennis Schade, Ken Abel und Nora Barakat für die Unterstützung und die hilfreichen Anregungen und Diskussionen bedanken.

Lebenslauf

Persönliche Daten

Name	Meike Simone Motika
Geburtsdatum	12. September 1980
Geburtsort	Leverkusen
Staatsangehörigkeit	deutsch

Schulausbildung

1987 – 1991	Grundschule Marne
1991 – 1997	Gymnasium Marne
1997 – 1998	Tullahoma High School, Tennessee, USA (High-School-Abschluß: Mai 1998)
1998 – 2000	Gymnasium Marne
Juni 2000	Allgemeine Hochschulreife

Studium

2000 – 2004	Studium der Pharmazie an der Christian-Albrechts-Universität zu Kiel
01.01. – 30.06.2005	1. Hälfte des Praktischen Jahres: Diplomarbeit durchgeführt bei Prof. Dr. Kadlubar am National Center for Toxicological Research in Little Rock, USA, unter der Leitung von Prof. Dr. Clement (Diplomprüfung: 01.09.2005)
01.07. – 31.12.2005	2. Hälfte des Praktischen Jahres in der Esmarch Apotheke, Kiel
Februar 2006	Erteilung der Approbation als Apothekerin

Berufstätigkeit und Promotion

01.02.06 – 31.03.06	Neue Apotheke, Marne, Apothekerin
01.04.06 – 31.03.07	Wissenschaftliche Mitarbeiterin am Pharmazeutischen Institut der Christian-Albrechts-Universität zu Kiel, Abteilung Pharmazeutische Chemie, Arbeitsgruppe Prof. Dr. Clement
01.04.07 – 31.03.09	Forschungsaufenthalt am Human BioMolecular Research Institute in San Diego, USA, unter der Leitung von Prof. Dr. Clement und Dr. Cashman
01.04.09 - heute	Wissenschaftliche Mitarbeiterin am Pharmazeutischen Institut der Christian-Albrechts-Universität zu Kiel, Abteilung Pharmazeutische Chemie, Arbeitsgruppe Prof. Dr. Clement